

Technical Report

522

**Millstone Hill
Thomson Scatter Results
for 1970**

J. V. Evans
J. M. Holt

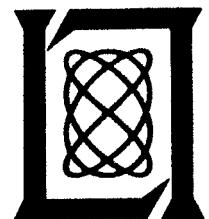
11 May 1976

Prepared for the National Science Foundation
under NSF Grant No. GA-42230 by

Lincoln Laboratory

MASSACHUSETTS INSTITUTE OF TECHNOLOGY

LEXINGTON, MASSACHUSETTS



ABSTRACT

During 1970, the incoherent scatter radar at Millstone Hill (42.6°N, 71.5°W) was employed to measure the electron density, electron and ion temperatures, and vertical velocity of the ions in the F-region over periods of 24 hours on an average of twice per month. The observations spanned the height interval 200 to 900 km, approximately, and achieved a time resolution of about 30 minutes. This report presents the results of these measurements in a set of contour diagrams.

Commencing with the data presented in this report, a method of data reduction has been used which supersedes the older one of constructing the contour diagrams by hand. In the new method the set of points for any given parameter is matched by a two-dimensional polynomial surface in a least-squares fit. The program that carries this out is described fully in the report. By obtaining a continuous analytical description of the data with respect to height and time, machine-drawn contouring becomes possible and is now employed. The new program also provides a means of transferring the results to other users in machine-readable form. In addition, the new program yields a more repeatable smoothing of the data with respect to height and time, thereby allowing parameters that depend upon gradients (e.g., heat and particle fluxes) to be estimated more accurately.

CONTENTS

Abstract	iii
I. INTRODUCTION	1
II. EQUIPMENT, OBSERVING, AND DATA-ANALYSIS PROCEDURES	3
A. Equipment	3
B. Observing Procedure	3
C. Observations	5
D. Data Analysis	8
III. DATA REDUCTION	9
A. Preparation of the Data	9
B. Least-Mean-Squares Polynomial Fitting	11
C. Contour Plots	14
D. Punched Card and Magnetic Tape Output	14
E. Recovery of Height Profiles or Time Variations	15
F. Vertical Gradients	16
G. Weighted Mean Height Correction	16
H. Total Electron Content	18
I. Uncertainties	18
IV. RESULTS	19
A. Electron Density	19
B. Electron Temperature	49
C. Ion Temperature	79
D. Vertical Velocity	79
References	133
APPENDIX - RCVR, RCVR1, RCVRP: Users Instructions, Listing and Sample Printed Output	135

MILLSTONE HILL THOMSON SCATTER RESULTS FOR 1970

I. INTRODUCTION

Since 1963, incoherent (Thomson) scatter radar measurements of F-region electron densities, and electron and ion temperatures have been conducted at Millstone Hill, Westford, Massachusetts (42.6°N, 71.5°W) (Refs. 1 to 7). This paper is the eighth in a series of annual reports, and presents the results gathered in this program during the calendar year 1970. The observations reported were made for periods of 24 hours, approximately twice a month. The results

TABLE I PUBLICATIONS CONCERNING THE MILLSTONE HILL UHF (68-cm Wavelength) THOMSON SCATTER RESULTS		
Year	Months Covered	Publication
1963	February 1963 to January 1964	Ref. 1
	March, July, August, September	Ref. 8
	April, July, November	Ref. 9
1964	January through December	Ref. 2
	April, July, November	Ref. 10
1965	January through December	Ref. 3
	January, April, August	Ref. 11
	June	Ref. 12
	June, August, September	Ref. 13
1966	January through December	Ref. 4
	January, March, July, September	Ref. 14
1967	January through December	Ref. 5
	February, June, October, December	Ref. 14
1968	January through December	Ref. 6
	October	Ref. 15
1969	January through December	Ref. 7
	February, April, July	Ref. 16
	September, October	Ref. 16

obtained in earlier years have been published in the articles listed in Table I, and have been transmitted to the World Data Center A, Boulder, Colorado.

In addition to the measurements reported here of F-region electron densities, electron and ion temperatures, and vertical velocity, a number of measurements were conducted in 1970 of the electron density in the D- and E-regions of the ionosphere employing a digital filter to

subtract out coherent echoes from distant hills at the same range.¹⁷ For these measurements, two new modes of operating the radar were developed. The E-mode provided a power profile over the altitude interval 90 to 600 km, approximately, with an altitude resolution of 15 km, while the I-mode covered the interval 65 to 130 km with 3-km height resolution. These programs afforded another improvement over the older method of operating the radar in that the repetition frequency was considerably increased, thereby providing a larger number of independent samples per second. Advantage was taken of this to try to measure rapid changes in the ionosphere introduced, for example, by Traveling Ionospheric Disturbances (TIDs) by simply repeating the E-mode runs with only 2 minutes integration. This program known as RASEM (Rapid Sequence E-Mode) was operated for eight days in 1970 and the results have been reported elsewhere.¹⁸

The principle of digital clutter subtraction was later extended to measurements of the autocorrelation functions of the signals; these permitted the first measurements at Millstone of electron and ion temperatures in the E-region in which good height resolution was achieved.¹⁹

The measurements of the echo autocorrelation function were accomplished by transmitting pairs of short pulses and calculating in the digital computer the correlation between samples of the echoes taken with the same spacing. This method of operation allows the height and frequency resolution of the measurements to be set independently of one another, while in the measurements reported here, the length of the single long pulse used establishes both parameters.

During 1970, three new operating modes (F, G, H) spanning the height interval 100 to 500 km were developed that employed the autocorrelation method. These became known as the "double-pulse" experiments to distinguish them from the earlier single-pulse measurements.

Double-pulse measurements were made at irregular intervals in 1970 commencing with observations conducted during a partial solar eclipse on 7 March. Results of the eclipse measurements have been reported elsewhere.²⁰ Routine measurements using the double-pulse method commenced in 1971 and have been used extensively to study the propagation of thermal tides from the mesosphere into the lower thermosphere,^{21,22} These measurements also permit the determination of the neutral density in the lower thermosphere (in the region where ion-neutral collisions become important) and the ion composition in the F1-region,²³ but as yet no complete reduction of these data for this purpose has been undertaken.

In this report, we present only the results of the measurements made with single long pulses. These covered the altitude interval 200 to 800 km, approximately, with a height resolution (for the measurements of temperature) of 75 km. These data can be used to deduce the temperature of the exosphere from thermal balance arguments,²⁴ and results obtained in this way for the period March 1969 through March 1971 have already been reported.²¹

Section II describes the equipment, data gathering, and data reduction procedures. During 1970, these were little changed from those employed in 1969,⁷ except that a new method of data smoothing and presentation was developed that replaced the earlier manual method employed since the program began. This method of data compression is described in detail in Sec. III. Results for electron density, electron and ion temperatures, and vertical velocity are presented and discussed in Sec. IV.

II. EQUIPMENT, OBSERVING, AND DATA-ANALYSIS PROCEDURES

A. Equipment

The UHF incoherent scatter radar equipment has been described.¹ During 1968, the spectrum analyzer portion of the receiver was replaced by one of newer design that was interfaced directly into the XDS 9300 computer. These changes are fully documented in Ref. 25 and discussed further in Ref. 7. As mentioned above, the principal changes made during 1970 were the development of the double-pulse modes for operating the equipment. A brief description of one of these (the F-mode) has been given elsewhere²² and a full account of the complete system is reserved for a separate report.

One other change made in (June) 1970 was the relocation of the parametric amplifier from a shelter beneath the 220-foot-diameter antenna to the room in the main building where the remainder of the receiver is located. This required extending the receiver waveguide by 330 feet. The resulting increase in the system temperature (20°K) was considered a small drawback in comparison to the greater ease with which the equipment could be adjusted. However, with the parametric amplifier in the same room as the exciter, it became necessary to exercise great care to prevent unwanted CW leakage into the receiver.

The performance of the receiver was further improved in August 1970 when the old gas discharge TR device used to protect the receiver was replaced by a new solid-state device (employing diode switches) built to a design provided by L. M. LaLonde (Cornell University). This introduced less loss and provided a faster recovery. More importantly, the new device did not suffer any of the aging problems to which the gas discharge tubes were prone, causing them to become noisy and introduce irregular variations in the noise level along the timebase.

In order to extend the measurements to low altitudes, it was also necessary to improve the transmitter switching of the beam current in the klystron amplifiers. The decay time for this with the original modulator was 200 μ sec and by rebuilding the modulator deck (in August), this was reduced to about 70 μ sec.

The most serious difficulty encountered with the equipment in 1970 was the loss of gain that occurred when snow collected in the 220-foot antenna to a depth of over two feet during a storm on 30 December 1969. Although the snow was removed manually during the course of the next few days, its weight (together with that of the people engaged in snow removal) aggravated the distortion of the mesh caused by a similar event the previous winter.⁷ To remedy this, a program of surface improvement was undertaken during the summer in which the wire ties holding the mesh to its supporting pipe purlins were selectively cut and the mesh retensioned. Sufficient mesh had "gathered" at the apex of the parabola to permit the removal during these operations of a 3-foot-wide span. In addition to this retensioning, the sag of the mesh between the pipe purlins (spaced 14 feet apart) was reduced by introducing a set of cables laid diagonally in orthogonal directions across the pipe purlins. These cables were separately tensioned and the mesh then tied to them.

B. Observing Procedure

During 1970, we attempted to make F-region observations twice per month for periods of 24 hours. These were carried out using the single-pulse experiment modes A to C described previously²⁵ which provide the coverage indicated in Table II. Two types of measurements were conducted. In one, the experiment sequence A to C (Table II) was repeated every 30 minutes,

TABLE II THE NORMAL "ONE-PULSE" EXPERIMENT MODE SEQUENCE						
Mode	Pulse Length (μsec)	Height Resolution (km)	Sample Spacing (km)	Altitude Coverage (km)	Measured Parameters	
					Direct	Deduced
A	100	15	7.5	100-1000	Power	N_e
B	500	75	30	150-1500	Power	N_e
			75	225- 675	Power spectrum	T_e, T_i, v_z
C	1000	150	30	300-2000	Power	N_e
			75	450-1125	Power spectrum	T_e, T_i, v_z

TABLE III THE NORMAL "TWO-PULSE" EXPERIMENT MODE SEQUENCE						
Mode	Pulse Length (μsec)	Height Resolution (km)	Sample Spacing (km)	Altitude Coverage (km)	Measured Parameters	
					Direct	Deduced
E	100	15	6, 9, 15	90-600	Power	N_e
F	40	6	3, 6	105-165	Autocorrelation	$\left\{ \begin{array}{l} z < 120 \text{ km: } T_i, v_{in} \\ z > 120 \text{ km: } T_e, T_i, \\ \frac{n(O^+)}{N_e}, v_z \end{array} \right.$
						$\left\{ \begin{array}{l} z < 225 \text{ km: } T_e, T_i, \\ \frac{n(O^+)}{N_e}, v_z \\ z > 225 \text{ km: } T_e, T_i, v_z \end{array} \right.$
G	100	15	15	165-315	Autocorrelation	T_e, T_i, v_z
H	200	30	30	215-515	Autocorrelation	T_e, T_i, v_z

thereby yielding about 50 profiles of electron density, and electron and ion temperatures during a 24-hour run. These operations were termed "regular." A second type in which the C-mode experiment was repeated four times in each sequence was employed to achieve better measurements of the vertical drift above h_{\max}^{F2} . These observations were termed "drift" runs. The time to complete a cycle of measurements during the "drift" runs was 45 minutes, so that only about 30 separate density and temperature profiles were obtained in 24 hours.

The value of N_{\max} to be employed in the data reduction was made available in the form of a measurement of the F-region critical frequency f_o^{F2} in megahertz at the start of each cycle.* This measurement was made by the radar operator, who then typed the value into the computer which stored it, along with all the other information, on magnetic tape. To make the measurement, the C-4 ionosonde was modified to permit it to be turned on and monitored remotely, as well as to have its frequency controlled by a remote frequency synthesizer. Thus, the operator would turn on the sounder and advance the frequency of the synthesizer until the F2 ordinary return was just perceived at great range. The synthesizer dials then gave the required value of f_o^{F2} .

The intent of this procedure was to create a data tape that contained all the information required for processing, so that this could be carried out immediately upon completion of a run. However, the radar operators frequently encountered difficulty in reading f_o^{F2} , especially at night. Thus, as a rule, these real-time estimates were not employed in the data analysis; instead, they were plotted as a function of time, together with those derived from the film records and values recorded at Ottawa, Canada, Maynard, Massachusetts (if available), and Wallops Island, West Virginia. A smooth curve was then drawn through this collection of points that followed the variation at Millstone, except when this was clearly at variance with the observations at all the other stations. Values were read from this curve at 30-minute intervals and punched onto IBM cards. The recorded data were then processed employing values of N_{\max} for the electron-density profiles obtained by linear interpolation between the values available at half-hour intervals. The measurements made with single long pulses (modes A to C) essentially yield N_e , T_e , T_i , and v_z over the altitude range 200 to 1000 km, approximately (Table II), and recently have been used to obtain the H^+/O^+ ratio at high altitudes.¹⁶

For completeness, mention should be made that the measurements made with pairs of pulses provide results at lower altitudes. Normally, a sequence of modes E through H is employed to gather data on N_e , T_e , and T_i over the altitude range 100 to 500 km, approximately (Table III). However, as noted above, these data are not included in this report.

The quantities measured in each observing mode (echo power vs delay and frequency) are stored on magnetic tape for later processing. This is conducted on the XDS 9300 computer using FORTRAN programs written specifically to handle the "one-pulse" and "two-pulse" data sets. A program known as "ANALYSIS" is employed for the one-pulse data and "MUPMAP" for the multiple-pulse data.

C. Observations

The dates and times on which the "regular" and "drift" single-pulse measurements were made in 1970 are listed in Table IV. An effort was made to operate the radar in each mode for 24 hours every month. In one instance (30-31 October 1970), a large portion of the measurements

* $N_{\max} = 1.24 \times 10^4 (f_o^{\text{F2}})^2 \text{ e1/cm}^3$ when f_o^{F2} is expressed in megahertz.

TABLE IV
INCOHERENT SCATTER OBSERVATIONS - 1970

Begin			End			Mean K_p	Obs [†]	Comments
Date	C*	EST	Date	C*	EST			
6 January	Q	0900	7 January	Q	0900	1 _o	Reg	Low antenna gain. Poor drift data at night.
20 January		1130	21 January		1200	2-	Drift	Noisy TR tube. Frequency synthesizer out of lock - poor drift data.
17 February		0930	18 February		0930	2+	Reg	
23 February		1500	24 February	D	1500	3-	Drift	
8 March	D	2000	9 March	D	0600	4+	Reg	Very disturbed. Auroral period.
17 March		1030	18 March		1030	2-	Reg	
23 March	Q	1600	24 March	QQ	1545	0+	Drift	Very quiet
14 April		0900	15 April		0900	1-	Reg	
28 April		0800	29 April		0800	1+	Drift	
12 May		1500	13 May		1500	2+	Reg	
18 May		1500	19 May		1500	1+	Drift	
10 June		0400	11 June		0200	2-	Reg	
23 June		1900	24 June		1900	1+	Drift	
7 July	QQ	1300	8 July		1300	2-	Reg	
18 July	QQ	0830	19 July	QQ	1100	1 _o	Drift	
17 August	D	1430	18 August	D	1500	5-	Drift	Disturbed. Storm sudden commencement at 1704 EST on 16 August. Poor data between 1700 and 2200 EST.
24 August	QQ	1400	25 August		1400	2-	Drift	
31 August		1400	1 September	D	1430	3-	Reg	
16 September		0930	17 September		0930	2-	Reg	
28 September	Q	1500	29 September	QQ	1400	1 _o	Drift	
5 October	Q	1500	6 October		1500	1+	Reg	
13 October		1400	14 October		1500	2 _o	Drift	
31 October	Q	0730	1 November		1900	1-	Reg	
7 November storm		0830	9 November		0800	2+	Drift	Follows geomagnetic
21 December	Q	1530	22 December		1600	1+	Reg	
28 December		1600	29 December		1600	2+	Drift	

* Condition:

- QQ One of five quietest days in month
- Q One of ten quietest days in month
- D One of five most disturbed days in month.

† Observations:

Data gathered and analyzed as described in Lincoln Laboratory Technical Report 477 (Ref. 25).
Reg = Regular; Drift = Drift Measurement.

was destroyed by a computer malfunction and only 11 hours of useful data were obtained. We have discarded these results in what follows. Likewise, a second short run (5 hours) on 24 November has not been included.

Beginning in 1968, a number of observations were scheduled to coincide with passes of Alouette II at the request of scientists at the NASA Goddard Space Flight Center. During 1970, there were many close passes of the satellites ISIS I, OGO VI, and Alouette II by Millstone Hill. Where possible, the regular monthly operations were scheduled to coincide with favorable passes, and Table V lists the satellite overflights of Millstone that occurred in routine operations scheduled with this in mind. The primary purpose of the measurements made during the passes of

Date	Time (EST)	Height (km)	Satellite	Date	Time (EST)	Height (km)	Satellite
6 January	1544	1060	OGO VI	18 May	1809	576	Alouette II
7 January	0207	630	OGO VI	18 May	2233	850	OGO VI
20 January	1426	870	OGO VI	10 June	0632	470	OGO VI
21 January	0048	450	OGO VI	10 June	1921	505	OGO VI
17 February	1000	470	OGO VI	23 June	0508	645	OGO VI
23 February	2025	615	OGO VI	23 June	1757	405	OGO VI
24 February	0914	420	OGO VI	8 July	0208	560	OGO VI
17 March	1709	950	OGO VI	18 July	1213	545	OGO VI
23 March	1709	1010	OGO VI	19 July	0211	1000	OGO VI
24 March	0557	570	OGO VI	25 August	1055	1000	OGO VI
24 March	1620	1020	OGO VI	31 August	2001	545	OGO VI
14 April	1350	950	OGO VI	29 September	0500	560	OGO VI
14 April	2320	780	Alouette II	10 October	1532	495	OGO VI
15 April	0232	690	ISIS I	13 October	1406	590	OGO VI
15 April	0236	980	OGO VI	14 October	0254	400	OGO VI
28 April	1201	720	OGO VI	30 October	1154	860	OGO VI
28 April	2329	1075	OGO VI	31 October	1230	860	OGO VI
12 May	1859	525	Alouette II	1 November	1134	895	OGO VI
12 May	2246	930	OGO VI				

OGO VI was to permit comparisons of electron and ion temperatures deduced by remote sounding and *in situ* probe measurements, and most of the results of this exercise have been reported.²⁶

During 1969, the first attempts were made to conduct coordinated measurements with Dr. J. Noxon (Harvard University) who, at that time, was measuring the 5577 Å, 6300 Å, and other emission lines from the night sky, at the Blue Hills Observatory, Boston, Massachusetts. The principal objective of this joint effort was to observe a stable auroral red (SAR)-arc, and determine if the 6300 Å emission could be accounted for in terms of impact excitation due to the

high temperature of the electrons. In this the effort proved to be disappointing, as no overhead SAR-arcs were observed. However, on three occasions (one in 1970) Dr. J. Noxon alerted us to the presence of low-latitude auroral activity and valuable optical and radar results were gathered simultaneously. These joint observations have been the subject of a separate report.²⁷

D. Data Analysis

Beginning in July 1968, the results were gathered in a manner that placed together all the quantities of interest on a single data tape so that complete machine reduction became possible. The computer programs employed are described in Ref. 25. Basically, the electron-density profiles were obtained in a way that: (1) combined measurements made with the three pulse lengths, (2) removed spurious echoes due to satellites, (3) adjusted the absolute value to yield the correct value of $N_{\text{max}} F2$ as measured on the ionosonde, and (4) removed the dependence on altitude variations of T_e/T_i , and on the Debye length. This profile was available as a graph plotted by a Calcomp plotter, and on a printout as $\log_{10} N_e$ vs altitude.²⁵ Estimates of T_e and T_i also were provided on plots and on the printout. The values of T_e were corrected for the effects of the changing Debye length with altitude.²⁵

It should be noted that the estimates of T_e and T_i were obtained by extracting two parameters from the measured spectra, viz., the half-peak-power width (proportional to T_e) and the ratio of the peak power in the wings to that at the center frequency (proportional to T_e/T_i). These values were inserted into analytical expressions that had been obtained to represent T_e and T_i , as functions of the ratio and width through scaling theoretical power spectra computed assuming only O^+ ions are present and that the Debye length is extremely small. In computing these theoretical power spectra, the effects of the transmitter pulse and the finite width of the filters in distorting the measurement were included.

To correct the estimate of the electron temperature $T_{e_{\text{obs}}}$ obtained in the above manner for the effect of the change in the Debye length on the spectrum, use was made of the expression²⁵

$$T_e = T_{e_{\text{obs}}} \left(1 - \frac{1.62 \times T_{e_{\text{obs}}}}{N_e} \right)^{-1} .$$

Unfortunately, this expression holds only so long as the second term in the parentheses remains ≤ 0.3 . At high altitudes, $T_{e_{\text{obs}}}$ may be of the order of 2000 to 3000°K and the correction then becomes inaccurate as N_e approaches 10^4 el/cm³. Thus, the electron temperatures obtained near or above this level are believed to be overestimates.

The results presented in this report extend only to 900 km altitude and hence, as a rule, the daytime temperatures do not suffer from this source of error. At night, the echoes returned from altitudes where the electron density is less than 10^4 el/cm³ are frequently so weak that the temperatures obtained from the spectra exhibit considerable scatter and are not reliable. The automatic data compression scheme described in Sec. III usually eliminates such data points so that the contour diagrams for the electron and ion temperatures generally are left blank in these regions.

A second source of error in the temperature estimates obtained at high altitudes has been the neglect of the presence of H^+ ions in the interpretation of the spectra. Recently, a computer program has been written that permits these spectra to be reanalyzed to yield estimates of T_e , T_i .

and the ratio of O^+ to H^+ ions.²⁸ This program attempts to match the observed spectra computed for various temperatures and composition ratios. Unfortunately, the program is quite slow and requires several hours of computer time (using the Millstone Hill XDS 9300 computer) to analyze a single day's measurements. Accordingly, no attempt has been made to reanalyze all the 1970 results. However, based on the results obtained for five days in 1969,¹⁶ it appears that the temperatures below 900 km will be in error only for a short interval between midnight and sunrise and that the error will be confined largely to altitudes above 750 km. In practice, this is also the region that is suspect because of the large correction that must be made for the effect of the Debye length.

A third source of error in the temperature results is introduced (chiefly at low altitudes) by the imperfect match provided by the filters used to measure the spectra when transmitting 0.5-msec pulses (B-mode). Empirical corrections were derived to compensate for this effect⁷ and the ANALYSIS program modified to print out both the corrected and uncorrected results.

The ANALYSIS program provides a data plotting tape from which plots of N_e , T_e , and T_i vs altitude are generated on a Calcomp plotter. To reduce the large number of independent profiles as well as smooth the data with respect to time (and thereby reduce some of the scatter in the measurements), it has been the custom to prepare diagrams which show, as a function of altitude and time, the variation of contours of constant density and temperature. As described previously,⁴ the first step in this process is to transfer from the vertical profiles sets of points representing particular values (of density or temperature) to their correct locations in height and time on the contour plot. These points are next connected by straight lines. The second step is to trace this "coarse" diagram using a French curve to best follow the trend of each contour. In this process the random errors from profile to profile are reduced, albeit with some smoothing of real variations.

This last step is somewhat subjective and the presence of true fluctuations from cycle to cycle introduced, for example, by TIDs makes it difficult to be consistent in the amount of smoothing one introduces.

This method of data presentation also has the drawback that it renders the results unsuited to machine processing. Consequently, we have frequently been asked to provide other users with copies of the ANALYSIS printouts. That is, although height profiles of a given parameter (or the time variation of a parameter at a given height) can be recovered from the contour diagrams, some detail is invariably lost and the operation is tedious and time-consuming.

In 1970, the hand production of contour diagrams was superseded by a method of data compression in which the results are represented in analytical form by fitting a two-dimensional polynomial expression. This is performed by the XDS 9300 computer using a program called INSCON. This is a flexible, modular FORTRAN program which also prepares contour plots from the fits and punches the parameters of the fit on IBM cards so that the smoothed results may be recovered later. INSCON is described in the next section.

III. DATA REDUCTION

A. Preparation of the Data

Prior to fitting an analytical function to the derived value of N_e , T_e , T_i , or v_z , an effort is made to eliminate bad points and assure that there are sufficient points in each height-time cell for the fit to be meaningful. INSCON reads the one-pulse (or two-pulse) data from the

master tape written by either the ANALYSIS or MUPMAP programs used to analyze the raw data.

One-pulse electron-density data are read from the Analysis Master Tape by a subroutine. These data are at altitudes ranging from 161 to 950 km. After these data have been read, they are filtered to remove bad points. *Density estimates between 161 and 229 km are first examined for contamination by clutter. These data points are required to decrease monotonically with decreasing altitude. If this condition is not satisfied at some altitude, the data from that point down are rejected. Since the polynomial fitting procedure requires initial guesses for the rejected data, the rejected densities are estimated by extrapolating linearly downward from the two lowest accepted points. Data above 400 km are next examined to insure that the density decreases monotonically with height. If the density at any height is greater than at the next lowest height, it is rejected. Rejected densities are estimated to be equal to the next lower acceptable point. All previously accepted data are now checked to insure that $2.5 \leq \log_{10} (N_e) \leq 8.0$. If this condition is not satisfied, all data at this time are now rejected.*

A "box score" is now developed. This is an $M \times N$ table, where M is the number of experiment times and N is the number of experiment altitudes. The tabulated number is 1 if the corresponding datum has been accepted and 0 if the corresponding datum has been rejected. The box score is next examined to determine which regions contain too many rejected points for the polynomial fit to be trustworthy. All box-score entries in regions where the fit is expected to be good are set equal to 1. The table is then examined to determine if there are any time gaps of more than two hours. If so, the tabular entries flanking the time gap are set equal to 2. The resulting status table is then printed.

One-pulse electron temperature and ion temperature data are next read from the Analysis Master Tape by another subroutine. These data are at 75-km intervals from 225 to 1125 km. INSCON uses B-mode (0.5-msec pulse) data at 225, 300, and 375 km and C-mode data from 450 to 1125 km. If there is more than one set of C-mode observations, the data at each height are averaged. No account is taken of the variation in returned power from different points within the scattering volume. A procedure for correcting for this effect has been developed that entails integrating the analytic expressions obtained from the INSCON fit (Sec. III-G).

After the temperatures at each experimental time have been read from the Analysis Master Tape, the B-mode data are empirically corrected for known systematic errors.⁷ The data are then filtered to remove bad points. The corrected B-mode data are first compared with the C-mode data to insure that the data from the two modes are reasonably consistent. The ion temperatures at 450 and 525 km are averaged for each mode. If the two averages differ by more than 20 percent, all three B-mode temperatures are rejected. The data also are checked to insure that all temperatures above 825 km are greater than 1000°K and that no temperatures are greater than 6000°K.

The rejected data are now estimated by passing a cubic through the nearest five accepted points. An "anchor point" is then added at 150 km by extrapolating exponentially downward from the temperatures at 225 and 300 km. This anchor is designed to prevent unreasonable behavior of the fit near 225 km and not to provide a realistic estimate of the temperature below 225 km.

The data at 975, 1050, and 1125 km are now replaced by a linear fit. This procedure helps to keep the final INSCON fit reasonable at high altitudes. Finally, all temperatures are checked to insure that they are less than 6000°K. As with one-pulse electron densities, the box-score and status table are now determined and printed.

One-pulse vertical ion drift data are read from the Analysis Master Tape. These data are at 75-km intervals from 225 and 1125 km. As with one-pulse temperature data, the velocities at 225, 300, and 375 km are B-mode data, the velocities above 300 km are C-mode data, and all altitudes are "nominal" altitudes.

After the velocities at each experimental time have been read from the Analysis Master Tape, they are filtered to remove bad points. First, the velocity at any time and altitude is rejected if the temperature data at that point do not lie within the bounds specified in the discussion of one-pulse temperatures. Next, the values for any missing points are estimated by passing a straight line through the four good velocities nearest the rejected value. The velocities at 975, 1050, and 1125 km are replaced by values obtained by fitting a straight line to the velocities between 750 and 1125 km. Finally, the velocity at 900 km is replaced by a value obtained by passing a parabola through the velocities between 750 and 1050 km. This high-altitude smoothing helps to keep the final INSCON fit reasonable at high altitudes. As with one-pulse electron densities and temperatures, the box-score and status table are now determined and printed.

B. Least-Mean-Squares Polynomial Fitting

The algorithm used by INSCON to fit a two-dimensional polynomial to the input data is discussed in this section. This procedure is identical for all types of input data. A good reference on least-squares estimation is Hauck's "Foundations for Estimation by the Method of Least Squares."²⁹

Consider m experimental data z_1, z_2, \dots, z_m , each of which corresponds to a particular value x_1, x_2, \dots, x_m of the variable x . We wish to find coefficients b_j which minimize the sum of squares

$$S = \sum_{i=1}^m \left[z_i - \sum_{j=1}^M b_j P_j(x_i) \right]^2 \quad (1)$$

where the $P_j(x_i)$ are M linearly independent functions of x_i . Defining $P_{ij} = P_j(x_i)$, differentiating Eq. (1) with respect to b_k and setting $\partial S / \partial b_k = 0$, one arrives at the normal equations,

$$\sum_{j=1}^M b_j \sum_{i=1}^m P_{ik} P_{ij} = \sum_{i=1}^m P_{ik} z_i \quad (2)$$

To solve this equation for the b_j , one must invert the matrix $\underline{P}^t \underline{P}$ where

$$\underline{P} = \begin{bmatrix} P_{11} & \cdots & P_{1M} \\ \cdot & & \cdot \\ \cdot & & \cdot \\ \cdot & & \cdot \\ P_{m1} & \cdots & P_{mM} \end{bmatrix} .$$

If M is large, the inversion of \underline{P} may be very difficult. In INSCON, M may be as large as 1024. For most choices of the functions $P_j(x)$, the inversion of $\underline{P}^t \underline{P}$ would then be completely

impractical. Suppose, however, that there exists a set of P_j which satisfies the orthonormality condition for the data set under consideration, that is:

$$\sum_{i=1}^m P_{ik} P_{ij} = \delta_{kj} \begin{cases} \delta_{kj} = 1 & , & k = j \\ \delta_{kj} = 0 & , & k \neq j \end{cases} \quad (4)$$

In this special case, the solution of the normal equations is simply

$$b_j = \sum_{i=1}^m P_{ij} z_i \quad (5)$$

In general, given a complete, linearly independent set of functions $P_{j_1}(x)$, a complete, linearly independent and unique orthonormal set may be derived from the $P_{j_1}(x)$ by means of the Gram-Schmidt orthogonalization procedure. If the P_{j_1} are polynomials in x , there also exists a recursion relation for the orthonormal P_j , namely

$$P_j(x) = (x - \gamma_j) P_{j-1}(x) - \delta_j P_{j-2}(x) \quad j = 1, 2, \dots, n$$

with

$$\begin{aligned} P_{-1}(x) &= 0 \\ P_0(x) &= 1 \end{aligned} \quad (6)$$

and

$$\begin{aligned} \gamma_j &= \frac{\sum_{i=1}^m x_i P_{i,j-1}^2}{\sum_{i=1}^m P_{i,j-1}^2} \\ \delta_j &= \frac{\sum_{i=1}^m x_i P_{i,j-1} P_{i,j-2}}{\sum_{i=1}^m P_{i,j-2}^2} \end{aligned}$$

So far we have assumed that the data z_i are functions of a single parameter x_i . In fact, INSCON deals with data which are functions of two variables, time and altitude. Consider then, two-dimensional polynomials in x and y . Equations (2) through (5) are still valid if i is assumed to run over all experimental points and j runs over all combinations of the one-dimensional polynomials in x and y . For a general data set, there is no recursion relation corresponding to Eq. (6). However, if the data lie on a rectangular grid, the required orthonormal polynomials are simply the products of the one-dimensional orthonormal polynomials given in Eq. (6). That is, if

$$\sum_{i=1}^m P_j(x_i) P_k(x_i) = \delta_{kj} \quad x_i = x_1, x_2, \dots, x_m$$

and

$$\sum_{i=1}^n Q_j(y_i) Q_k(y_i) = \delta_{kj} \quad y_i = y_1, y_2, \dots, y_n \quad (7)$$

then

$$\sum_{i=1}^m \sum_{i'=1}^n P_j(x_i) P_k(x_{i'}) Q_{j'}(y_{i'}) Q_{k'}(y_{i'}) = \delta_{kj} \delta_{k'j'}$$

and the desired two-dimensional orthonormal polynomials are

$$T_{jj'}(x_i, y_{i'}) = P_j(x_i) Q_{j'}(y_{i'}) \quad j = 1, M; j' = 1, N \quad (8)$$

The $M \times N$ term INSCON polynomial will then be

$$V(x_i, y_{i'}) = \sum_{j=1}^M \sum_{j'=1}^N b_{jj'} T_{jj'}(x_i, y_{i'}) \quad (9)$$

The method described above is used in INSCON. The independent variables x and y are time and altitude, respectively. The experimental measurements z may be electron density, electron temperature, ion temperature, etc. INSCON first uses Eq. (6) to calculate one-dimensional polynomials which are orthonormal over the experimental times and altitudes, respectively. These polynomials are then combined as in Eq. (8) to form two-dimensional orthonormal polynomials. Finally, coefficients b_j are evaluated by means of Eq. (5).

In practice, good data may not be present at certain times and altitudes. In this case Eq. (5) is invalid. However, the method may still be used by applying Eq. (5) iteratively. For the first iteration, a first guess based on surrounding data is used in place of the missing datum. During subsequent iterations, the fit value from the preceding iteration is used as an approximation to the missing datum. This procedure usually converges very quickly.

A further complication is the deterioration of the fit near its end points, e.g., near the lower and upper altitude limits and the earliest and latest experimental times. This is due to the well-known Runge phenomenon³⁰ which often afflicts high-order polynomial interpolation and least-squares fitting. Ideally, one would like to use a basis set less subject to such difficulties; for example, piecewise polynomial functions.³¹ Unfortunately, the matrix inversion required, were such a basis set to be adopted, would be too time consuming to be practical.

An alternative approach, which has been implemented in INSCON, is the addition of "anchor points" beyond the end points of the experimental data. In general, anchor data are added at two times preceding the earliest experimental time and at two times following the latest time. The datum at each of these points is estimated by least-squares linear extrapolation of the three data points nearest in time and at the same altitude as the anchor points. The procedure used to anchor the data near the altitude limits of the experimental points varies with the type of data. In some cases additional anchor points are added by extrapolating from nearby experimental data. For example, anchor points at 150 km are used in the fits to one-pulse T_e , T_i , and v_z . On the other hand, at the upper altitude limit of these parameters additional data points are not added. Instead, the data at the three highest altitudes (975, 1050, and 1125 km) are smoothed before the INSCON polynomial is fit to the data. In any event, while the fit beyond the actual

data may behave reasonably due to the anchor points, it is not to be trusted. INSCON does not plot contours beyond the limits of the actual experimental data, and if an attempt is made to recover data in these regions by means of the recovery routines described in Sec. III-E, zero is returned.

For the INSCON fits to be really useful, the uncertainty of the polynomial must be known. This may easily be calculated from the punched INSCON output parameters. In general, the error bar on the polynomial fit at a given time and altitude will be less than the error bar on the corresponding experimental point.

Suppose that the variance σ^2 of the experimental data is known. Then given the INSCON error matrix $\mathbb{N} = (\underline{\mathbf{T}} \underline{\mathbf{T}})^{-1}$, the uncertainties in the polynomial coefficients b_{jj} may be calculated from

$$\Delta b_{jj'}^2 = \mathbb{N}_{jj',jj'} \sigma^2 \quad (10)$$

The error in the INSCON fit values $V(x_i, y_i)$ is then given by the well-known error propagation formula

$$\Delta V(x_i, y_i)^2 = \sum_{i=1}^m \sum_{i'=1}^n \left[\frac{\partial V(x_i, y_{i'})}{\partial b_{jj'}} \right]^2 \Delta b_{jj'}^2 \quad (11)$$

The variance of the experimental data may be estimated from the scatter of the data about the INSCON fit. The INSCON output deck includes the time averaged square deviation $s_{i'}^2$ of the experimental points from the INSCON fit at each experimental altitude. This gives a reasonable estimate of the variance at any point, since the variance is much more dependent on altitude than time. We can then estimate $\sigma_{i'}^2$ by

$$\sigma_{i'}^2 = \frac{m s_{i'}^2}{m - M} \quad (12)$$

Of course, another estimate of the variation of σ could be used in Eq. (10) based, for example, on the signal-to-noise ratio.

C. Contour Plots

After the least-squares fit to a data set has been calculated, a plotting subroutine is loaded into the computer, overlaying the data preparation subroutine. Separate subroutines exist for the types of data currently being routinely processed by INSCON. The contour plotting routines first evaluate the polynomial fit on a 121 (time) \times 37 (altitude) grid. A subroutine ZCONTR is then called to find contour paths through the table. Labeling, the separation of the contours, the range of the contours, and the altitude range are fixed for each of the conventional data types. All contour diagrams have been compared with those generated by hand for 1970. In general, the agreement appears to be good, but there are differences apparently stemming from the different amounts of smoothing applied in the two methods.

D. Punched Card and Magnetic Tape Output

For each polynomial fit calculated, INSCON punches a deck of cards from which the fit may later be recovered. These cards are a convenient medium for the external distribution of selected fits, but are somewhat unwieldy in applications which require the routine processing of many INSCON fits. Consequently, new INSCON decks are transferred to a magnetic tape known

as the CONSUM tape by means of the FORTRAN program CONSUM. Each deck is stored on this tape as one long (6949 word) record. The first two cards of each INSCON deck contain two numbers (FIT NO. and KDAT) which uniquely specify the fit. CONSUM first reads the new INSCON deck and stores them on tape. A new CONSUM tape is then created from the card images of the new decks and the old CONSUM tape. Each new fit is inserted in the new tape in proper chronological order. If a new deck has the same two identification numbers as a fit already on the old CONSUM tape, the old fit is replaced by the new fit. Finally, a summary of the new tape is printed.

Several years' data may be stored on a single magnetic tape. This tape may be used in two ways. First, if a copy of a particular fit or fits is needed for external distribution, the corresponding FIT NO.s and KDATs may be punched on IBM cards and input to CONSUM. CONSUM then scans the CONSUM tape and punches copies of the specified decks.

The INSCON summary table also includes test values which are used to assure that the parameters on the CONSUM tape indeed correspond to the parameters calculated by INSCON. Each time CONSUM generates a new summary tape, it evaluates the INSCON polynomial at the earliest experimental time and lowest altitude. This value is then printed in the INSCON summary table. Comparison with the original INSCON printed output ensures the integrity of the parameter set.

E. Recovery of Height Profiles or Time Variations

The INSCON fit to any data set may be recovered at a later time by means of the FORTRAN recovery subroutines RCVR, RCVR1 and RCVRP. Given the INSCON fit parameters, these subroutines recover the polynomial representation of the data at any time and altitude within the range of the data. The user of these routines is thereby relieved of the necessity of knowing in detail the meaning of the INSCON fit parameters.

Given the INSCON fit parameters, the time, and the altitude, RCVR returns the value of the polynomial fit at the specified time and altitude. The fit parameters are normally transferred to RCVR in a labeled common block, while the time, altitude, and fit value are transferred via the RCVR argument list. If an attempt is made to recover a fit value outside the time or altitude limits of the experimental data, RCVR returns 0. If an attempt is made to recover a fit value P in a region in which INSCON determined that the quality of the fit was questionable, RCVR returns $-P$. The user must then decide whether to risk using this value, which may in fact be a reasonable interpolated value. This procedure for indicating questionable points requires that the INSCON polynomial be positive definite. To ensure this, data which may be negative are shifted upward by a constant. For example, instead of fitting the vertical ion drift v_z directly, INSCON fits $v_z + 300$ m/sec. This shift is included among the INSCON fit parameters, but must be applied by the user in his applications program. RCVR1 is similar to RCVR, but in addition to the fit value, RCVR1 returns the time and altitude derivatives of the polynomial fit.

RCVRP may be used if the user wants a periodic approximation to the polynomial fit rather than the fit itself. This has proved useful in several applications. In addition to the time and altitude, the user must specify the 24-hour period on which the periodic approximation is to be based. RCVRP then returns values for the fit quantity and its time and altitude derivatives based on values RCVRP obtains from RCVR1. If the experimental data span is less than 20 hours, RCVRP makes no attempt to recover values within the gap; instead, zeroes are returned. If the

data span is more than 24 hours, RCVRP subtracts a linear trend from all recovered data. If the data span is between 20 and 24 hours, the Millstone cubic spline interpolation routine SPLN3A is used to calculate interpolated values of Q , $\partial Q/\partial t$, and $\partial^2 Q/\partial h^2$ within the gap.

Two FORTRAN subroutines are available to input INSCON fit parameters to a users application program: "CREAD" reads INSCON card decks and stores the fit parameters in labeled common storage; "TREAD" searches the CONSUM tape (Sec. D) for a specified fit and stores these parameters in labeled common storage. By using one of the input routines together with one of the recovery routines, the user is able to recover INSCON fit values without having detailed knowledge of the INSCON fit parameters or the way in which they are stored on cards or tape. Detailed instructions for using these routines have been made available to some users and are contained in the Appendix of this report.

F. Vertical Gradients

By using the FORTRAN subroutines RCVR, RCVR1 and RCVRP, the INSCON fit values and their first derivatives in altitude and time may be recovered from the fit parameters punched on cards by INSCON. The recovered values may then be combined to form derived quantities such as particle or heat fluxes. While, in principle, this is very simple, there are some fairly substantial practical difficulties stemming primarily from the large amount of information contained in each set of INSCON cards. Each fit requires 6949 words of storage in the XDS 9300. As a consequence, at Millstone, programs using INSCON results usually make extensive use of the rapid access drum (RAD), and must also be segmented.

In order to make the INSCON fits more useful in view of these difficulties, a general-purpose FORTRAN program (DERQ) to calculate derived quantities has been written. All segmentation, RAD usage, and major bookkeeping are handled by general-purpose routines. To calculate a specific derived quantity or set of quantities, the user need only supply a set of data cards and a subroutine to calculate the desired quantities.

In a single run of DERQ, up to 8 different derived quantities DQ may be calculated at as many as 32 altitudes and 64 times. The DQs may be functions of as many as 16 quantities Q , $\partial Q/\partial t$, $\partial Q/\partial h$, or $\partial^2 Q/\partial h^2$, where Q is any quantity for which an INSCON fit exists. The necessary INSCON cards may either be read in directly as cards or read from the INSCON summary tape on which all INSCON results are ultimately stored. In the latter case, the user need only specify the unique fit number which is assigned to each INSCON fit and which is listed on the summary printed after each update of the INSCON summary tape.

DERQ automatically writes an output tape which may later be used as input to INSCON if INSCON fits to the DQs are wanted. If desired, contour plots of the DQs are also automatically plotted by DERQ. These plots are produced by direct interpolation in the table of DQs calculated by DERQ and no INSCON type fit to the DQs is calculated.

G. Weighted Mean Height Correction

Measurements of electron and ion temperatures made with single long pulses represent a weighted average of the properties of the plasma illuminated by the pulse during the course of the measurement. At Millstone, a bank of filters matched to the pulse length T sec is used to explore the spectra. The return from a single electron in the ionosphere would cause the power at the output of the filter to rise linearly in a time T from zero to a peak and then fall to zero again in an equal time. Sampling the filters at any time t after the pulse has been transmitted

will permit the full power to be sampled from those electrons lying at a height $z_0 = ct/2$. Electrons at other altitudes z will contribute less power, i.e., their contribution will be weighted by the factor

$$W = \left(1 - \left|\frac{z - z_0}{w}\right|\right) \quad (13a)$$

$$= 0 \quad z_0 - w \leq z \leq z_0 + w \quad (13b)$$

where $w = cT/2$ is the instantaneous height interval occupied by the pulse. The electrons distributed over the altitude interval ($z_0 - w \leq z \leq z_0 + w$) that contribute to the estimate, yield an echo power $P(z)$ which depends upon their number density N_e , height z , and electron-to-ion temperature ratio, approximately as

$$P(z) \propto \frac{N_e}{z^2 [1 + (T_e/T_i)_z]} \quad (14)$$

Since the echo power $P(z)$ is measured in the profile measurements it is a simple matter to compute the effective or weighted height \bar{z} of the measurement

$$\bar{z} = \frac{\int_{z_0-w}^{z_0+w} W P(z) z dz}{\int_{z_0-w}^{z_0+w} W P(z) dz} \quad (15)$$

provided that $P(z)$ is known at shorter height intervals than the samples of spectra (gathered at intervals of every 75 km). Accordingly, weighted mean heights \bar{z} are computed for the 0.5- and 1.0-msec measurements from the A-mode (0.1 msec) power profile results and these are tabulated on the real-time data printout.²⁵ These values of \bar{z} typically differ from values of the nominal height $z_0 = ct/2$ by as much as 35 km for the C-mode (1 msec) results above h_{\max}^{F2} , where the N_e and z^2 terms in Eq. (14) cause less power to be returned from the higher altitudes. Thus, for precise work, allowance should be made for the difference between the nominal and effective pulse heights. This has been done in studies of the vertical particle fluxes¹⁶ but, in general, has tended to be ignored owing to the fact that the values of \bar{z} are not stored on the real-time (RETIAS) data tape.

Accordingly, one of the first applications of DERQ has been to correct the INSCON fits to one-pulse T_e , T_i , and v_z data for the inaccuracy arising from the use of nominal heights (i.e., the center of the pulse) in the initial INSCON fits. The version of DERQ which calculates this correction has been named HEQUIV. DERQ first reads the INSCON cards for N_e , T_e , T_i , and v_z . Values of these quantities are then recovered at all B- and C-mode nominal altitudes z_0 . At each experimental time, DERQ then calculates the equivalent height \bar{z} corresponding to each B- or C-mode nominal height. The relation used is

$$\bar{z} = \frac{\int_{z_0-w}^{z_0+w} W \left[\frac{N_e(z)}{1 + (T_e/T_i)_z} \right] \frac{dz}{z}}{\int_{z_0-w}^{z_0+w} W \left[\frac{N_e(z)}{1 + (T_e/T_i)_z} \right] \frac{dz}{z^2}}$$

where z_0 is the nominal height and w is 75 km for B-mode data and 150 km for C-mode data. The quadratures are performed by a cubic spline interpolation, differentiation, and integration

routine SPLN3A. This routine is always present in DERQ and has proved useful in several other versions of DERQ.

The experimental quantities T_e , T_i , and v_z are now calculated at their nominal heights z_0 by using SPLN3A to interpolate between the values recovered from the original INSCON fit, and now assumed to be the correct value at the equivalent height \bar{z} . As discussed above, DERQ produces an output tape which contains the results of these interpolations and which can be read by INSCON which then produces new fits and a new set of contour plots. All plots for T_e , T_i , and v_z given in this report are the corresponding plots after the equivalent height correction.

H. Total Electron Content

DERQ is also routinely used to calculate total electron content (TEC). This version of DERQ uses SPLN3A to integrate the measured electron density N_e from 161 to 1000 km. The results at each experimental time are then tabulated. An example of the TEC results from 23-24 March 1970 is shown in Table VI.

TABLE VI			
TOTAL ELECTRON CONTENT FOR 23-24 MARCH 1970			
DERIVED BY DERQ			
TOTAL ELECTRON CONTENT (161-1000 KM)		23-24, MAR, 1970	
EST	TOTAL CONTENT (CM-2)	EST	TOTAL CONTENT (CM-2)
1611	.34274E 14	0357	.73797E 13
1655	.33502E 14	0440	.75771E 13
1740	.30242E 14	0524	.85056E 13
1823	.26251E 14	0608	.10401E 14
1908	.22757E 14	0652	.13503E 14
1957	.20151E 14	0735	.17865E 14
2040	.18781E 14	0820	.23142E 14
2124	.17852E 14	0907	.28031E 14
2208	.17005E 14	0952	.31305E 14
2252	.15992E 14	1047	.33535E 14
2336	.14658E 14	1130	.34498E 14
0020	.13047E 14	1215	.35155E 14
0103	.11385E 14	1258	.35928E 14
0147	.98235E 13	1342	.37083E 14
0230	.85782E 13	1426	.38246E 14
0314	.77351E 13	1510	.38474E 14

I. Uncertainties

DERQ also has been used to investigate the uncertainty of quantities derived from INSCON fits. Error bars for the INSCON fits themselves may be derived as discussed in Sec. III-B. In principle, given the INSCON polynomial coefficients and their uncertainties, the uncertainty in any quantity dependent on these coefficients also may be calculated. However, this calculation will be rather complex if the quantity whose uncertainty is sought contains derivatives of the INSCON polynomial. Examples of such quantities are the protonospheric heat flux and the divergence of the ion flux. The assumptions behind the calculation might also be called into doubt since INSCON does not necessarily provide unbiased estimates of arbitrary functionals of the INSCON fits.

An alternative procedure for investigating the uncertainty of quantities derived from INSCON fits is to use DERQ to perform a simulation study. Given the known scatter S of the original experimental data about the corresponding INSCON fit, a random number generator may be used to produce simulated data sets whose scatter about the original INSCON fit has the same magnitude and altitude dependence as the original data. INSCON fits may then be calculated for each of these simulated data sets. Each of these fits is in turn used to calculate the quantity whose uncertainty is being investigated. The results of these calculations will fluctuate about the results calculated from the original INSCON fits, providing a direct measure of the uncertainty of the derived quantity. This procedure is too time-consuming to be performed for every data set. However, by carrying the calculation out for a few representative data sets, one may determine typical uncertainties for the derived quantity.

IV. RESULTS

A. Electron Density

The electron-density contours are presented in Figs. 1(a-z) for the days and times listed in Table IV. These span the height interval 160 to 900 km and the full time of each set of observations. The contours are drawn for values $\log_{10} N_e > 3.0$ at intervals of $\log_{10} N_e = 0.2$. However, values of $\log_{10} N_e \leq 4.0$ at altitudes above $h_{\max} F_2$ are not thought to be reliable.

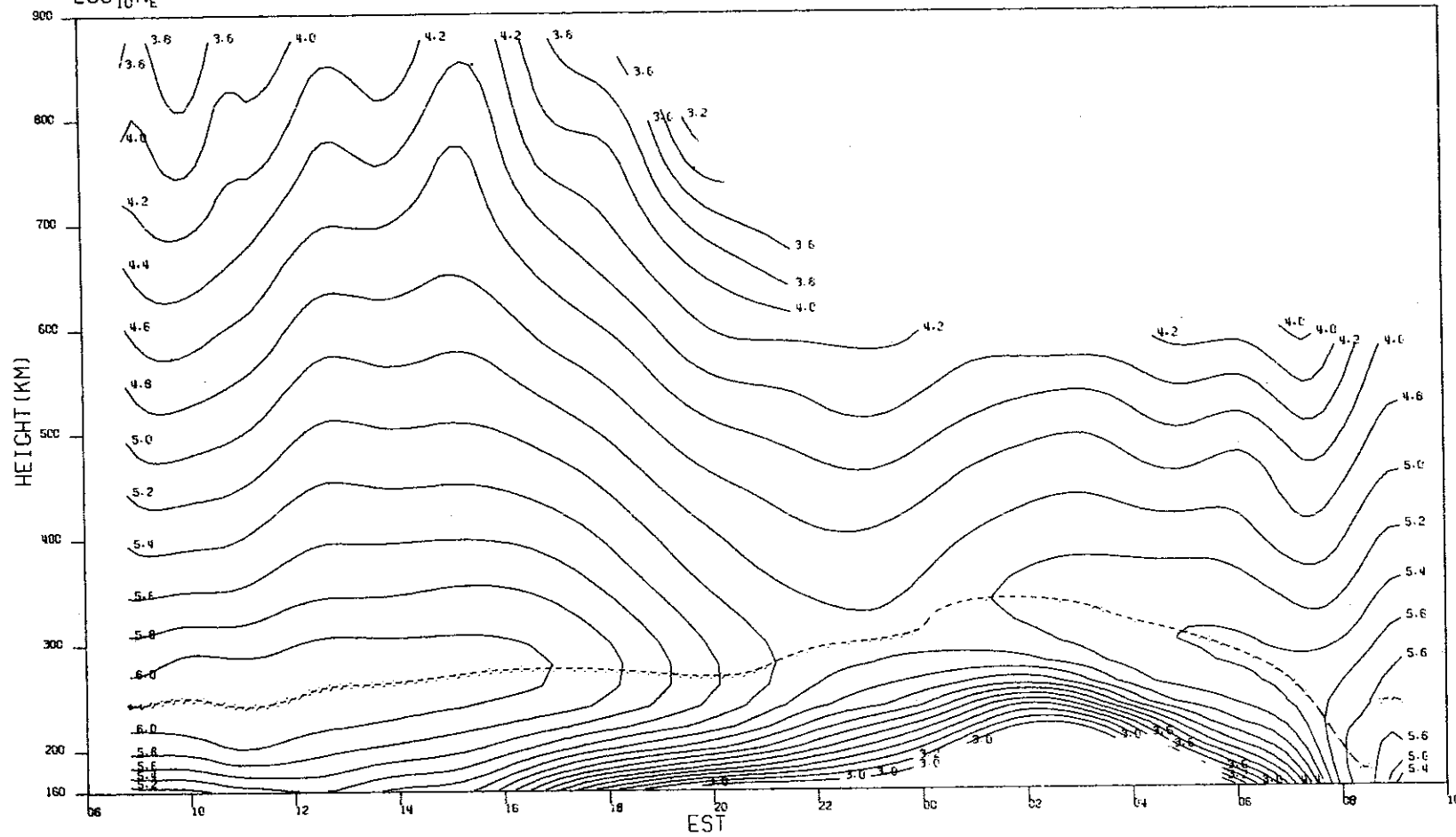
A few general comments deserve to be made concerning Figs. 1(a-z). The results for 6-7 January and 20-21 January [Figs. 1(a) and (b)] at high altitudes at night are suspect owing to the reduced antenna gain resulting from the snowstorm damage and the existence of a noisy gas discharge tube in the TR system. Also on 17-18 August [Fig. 1(p)] the results between 1700 and 2000 EST are thought to be poor either because of external interference or a receiver malfunction. Other small outages occurred, as a consequence of transmitter or computer failures, but unless these exceeded about 1 hour [as on 12-13 May - Fig. 1(j)], the INSCON program managed to smooth through the gap.

We have described previously the two types of electron-density variation seen at Millstone on quiet days.⁵⁻⁷ "Winter" type days exhibit higher daytime values of $N_{\max} F_2$ with a single peak near noon. The layer thickness is less than in summer and $h_{\max} F_2$ is typically ~240 to 260 km. Figures 1(a-c) provide good examples of this behavior. In the spring equinox, there is a rapid transition to the "summer" type of behavior, first seen in 1970 in the results obtained on 12-13 May [Fig. 1(j)]. The day-to-night variation of N_{\max} is reduced in summer, largely because the daytime values appear depressed. The peak value is usually reached near ground sunset. In summer the thickness of the layer (measured by almost any criterion) is much larger than in winter and $h_{\max} F_2$ is typically ≥ 300 km. In 1970 the transition back to winter behavior occurred around the end of September [Fig. 1(t)].

We have also described particular modifications to these basic patterns caused by magnetic storms.^{5,6} In 1970 there appear to have been no instances when the trough was observed to move to the latitude of the station in the late afternoon as seen in 1967 and 1968, i.e., around sunspot maximum. Nor were instances of abnormally large evening increase of N_{\max} observed that we have seen previously on the first day of a magnetic storm.¹⁵ However, it does appear that there was some manifestation of the lifting of the layer (induced by electric fields) that is responsible for this phenomenon on the evening of 17 August [Fig. 1(p)], as is evident by the very marked increase in $h_{\max} F_2$ seen at this time and the large upward drift velocity v_z observed.

MILLSTONE HILL
06-07, JAN, 1970
 $\text{LOG}_{10} N_e$

-9-5124

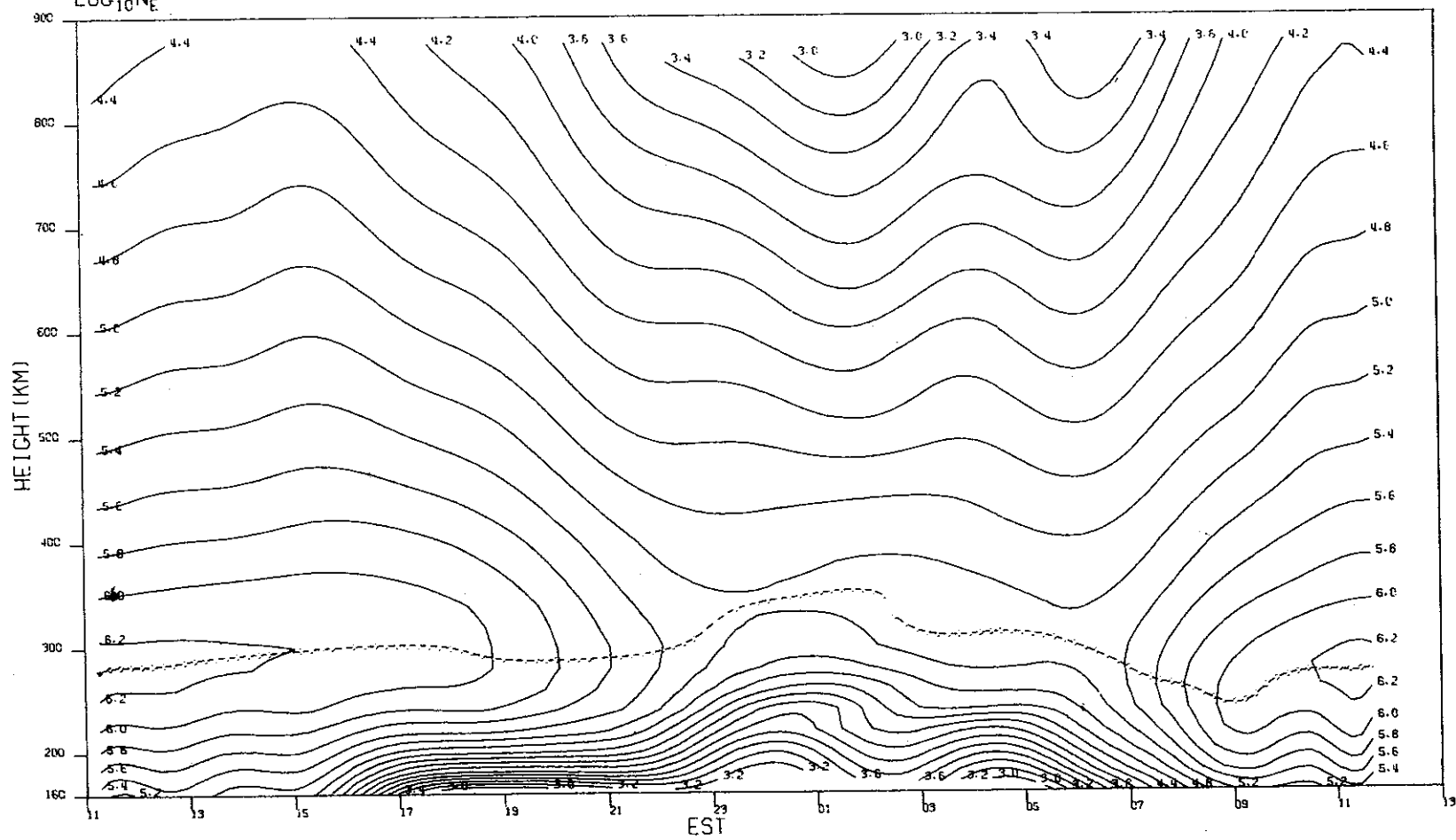


(a)

Fig. 1(a-z). Computer-drawn plots showing contours of constant $\log_{10} N_e$ (where N_e is the electron density/ cm^3) as functions of height and time for the measurements made in 1970 (Table IV).

MILLSTONE HILL
20-21, JAN. 1970
LOC₁₀N_E

-9-5125

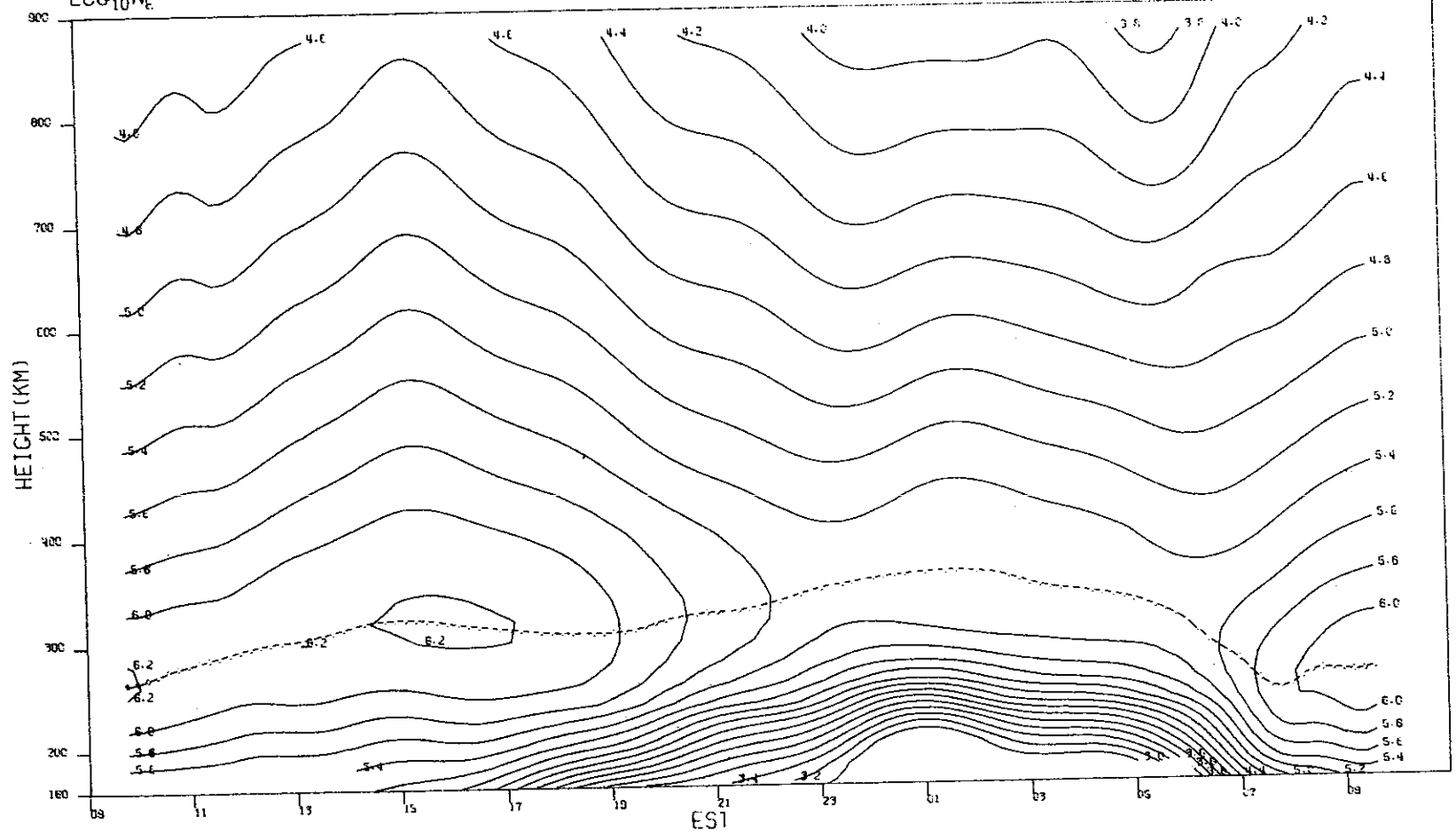


(b)

Fig. 1(a-z). Continued.

MILLSTONE HILL
17-18, FEB. 1970
 $\text{LOG}_{10} N_E$

-9-5126



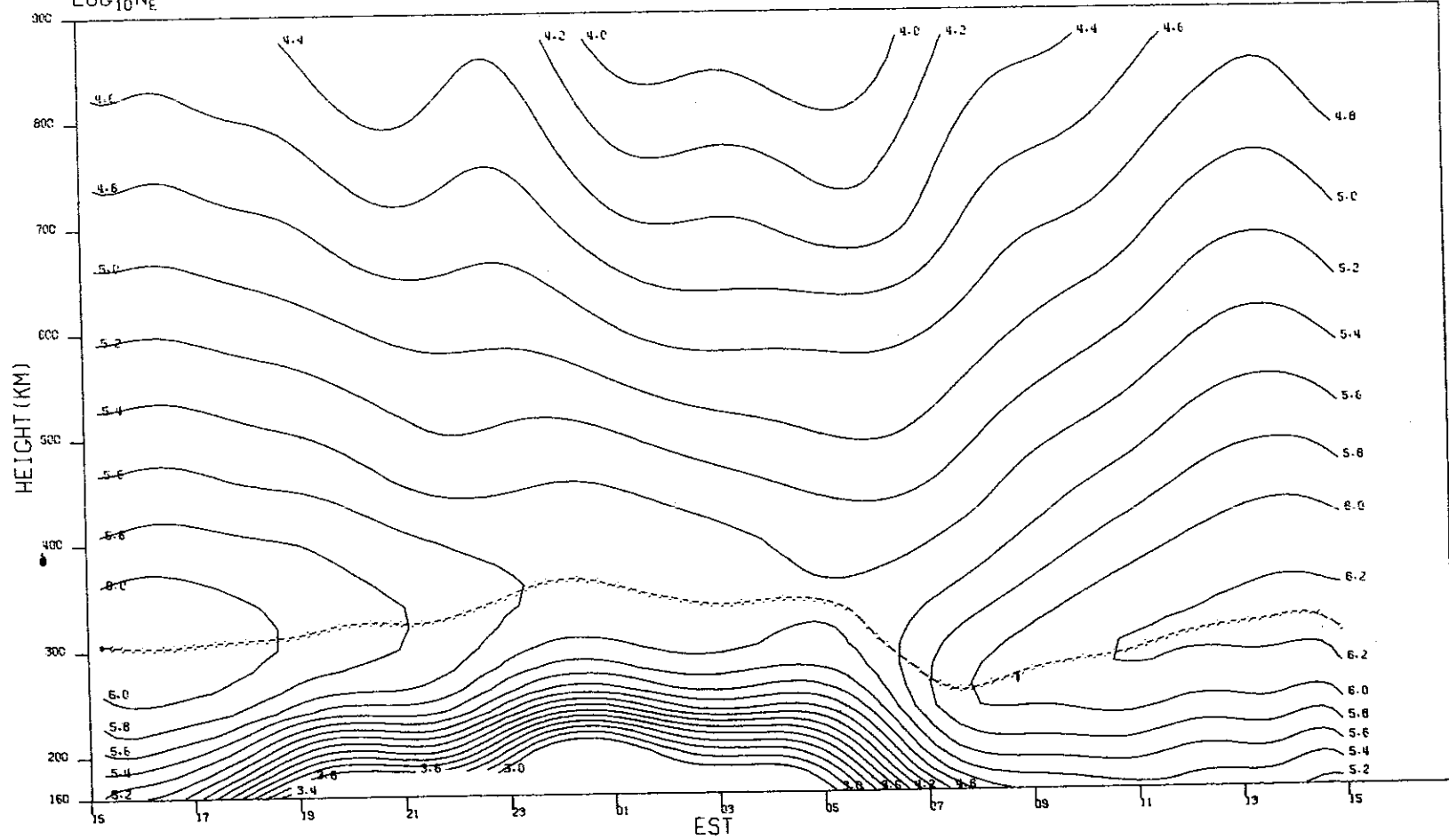
22

(c)

Fig. 1(a-z). Continued.

MILLSTONE HILL
23-24.FEB. 1970
LOG₁₀N_E

-9-5127

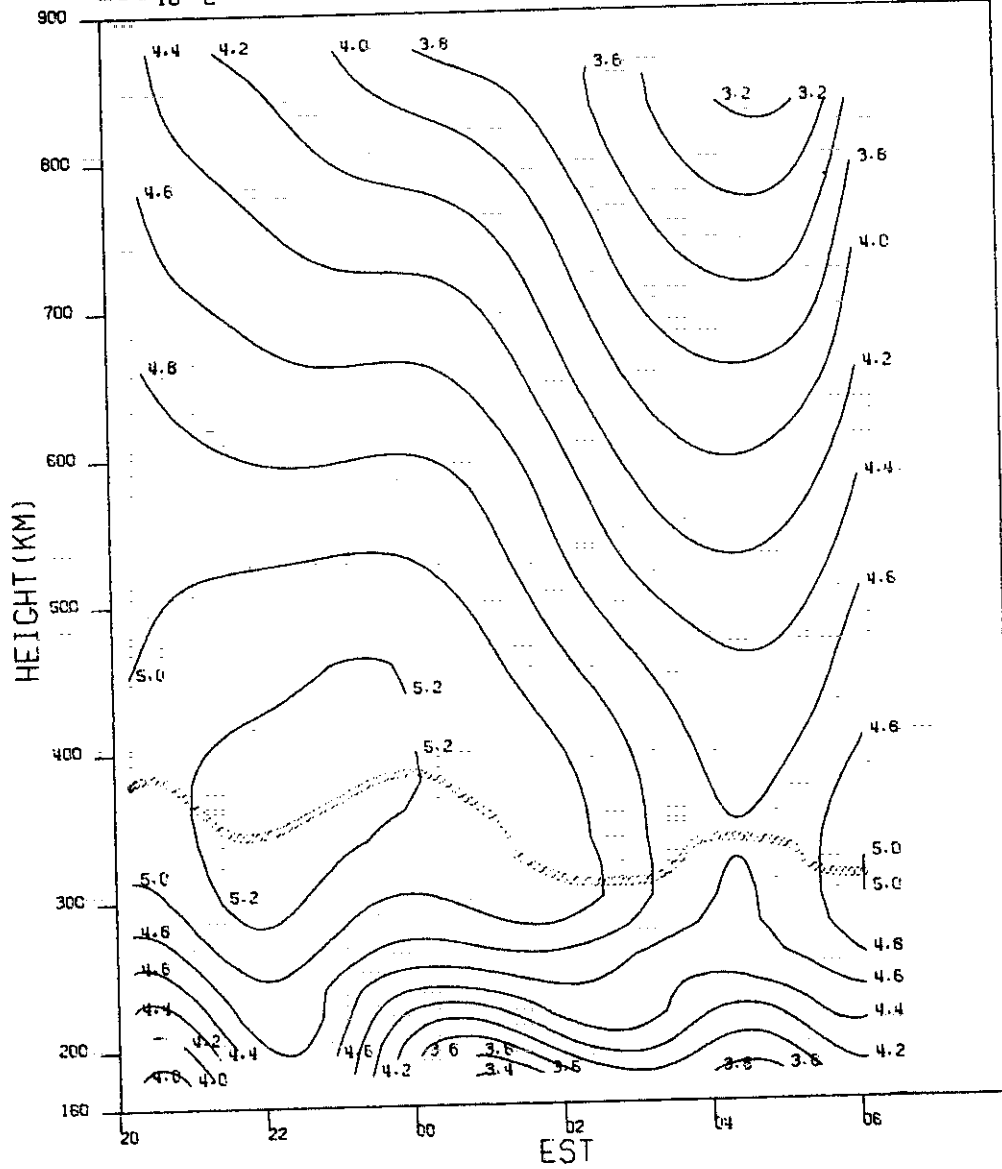


(d)

Fig. 1(a-z). Continued.

MILLSTONE HILL
09, MAR, 1970
LOG₁₀N_E

-9-5128

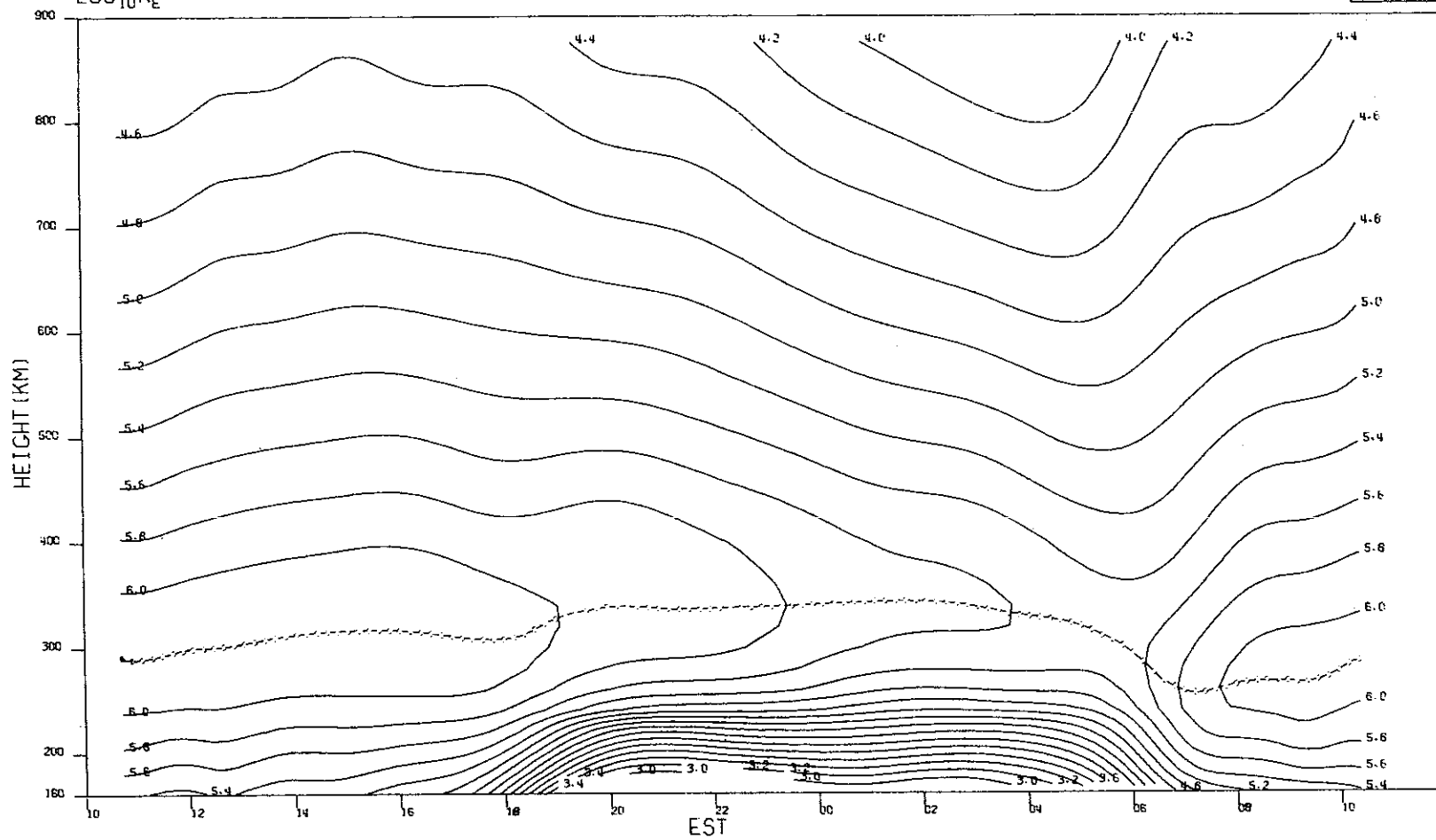


(e)

Fig. 1(a-z). Continued.

MILLSTONE HILL
17-18, MAR, 1970
 $\text{LOG}_{10} N_E$

-9-5129

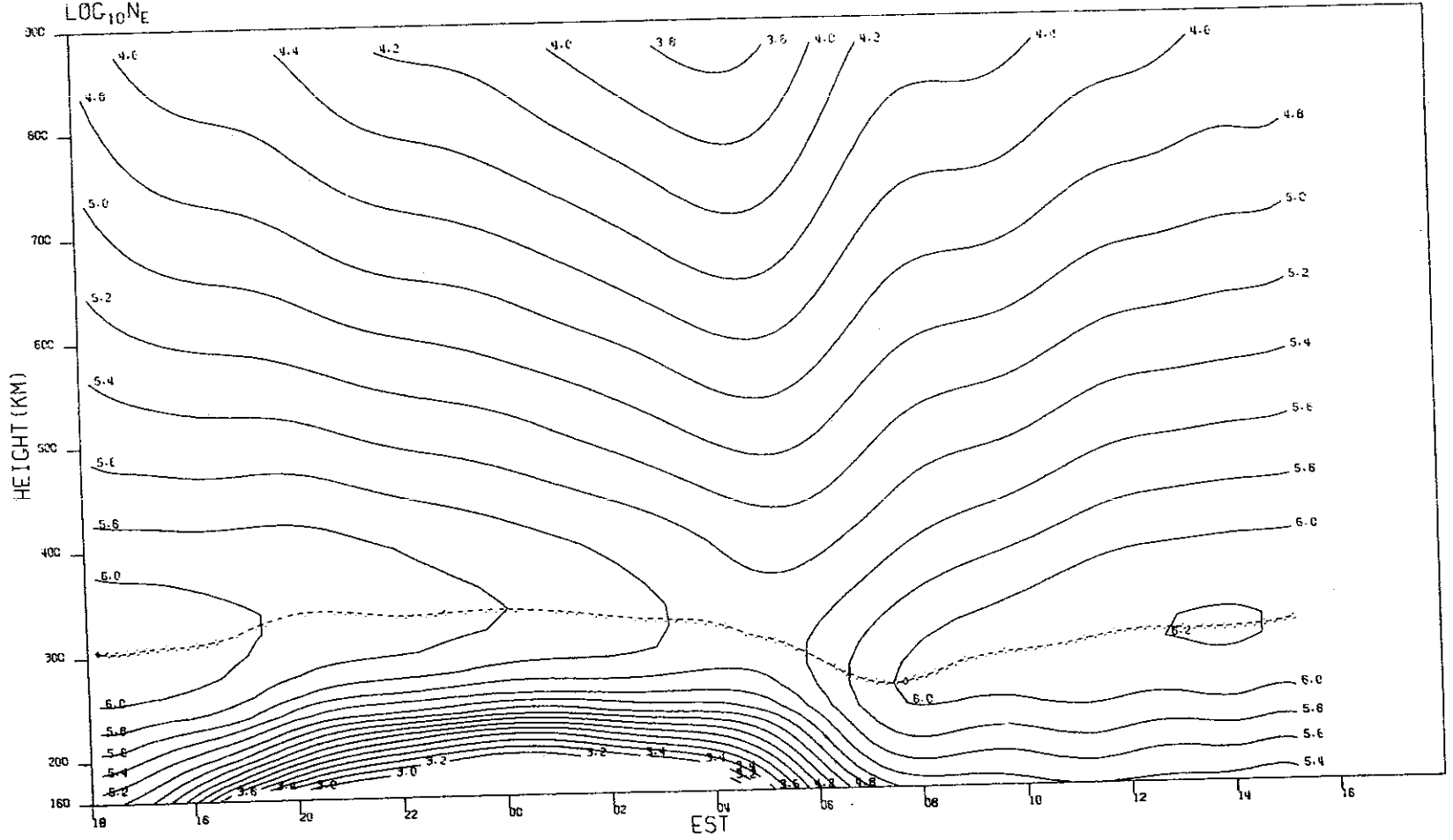


(F)

Fig. 1(a-z). Continued.

MILLSTONE HILL
23-24. MAR, 1970
LOC: 10NE

-9-5130



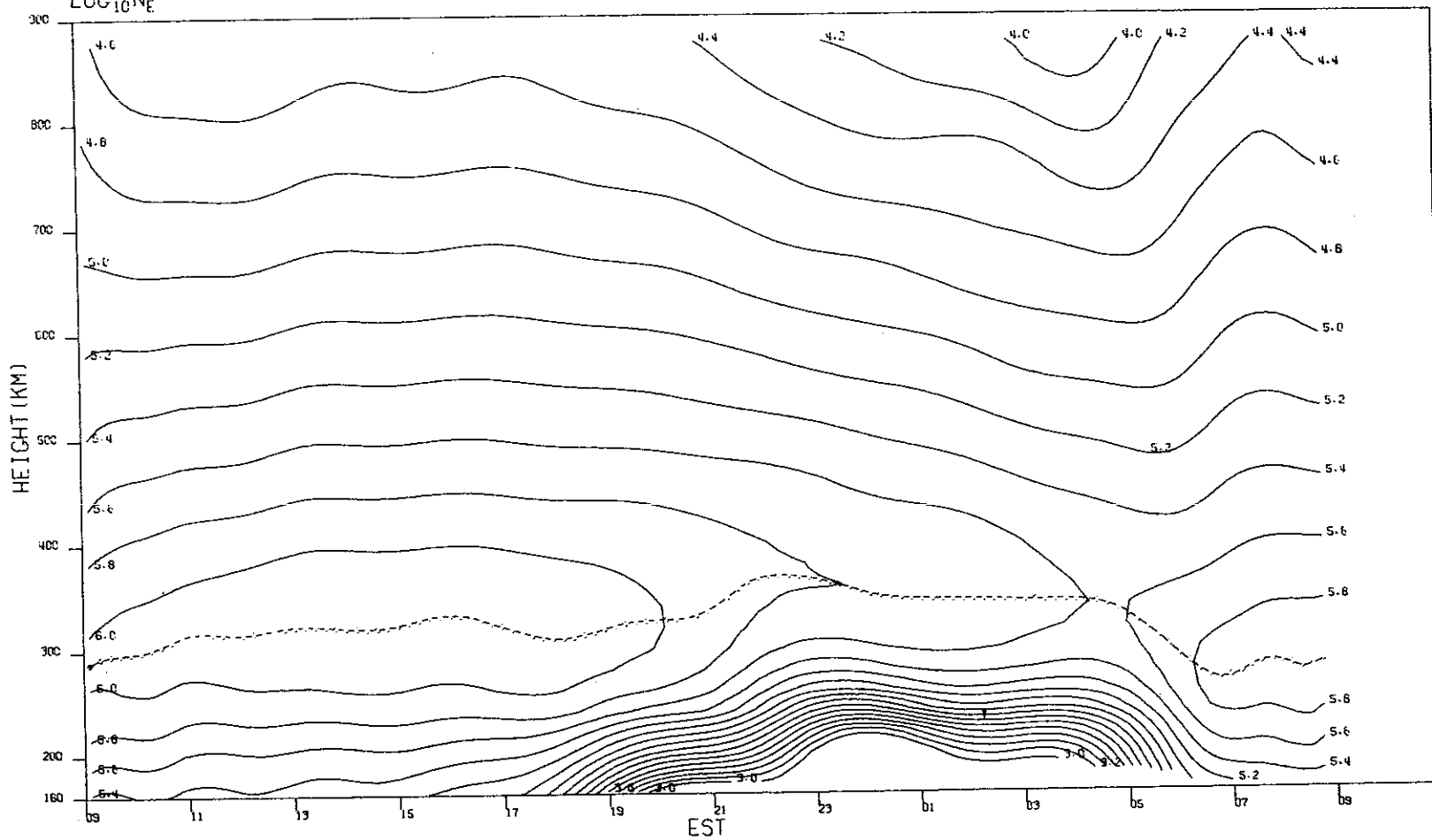
26

(g)

Fig. 1(a-z). Continued.

MILLSTONE HILL
14-15, APR. 1970
LCC₁₀N_E

-9-5131



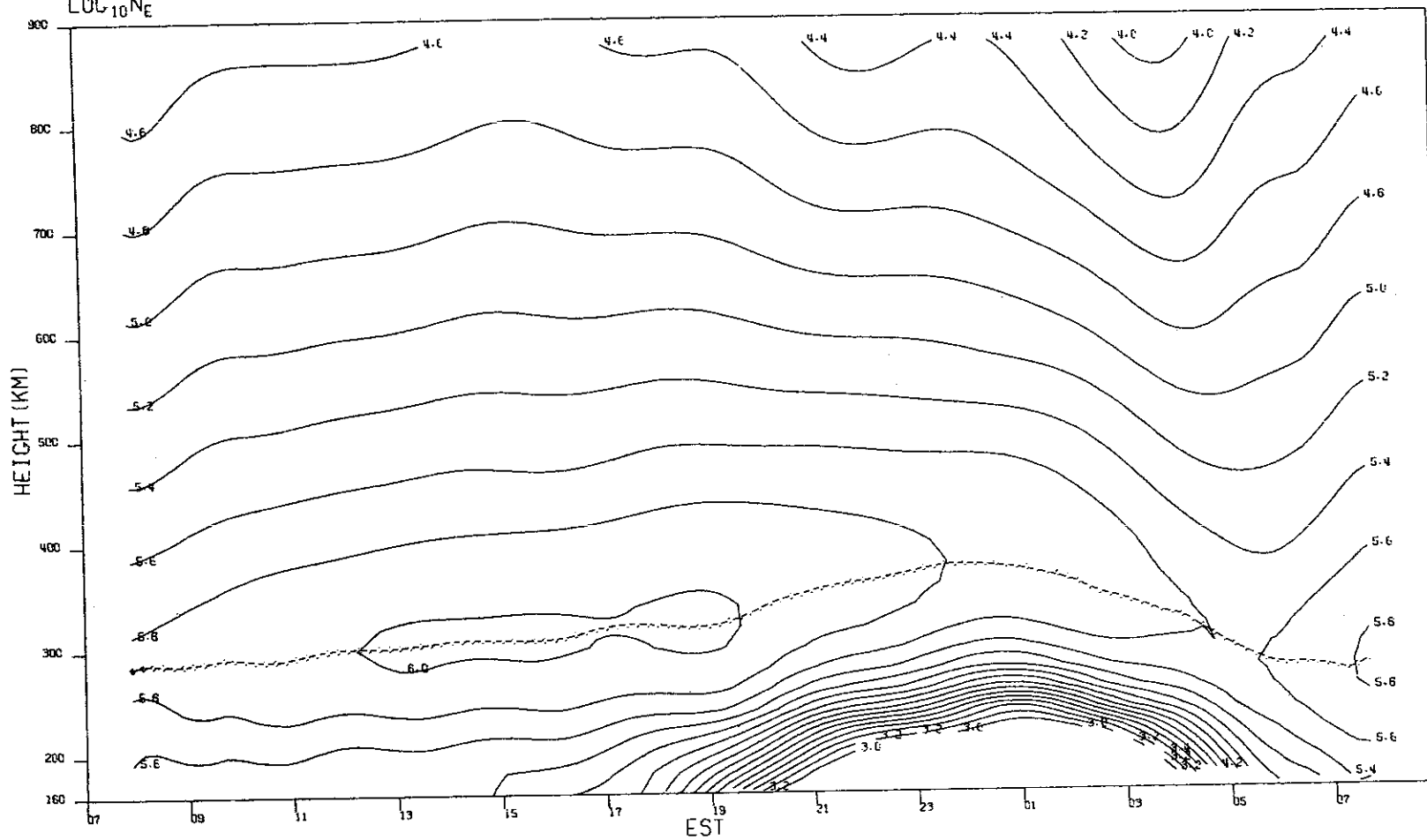
27

(h)

Fig. 1(a-z). Continued.

MILLSTONE HILL
28-29, APR, 1970
LOC 10NE

-9-5132



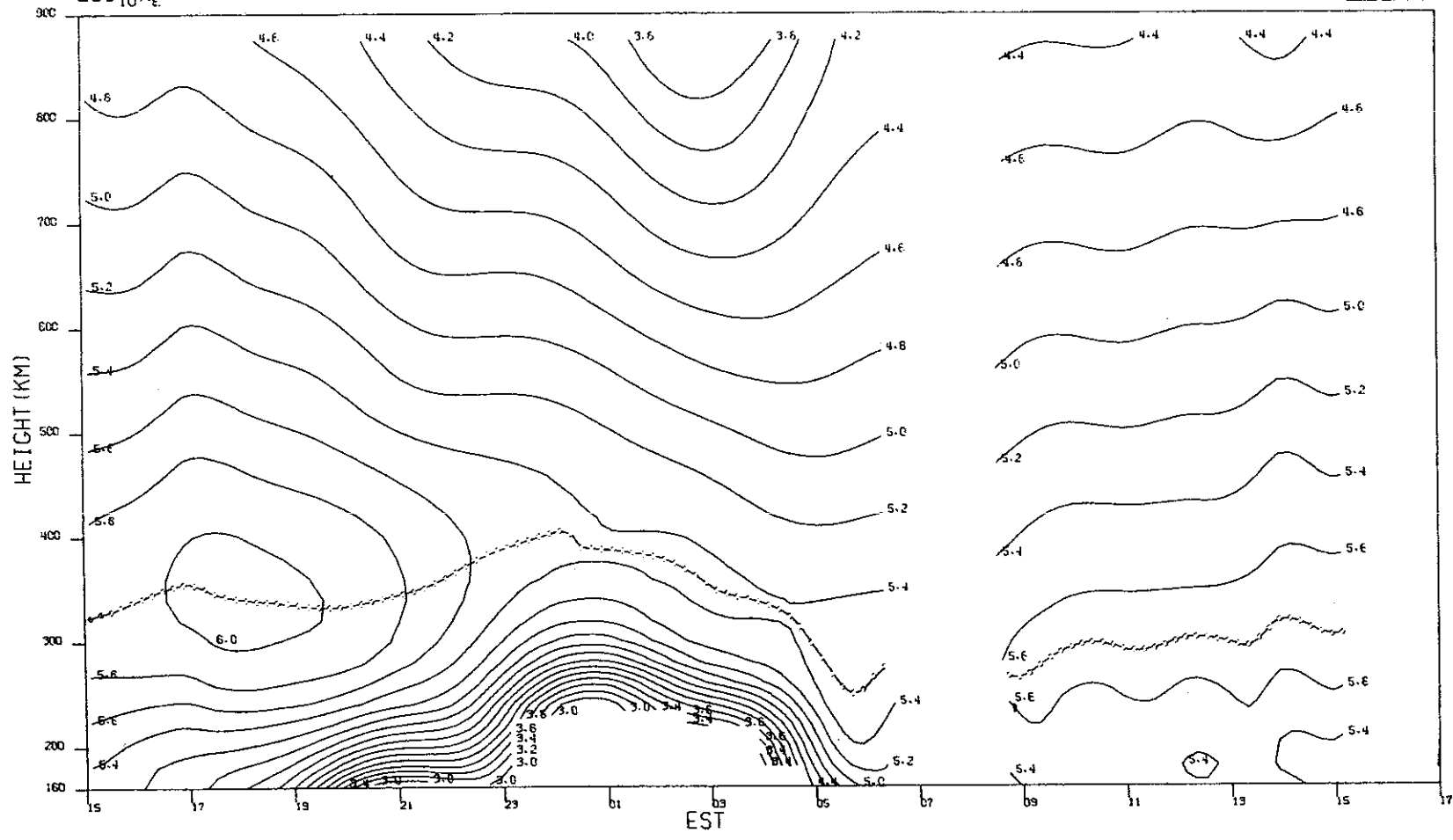
28

(i)

Fig. 1(a-z). Continued.

MILLSTONE HILL
12-13, MAY, 1970
LOG₁₀N_E

-9-5133



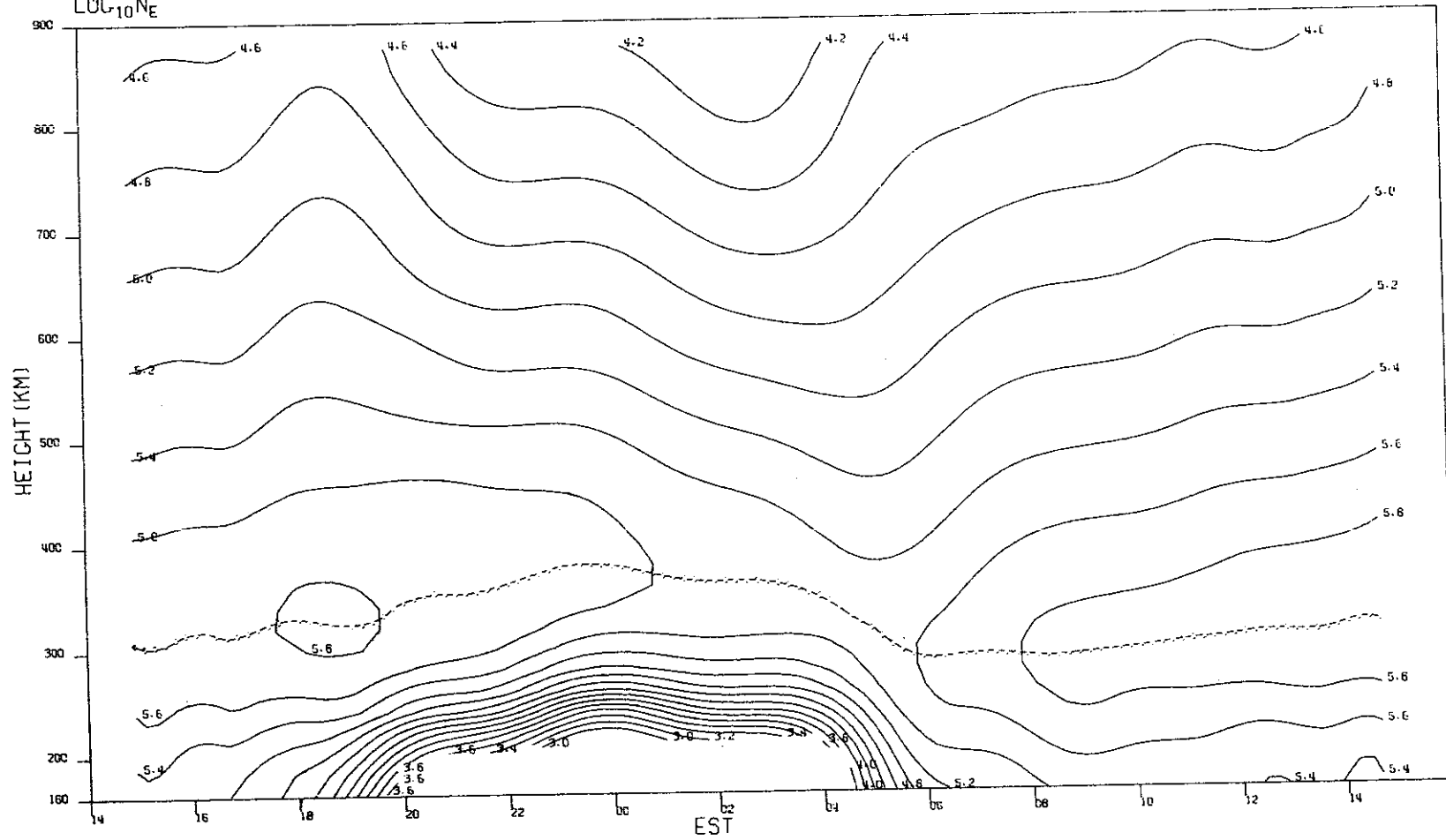
29

(j)

Fig. 1(a-z). Continued.

MILLSTONE HILL
18-19, MAY, 1970
LOG₁₀N_E

-9-5134



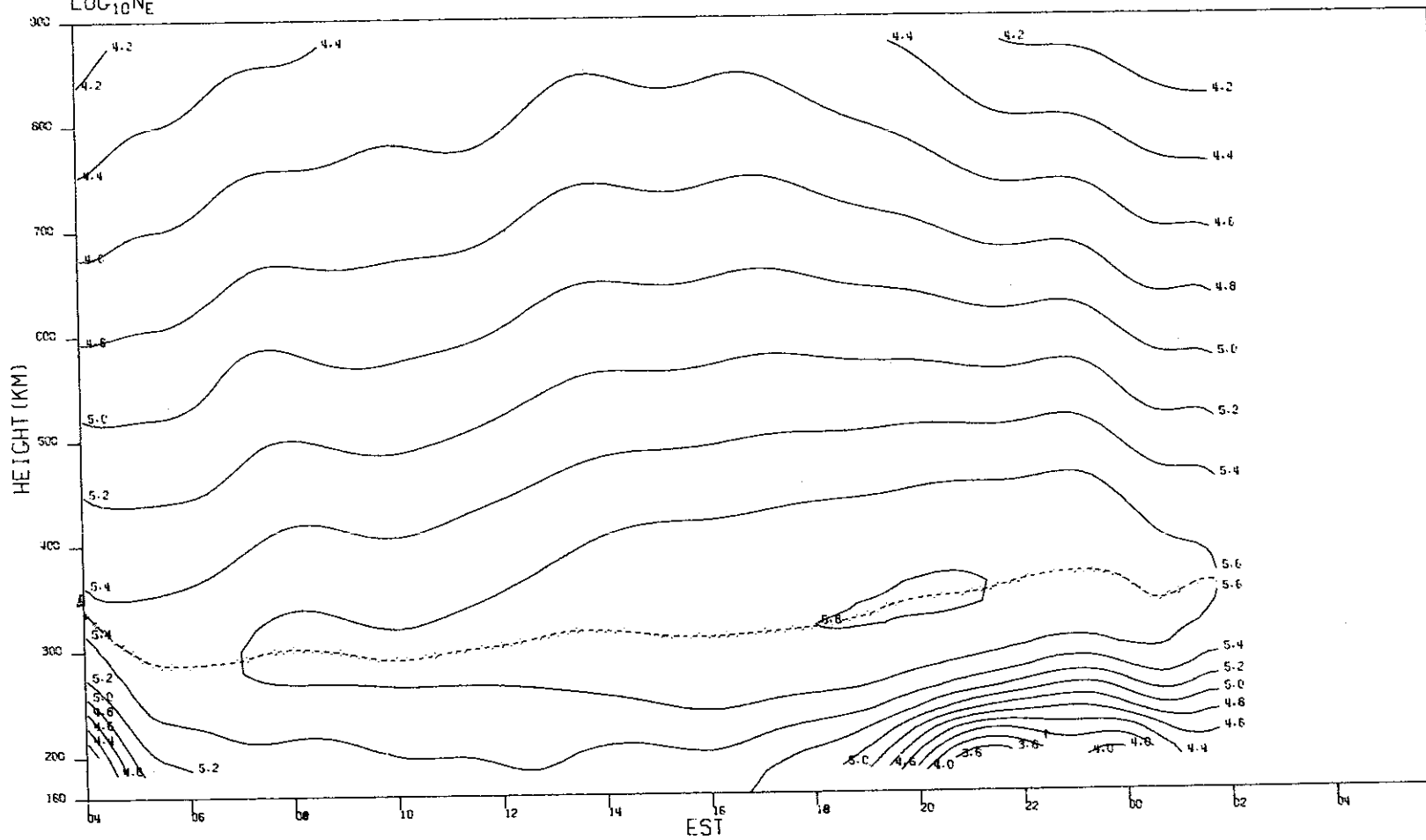
30

(k)

Fig. 1(a-z). Continued.

MILLSTONE HILL
10-11, JUN. 1970
LOC₁₀NE

-9-5135

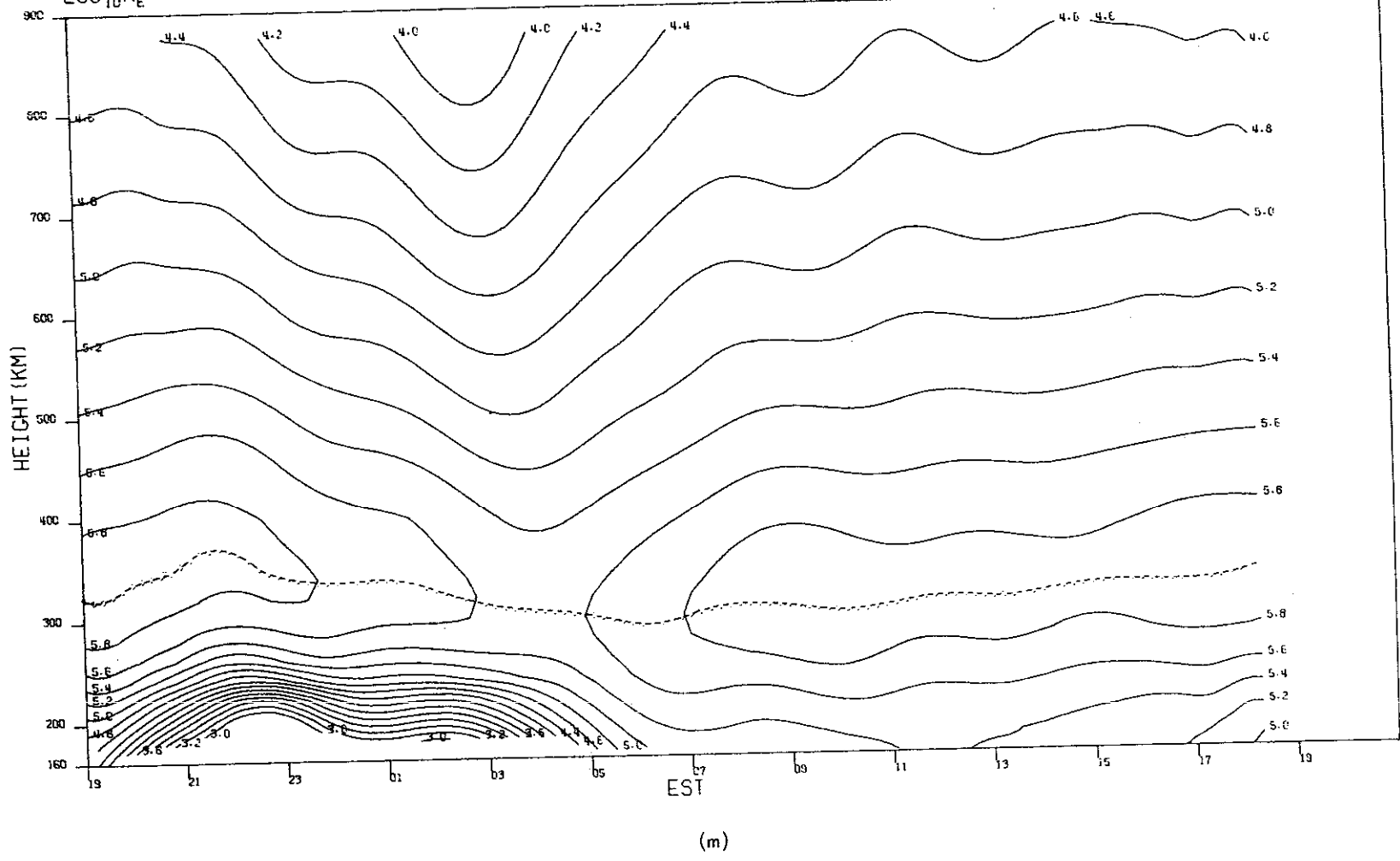


(I)

Fig. 1(a-z). Continued.

MILLSTONE HILL
23-24 JUN. 1970
 $\text{LOG}_{10} N_e$

-9-5136

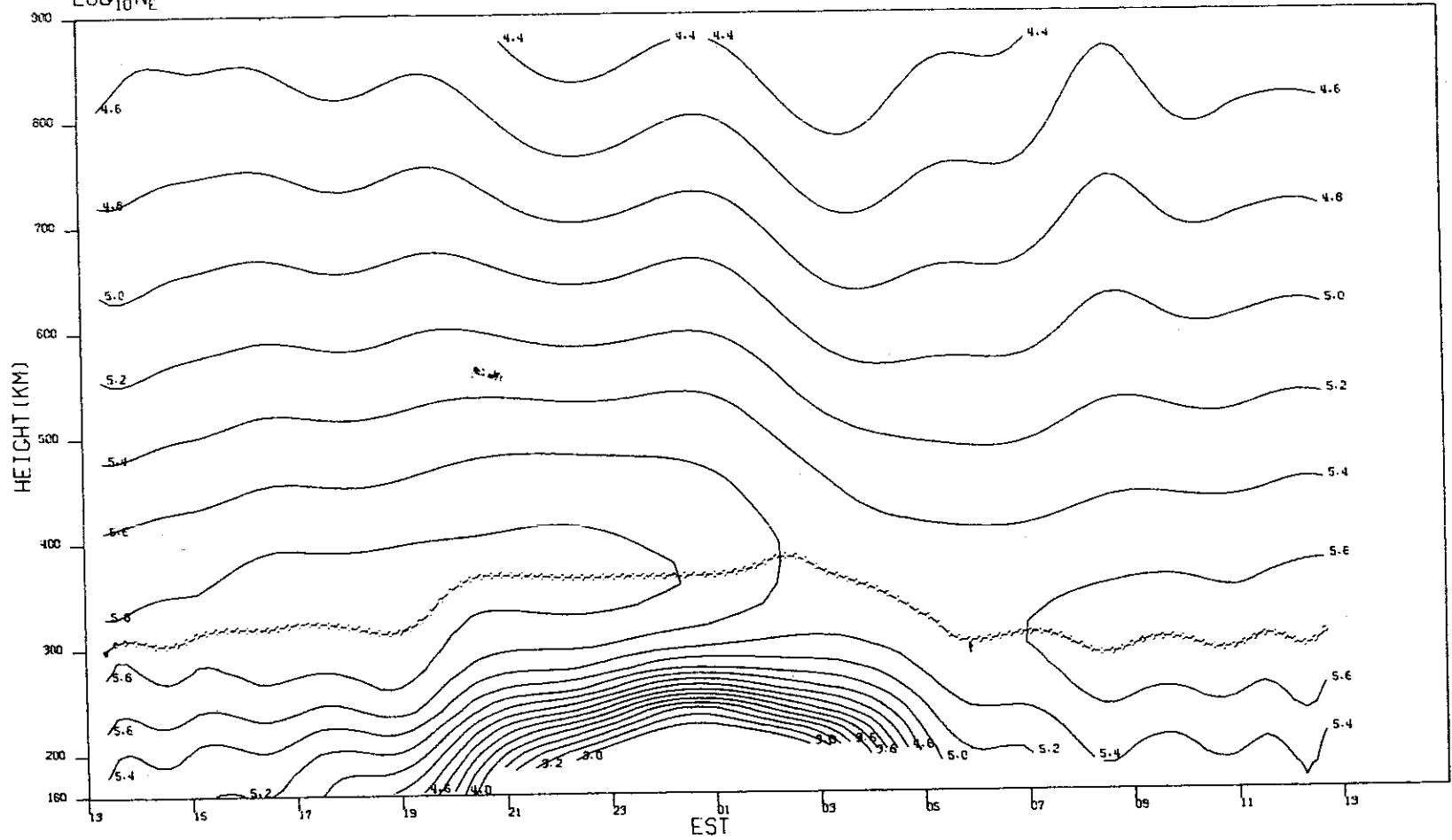


32

Fig. 1(a-z). Continued.

MILLSTONE HILL
07-08, JUL, 1970
LOC₁₀N_F

-9-5137

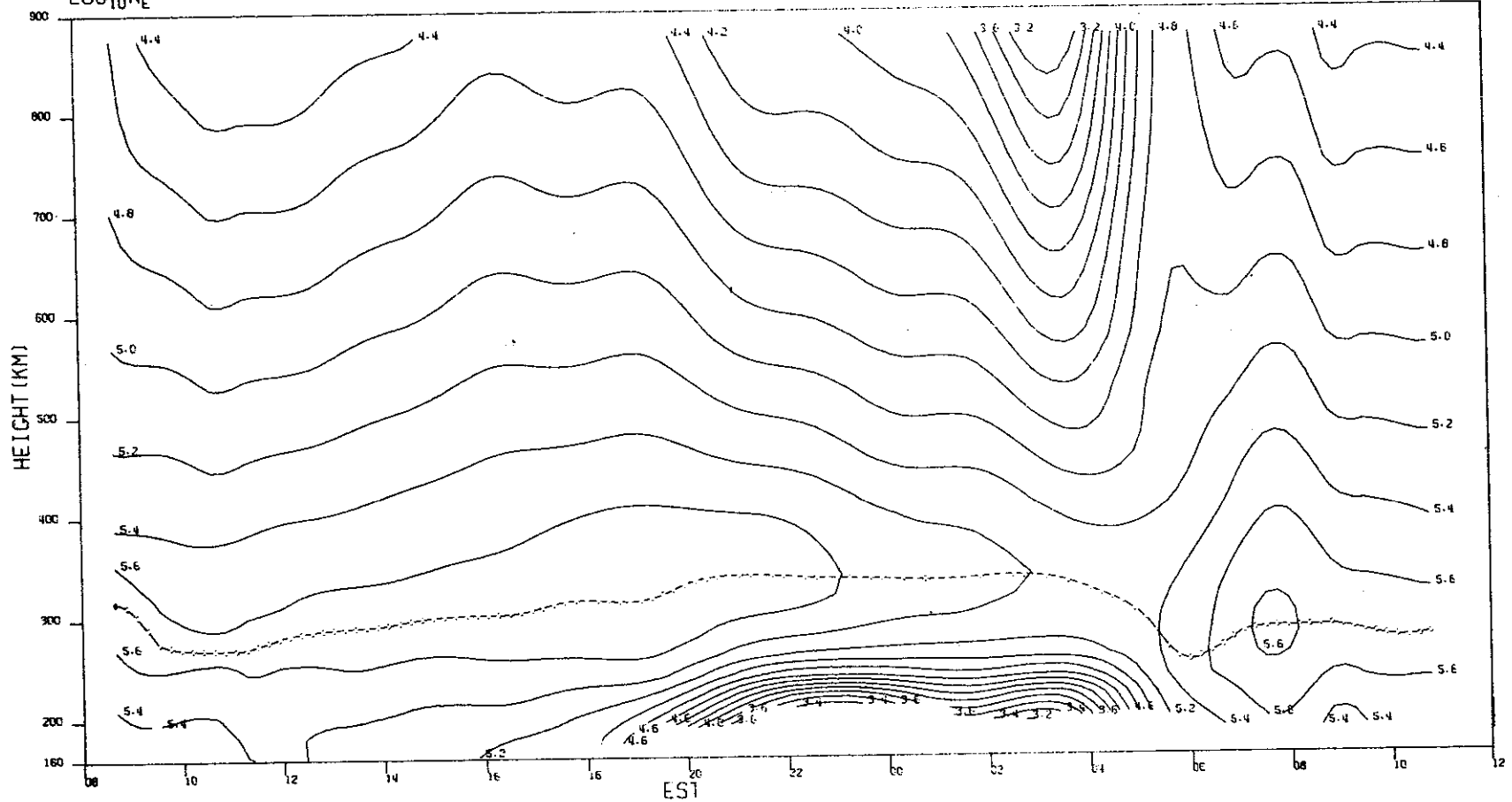


(n)

Fig. 1(a-z). Continued.

MILLSTONE HILL
18-19, JUL, 1970
LOC₁₀NE

-9-5130

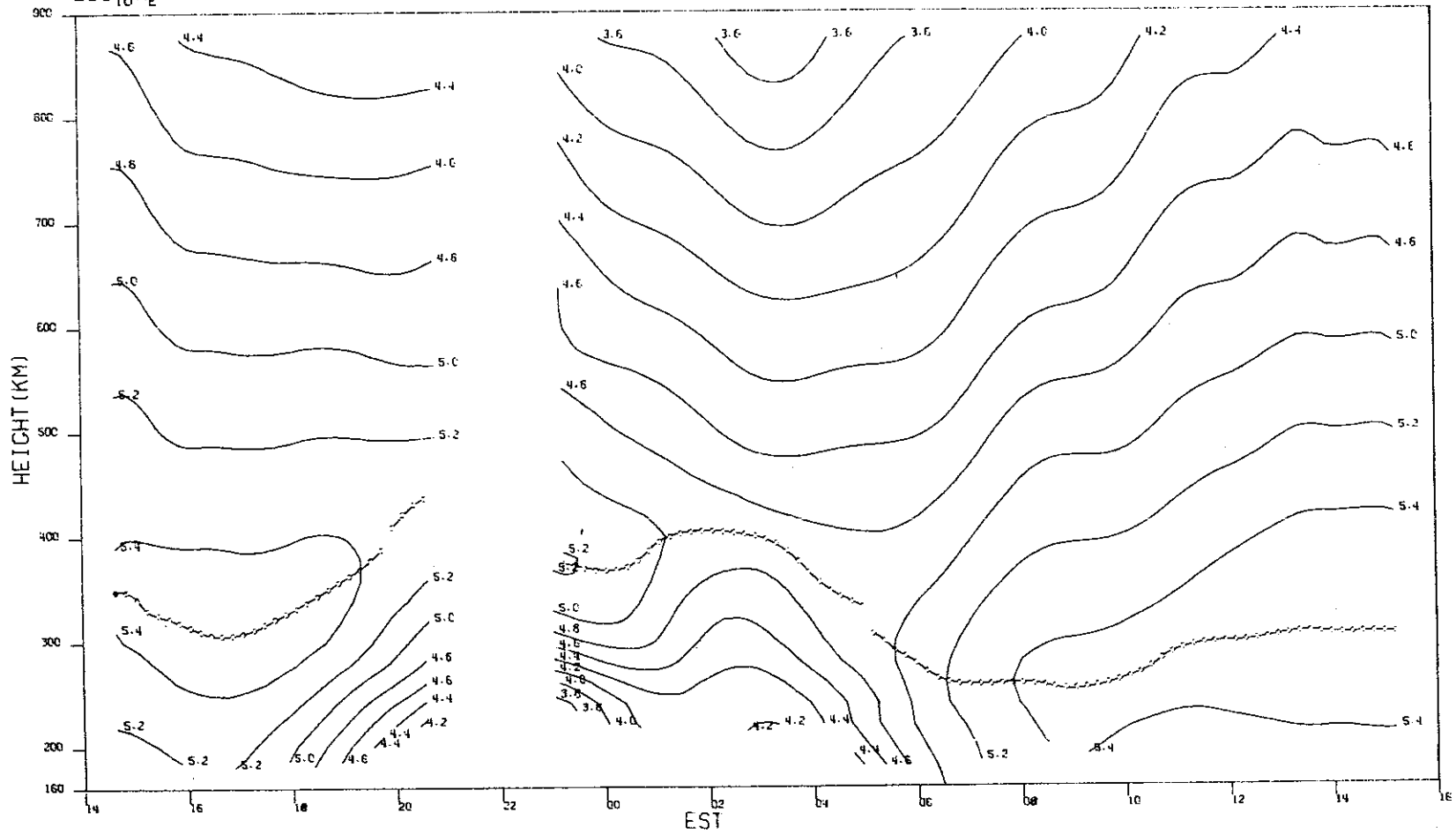


(o)

Fig. 1(a-z). Continued.

MILLSTONE HILL
17-18, AUG, 1970
LOC₁₀NE

-9-5139



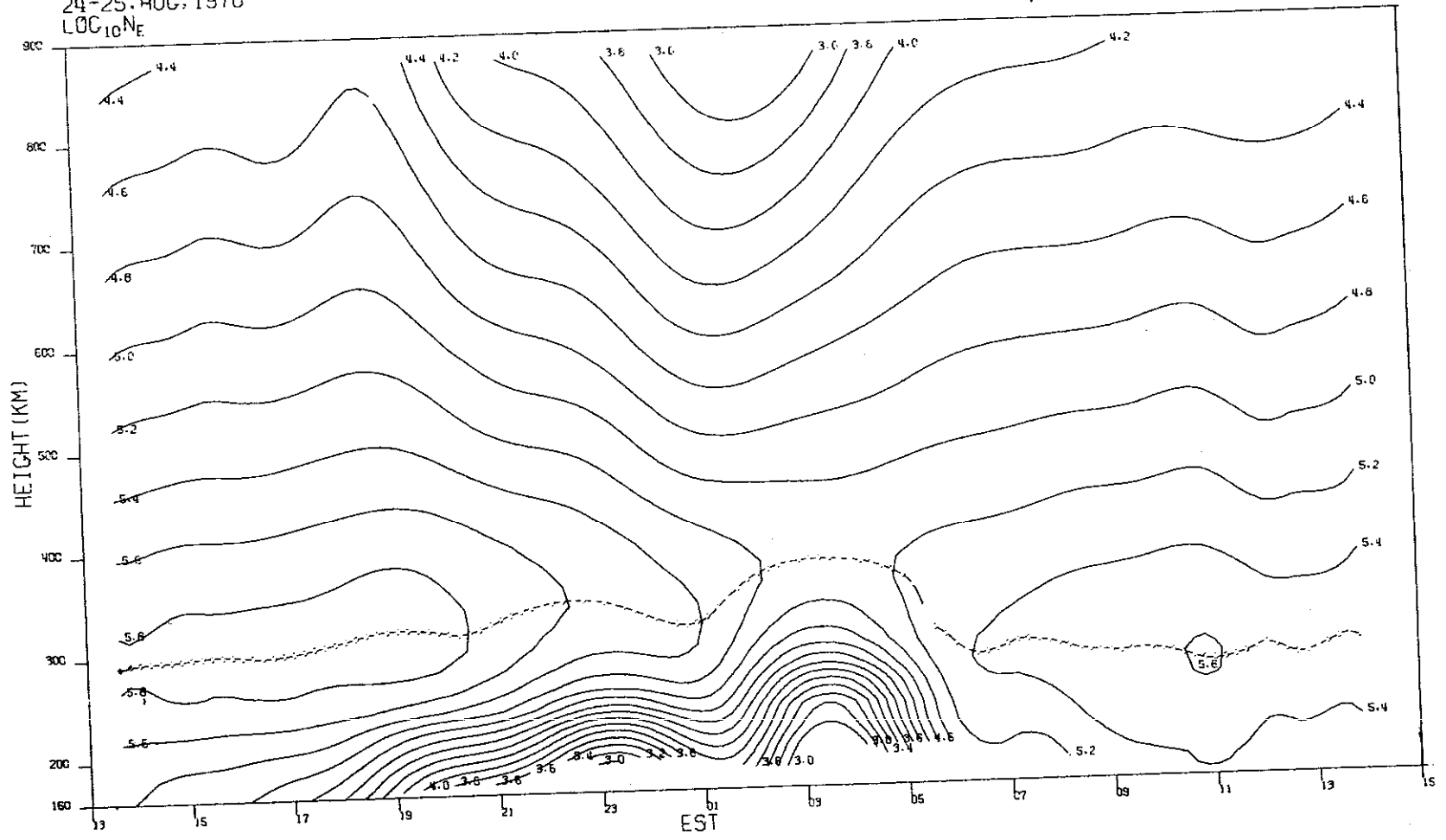
35

(p)

Fig. 1(a-z). Continued.

MILLSTONE HILL
24-25. AUG, 1970
LOC 10NE

-9-5140



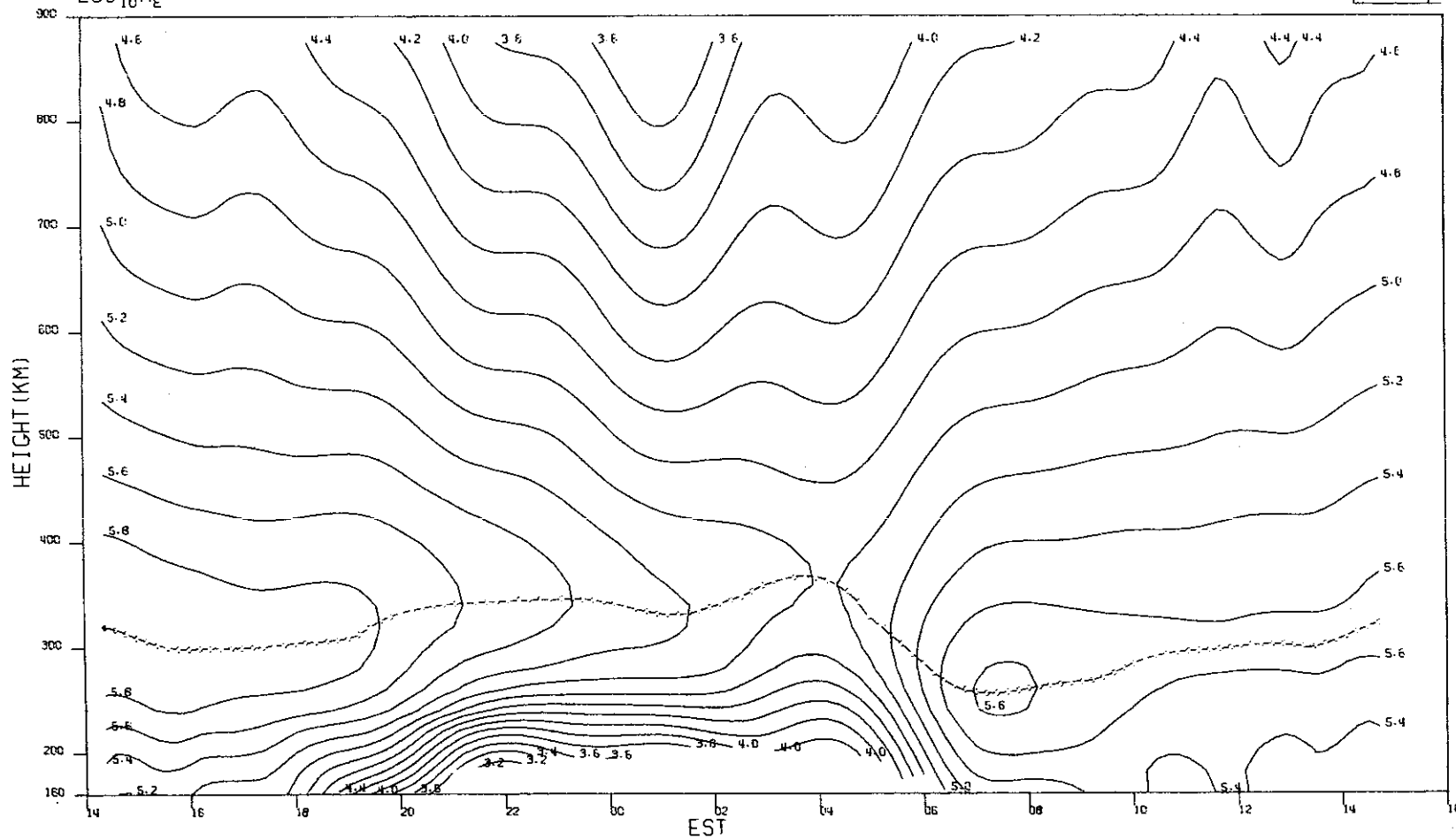
36

(q)

Fig. 1(a-z). Continued.

MILLSTONE HILL
31 AUG-01 SEP, 1970
LOC 10 NE

-9-5141



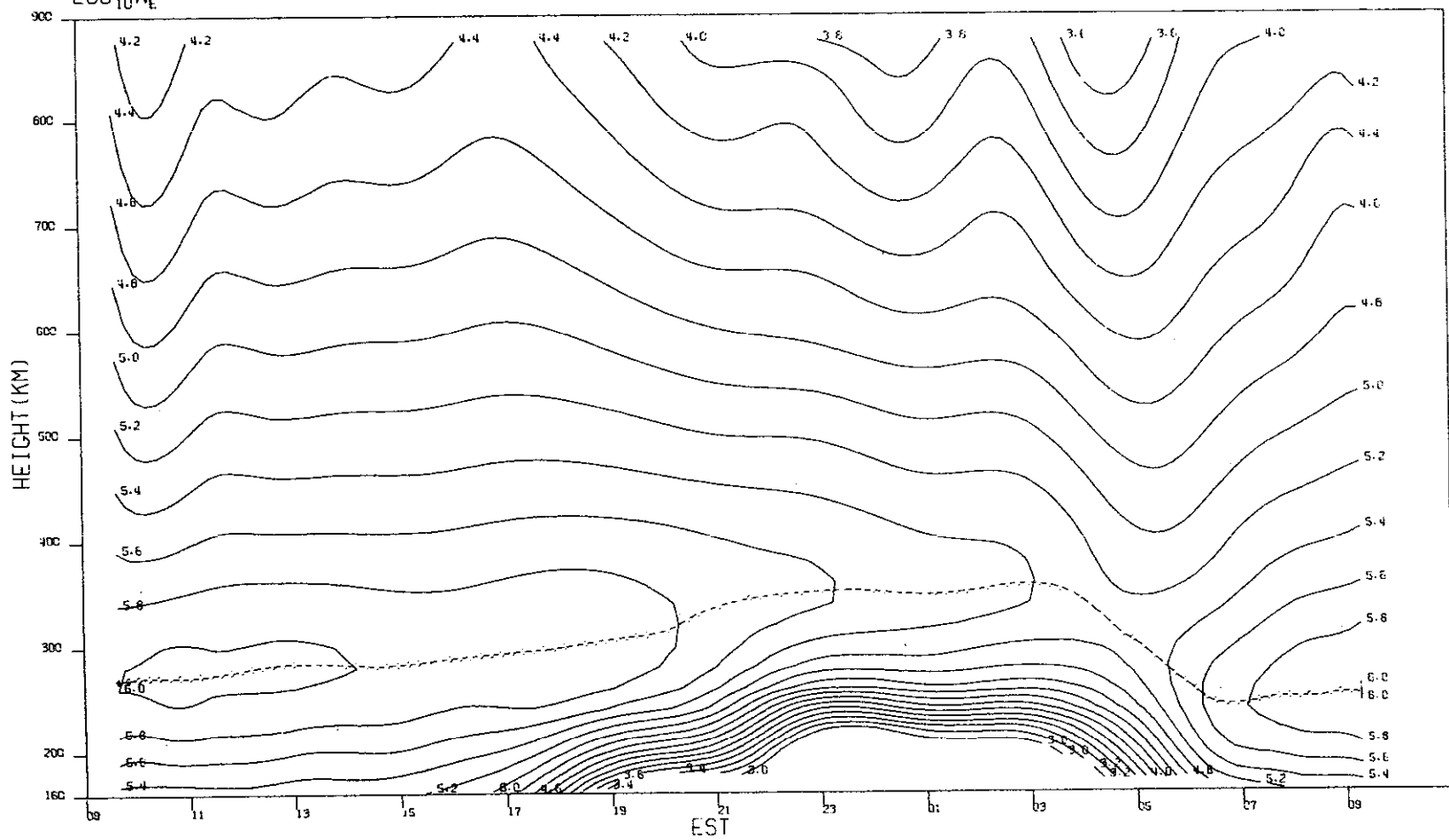
37

(r)

Fig. 1(a-z). Continued.

MILLSTONE HILL
16-17, SEP. 1970
 $\text{LOG}_{10} N_E$

-9-5142



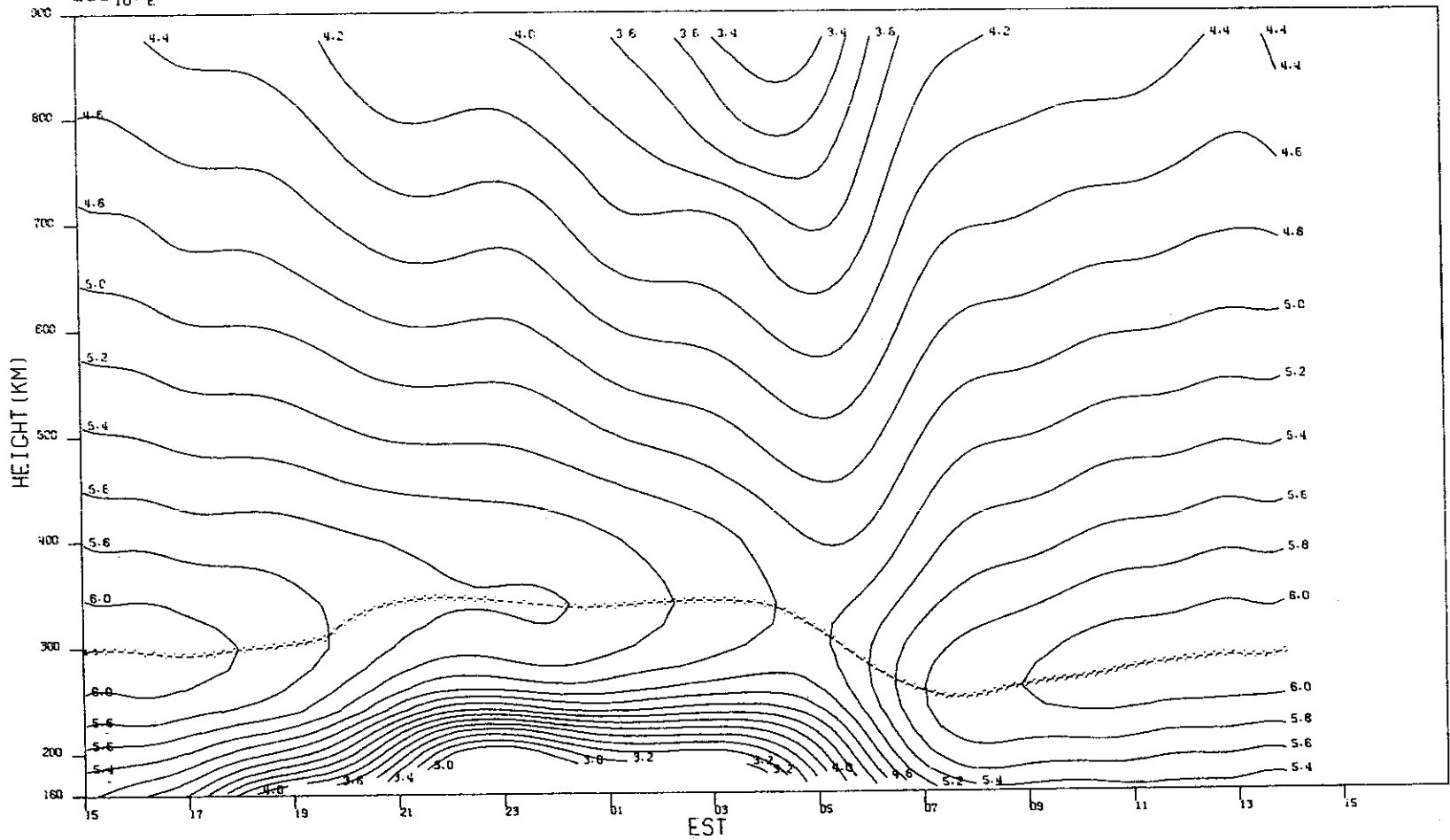
38

(s)

Fig. 1(a-z). Continued.

MILLSTONE HILL
26-29. SEP. 1970
 $\text{LOG}_{10} N_E$

-9-5143

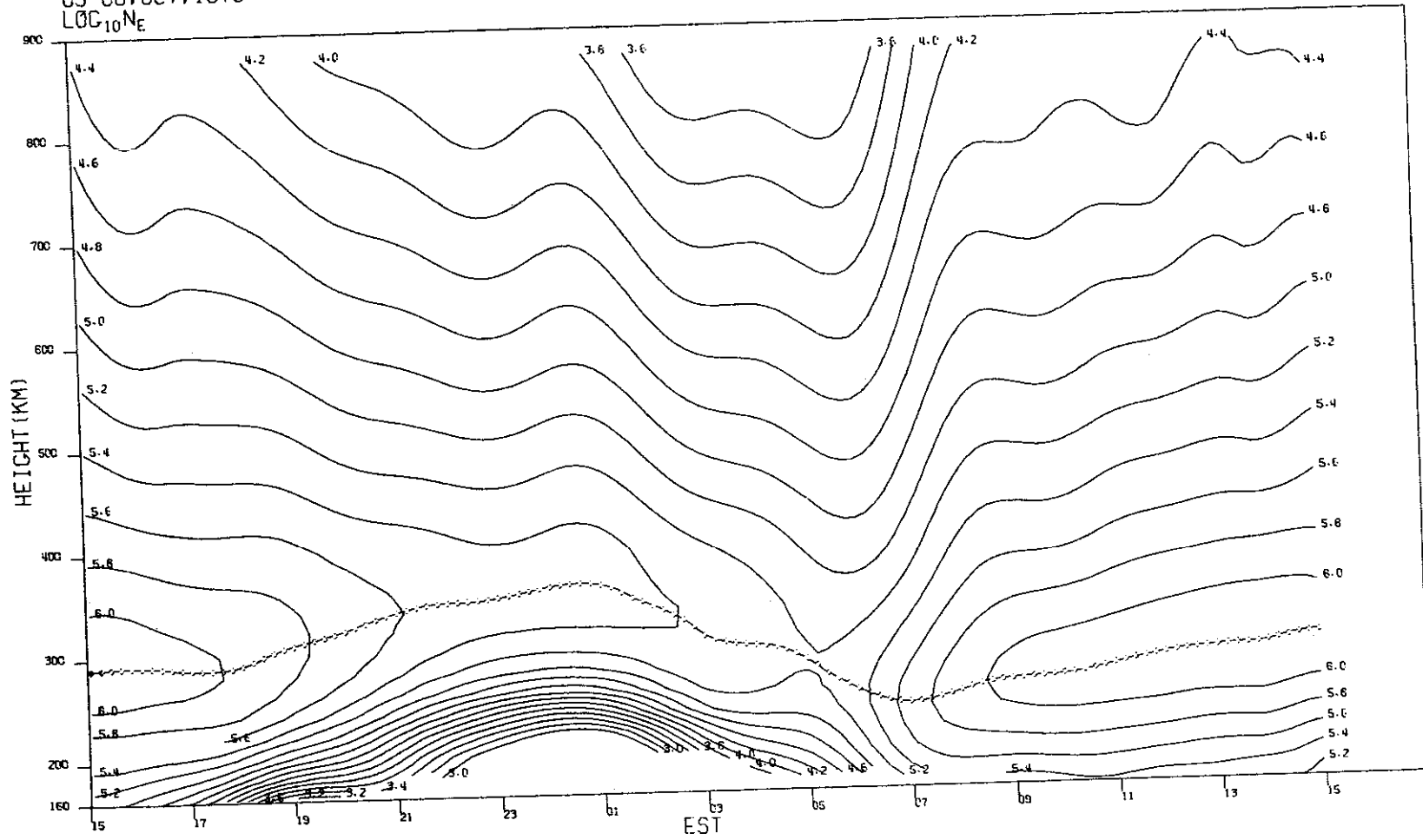


(t)

Fig. 1(a-z). Continued.

MILLSTONE HILL
05-06, OCT, 1970
LOC 10NE

-9-5144



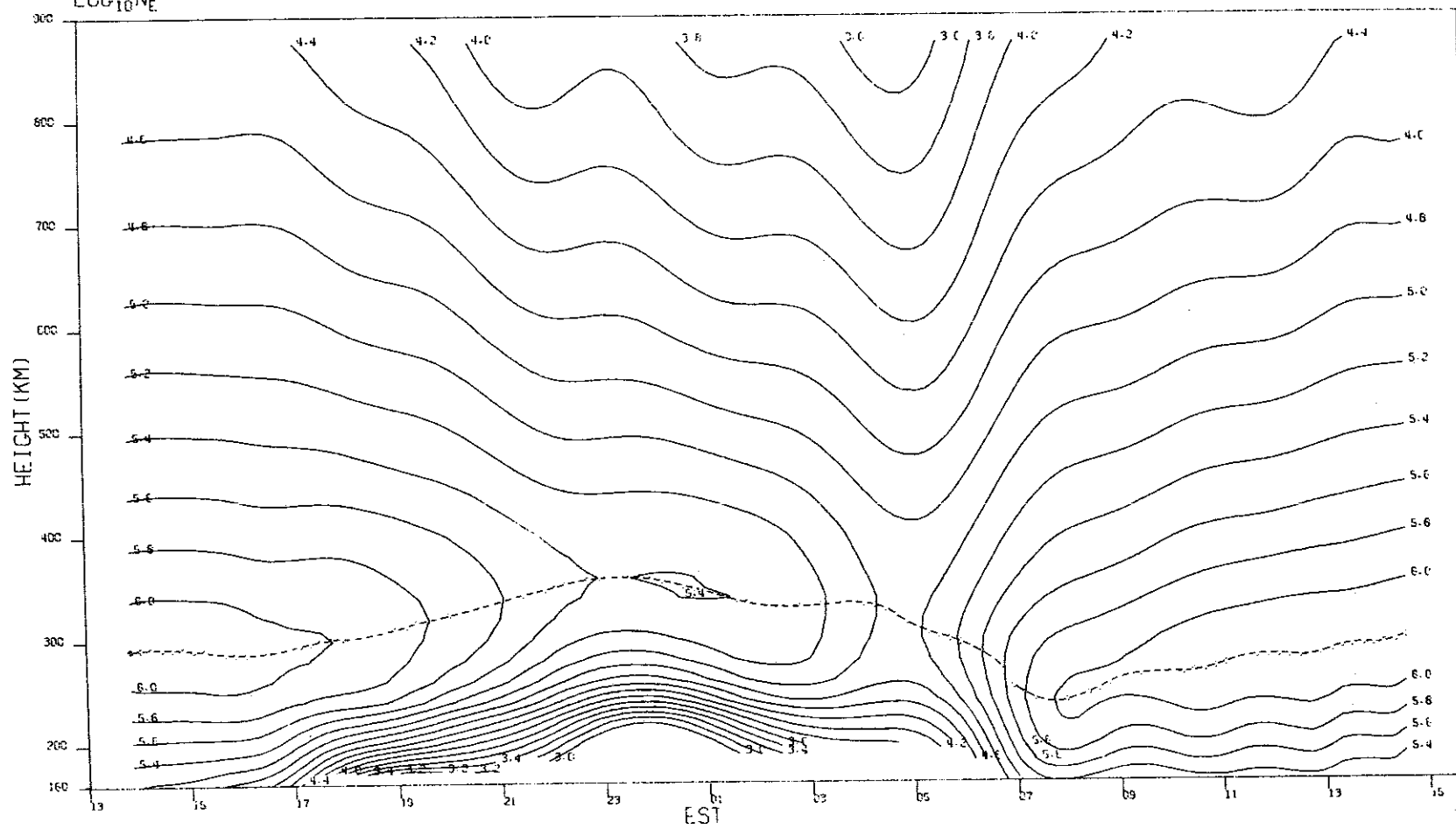
40

(u)

Fig. 1(a-z). Continued.

MILLSTONE HILL
13-14. OCT. 1970
LOG₁₀N_E

-9-5145

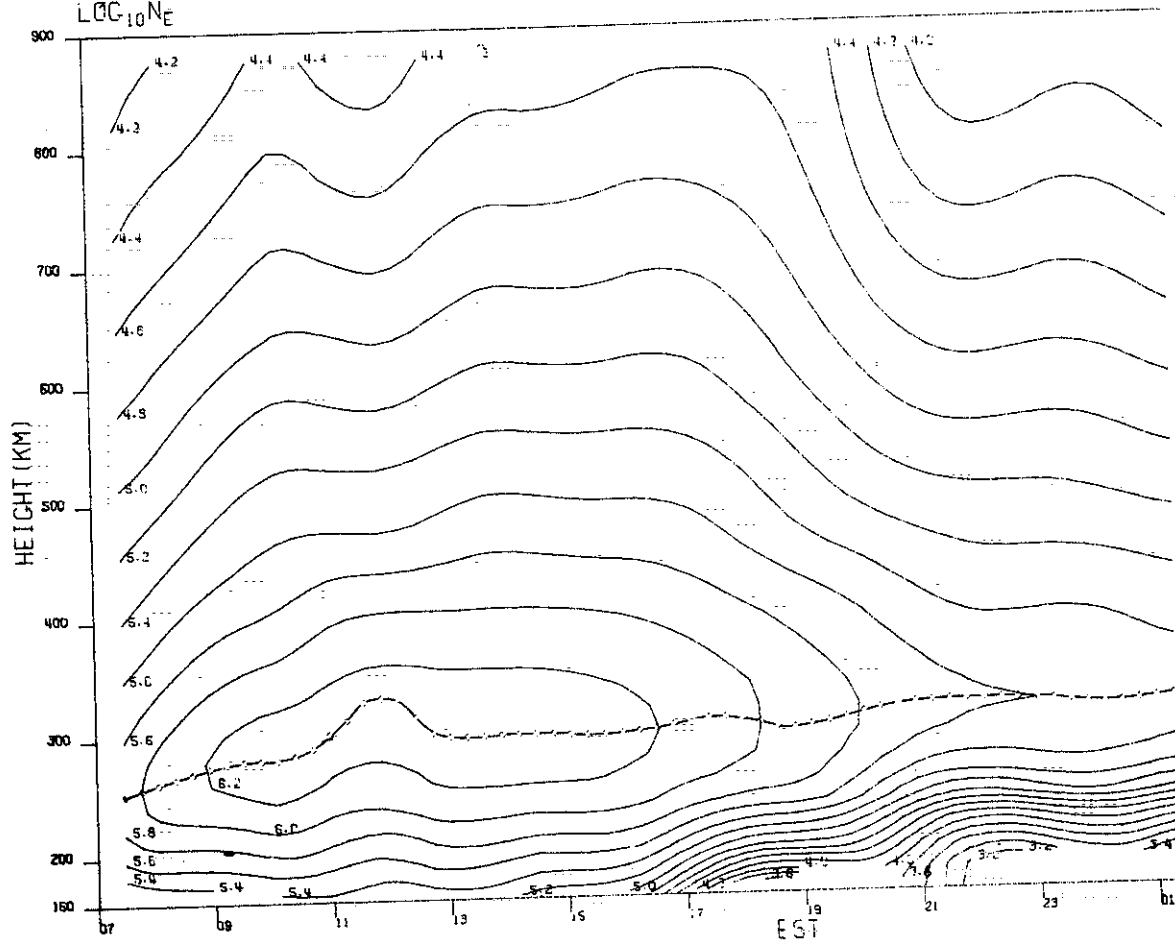


44

(v)

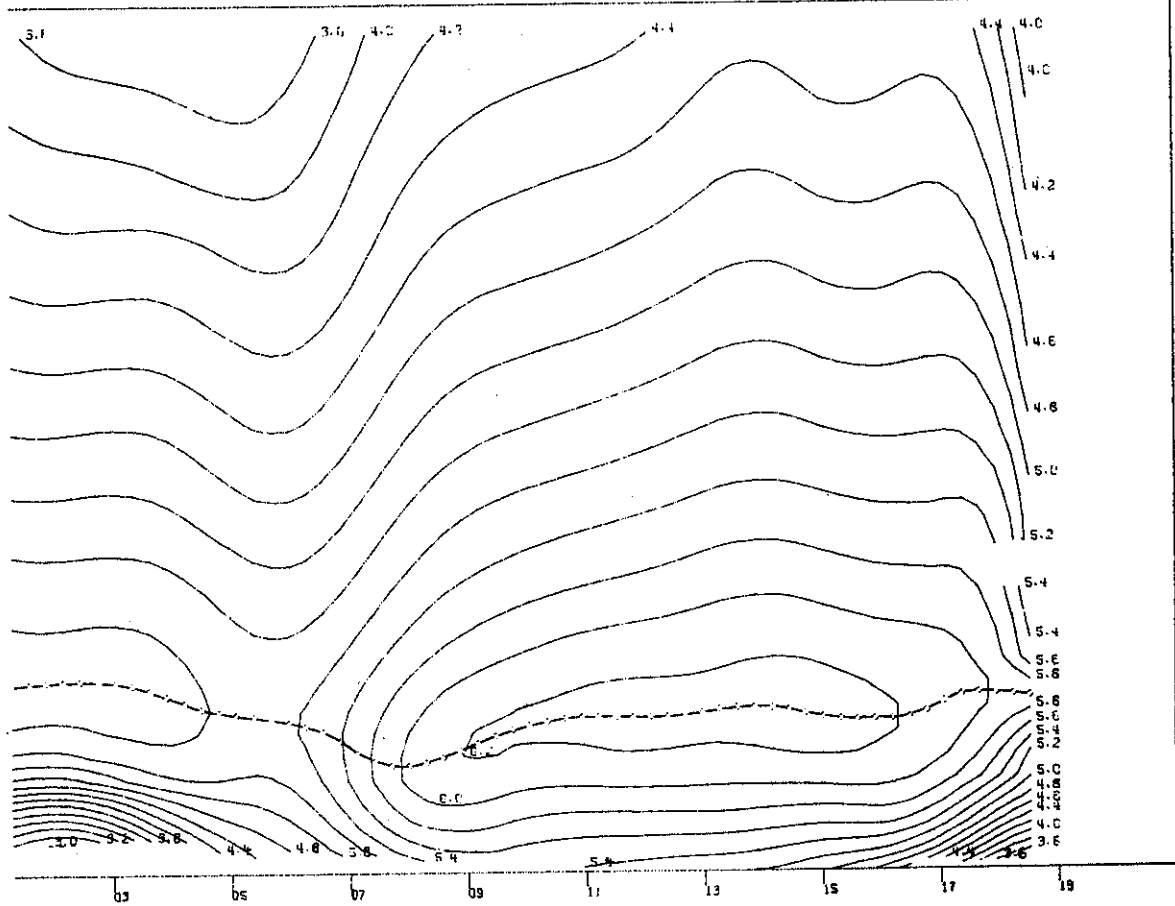
Fig. 1(a-z). Continued.

MILLSTONE HILL
31 OCT - 01 NOV 1970
LOG₁₀N_E



(w)

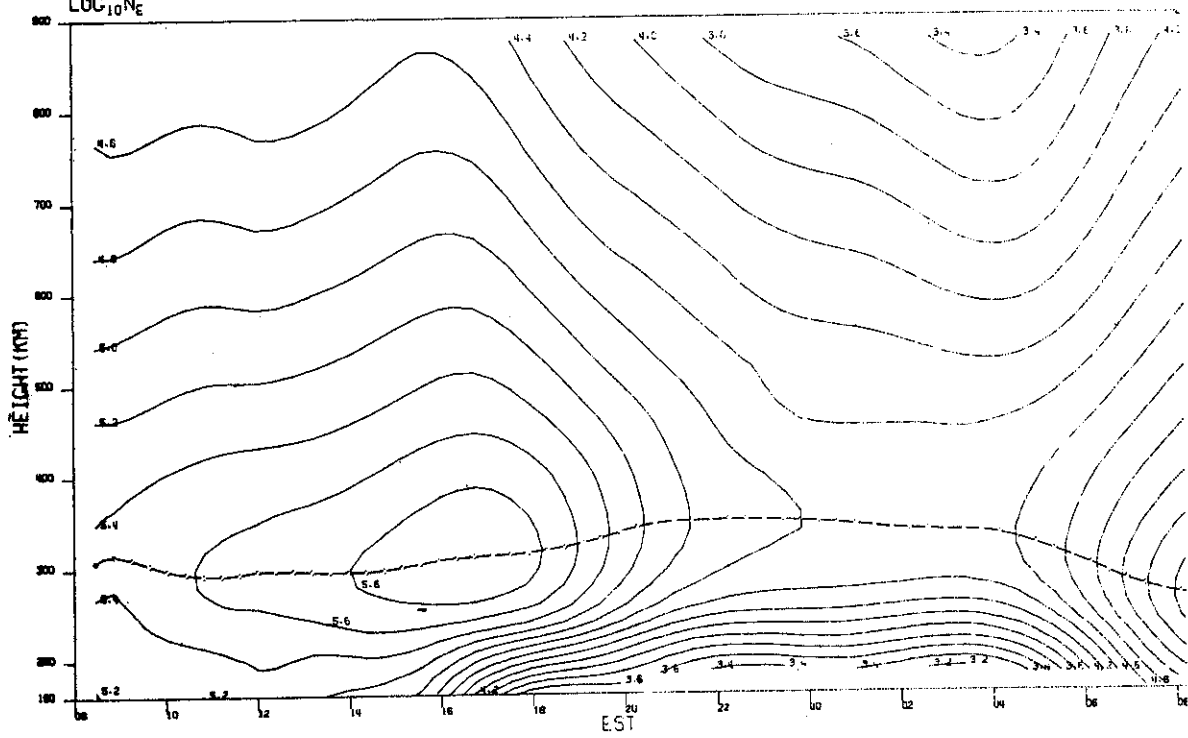
Fig. 1(a-z). Continued.



(w)

Fig. 1(a-z). Continued.

MILLSTONE HILL
 07-09, NOV, 1970
 $LOG_{10} N_E$



(x)

Fig. 1(a-z). Continued.

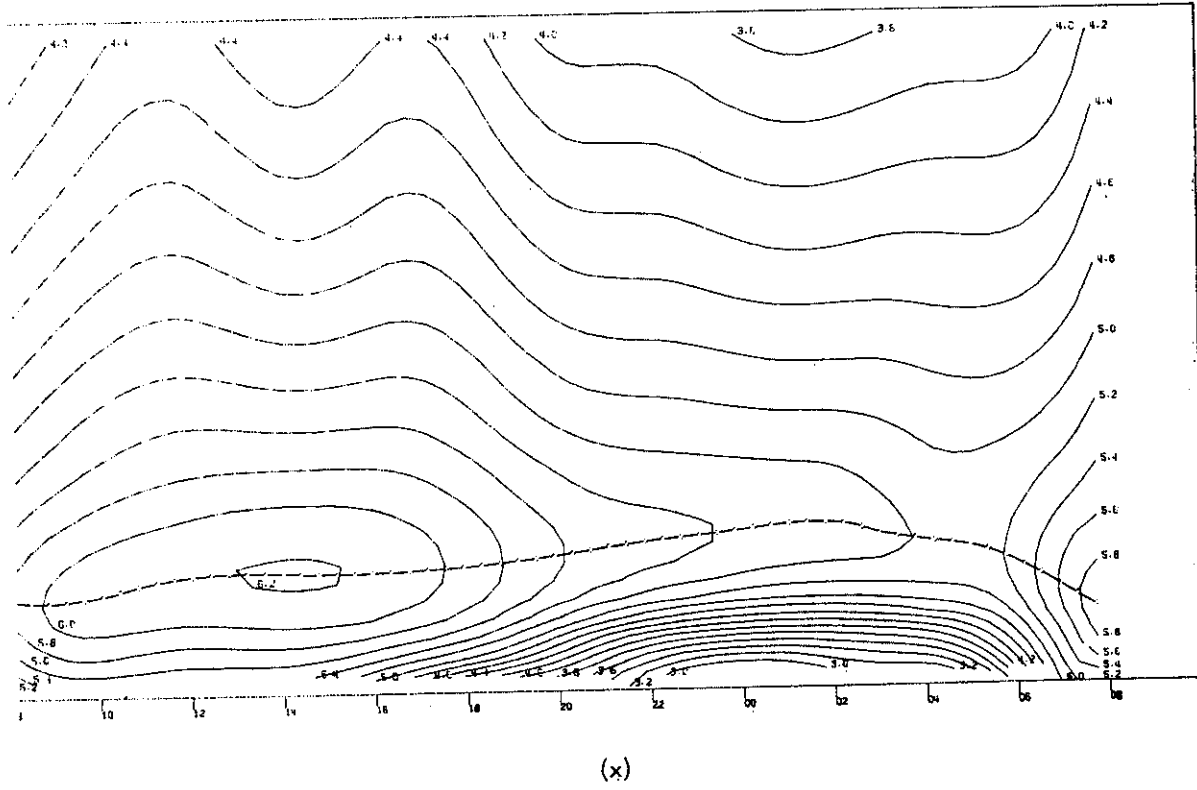
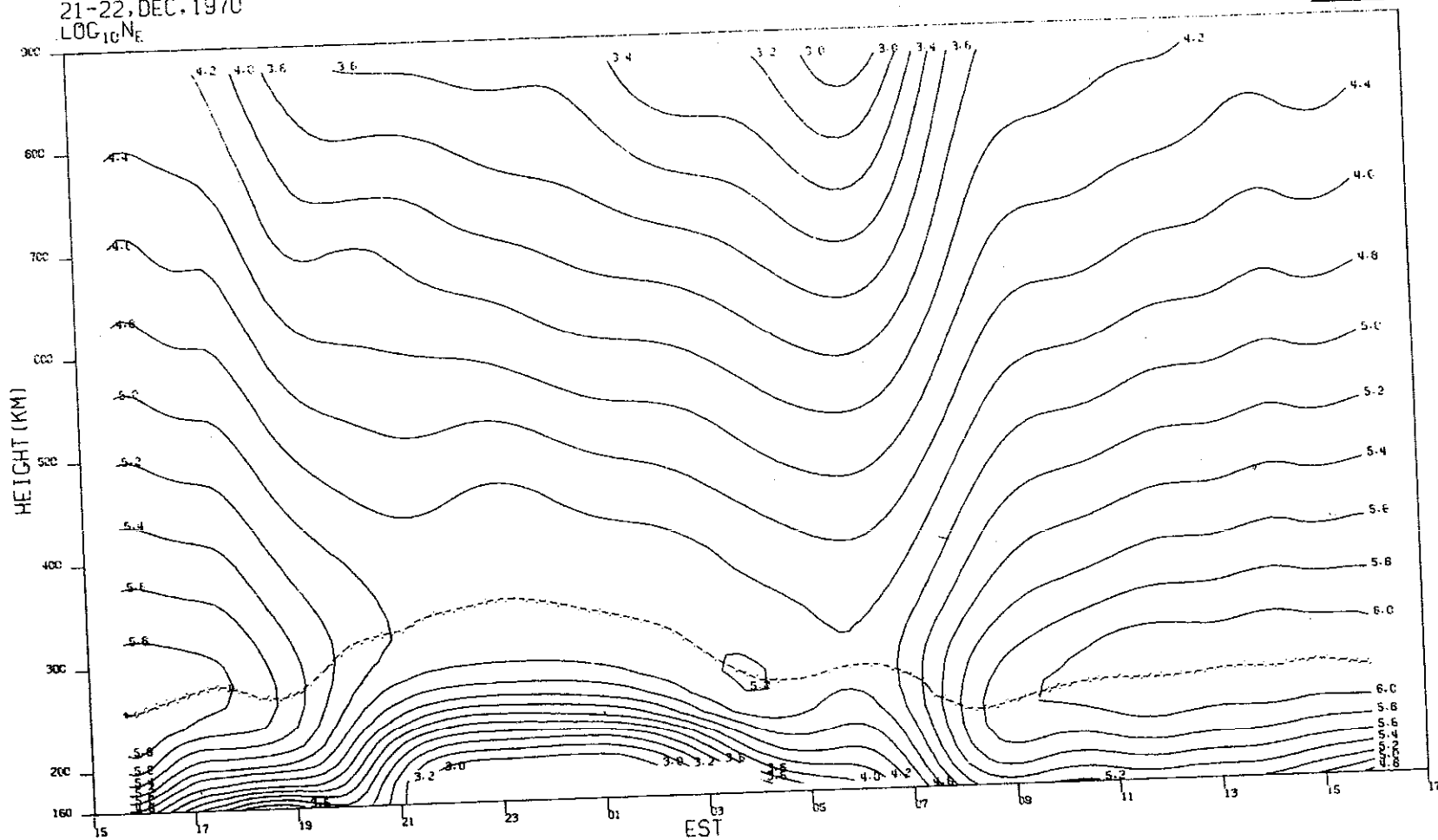


Fig. 1(a-z). Continued.

MILLSTONE HILL
21-22, DEC. 1970
LOG₁₀N_E

-9-5148



46

(y)

Fig. 1(a-z). Continued.

MILLSTONE HILL
28-29, DEC. 1970
LOC 10NE

-9-5149

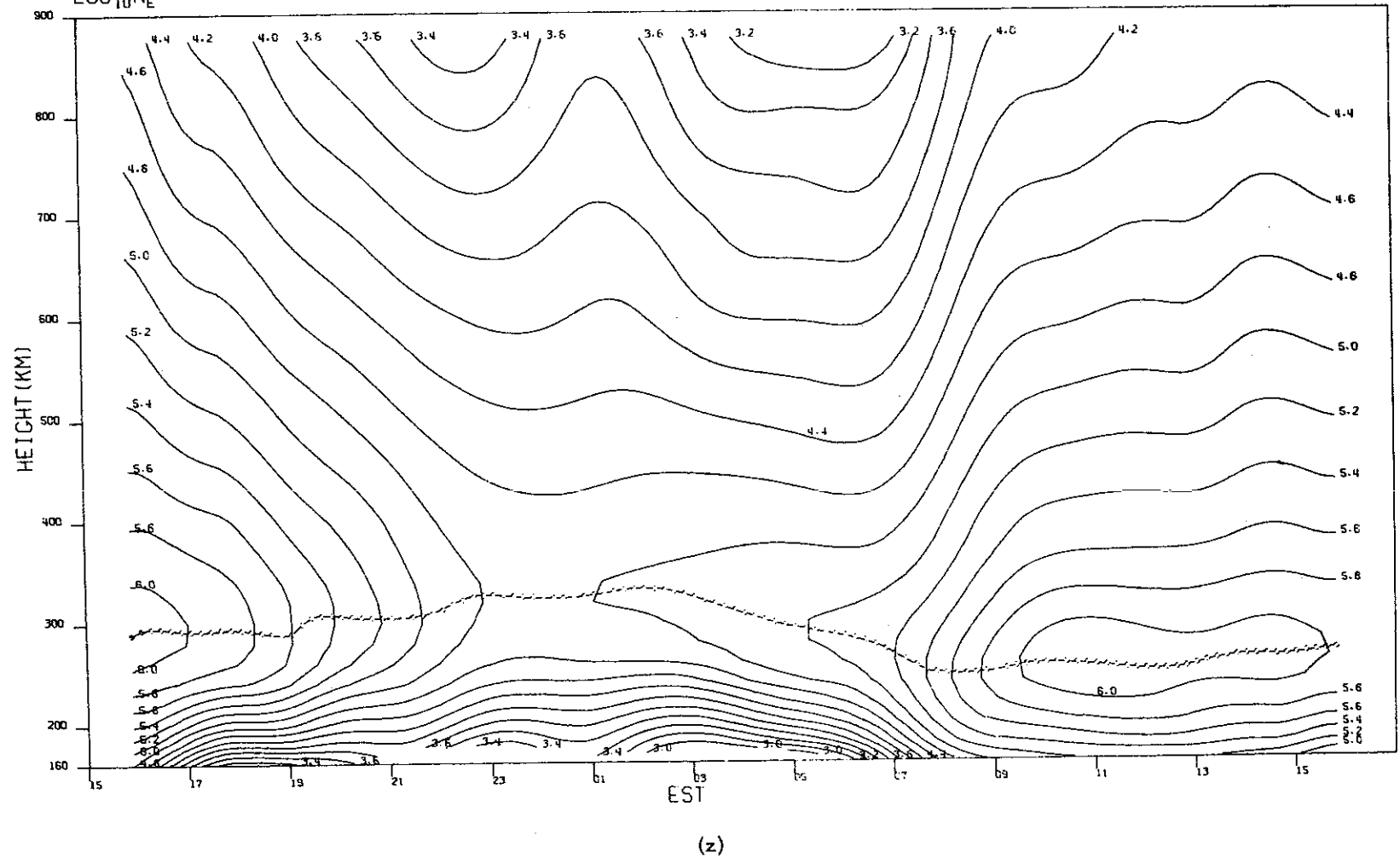


Fig. 1(a-z). Continued.

nighttime period of 17-18 August [Fig. 1(p)] is compared with that of the quiet day that followed 24-25 August [Fig. 1(q)], it appears that the electron density below h_{\max}^{F2} remained high ($>10^4 \text{ eI/cm}^3$) down to lower altitudes throughout much of the disturbed night in contrast to the quiet night. This suggests the presence of a weak ionizing flux of precipitating particles (electrons), and this interpretation is supported by the higher electron temperatures present on the disturbed night. During the day on 18 August, the density behaved much as expected, despite the fact that this was a very disturbed period.

The observations of 31 October through 1 November were conducted jointly with the other incoherent scatter radar facilities (St. Santin, Chatanika, and Arecibo) that participate in a program organized by the Incoherent Scatter Working Group of Commission G (then Commission 3) of the International Union of Radio Science (URSI). The intent was to gather observations during a magnetically disturbed period. A class 2B flare was seen on the sun on 28 October at 0750 EST and the joint observations were then scheduled to begin at 0900 EST on 30 October. This was the day on which computer malfunctions marred much of the data. As it transpired, no magnetic storm occurred and the observations were rescheduled.

On 4 November, a second 2B flare occurred on the sun at 2241 EST and this was followed by a proton event observed by ATS-1. Unfortunately, in this instance other operations at Millstone precluded our participation in the joint program prior to 0600 on 7 November. On this day, N_{\max} was very depressed until midafternoon. Normal behavior was exhibited on 8 November [Fig. 1(x)].

The observations conducted on the evening of 9 March [Fig. 1(e)] appear to have been made during an instance of overhead precipitation at Millstone that was responsible for a low latitude red aurora. The results for this night have been examined in considerable detail by Noxon and Evans,²⁷ and the reader is referred to that paper for a thorough discussion.

B. Electron Temperature

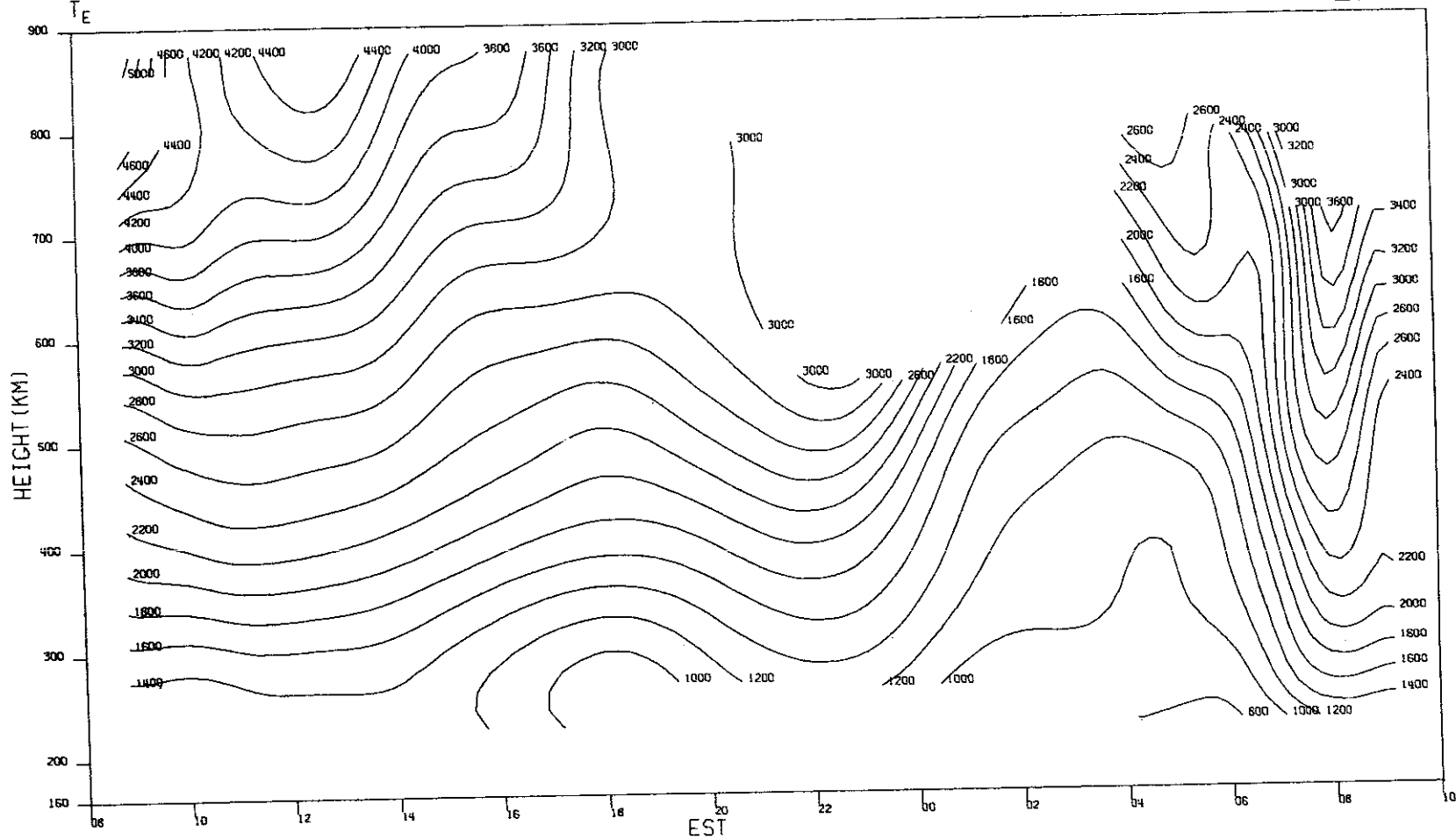
Contours of electron temperature spanning the range 225 to 900 km are presented in Figs. 2(a-z) at 200°K intervals. In summer the electron temperature is characterized by a very rapid increase ($\sim 2000^\circ\text{K}$) at sunrise which occurs at almost all levels in a space of 3 hours [e.g., Fig. 2(k)]. This rapid increase appears to commence when the solar zenith distance $\chi \approx 105^\circ$. During the daytime, the electron temperature remains roughly constant at all levels until mid-afternoon when a slow decrease to the nighttime level commences. The sunset decrease is less rapid than the sunrise increase and extends over a 6- to 8-hour interval. At night the temperature is again roughly constant with time.

In winter the time variation of T_e is more complex. There is a marked increase at local sunrise and T_e reaches a maximum a little after ground sunrise. Thereafter, there is often a decline as the electron density increases [e.g., Fig. 2(b)]. At sunset there is a further decrease which is arrested around 1700 to 1900 EST when heat from the magnetosphere is able to maintain the F-region temperature as the density decays [e.g., Fig. 2(y)]. The temperature may then increase to almost its daytime value and remain at this level throughout much of the night. The temperature usually decreases for a few hours prior to local sunrise [e.g., Figs. 2(a), 2(z)]. This decrease is thought to be caused by a density increase that commences a few hours after midnight [e.g., Figs. 1(a), 1(z)].

The winter behavior has been explained as a consequence of heat supplied to the magnetosphere by photoelectrons escaping from the conjugate point which remains sunlit. During March

MILLSTONE HILL
06-07, JAN. 1970

-9-5150

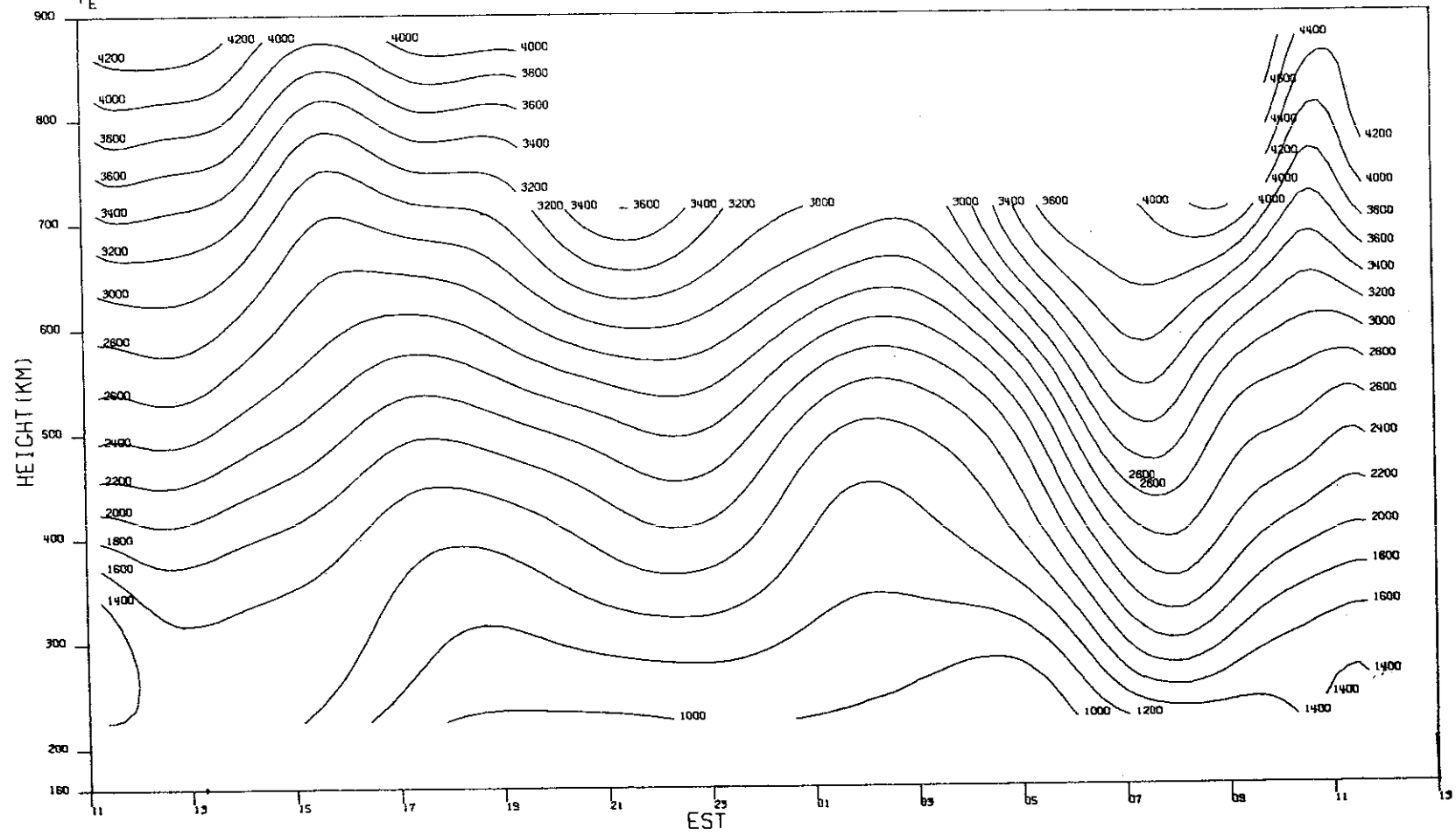


(a)

Fig. 2(a-z). Computer-drawn plots showing contours of constant electron temperature T_e (in $^{\circ}\text{K}$) as functions of height and time for the measurements made in 1970 (Table IV).

MILLSTONE HILL
20-21, JAN, 1970
T_E

-9-5151



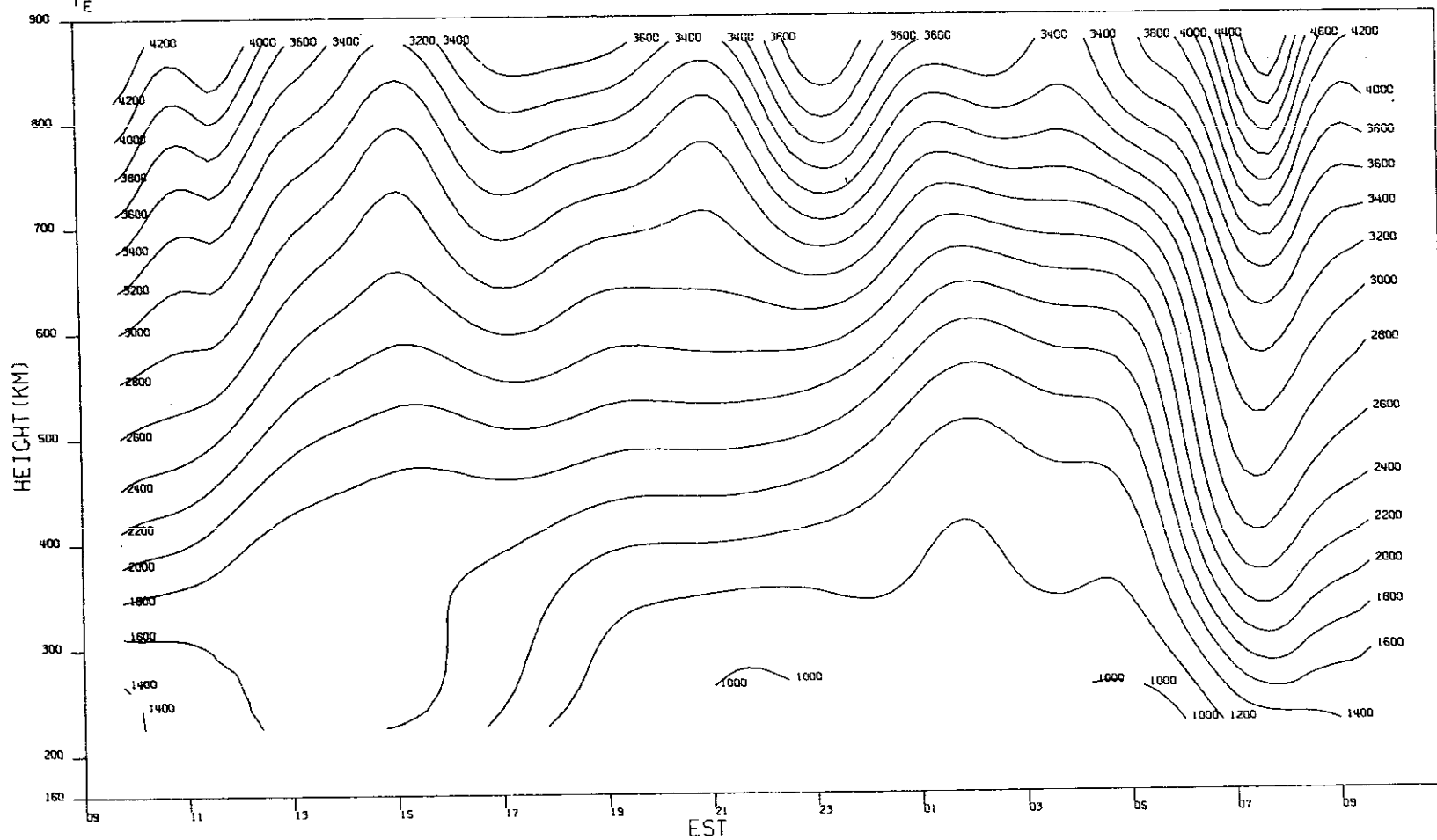
51

(b)

Fig.2(a-z). Continued.

MILLSTONE HILL
17-18. FEB. 1970
T_E

-9-5152



(c)

Fig. 2(a-z). Continued.

MILLSTONE HILL
23-24.FEB.1970

T_E

-9-5153

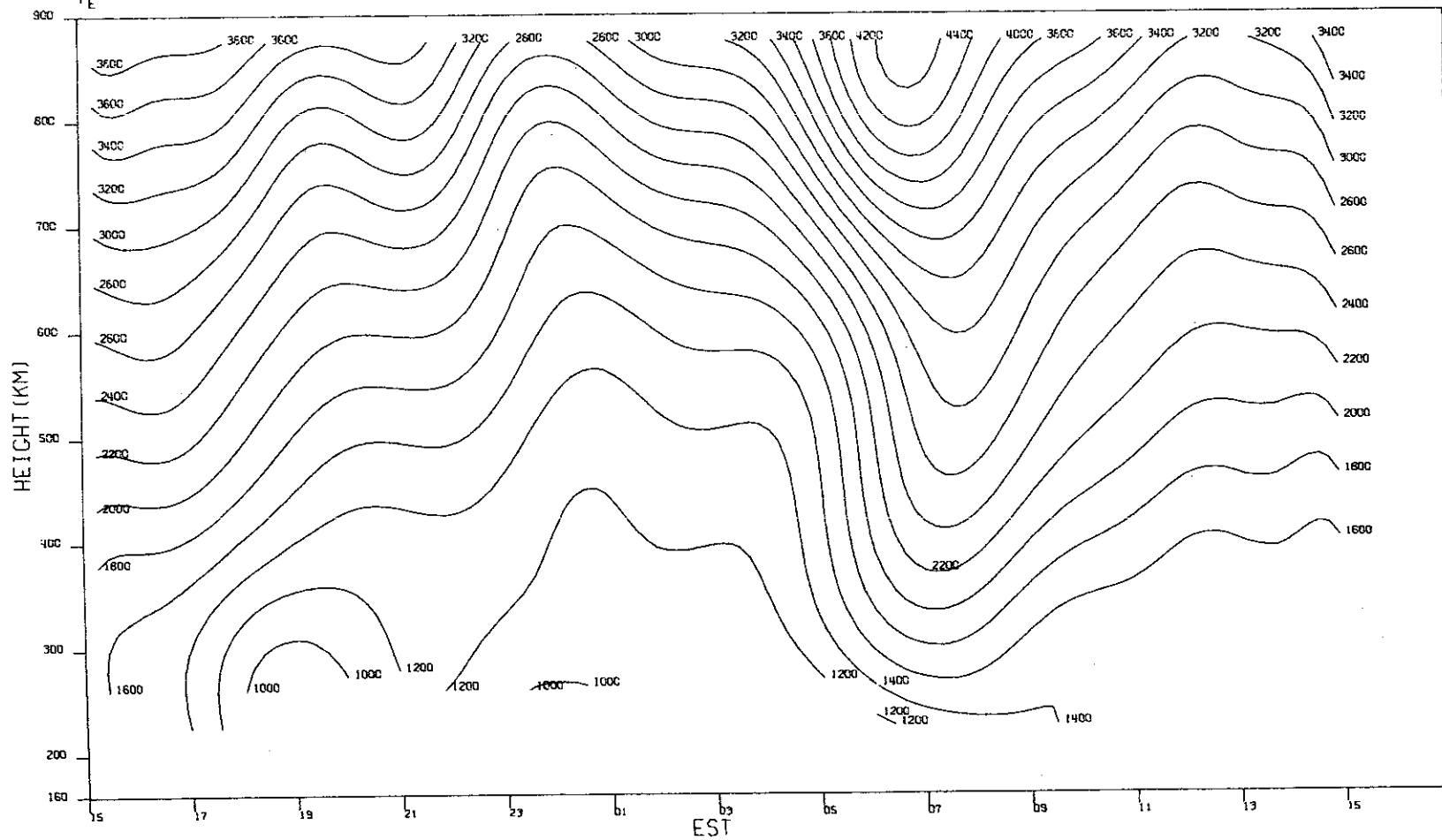
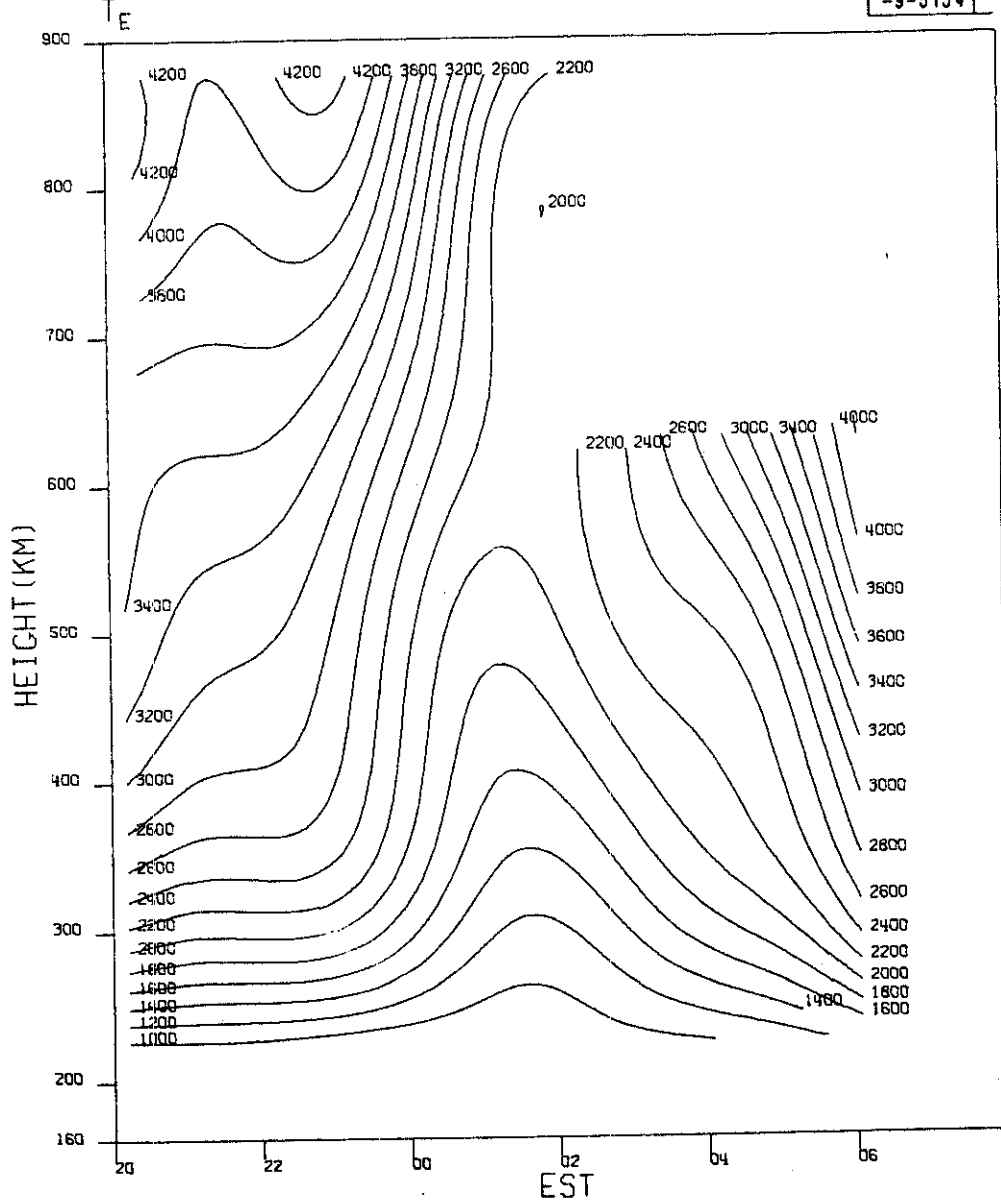


Fig.2(a-z). Continued.

MILLSTONE HILL
09, MAR, 1970

-9-5154

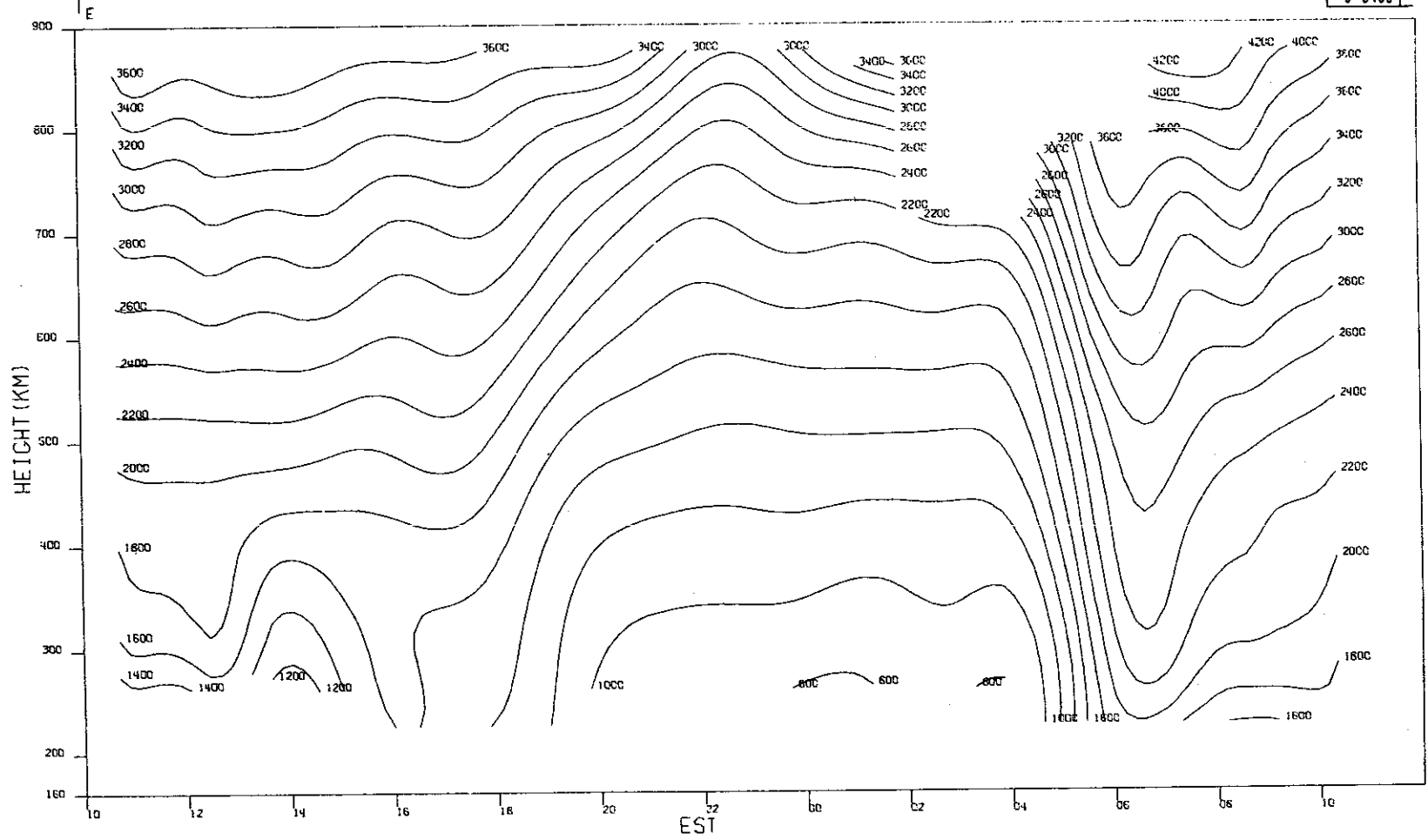


(e)

Fig. 2(a-z). Continued.

MILLSTONE HILL
17-18, MAR, 1970

-9-5155

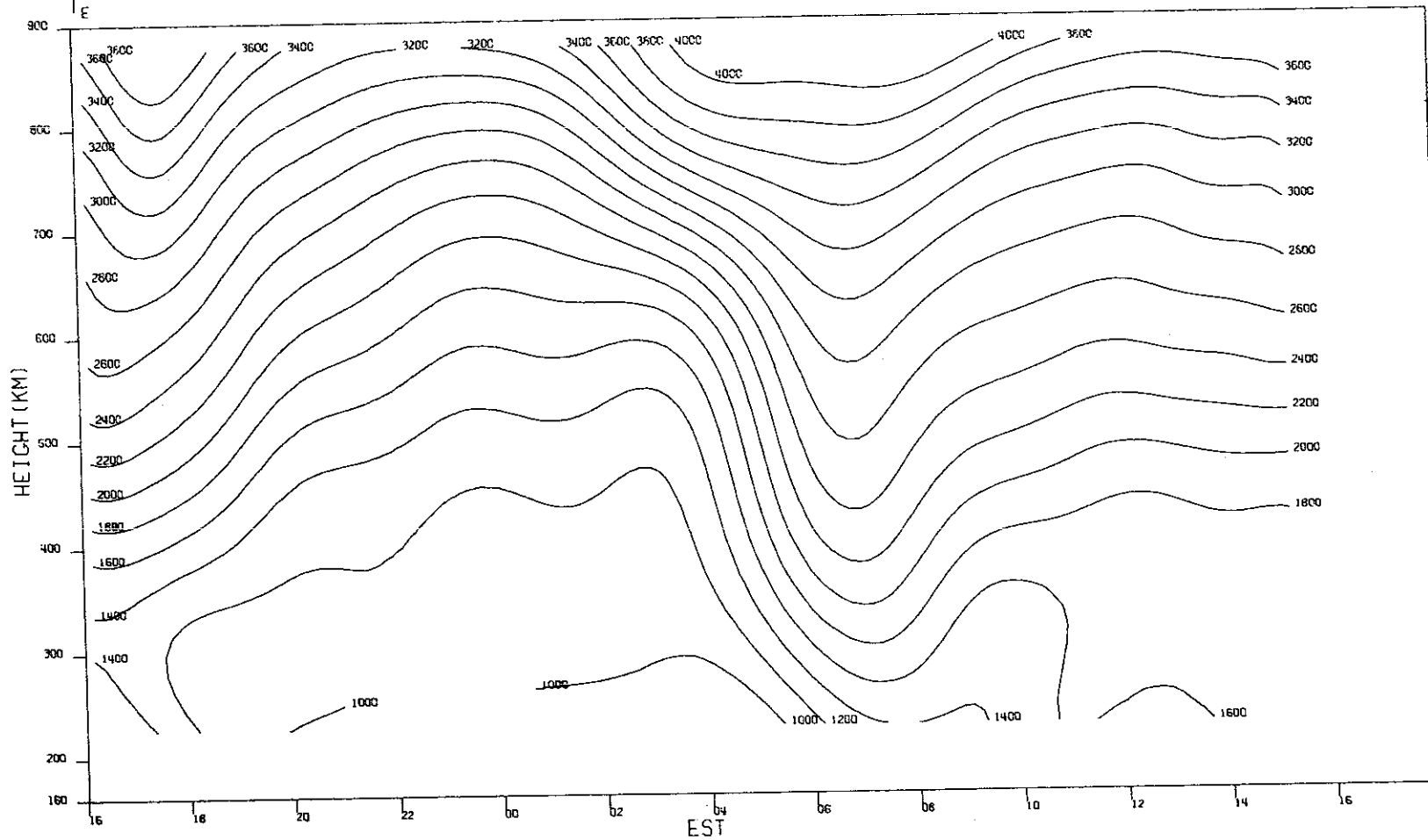


(f)

Fig. 2(a-z). Continued.

MILLSTONE HILL
23-24, MAR. 1970

-9-5156

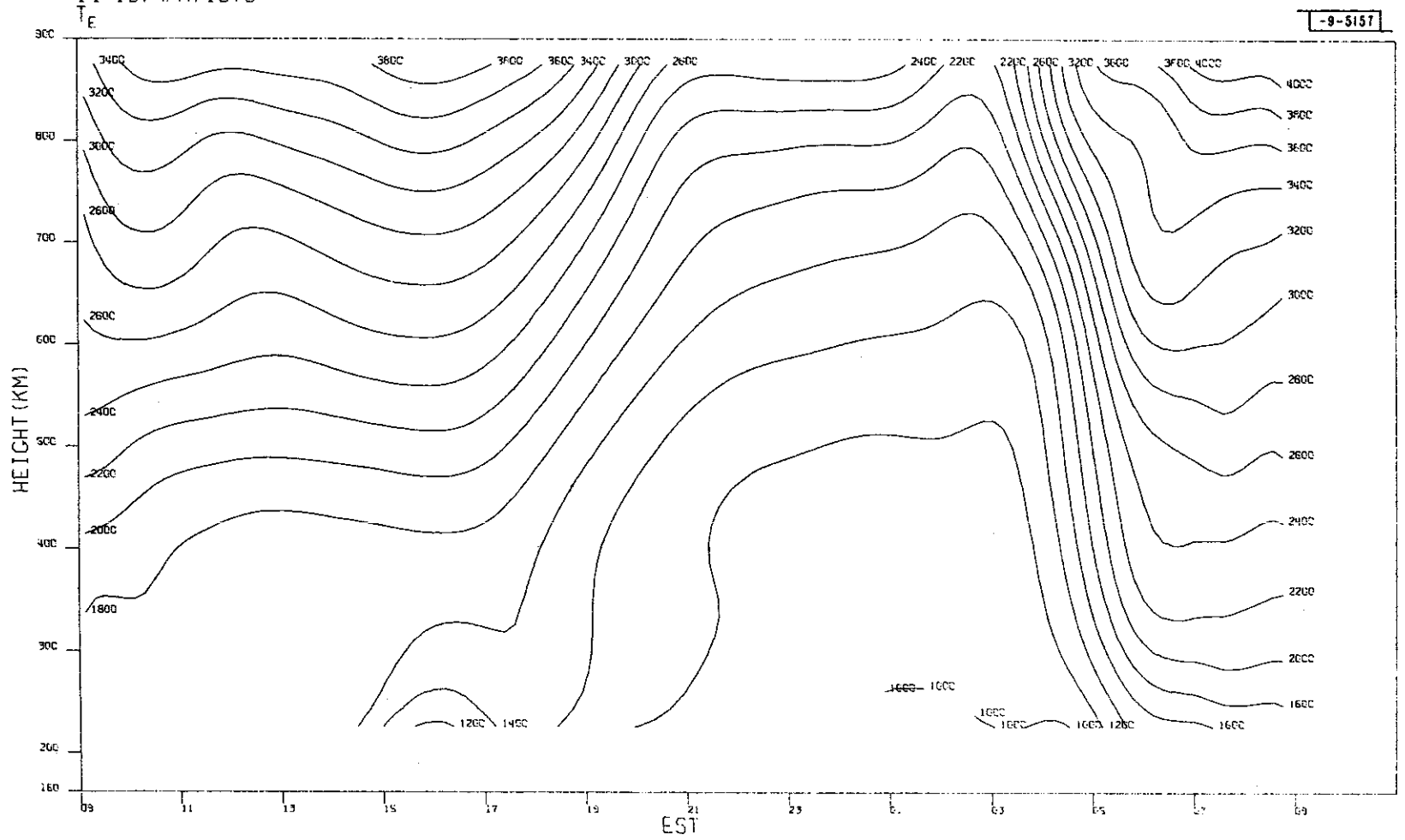


56

(g)

Fig.2(a-z). Continued.

MILLSTONE HILL
14-15, APR, 1970

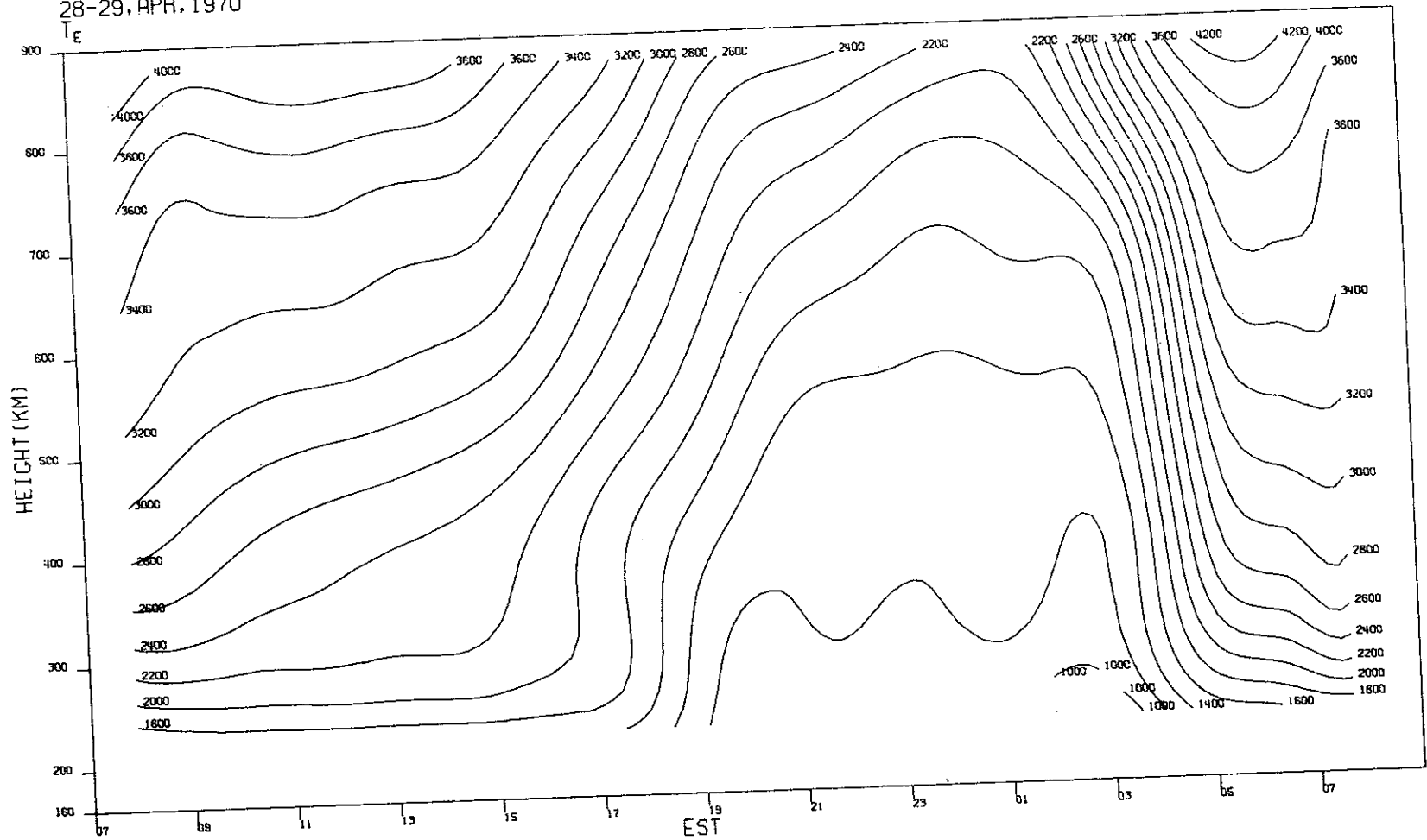


(h)

Fig.2(a-z). Continued.

MILLSTONE HILL
28-29, APR, 1970

- 9 - 5158



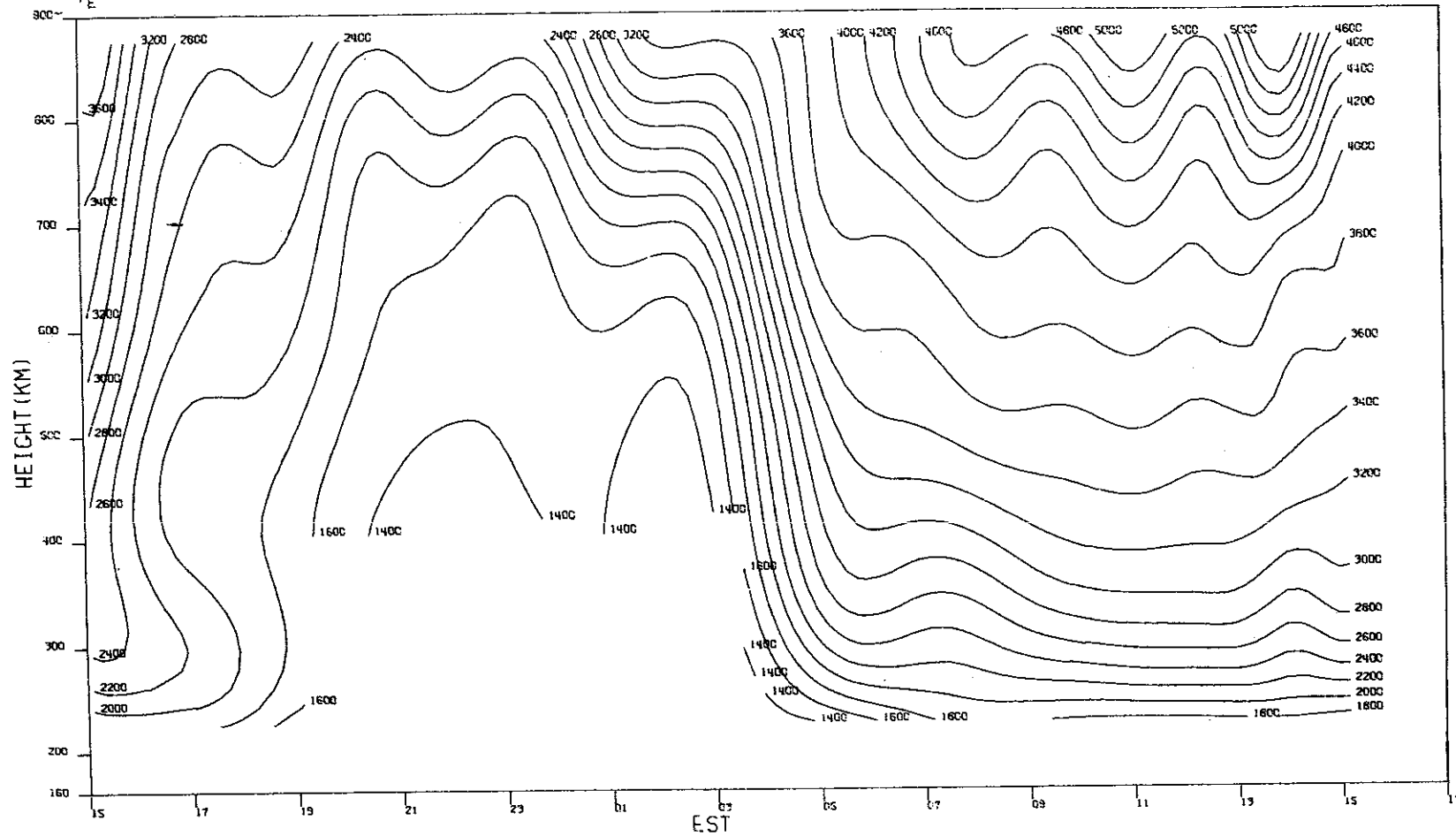
58

(i)

Fig. 2(a-z). Continued.

MILLSTONE HILL
12-13. MAY, 1970

-9-5159



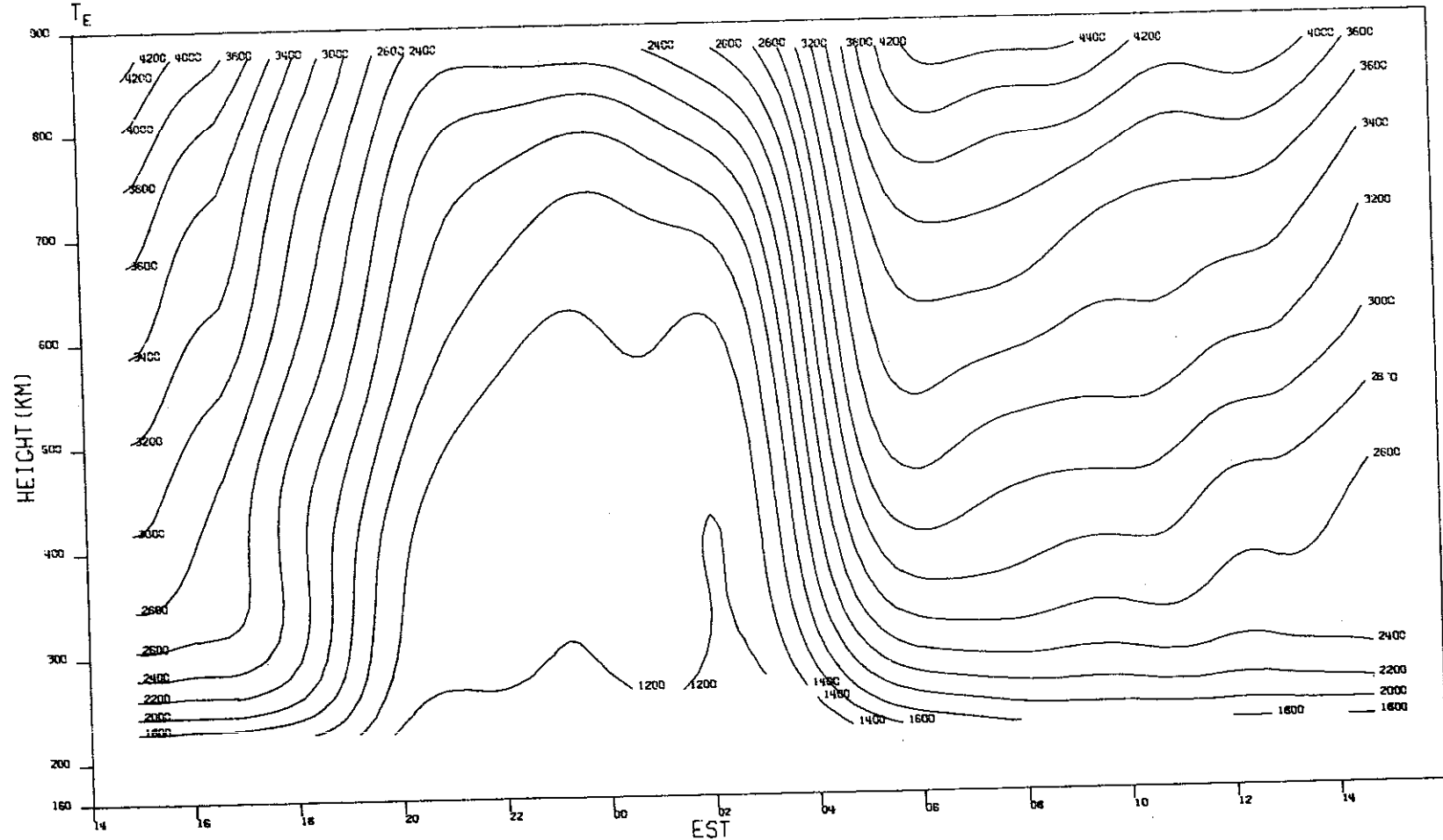
59

(j)

Fig. 2(a-z). Continued.

MILLSTONE HILL
18-19, MAY, 1970

-9-5160



09

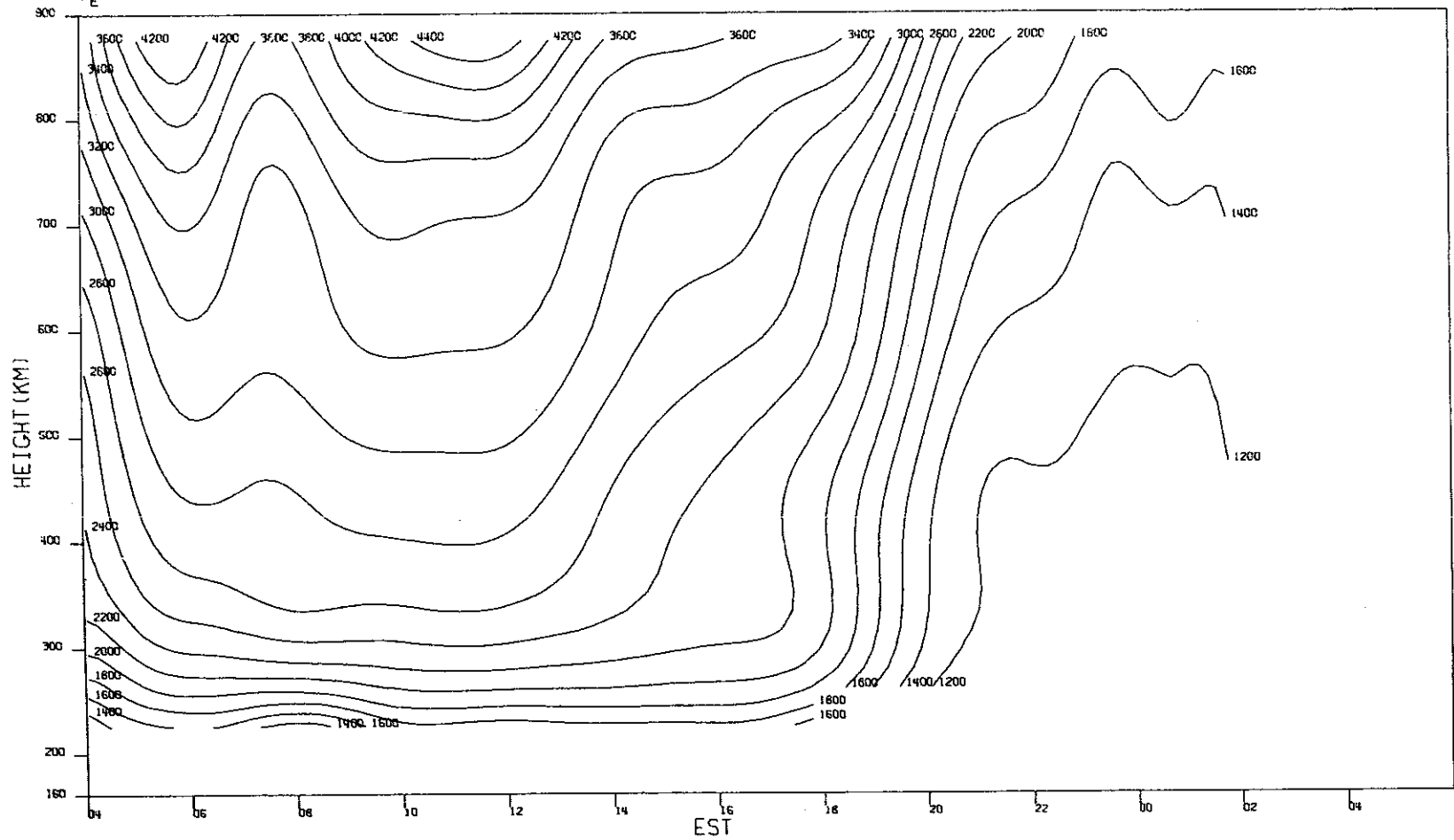
(k)

Fig.2(a-z). Continued.

MILLSTONE HILL
10-11, JUN, 1970

T_E

-9-5161



61

(I)

Fig.2(a-z). Continued.

MILLSTONE HILL
23-24, JUN. 1970

-9-5162

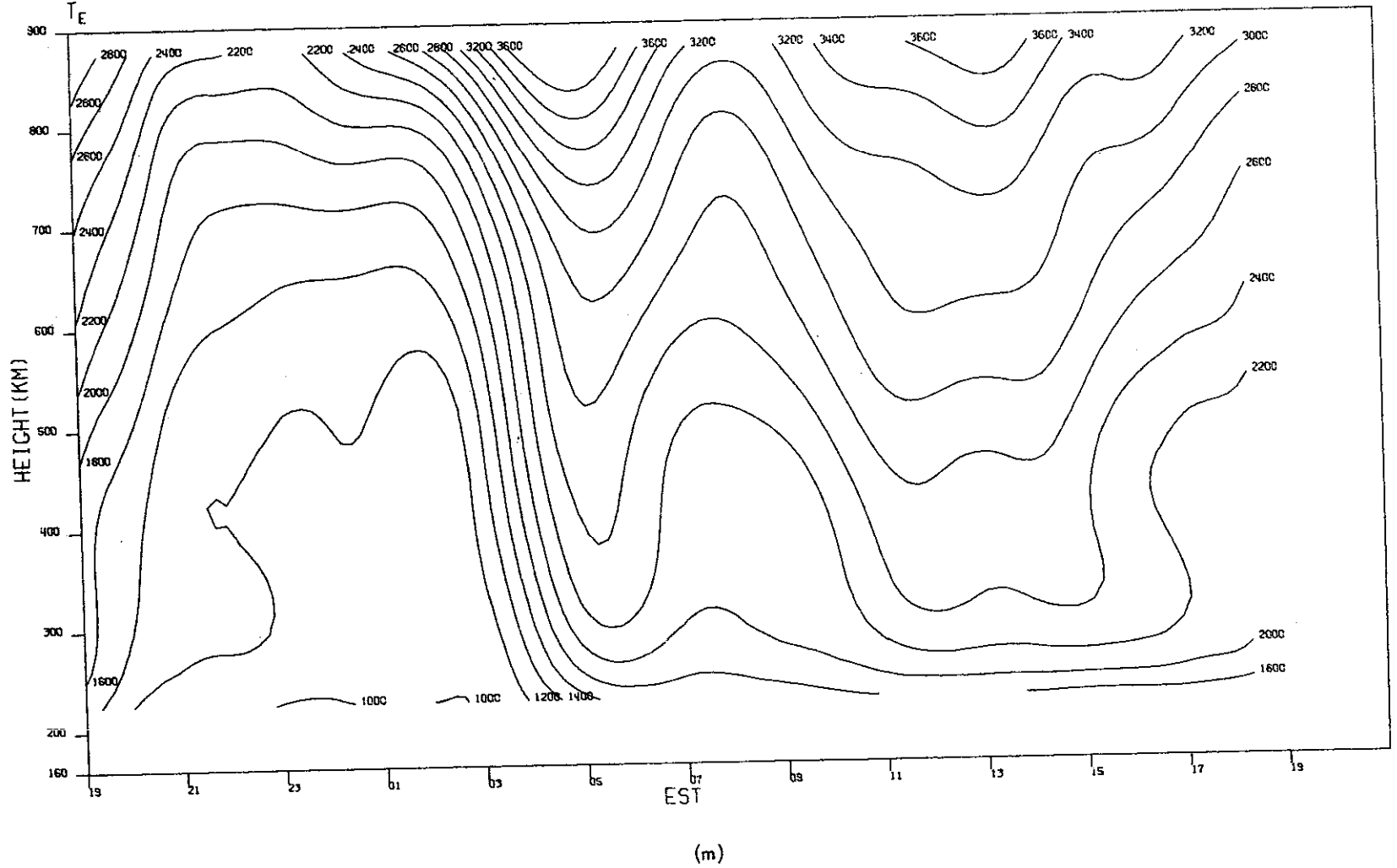


Fig. 2(a-z). Continued.

MILLSTONE HILL
07-08, JUL, 1970

-8-5163

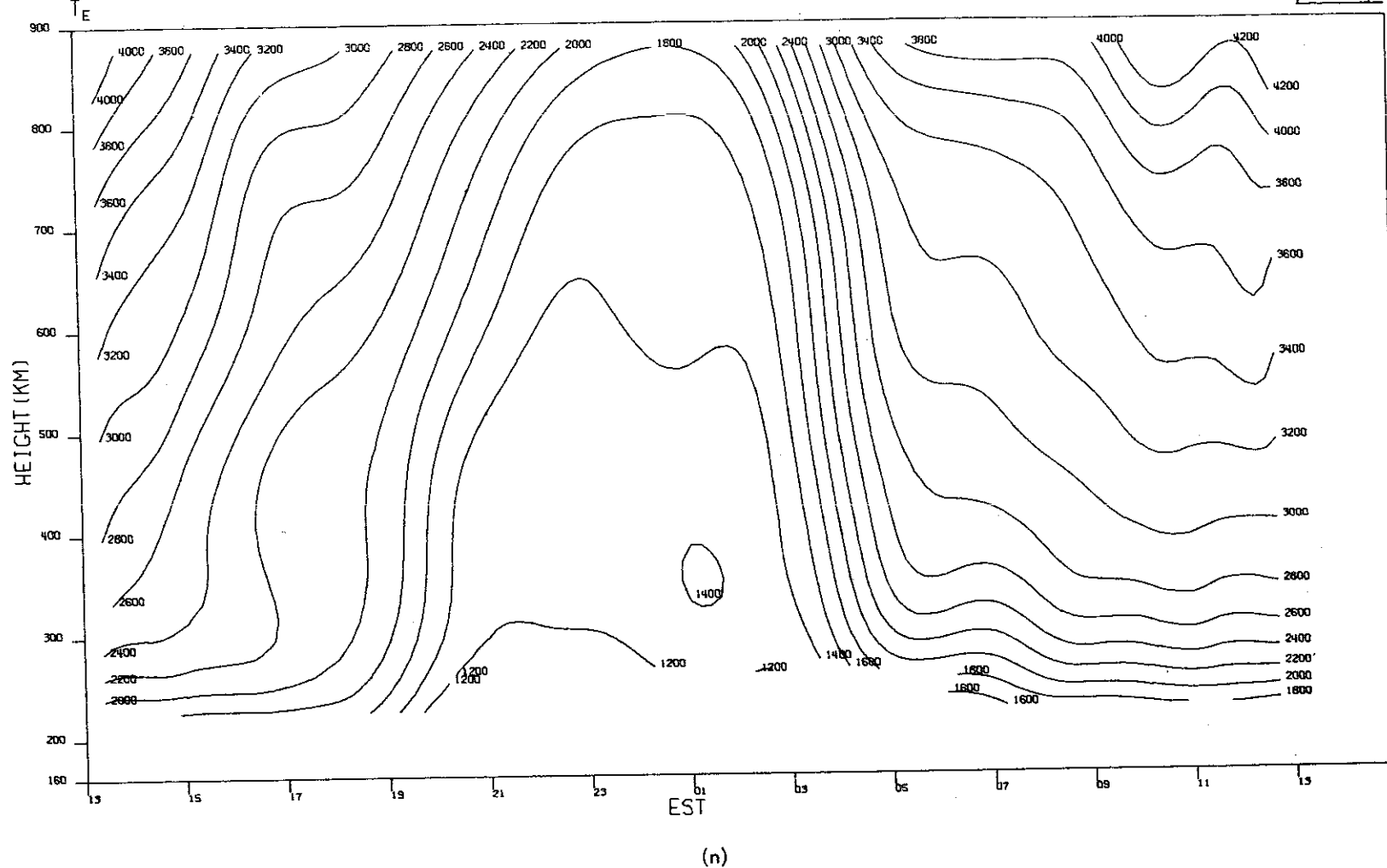
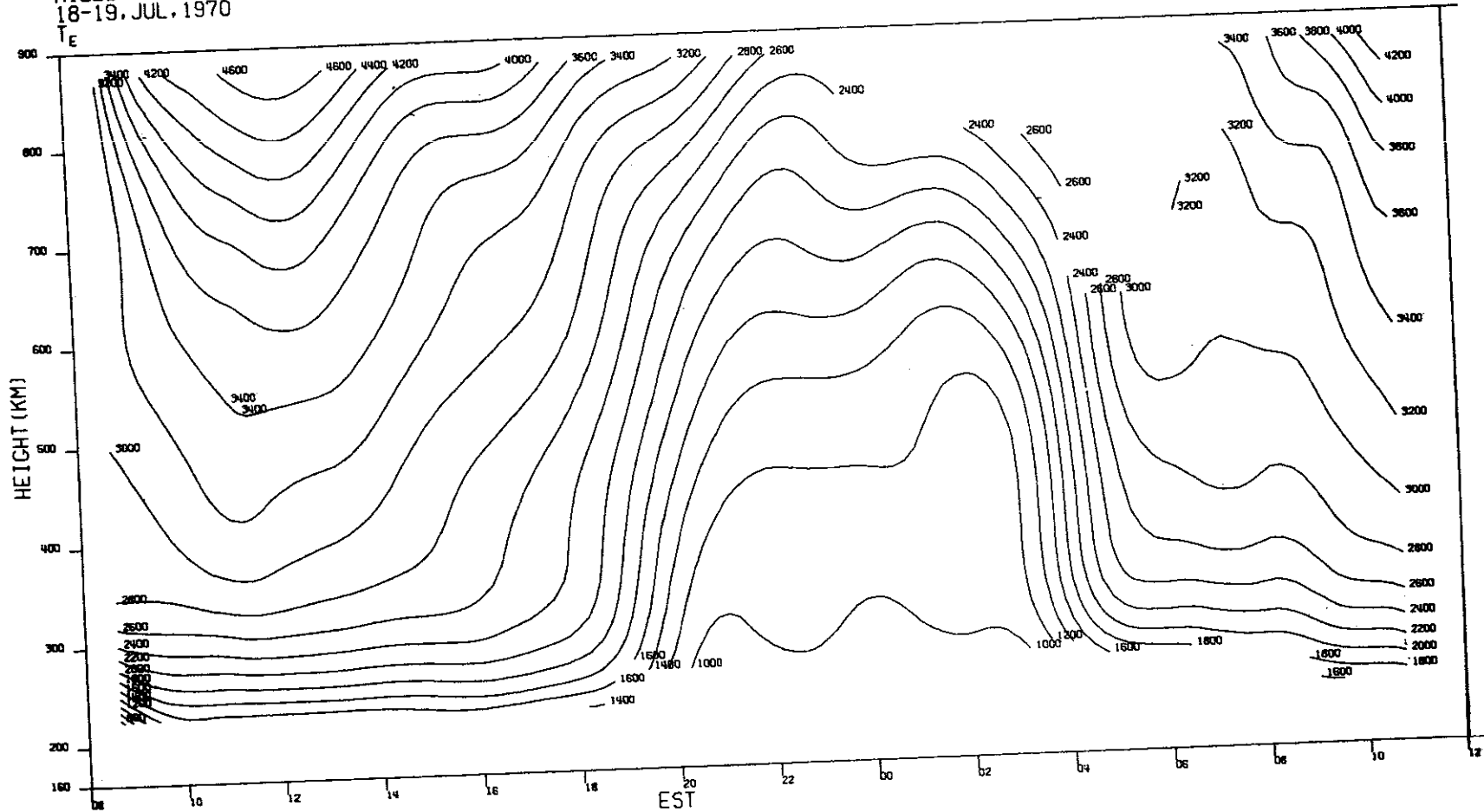


Fig. 2(a-z). Continued.

MILLSTONE HILL
18-19 JUL. 1970

-9-5164



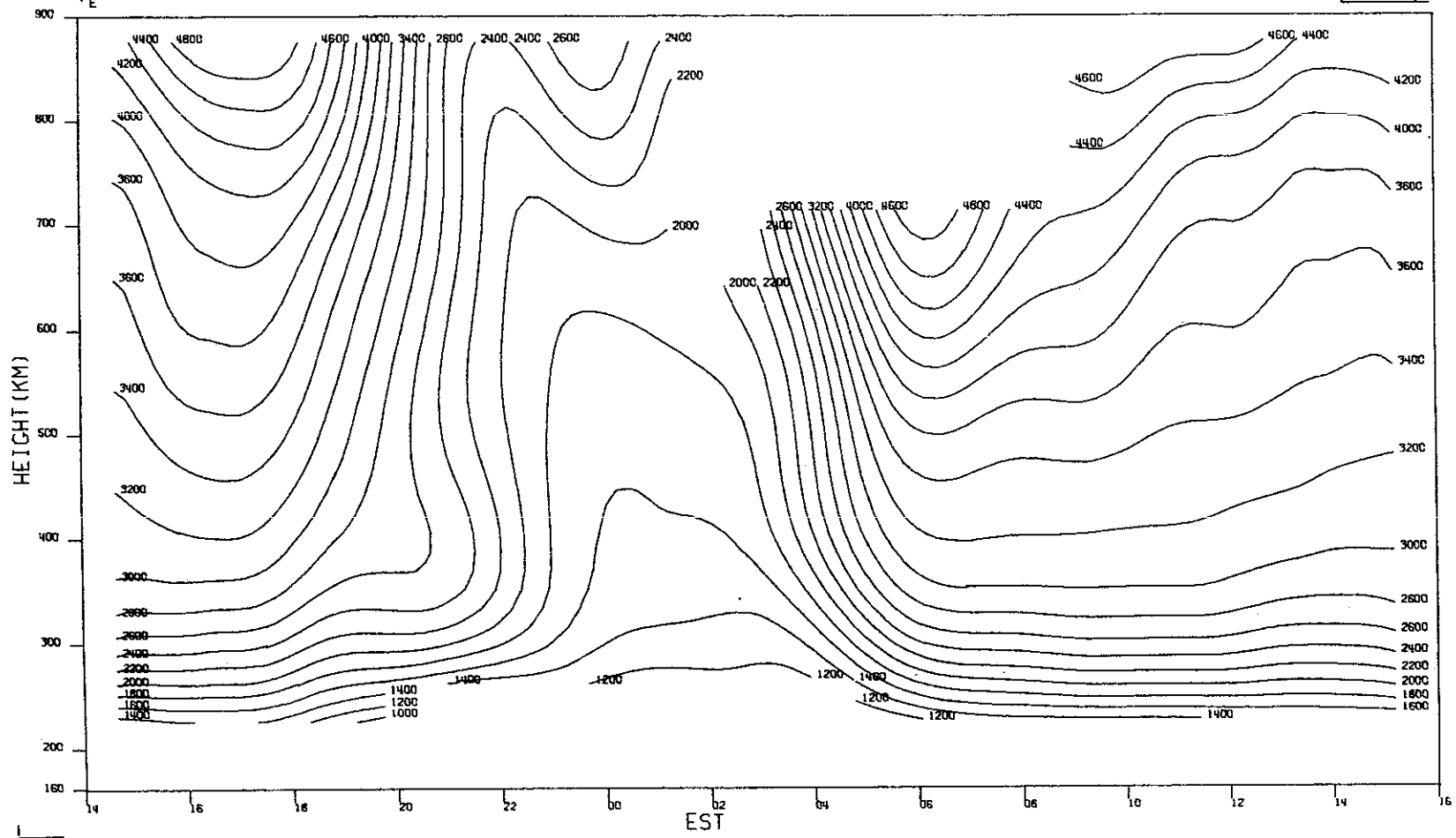
64

(o)

Fig.2(a-z). Continued.

MILLSTONE HILL
17-18. AUG. 1970

-9-5165



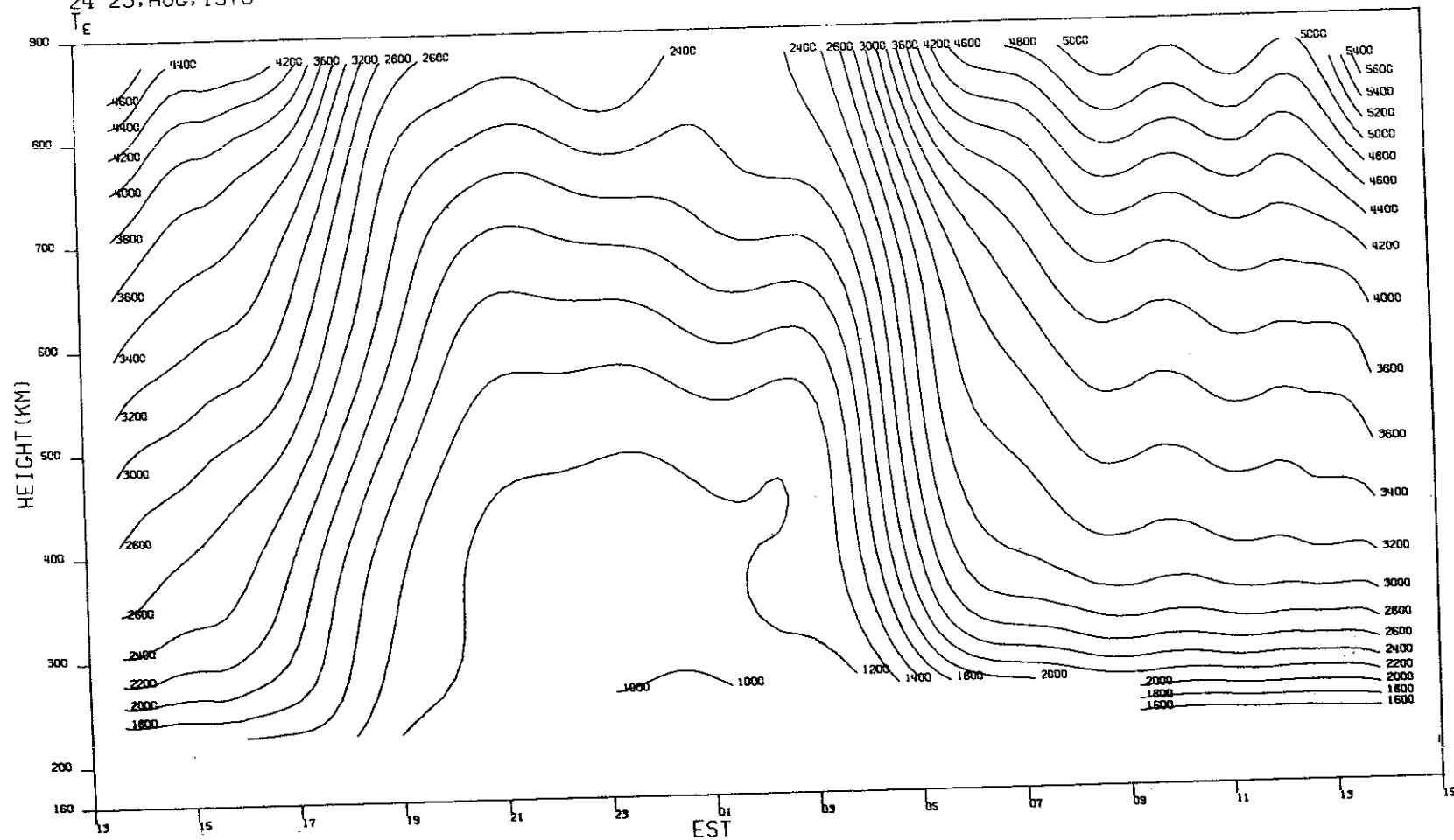
69

(p)

Fig.2(a-z). Continued.

MILLSTONE HILL
24-25, AUG, 1970

-9-5166

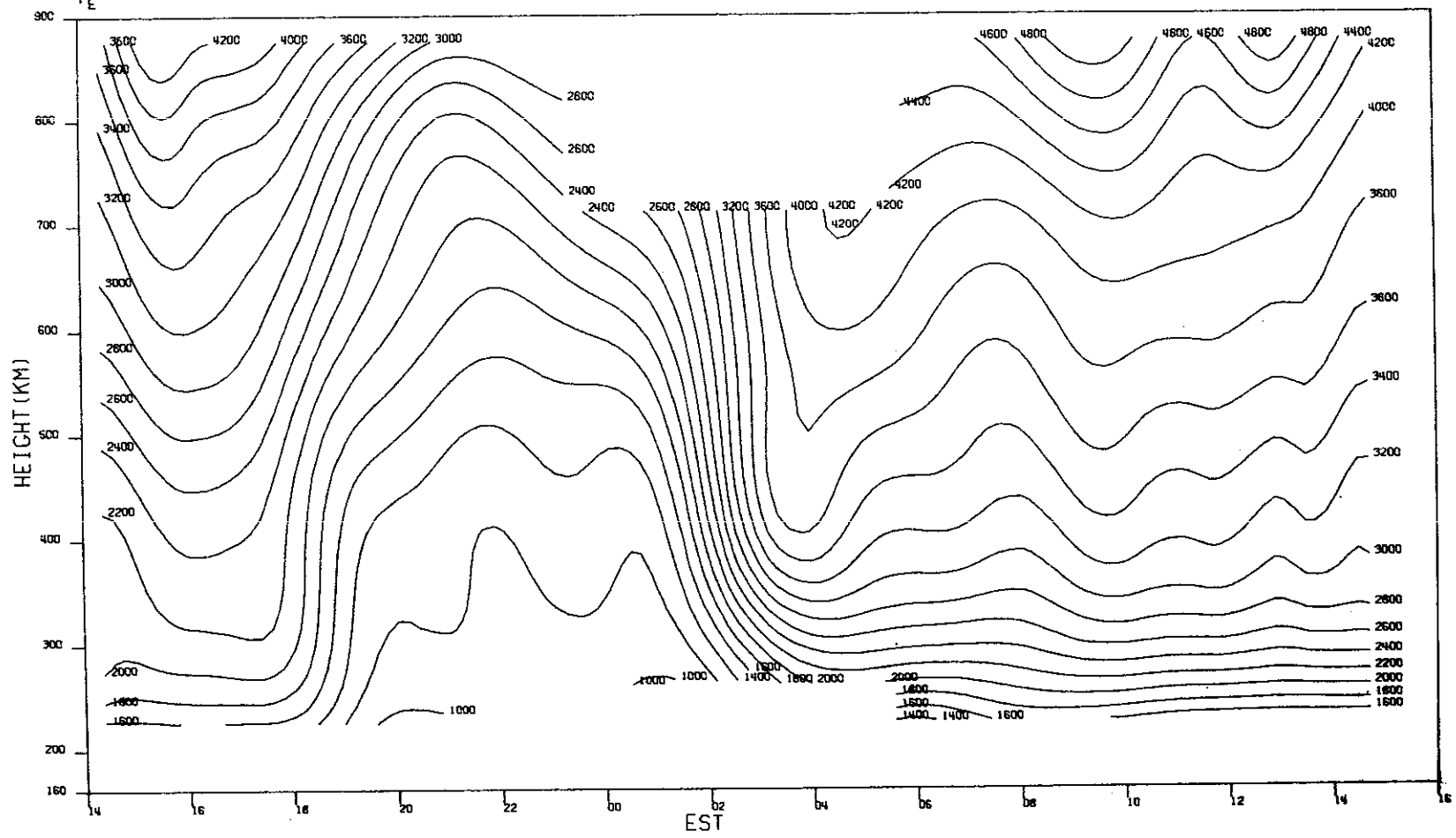


(q)

Fig.2(a-z). Continued.

MILLSTONE HILL
31AUG-01SEP. 1970

-9-5167



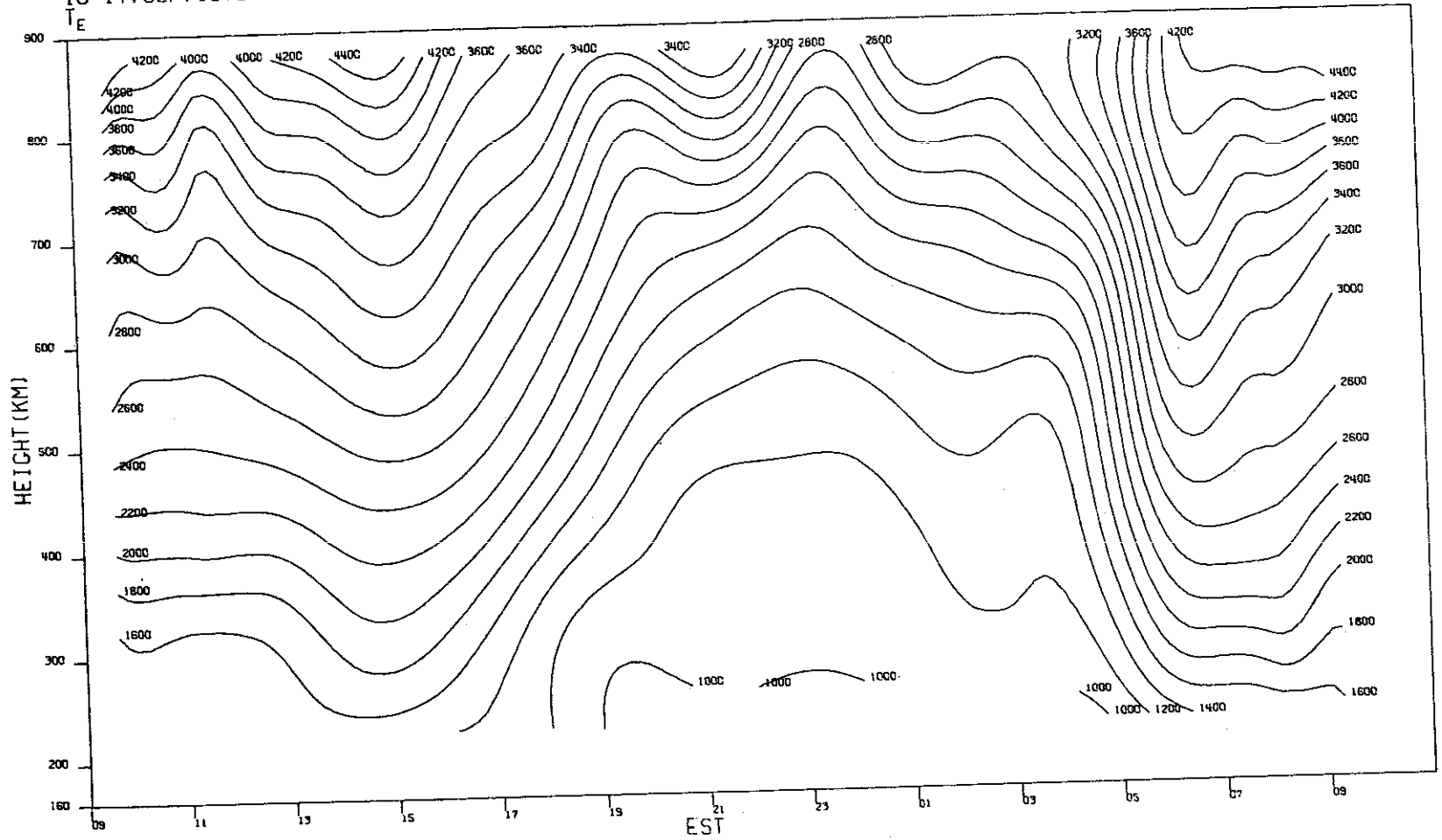
67

(r)

Fig.2(a-z). Continued.

MILLSTONE HILL
16-17. SEP. 1970

-9-5168



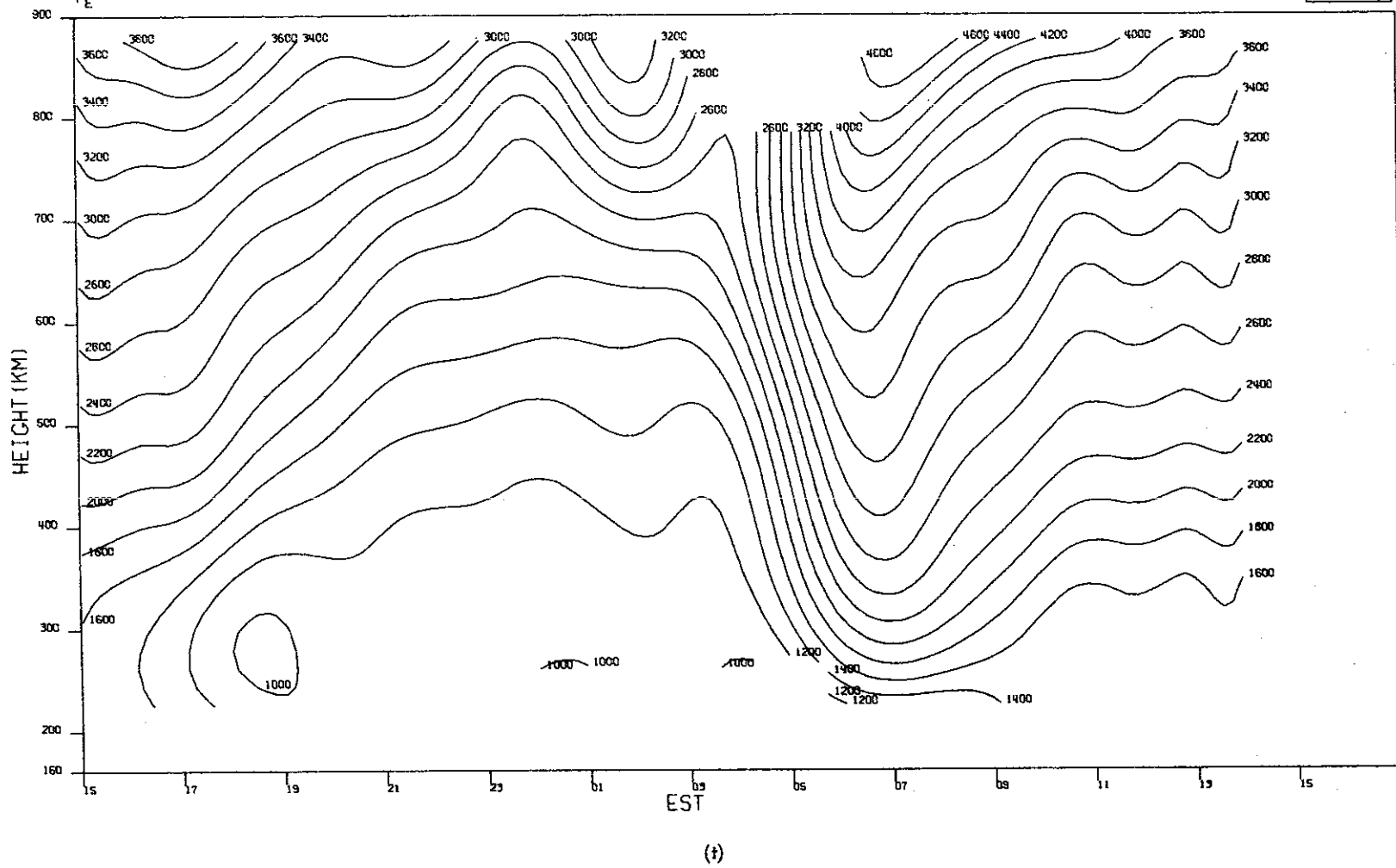
89

(s)

Fig. 2(a-z). Continued.

MILLSTONE HILL
28-29, SEP. 1970
T
E

-9-5169

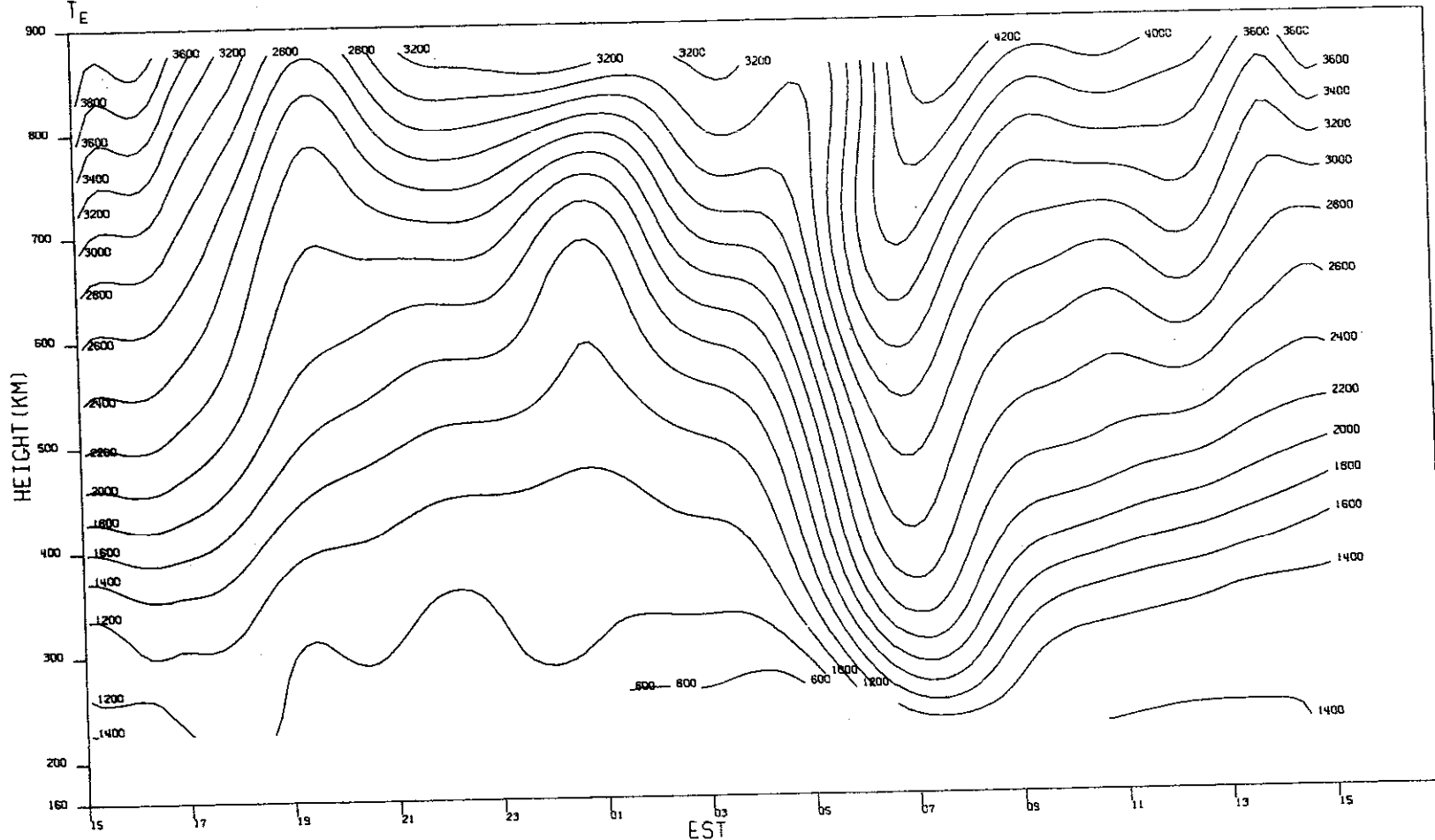


69

Fig. 2(a-z). Continued.

MILLSTONE HILL
05-06, OCT. 1970

-9-5170



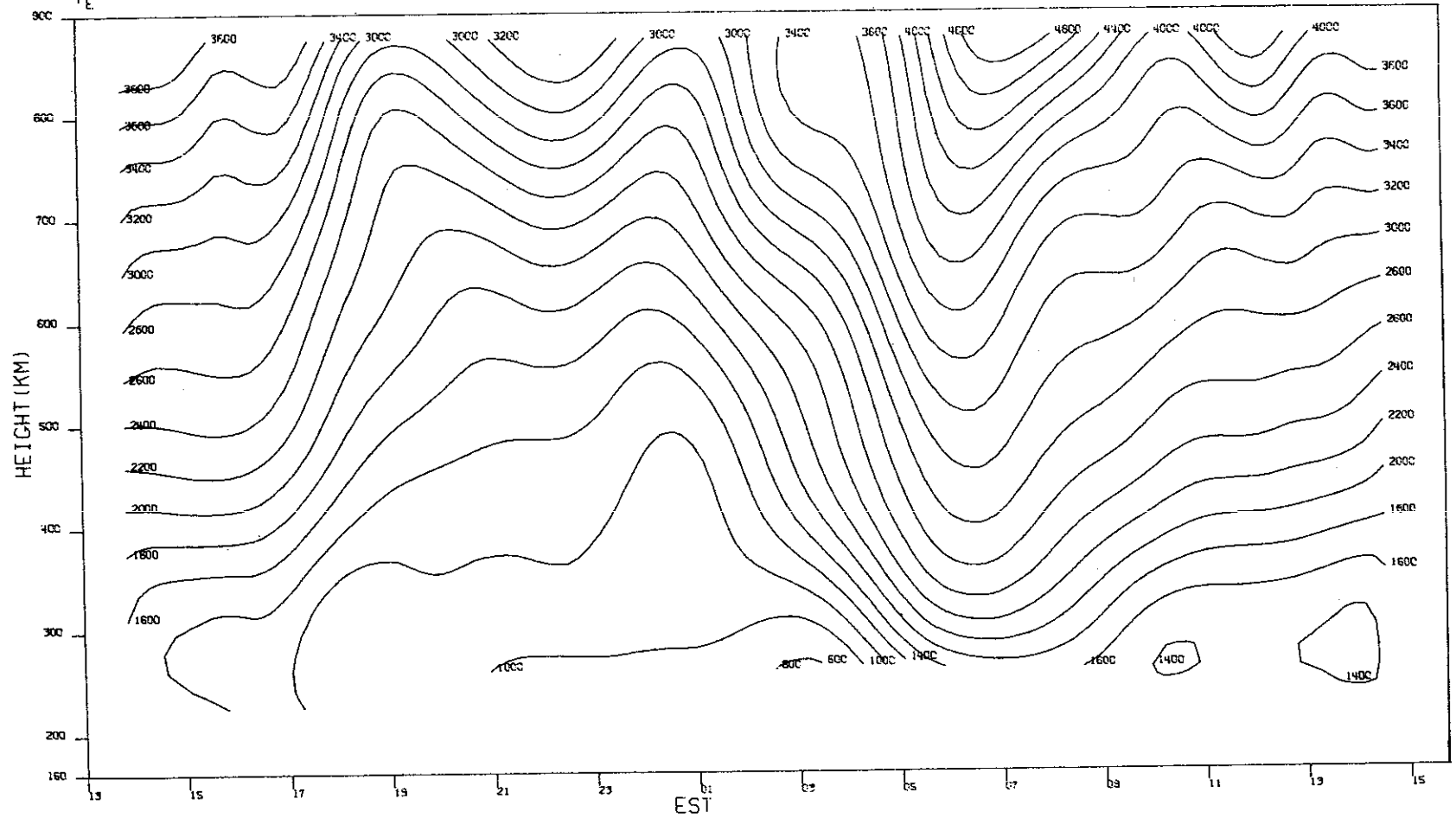
70

(u)

Fig.2(a-z). Continued.

MILLSTONE HILL
13-14. OCT. 1970

-9-5171

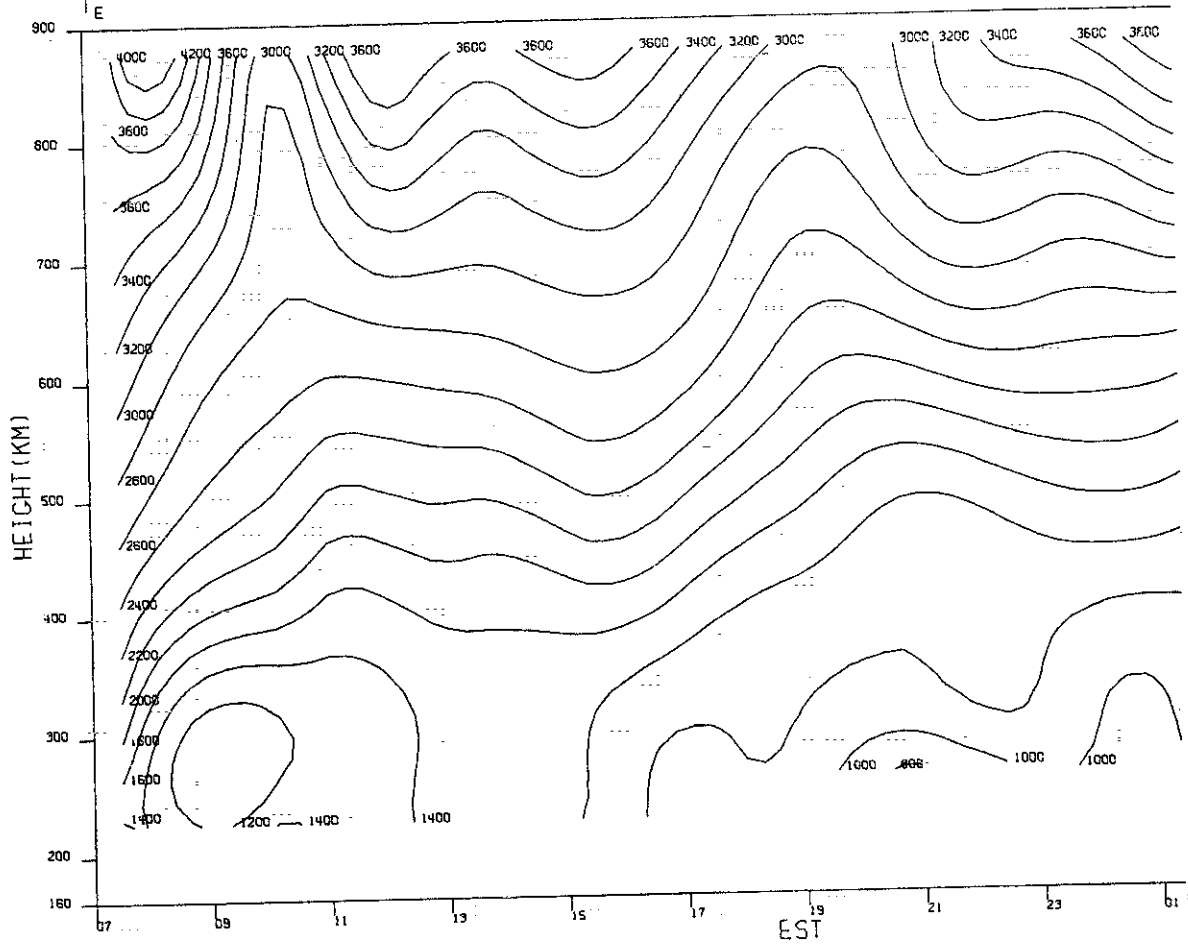


71

(v)

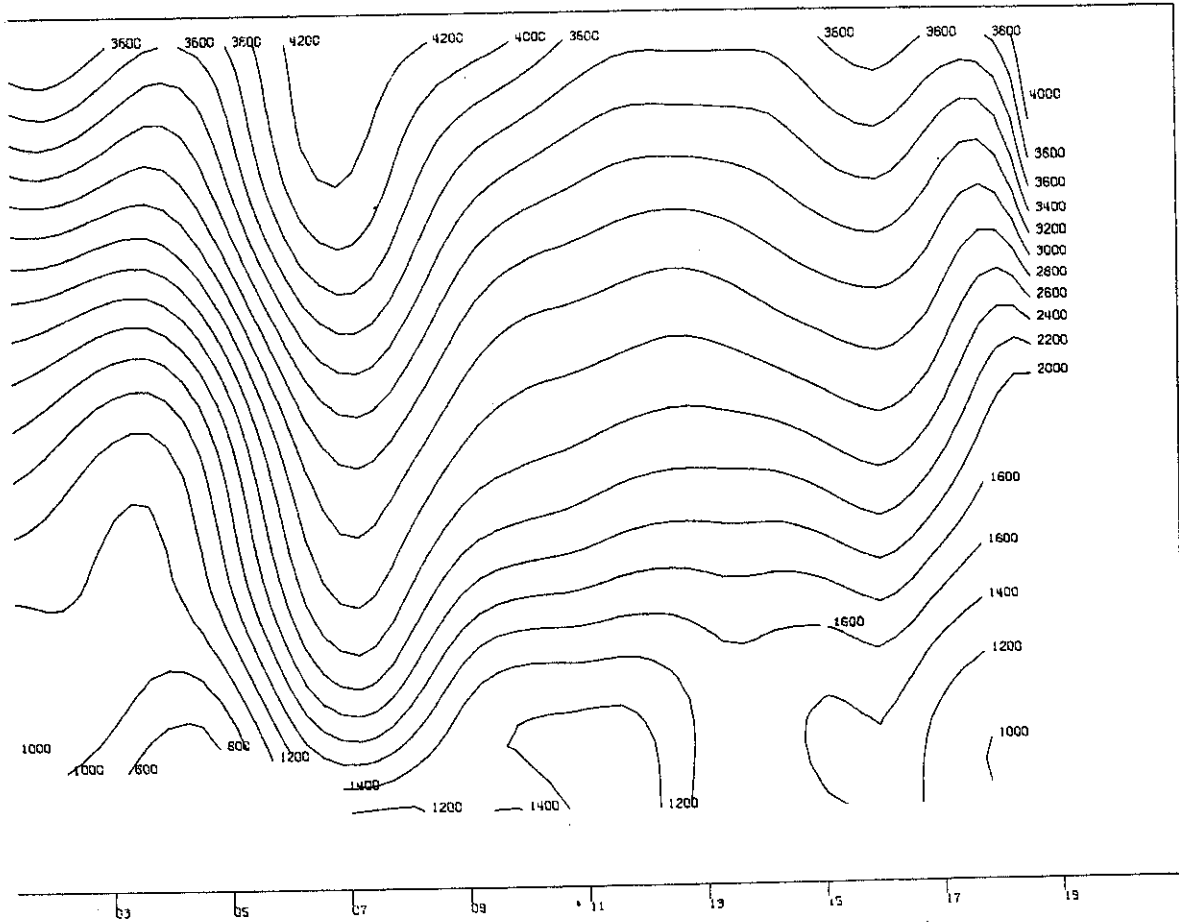
Fig. 2(a-z). Continued.

MILLSTONE HILL
31 OCT-01 NOV. 1970
T_E



(w)

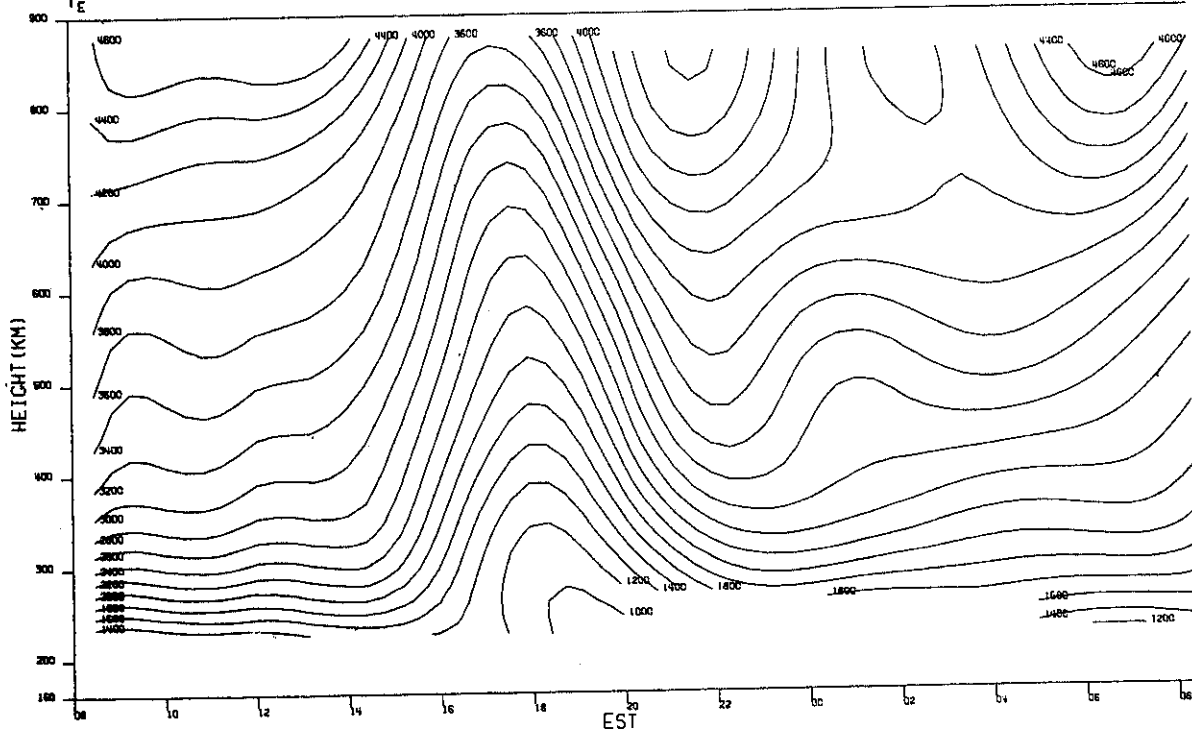
Fig. 2(a-z). Continued.



(w)

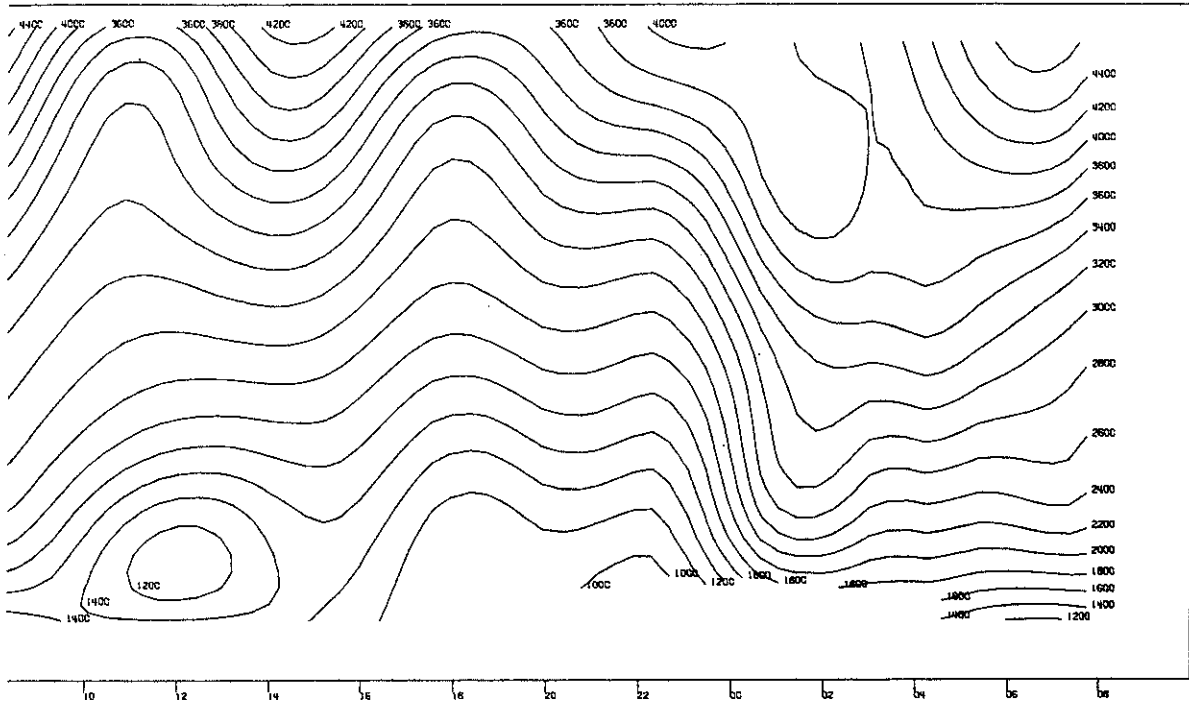
Fig.2(a-z). Continued.

MILLSTONE HILL
07-09. NOV. 1970
T_e



(x)

Fig. 2(a-z). Continued.

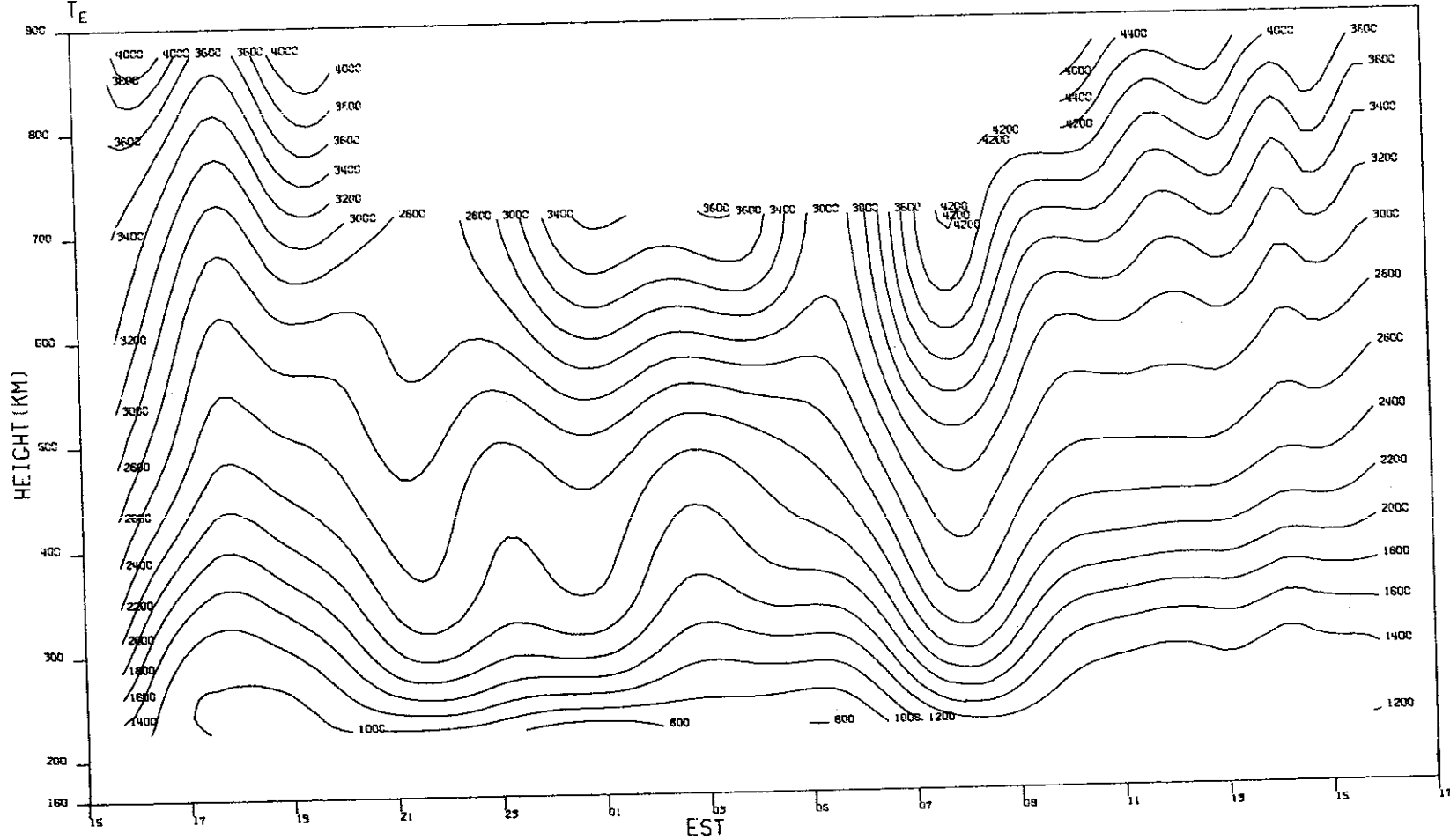


(x)

Fig.2(a-z). . Continued.

MILLSTONE HILL
21-22, DEC. 1970

-9-5174



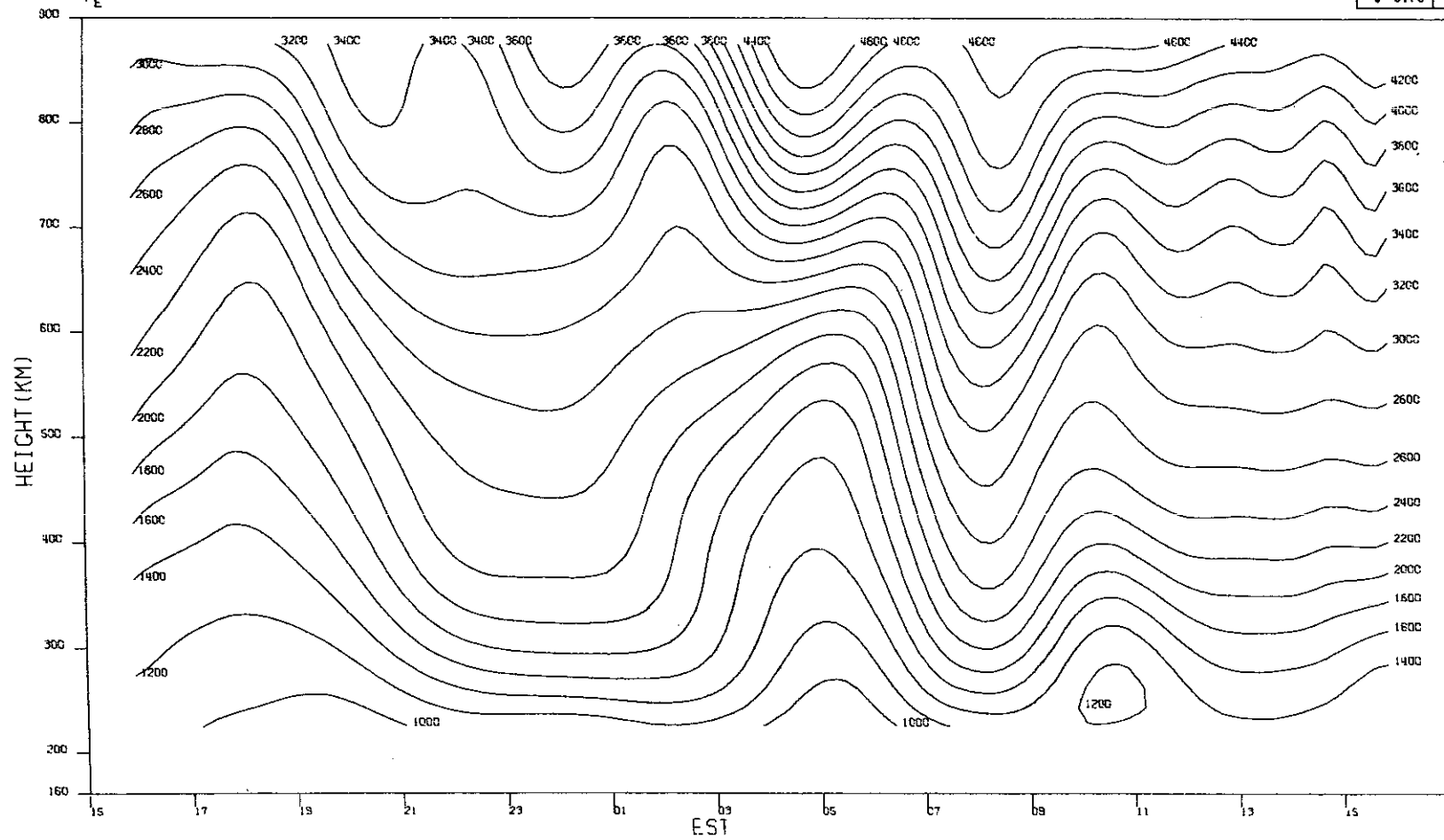
76

(y)

Fig.2(a-z). Continued.

MILLSTONE HILL
28-29, DEC. 1970
T_E

-9-5175



77

(z)

Fig.2(a-z). Continued.

and October, conjugate sunrise occurs a few hours before local sunrise. Depending on the magnitude of the local electron density, the photoelectron flux established at conjugate sunrise ($\chi_c < 105^\circ$) may cause the temperature to begin increasing prior to local sunrise. Figures 2(u) and 2(v) appear to provide clear examples of this behavior.

Anomalously high electron temperatures are associated with magnetically disturbed periods and may be caused by heat conducted from the magnetosphere where it is generated by the decay of ring current particles¹³ or created *in situ* by precipitation of soft electrons.²⁷ Often it is impossible to distinguish between these sources except at night when, at Millstone, particle precipitation tends to fill in the valley between the E- and the F-layers. The very high temperatures observed on 9 March [Fig. 2(e)] prior to midnight are thought to be associated with particle precipitation [cf., Fig. 1(e)]. The increase in T_e after midnight is thought to be caused by conjugate sunrise.²⁷ As noted above, there is also evidence for particle precipitation during the evening of 17 August [Fig. 1(p)] which appears to have maintained the electron temperature to high values as late as 2200 EST.

The very low values of electron density during the daytime on 7 November caused the temperature to be several hundred degrees above normal. This situation prevailed at least until midnight. The heat flux conducted into the layer was also considerably higher on this day, suggesting that during 7 November considerable heat was being supplied to the local ionosphere by the decay of ring current protons in the magnetosphere.

C. Ion Temperature

The ion temperature is plotted in the contour diagrams [Figs. 3(a-z)] at 100°K intervals. At low altitudes (<350 km), T_i varies in a similar fashion to the neutral temperature and values of the exospheric temperature T_∞ derived from these data have been reported by Salah and Evans.²¹ At higher altitudes (400 to 700 km), heat supplied to the ions via coulomb encounters with the electrons raises the ion temperature to a value intermediate between T_∞ and T_e . With increasing height, T_i tends toward T_e and begins to exhibit similar diurnal variations to those described above.

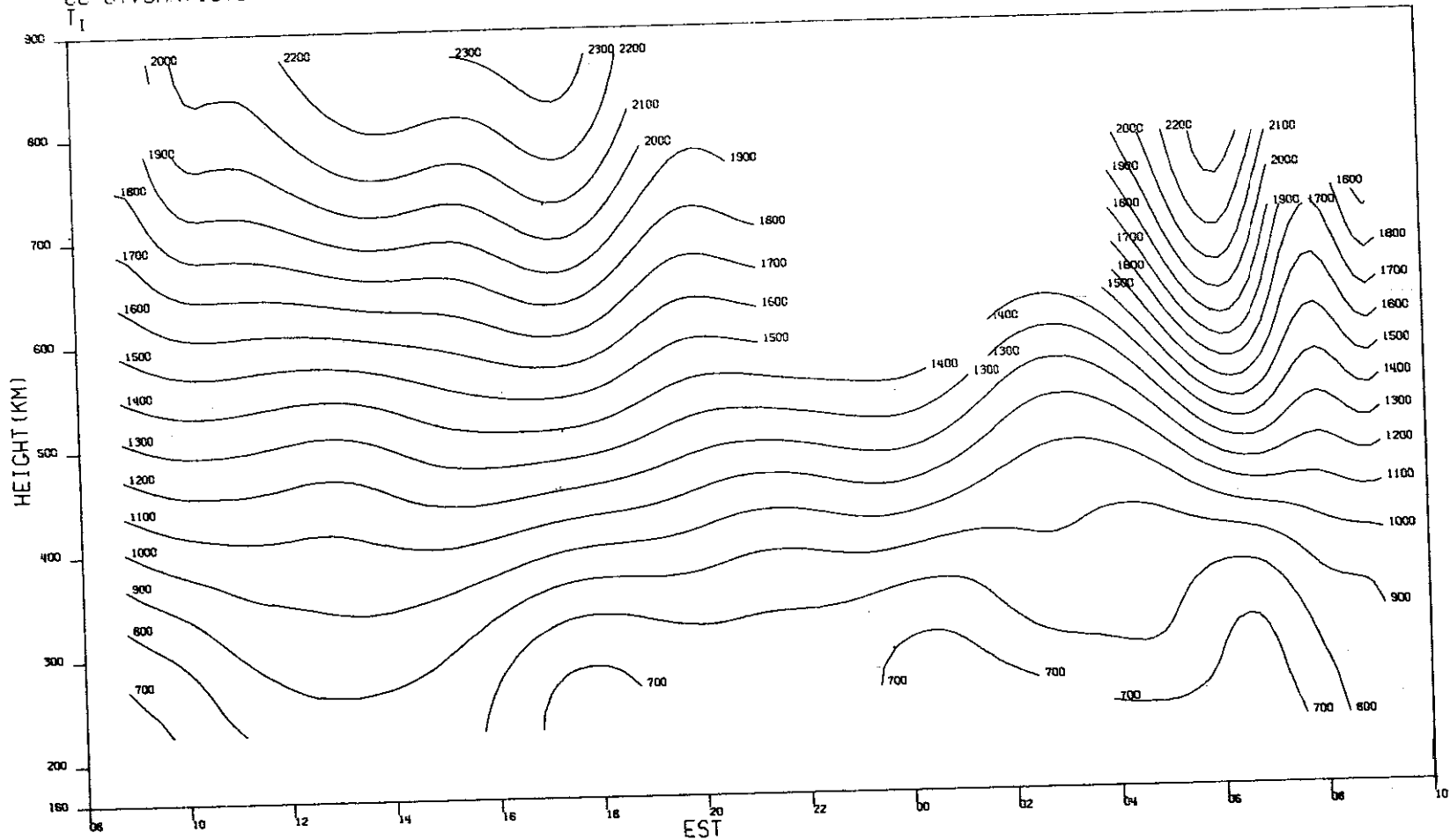
D. Vertical Velocity

Contour diagrams for the vertical velocity v_z are presented in Figs. 4(a-v). Owing to the difficulty in extracting this parameter from the measurements, it is the first quantity to be seriously degraded whenever the signal-to-noise ratio is reduced, or there are instrumental effects which reduce the quality of the spectra. Accordingly, useful results were not obtained for this quantity on 6-7 January, 20-21 January, 9 March and 7-9 November. On the first of these days, there appears to have been a systematic bias in the measurements which may have been introduced by the noise contributed by the poor gas discharge tube. On 20-21 January, the frequency synthesizer employed as one of the receiver local oscillators became unlocked with the site master frequency standard for a portion of the day, thereby introducing large errors in the drift velocity estimates.

We have not previously attempted to present contour diagrams for v_z owing to the large scatter in the data and the seeming existence of a time-varying systematic difference in the results gathered by the B- and C-modes.¹⁶ The source of this difference was thought to be the use (in 1969) of only half the B-mode filter bank for part of the year. However, analysis of data gathered in later years suggests that it persisted when the full filter bank was back in use.

MILLSTONE HILL
06-07, JAN. 1970

-9-5176



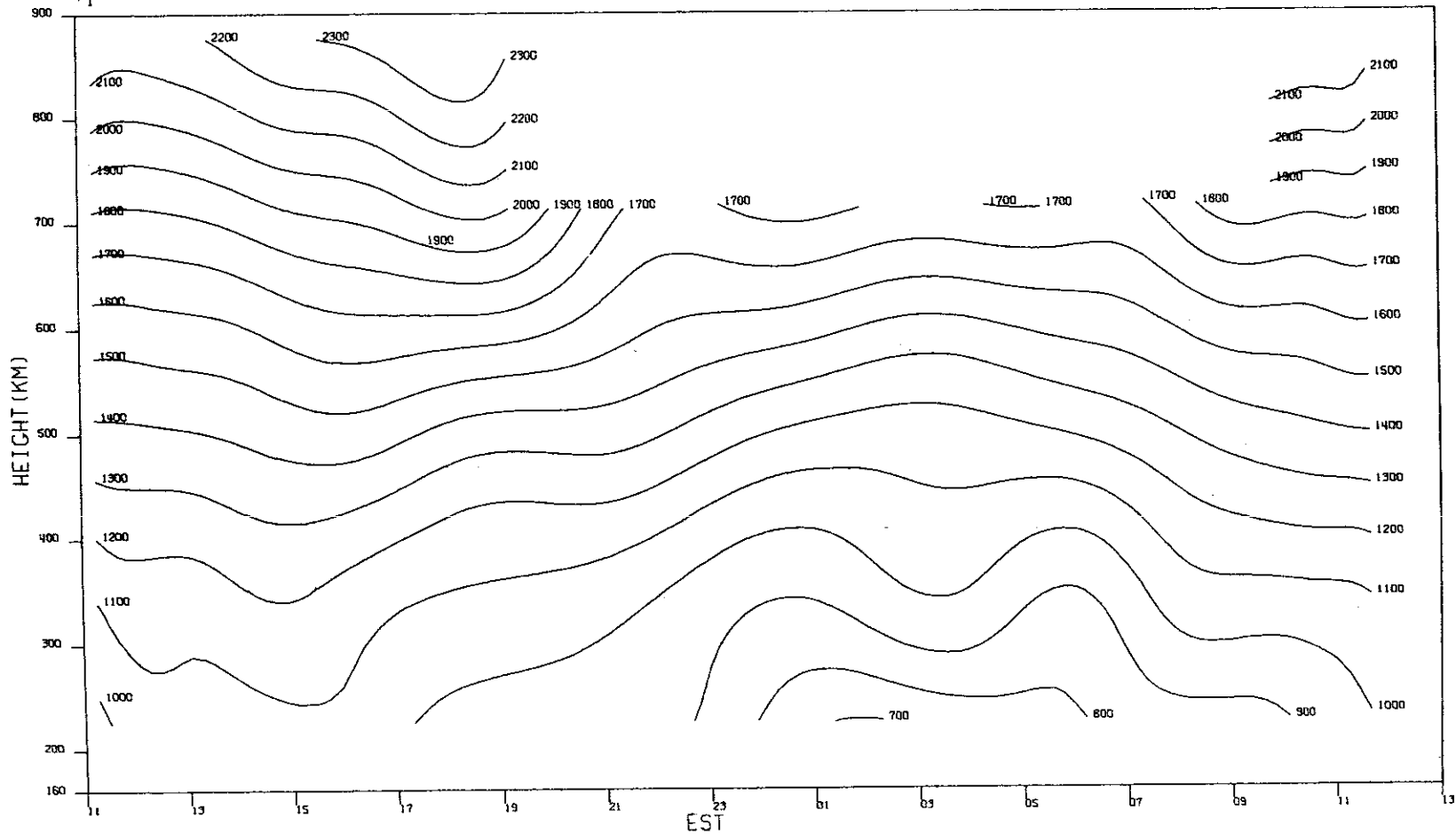
08

(a)

Fig. 3(a-z). Computer-drawn plots showing contours of constant ion temperature T_i (in $^{\circ}\text{K}$) as functions of height and time for the measurements made in 1970 (Table IV).

MILLSTONE HILL
20-21, JAN, 1970

-9-5177

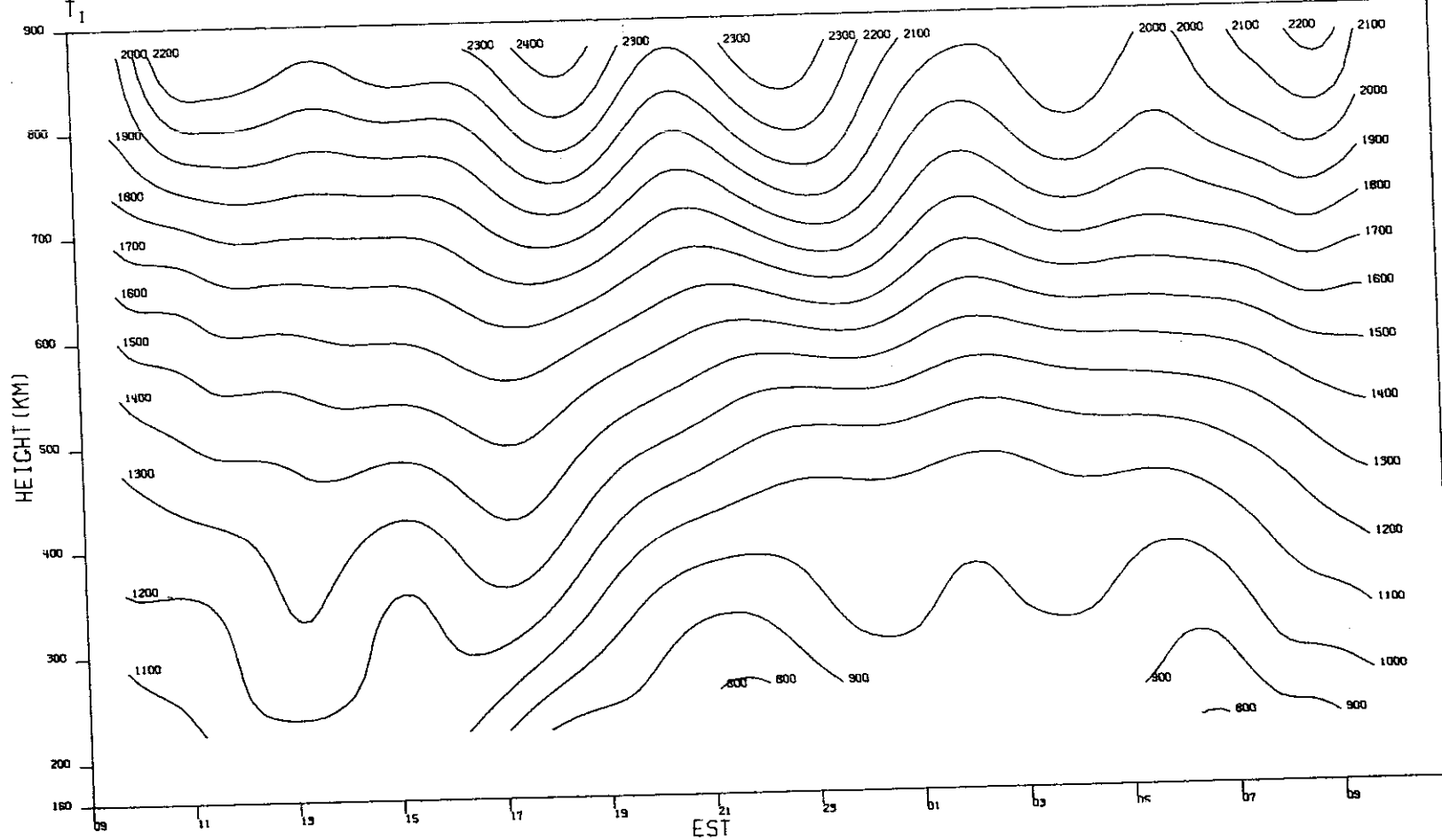


(b)

Fig.3(a-z). Continued.

MILLSTONE HILL
17-18, FEB. 1970

-9-5178

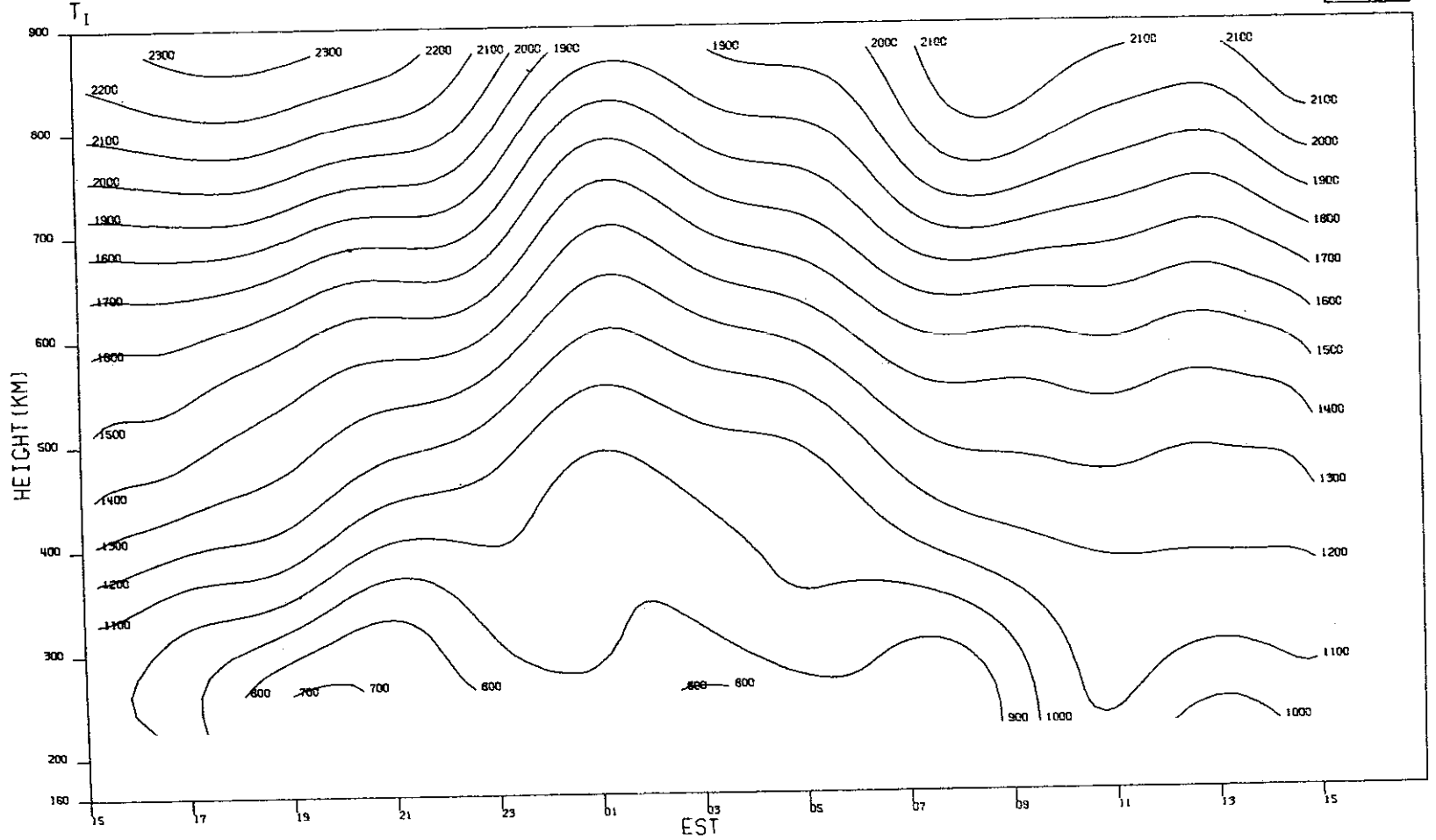


(c)

Fig. 3(a-z). Continued.

MILLSTONE HILL
23-24, FEB. 1970

-9-5179



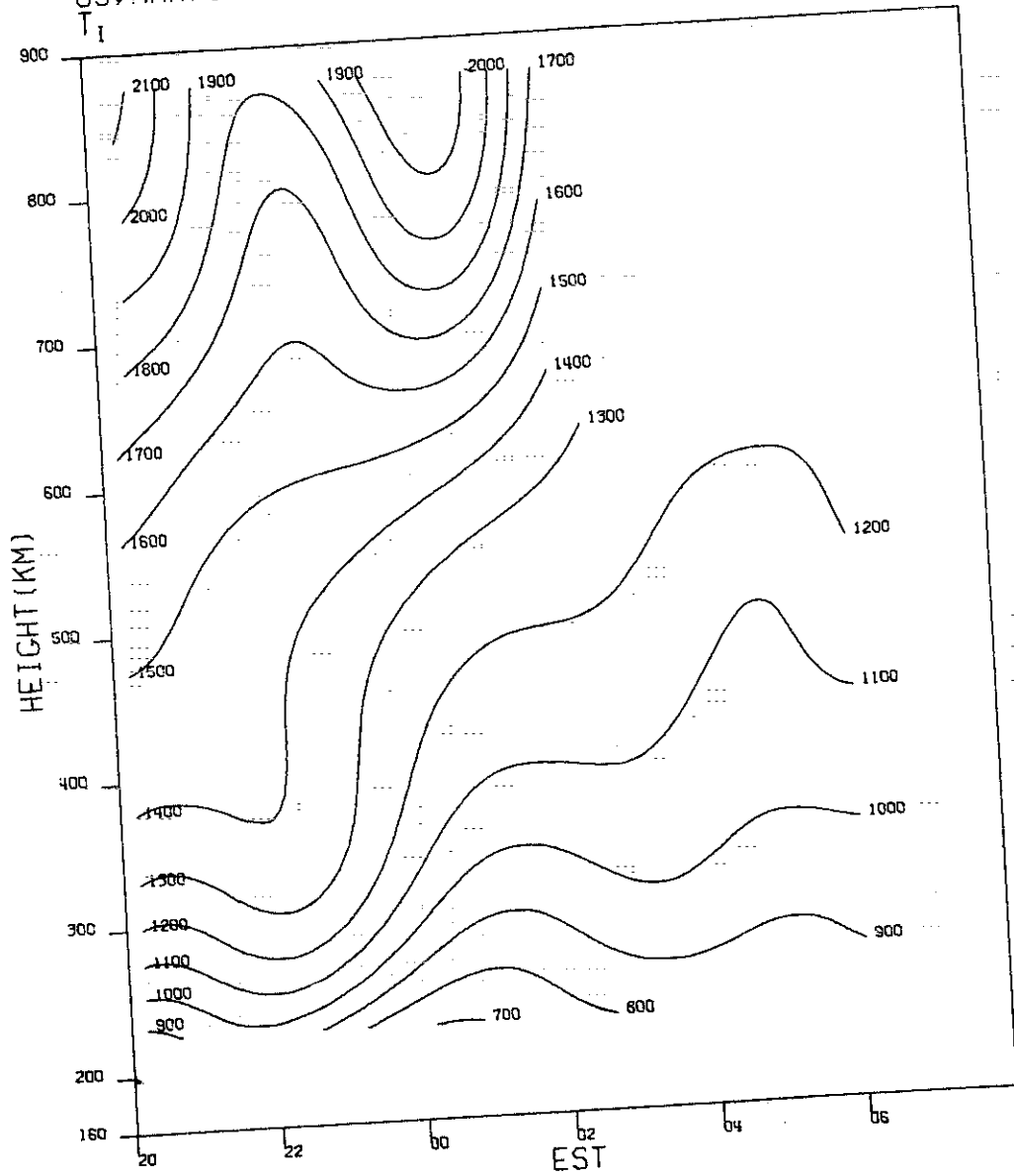
83

(d)

Fig.3(a-z). Continued.

MILLSTONE HILL
09, MAR. 1970

-9-5180

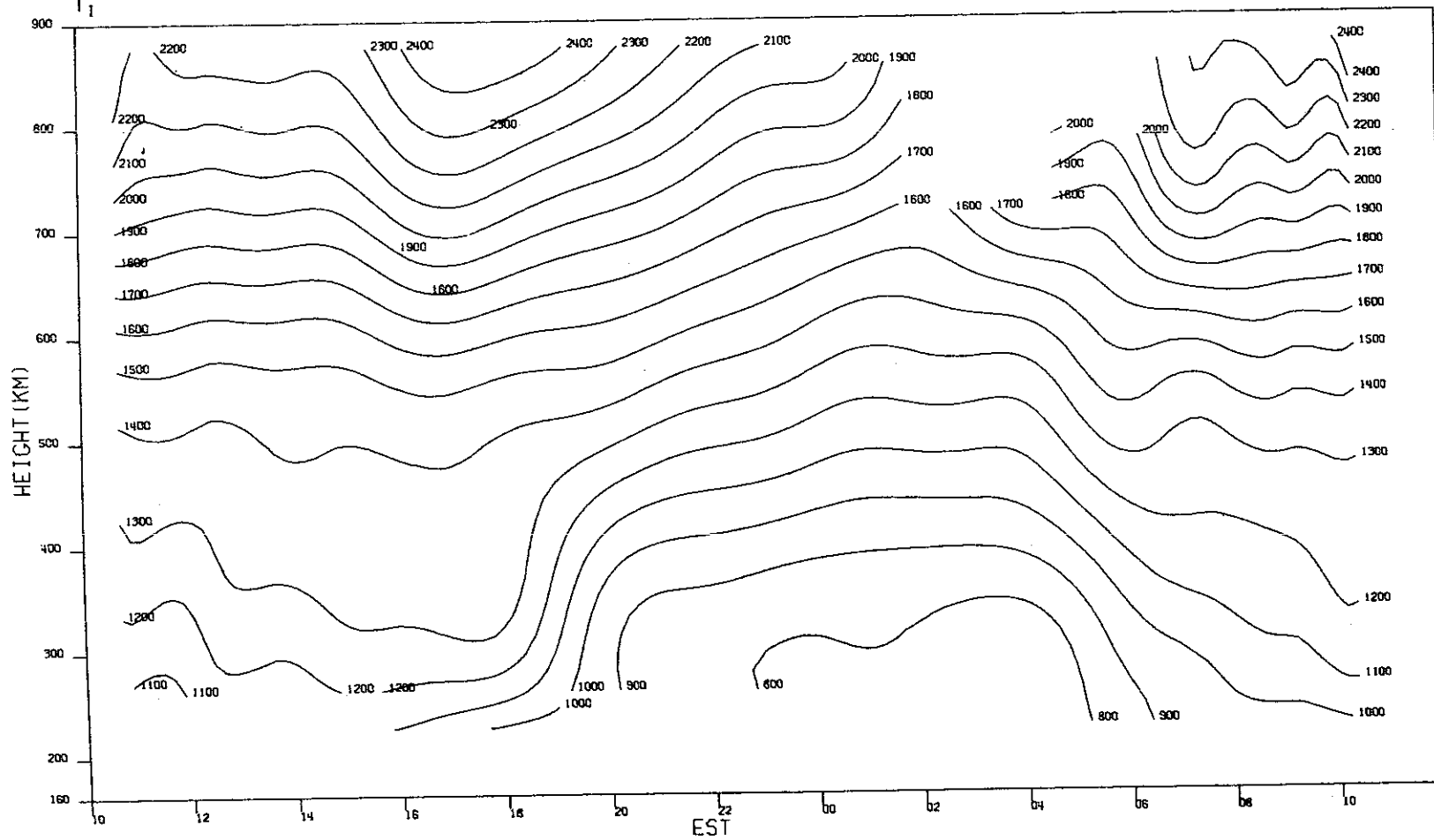


(e)

Fig. 3(a-z). Continued.

MILLSTONE HILL
17-18. MAR. 1970

-9-5181



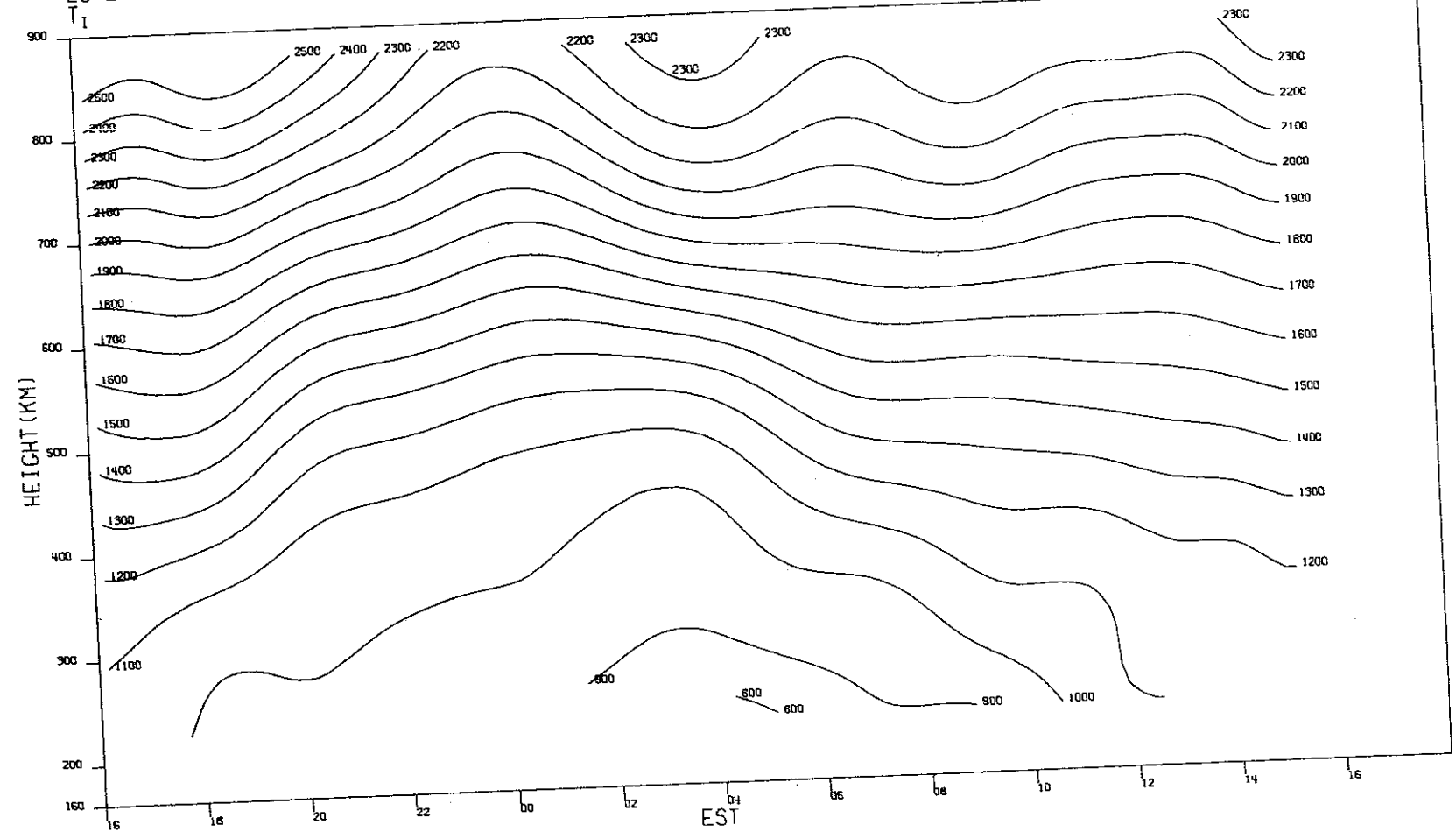
88

(f)

Fig.3(a-z). Continued.

MILLSTONE HILL
23-24, MAR. 1970

-9-5182



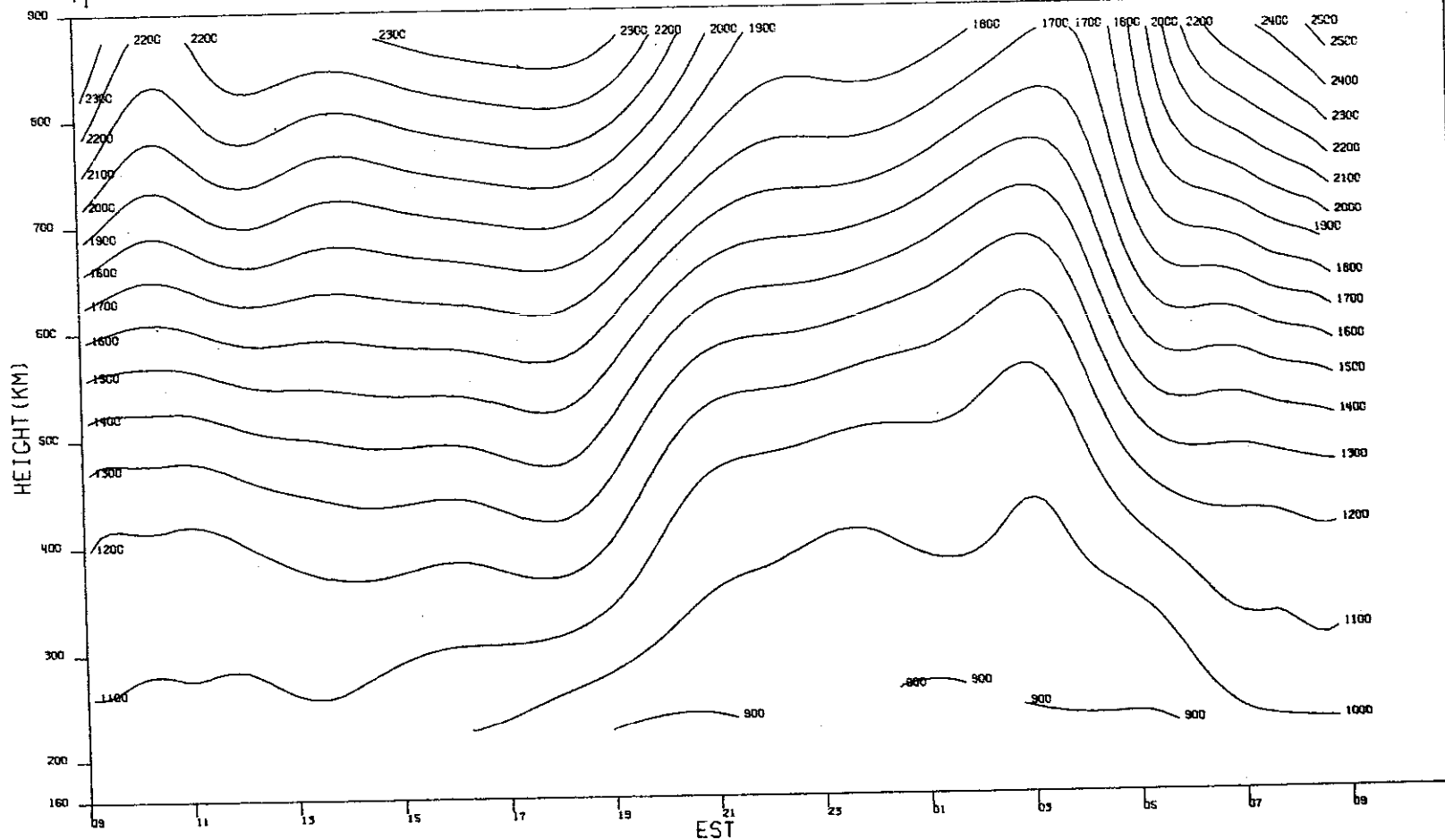
98

(g)

Fig.3(a-z). Continued.

MILLSTONE HILL
14-15, APR, 1970

-9-5183



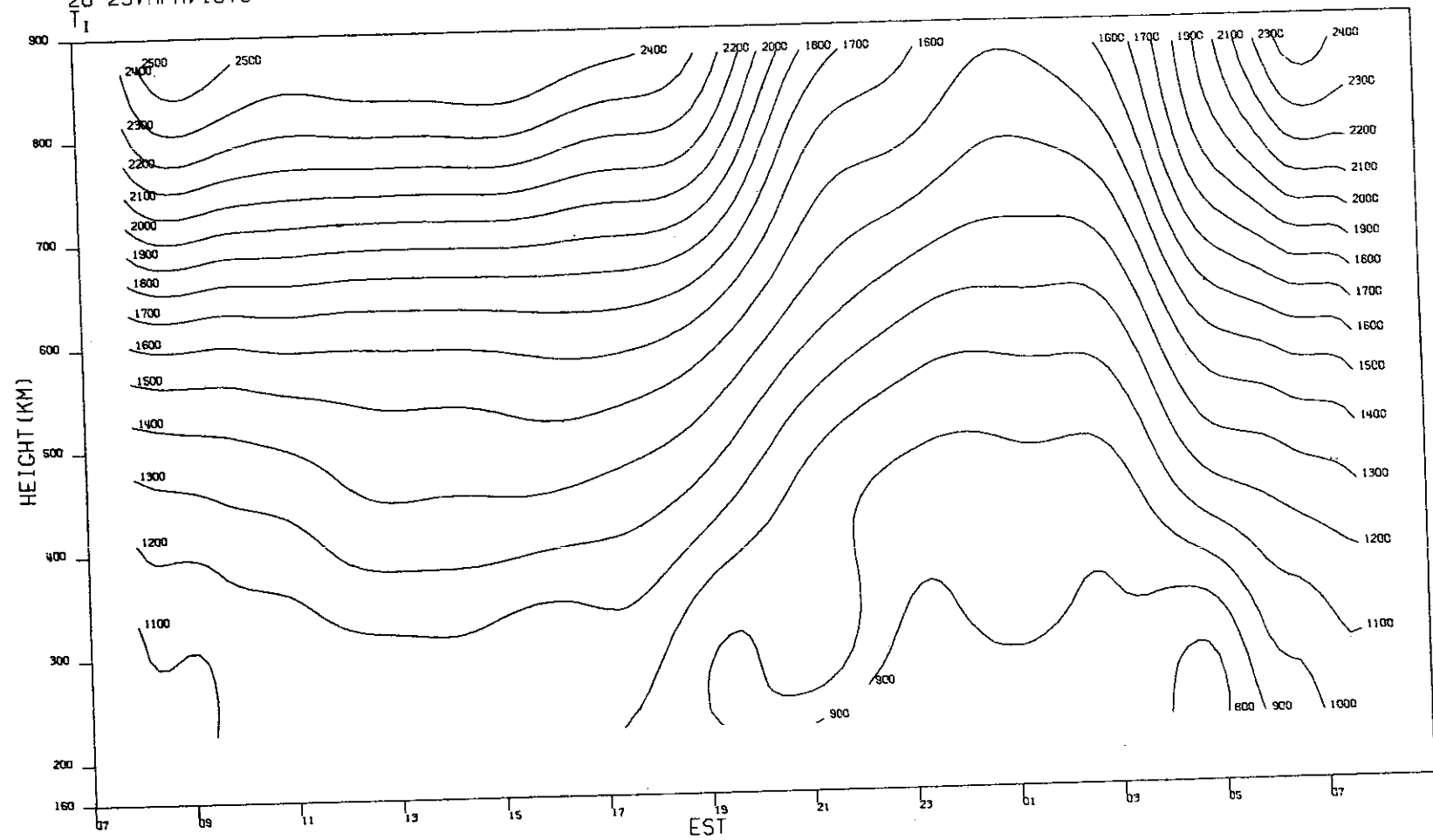
87

(h)

Fig.3(a-z). Continued.

MILLSTONE HILL
28-29, APR, 1970

-9-5184



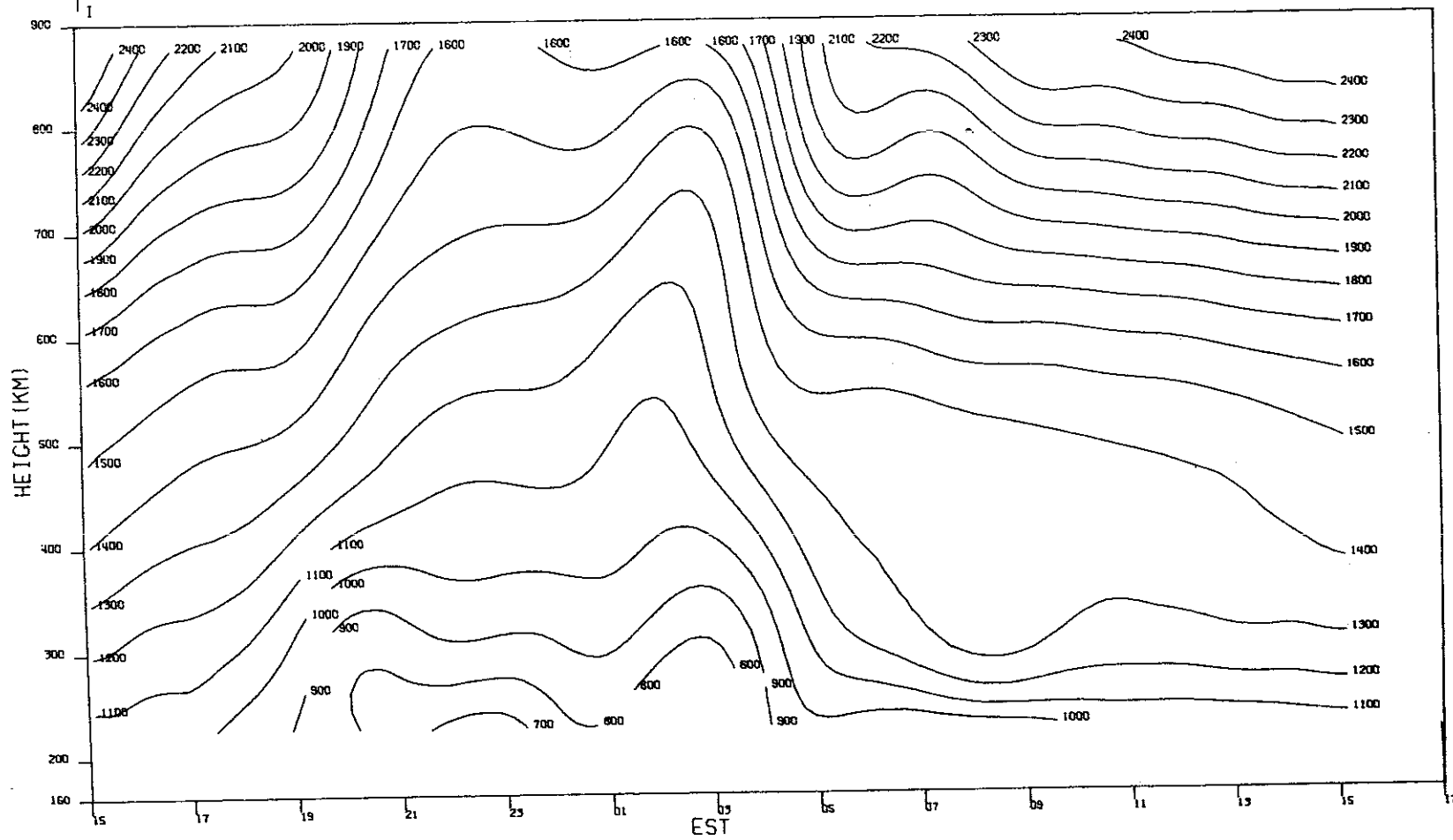
88

(i)

Fig. 3(a-z). Continued.

MILLSTONE HILL
12-13, MAY, 1970

-9-5185



(j)

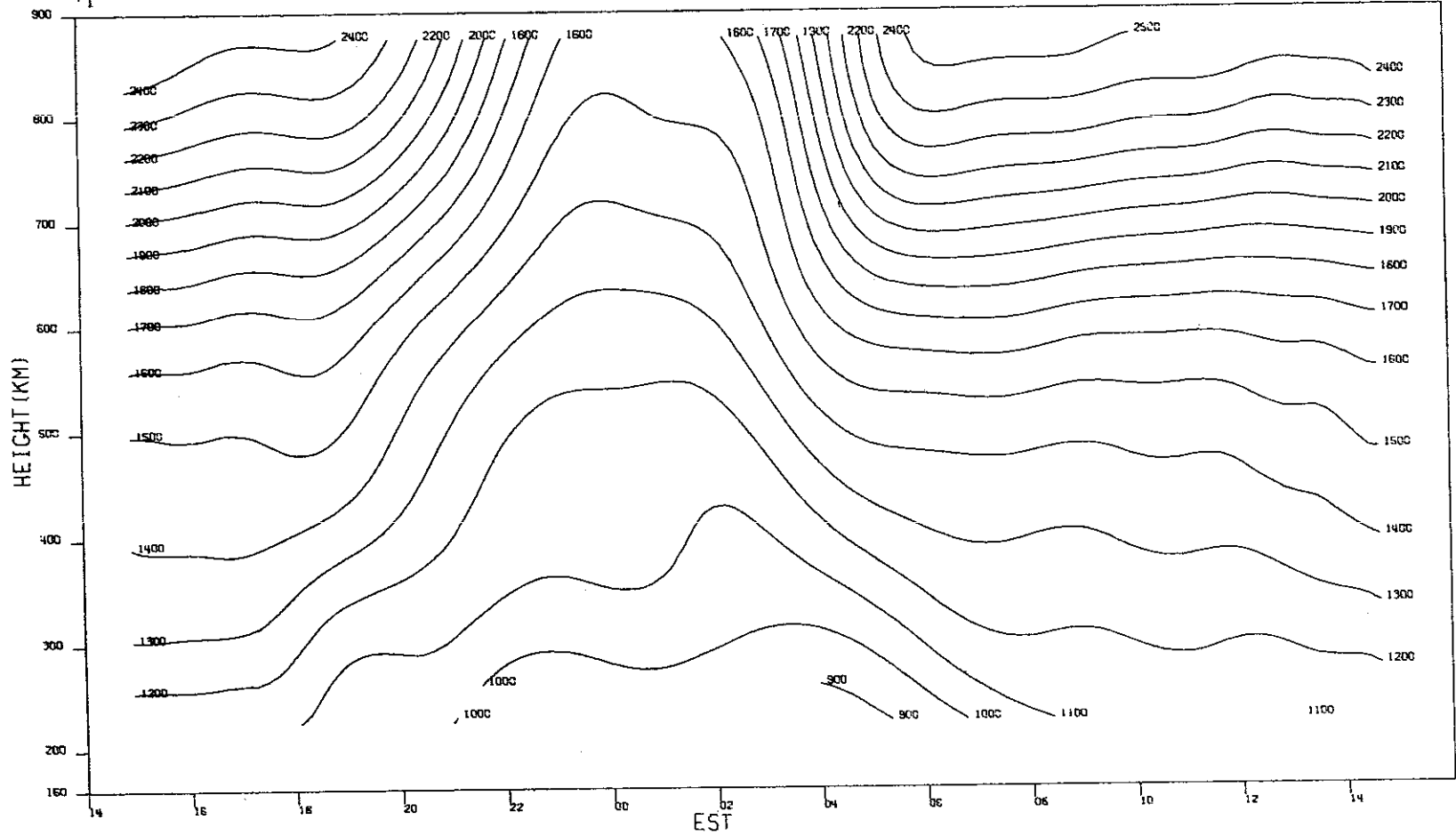
Fig.3(a-z). Continued.

MILLSTONE HILL
18-19, MAY, 1970

T₁

-9-5186

06

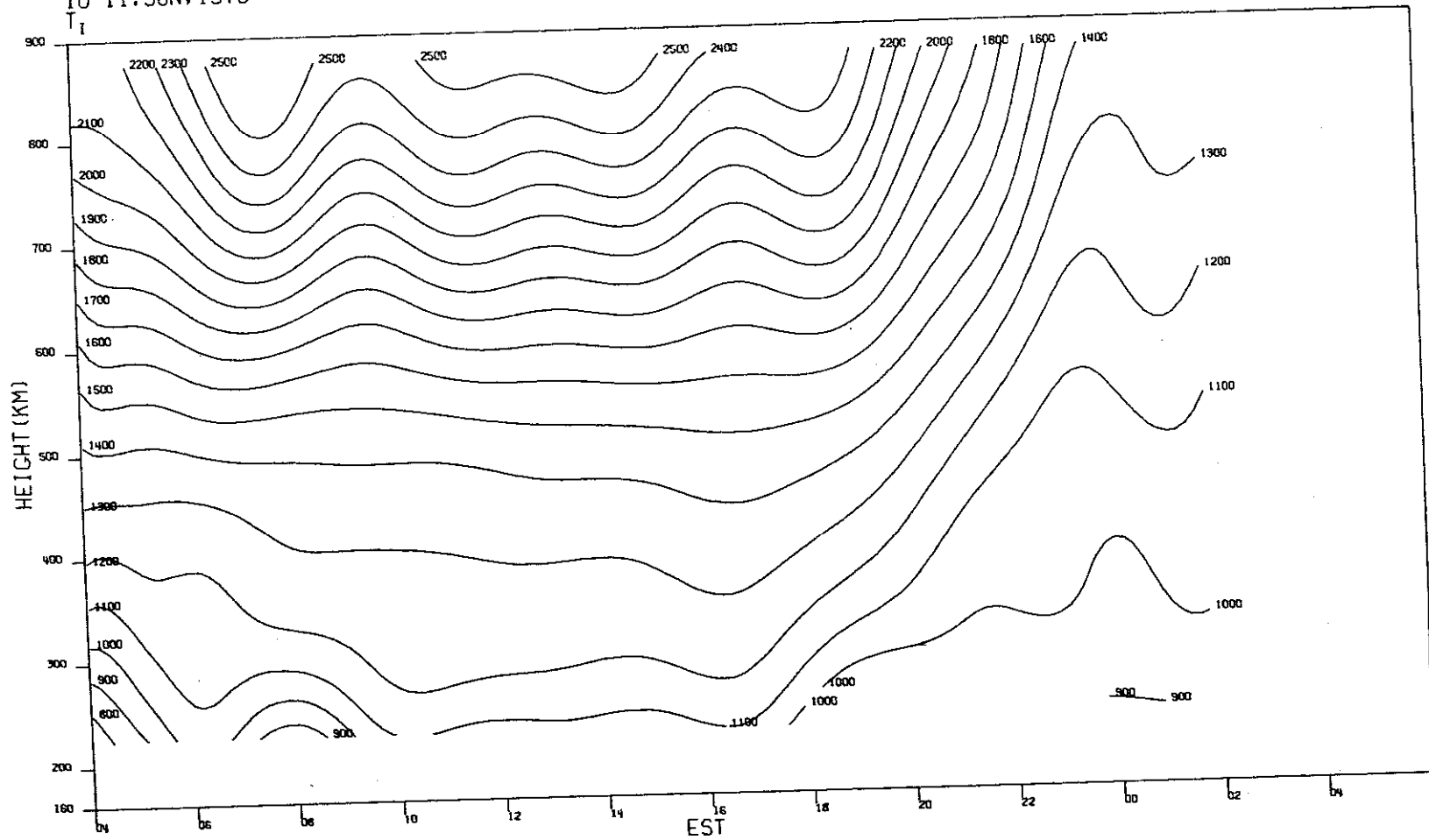


(k)

Fig. 3(a-z). Continued.

MILLSTONE HILL
10-11. JUN. 1970

-9-5187



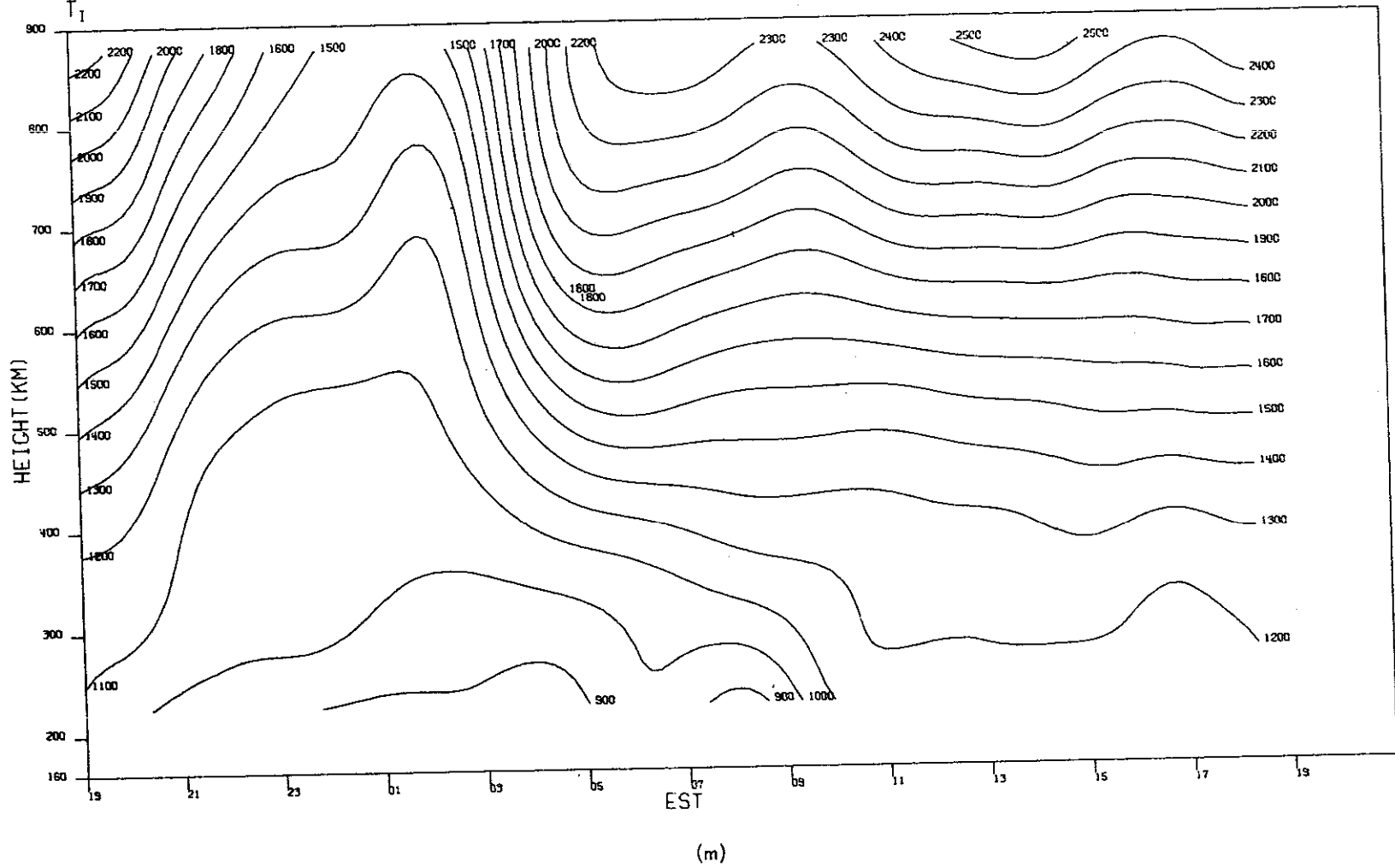
91

(I)

Fig.3(a-z). Continued.

MILLSTONE HILL
23-24, JUN. 1970

-9-5188

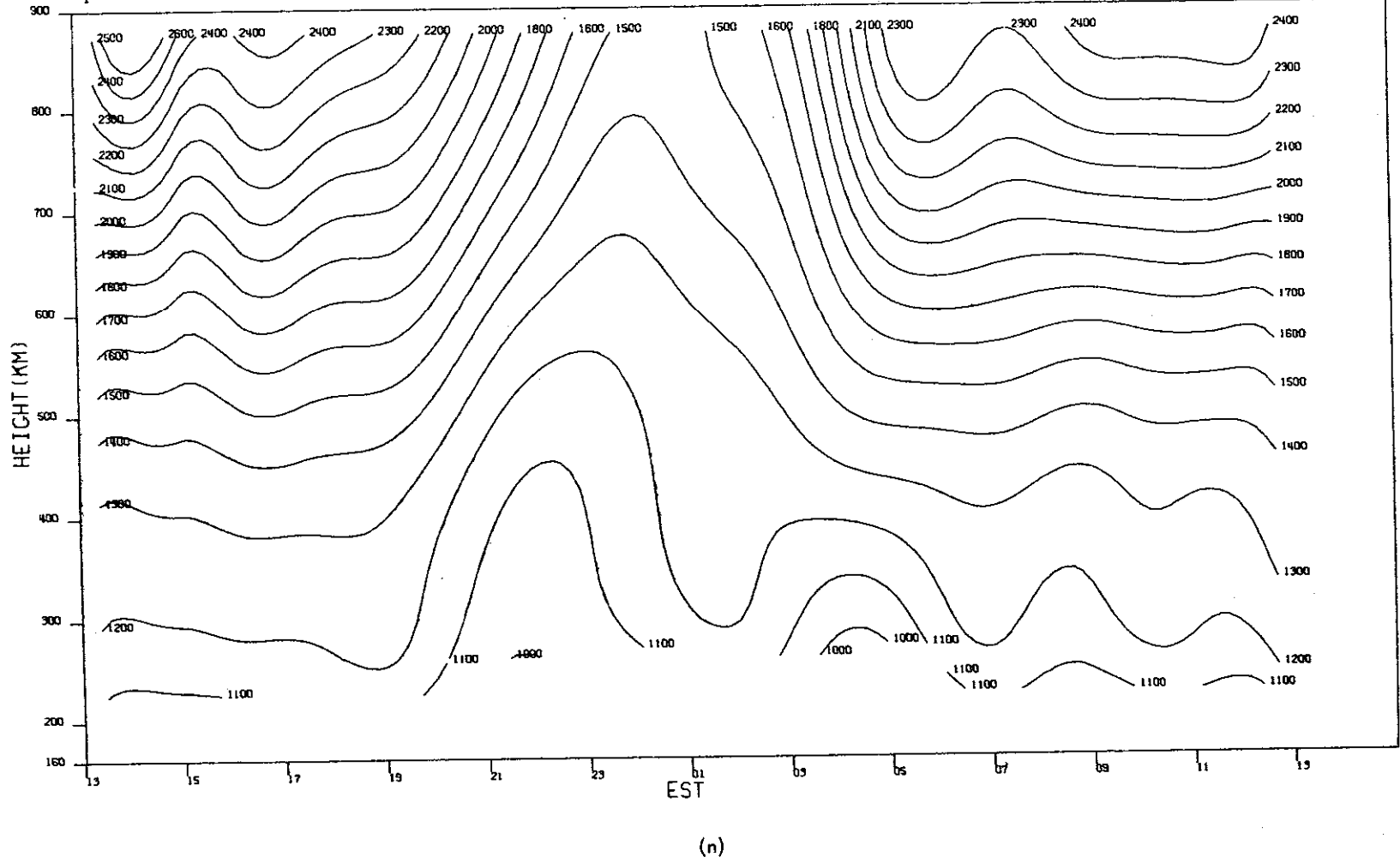


92

Fig. 3(a-z). Continued.

MILLSTONE HILL
07-08. JUL. 1970

-9-5189

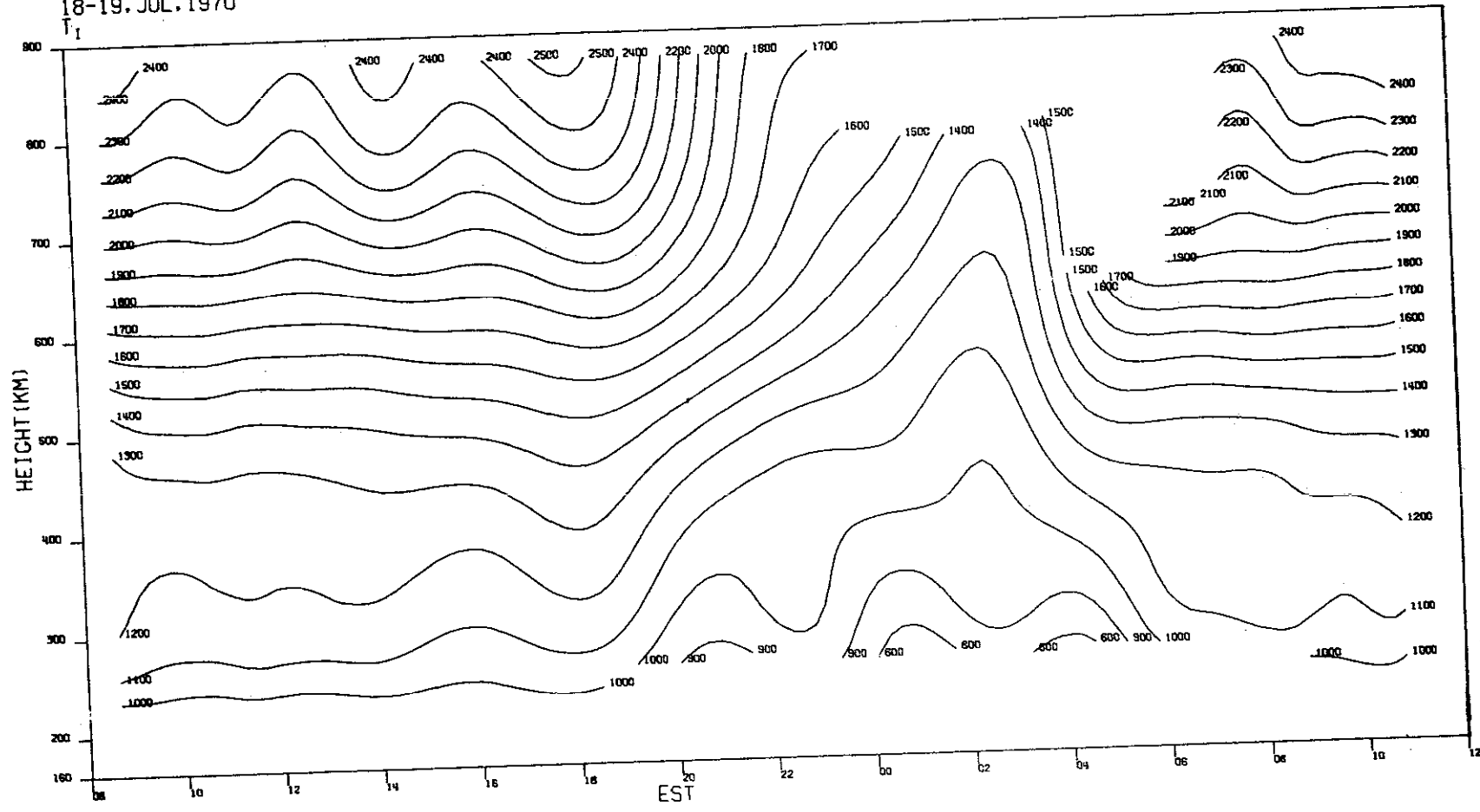


93

Fig. 3(a-z). Continued.

MILLSTONE HILL
18-19. JUL. 1970

9-5190



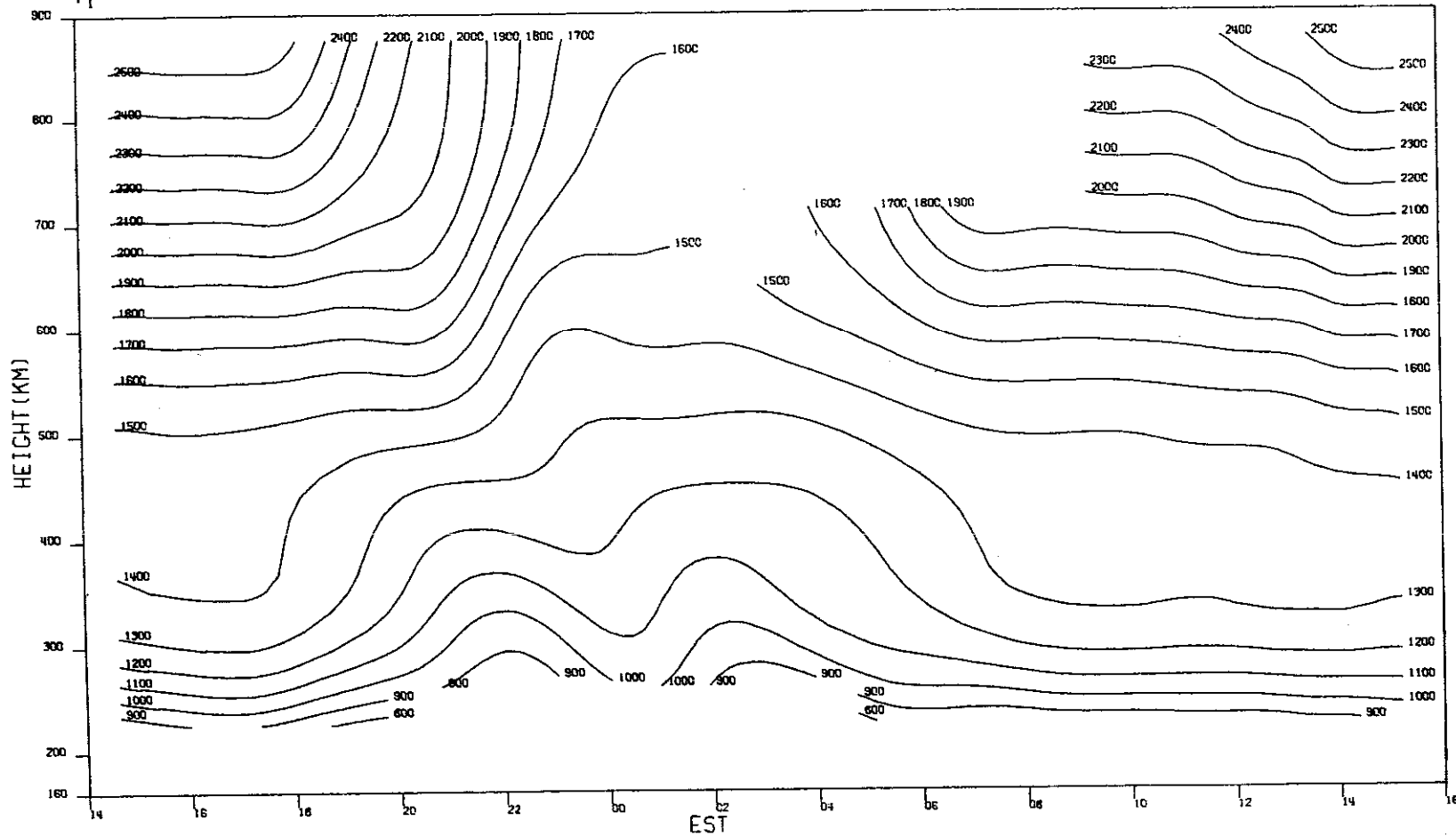
94

(o)

Fig. 3(a-z). Continued.

MILLSTONE HILL
17-18. AUG. 1970

-9-5181

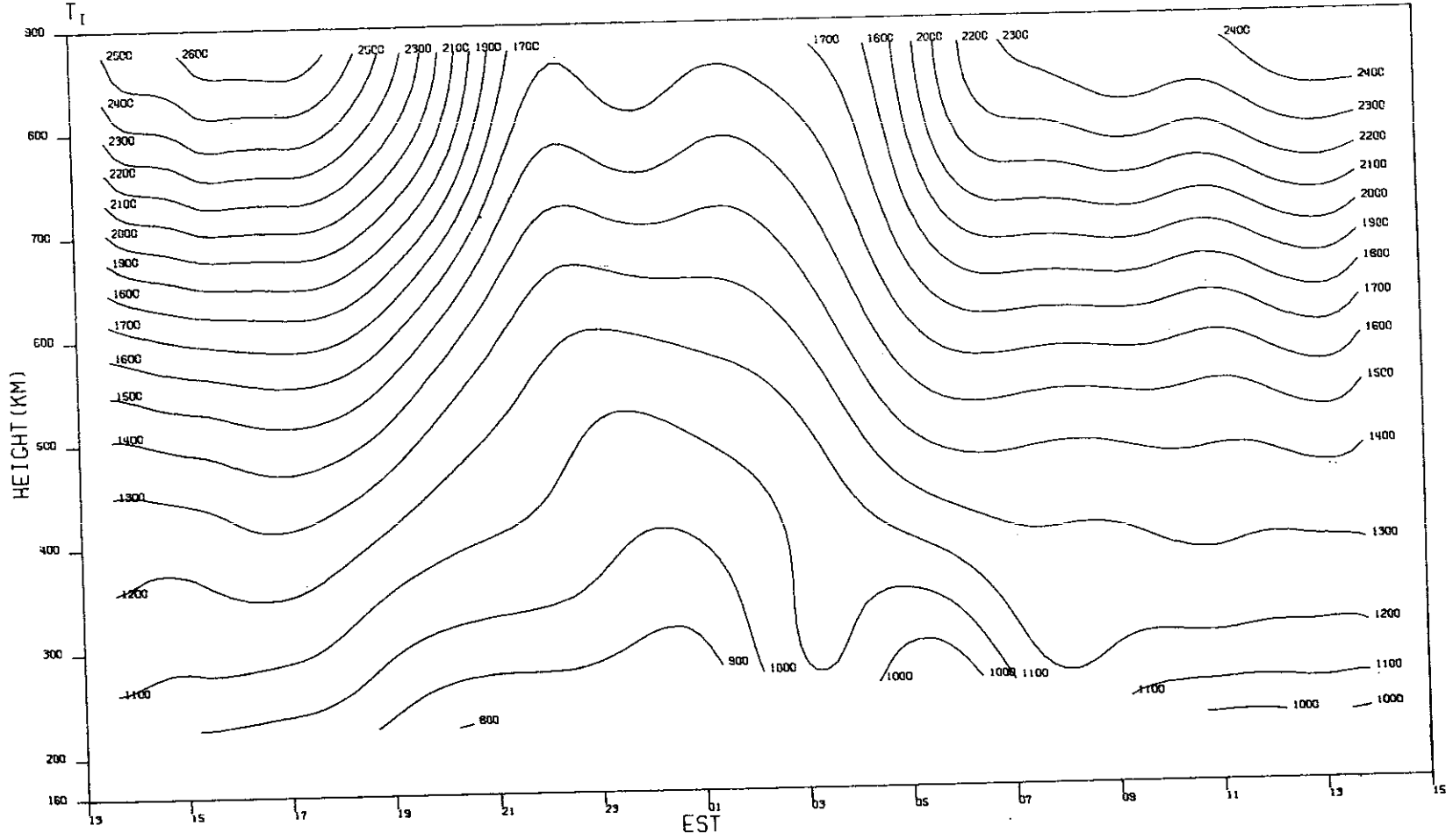


(p)

Fig.3(a-z). Continued.

MILLSTONE HILL
24-25, AUG, 1970

-9-5192



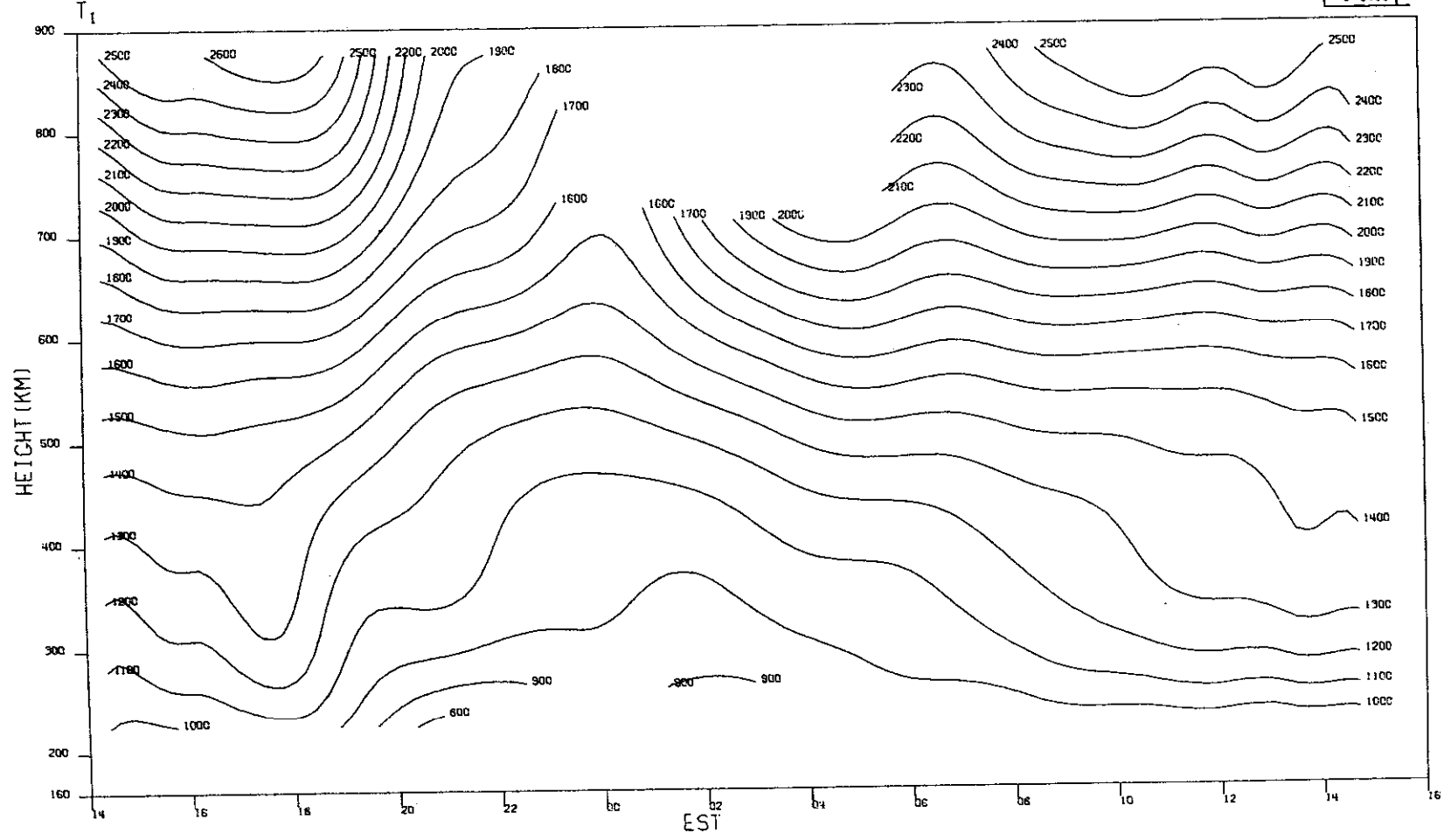
96

(q)

Fig.3(a-z). Continued.

MILLSTONE HILL
31AUG-01SEP, 1970

-9-5193

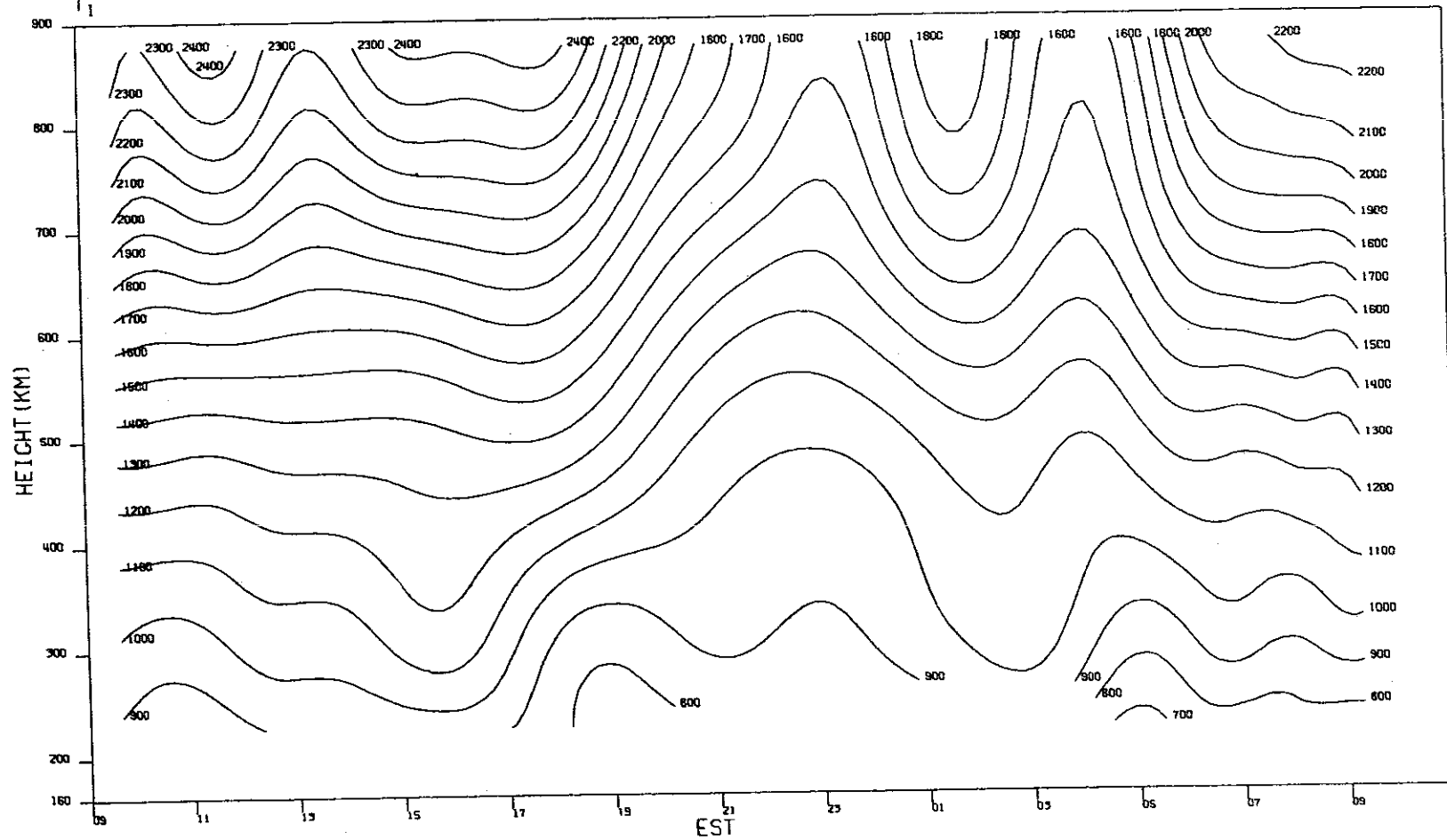


(r)

Fig. 3(a-z). Continued.

MILLSTONE HILL
16-17. SEP. 1970

-9-5194

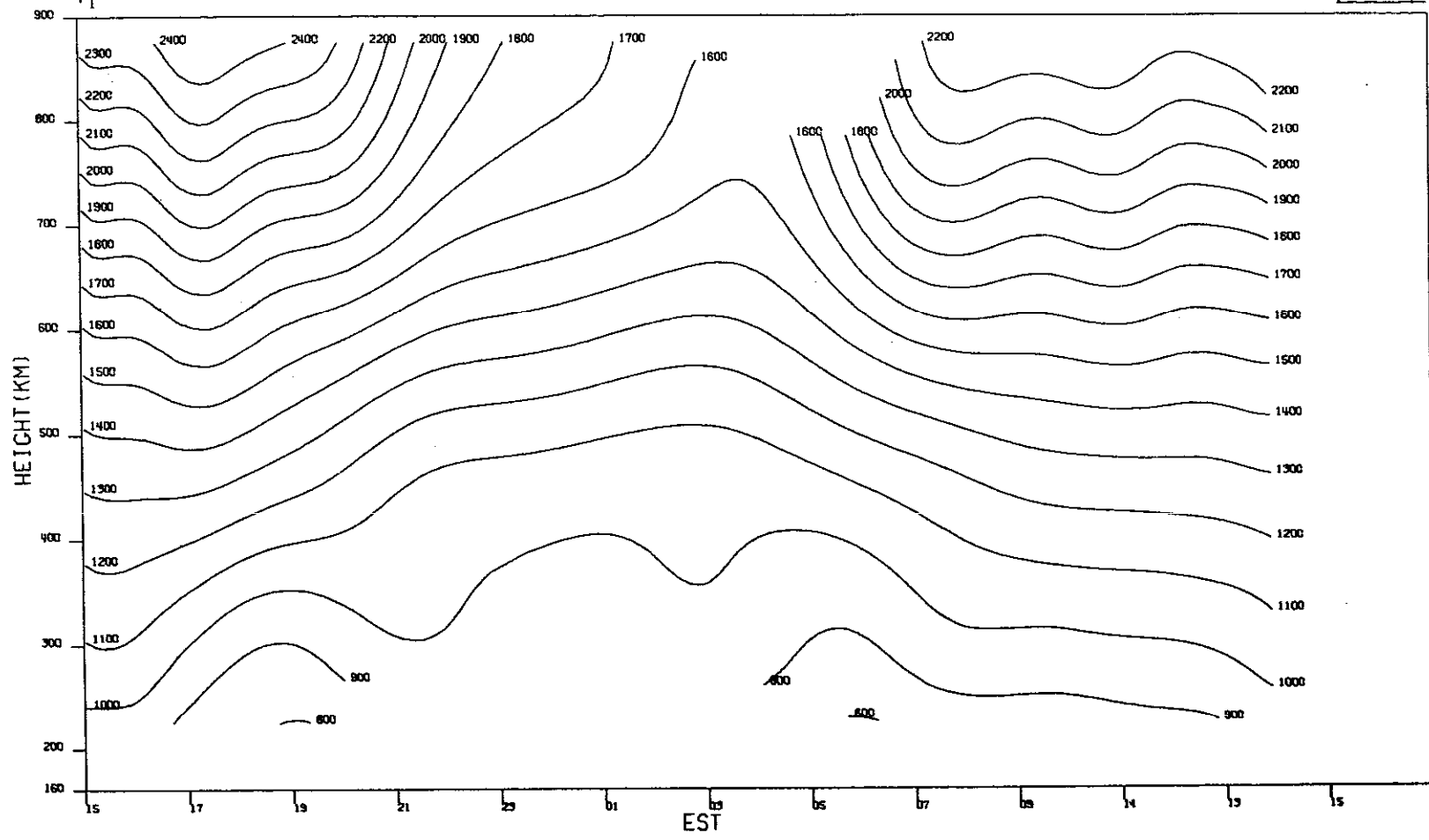


(s)

Fig. 3(a-z). Continued.

MILLSTONE HILL
28-29, SEP, 1970

-9-5195



66

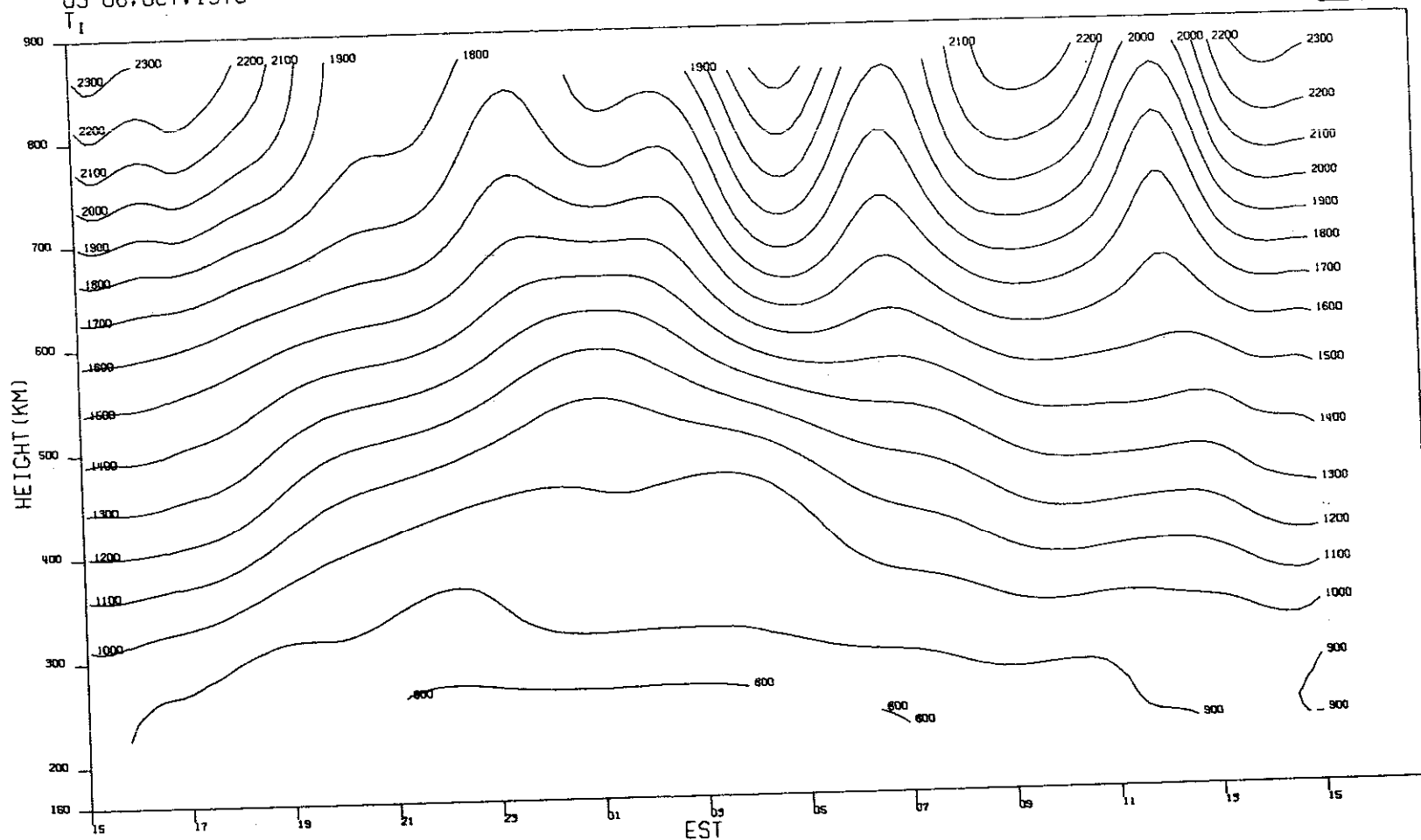
(t)

Fig. 3(a-z). Continued.

MILLSTONE HILL
05-06, OCT. 1970

-9-5196

100



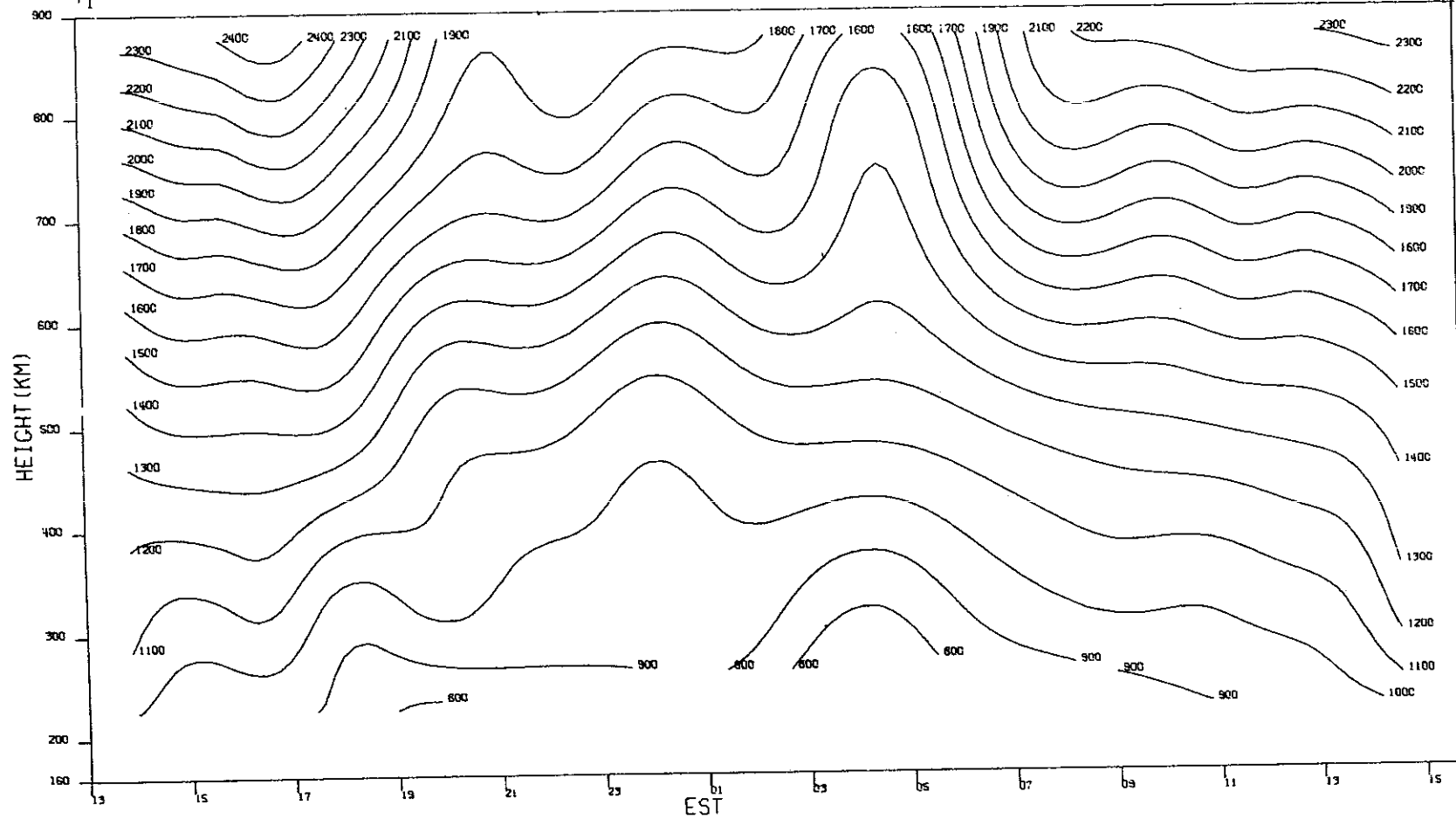
(u)

Fig. 3(a-z). Continued.

MILLSTONE HILL
13-14, OCT, 1970

-9-5197

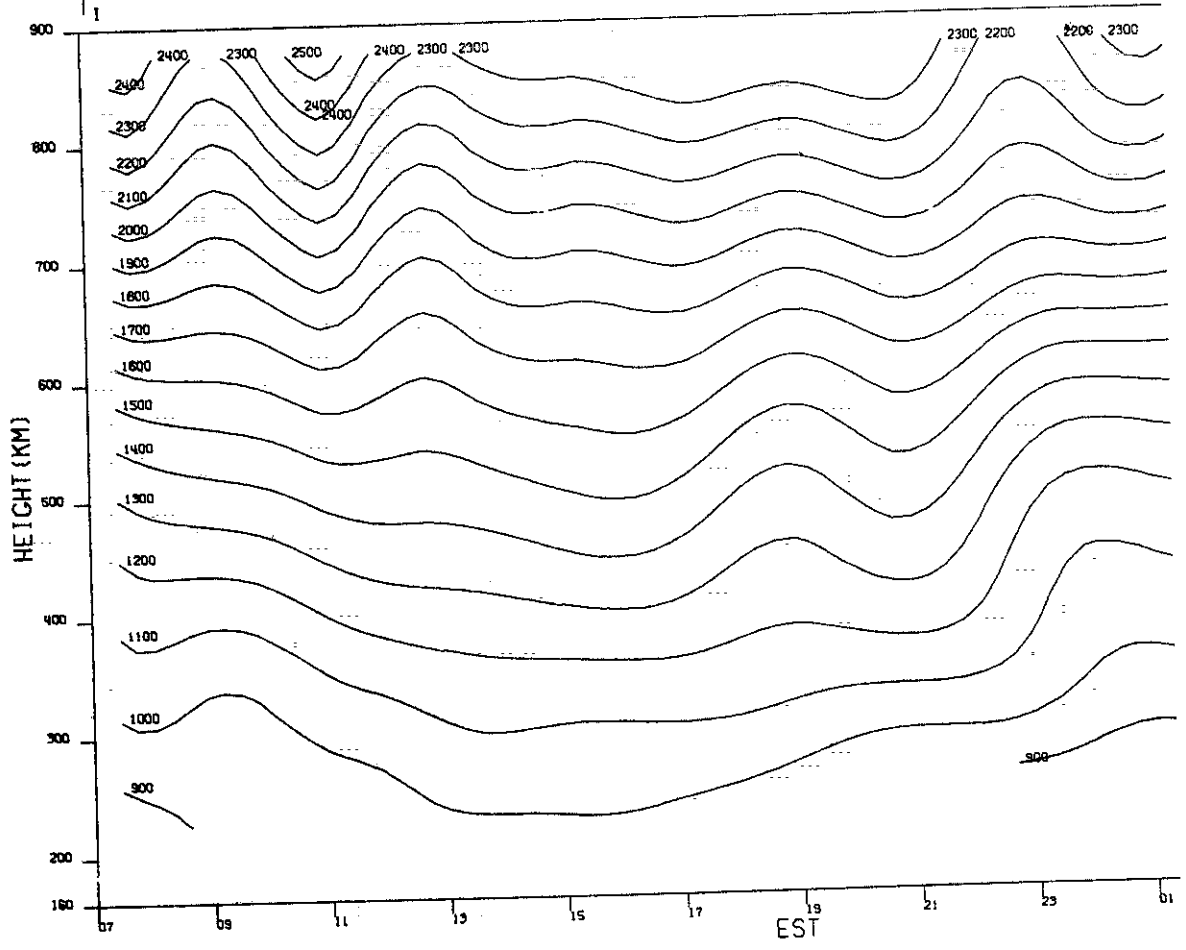
101



(v)

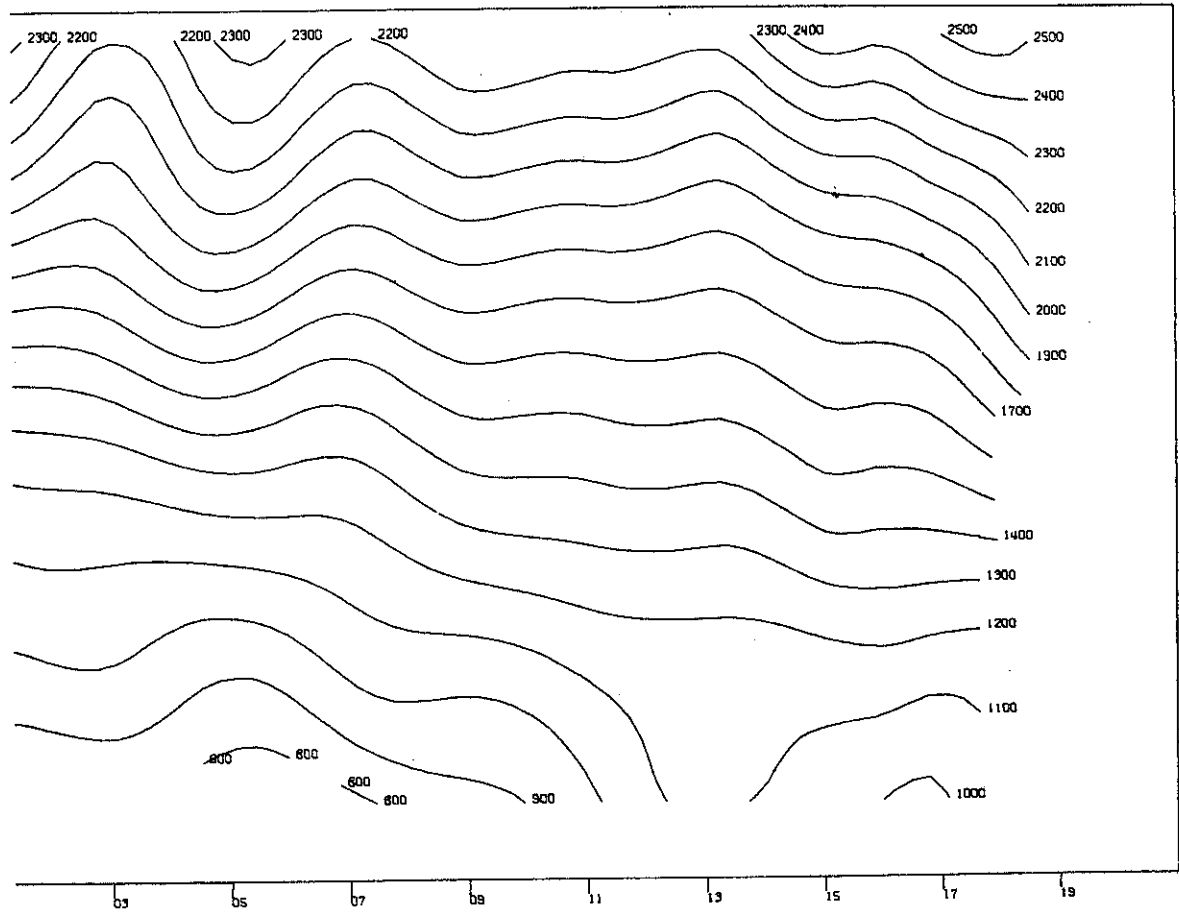
Fig. 3(a-z). Continued.

MILLSTONE HILL
31 OCT-01 NOV. 1970



(w)

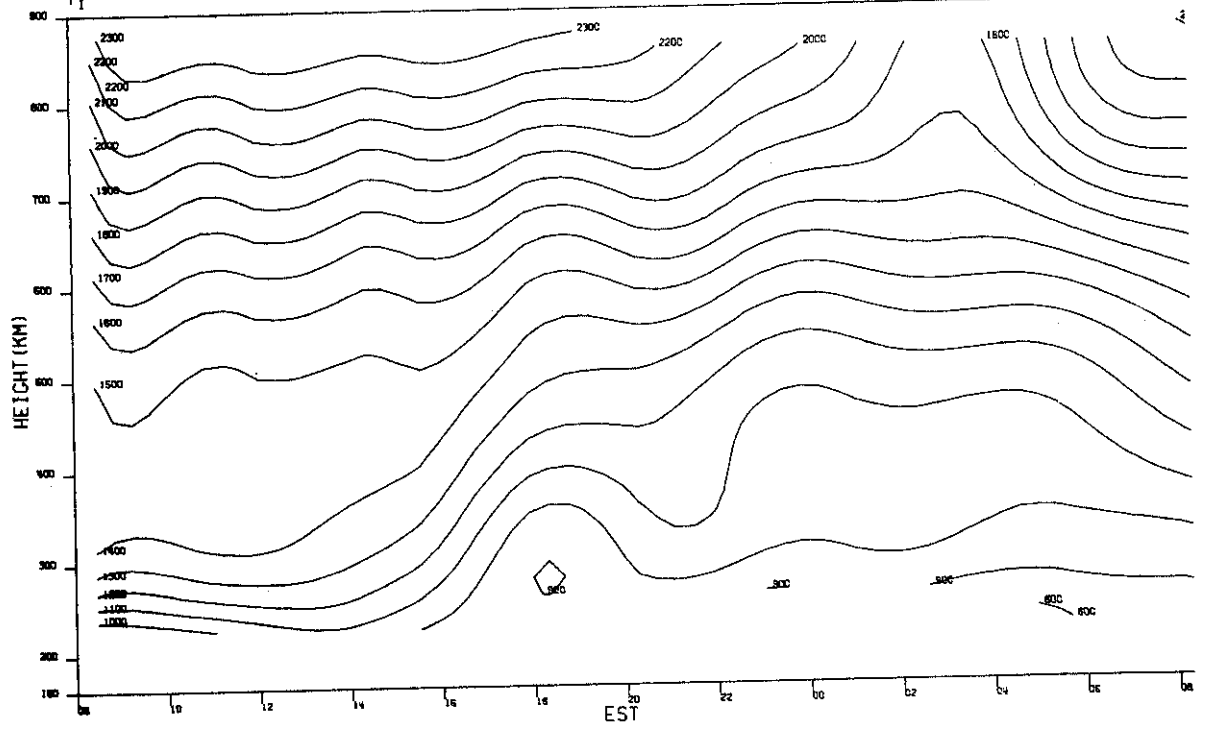
Fig. 3(a-z). . Continued.



(w)

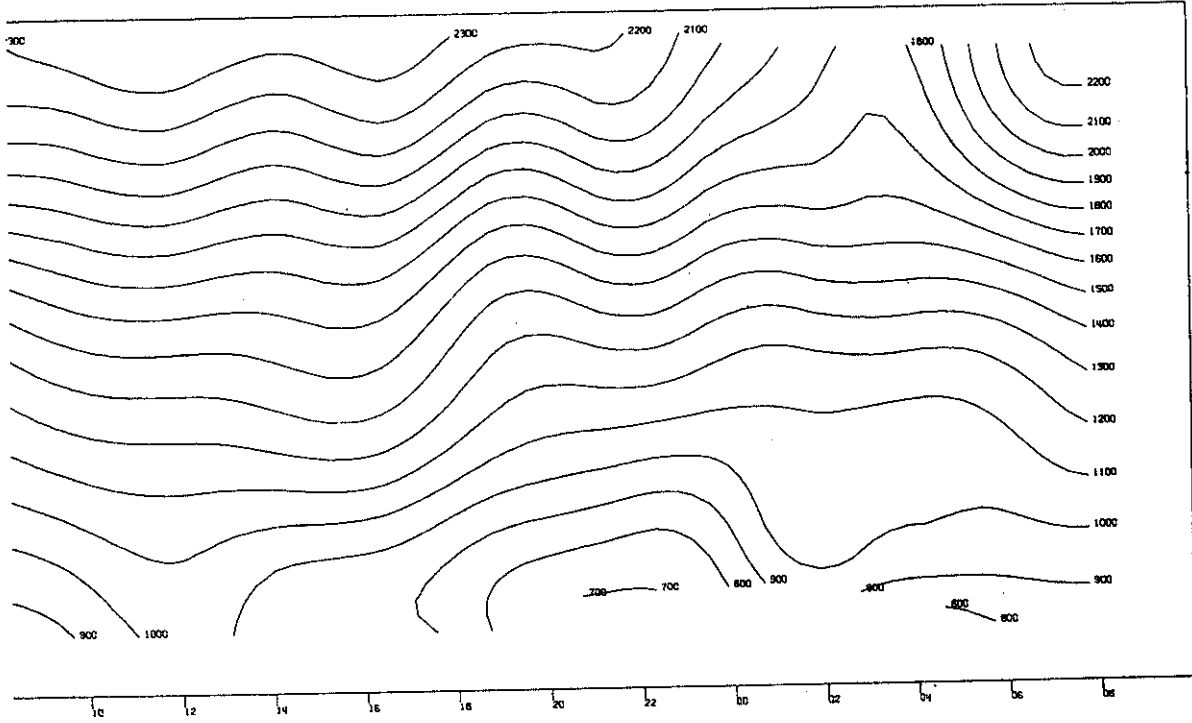
Fig.3(a-z). Continued.

MILLSTONE HILL
07-09. NOV. 1970
T₁



(x)

Fig. 3(a-z). Continued.

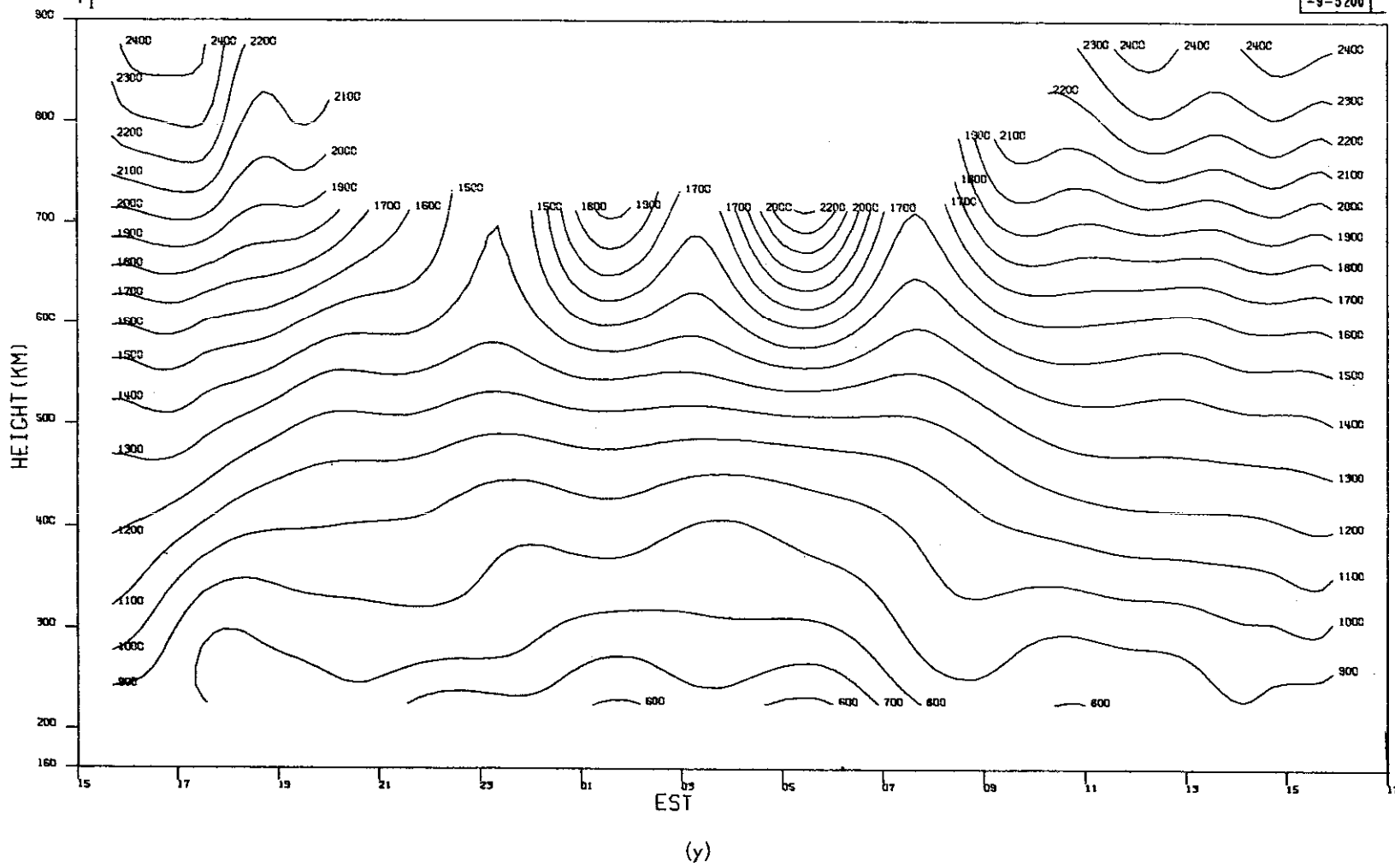


(x)

Fig. 3(a-z). Continued.

MILLSTONE HILL
21-22, DEC, 1970

-9-5200



106

Fig.3(a-z). Continued.

MILLSTONE HILL
28-29. DEC. 1970

-9-5201

4.07

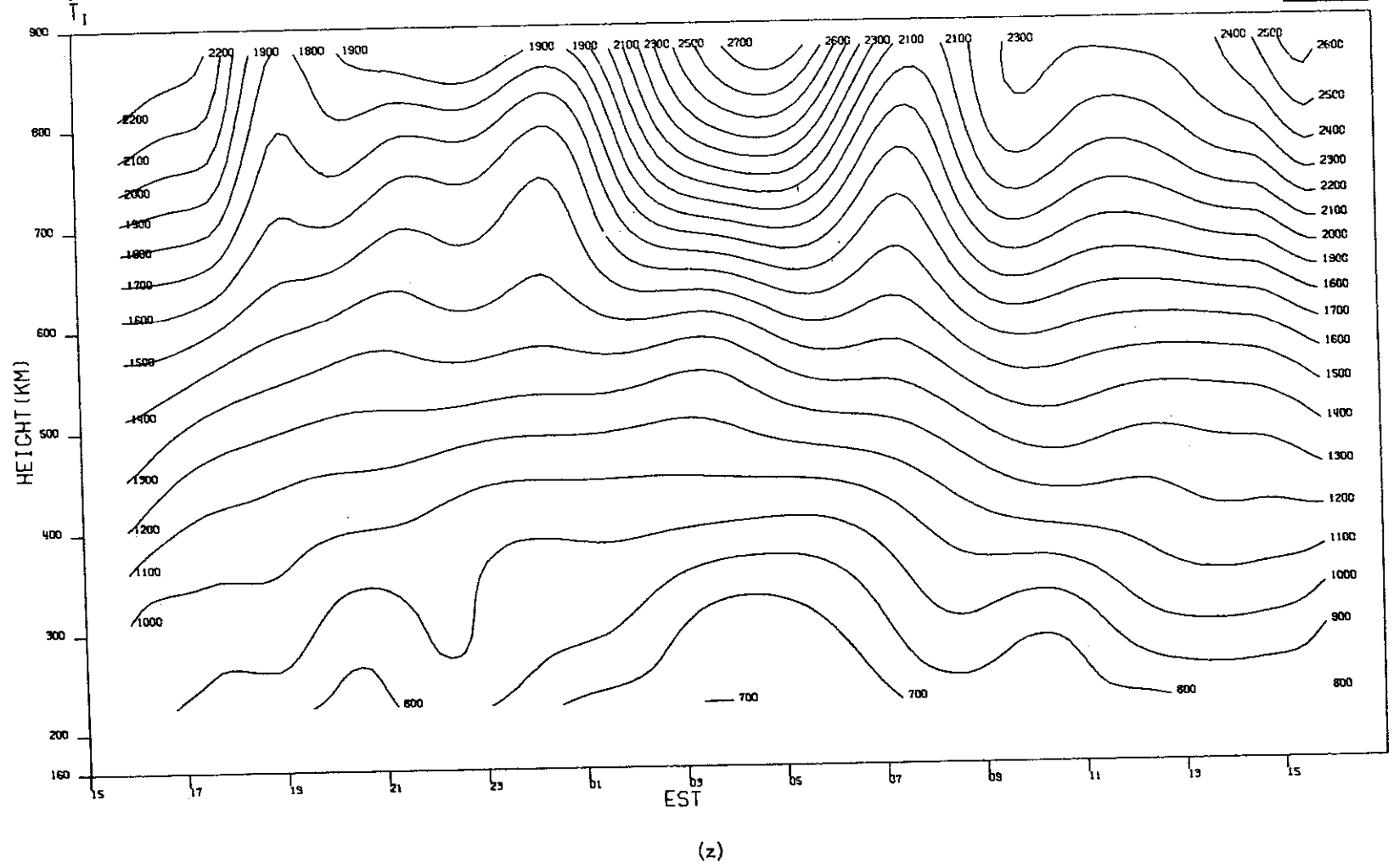
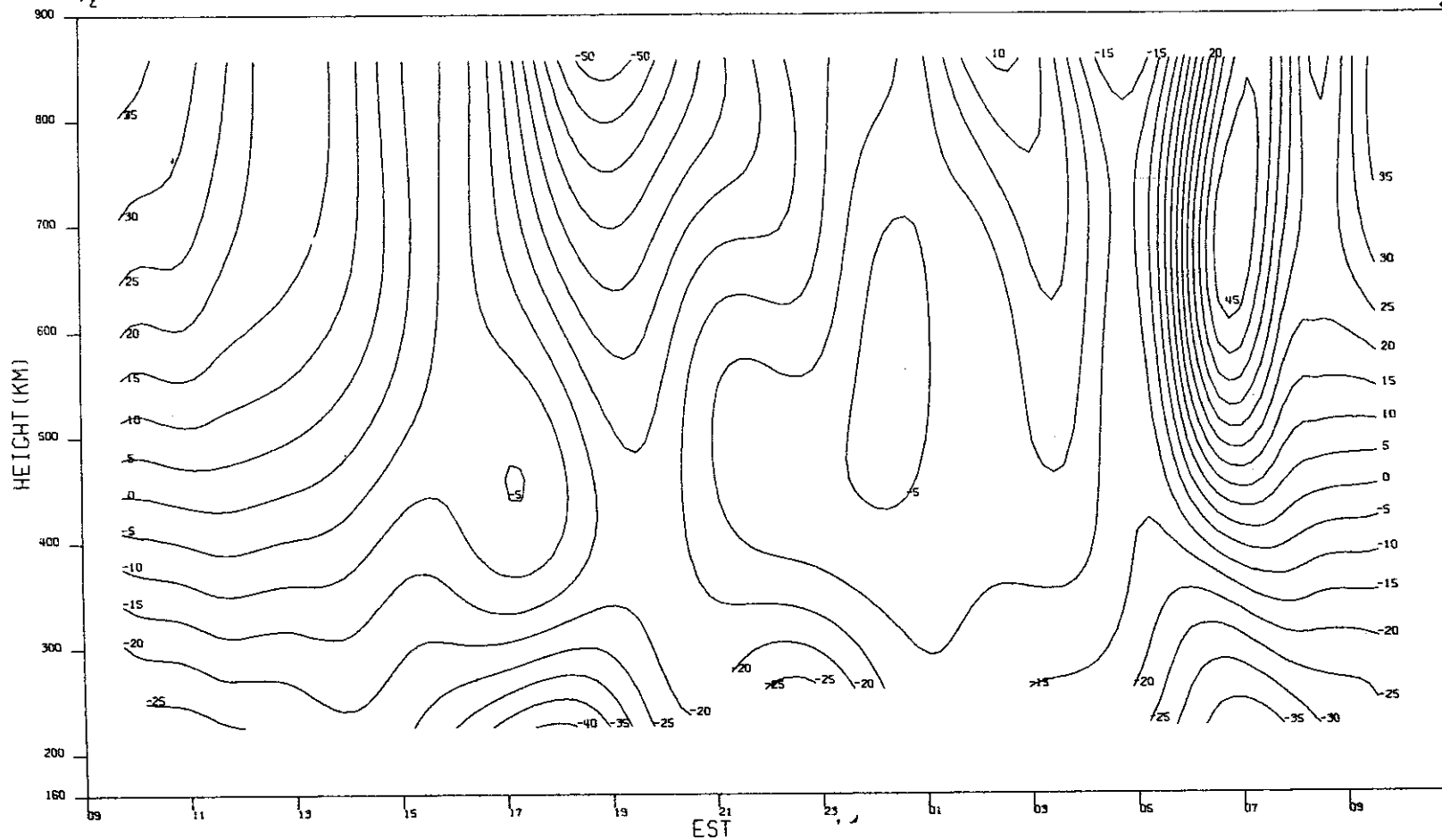


Fig.3(a-z). Continued.

MILLSTONE HILL
17-18, FEB. 1970
 V_z

-9-5202



109

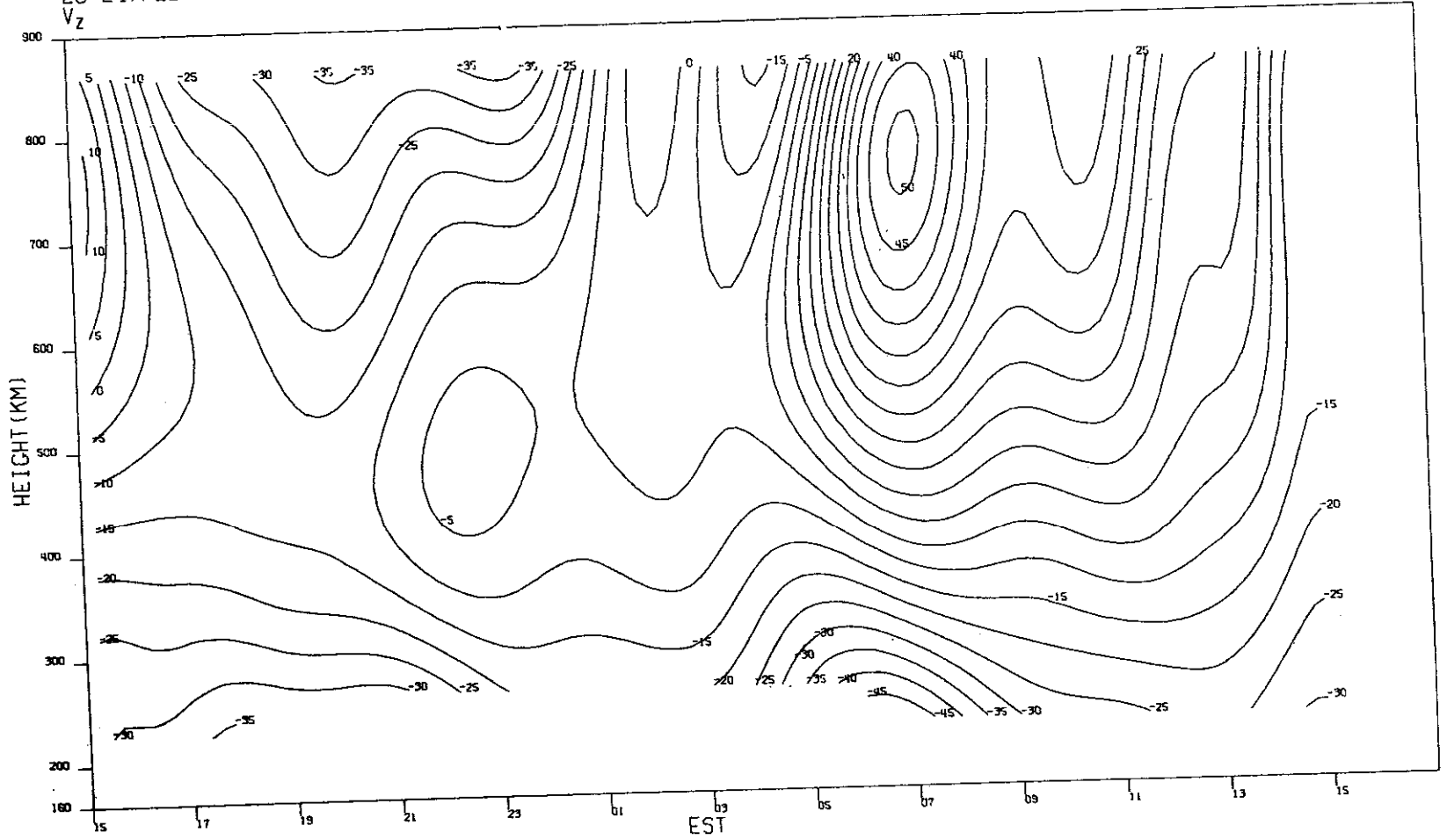
(a)

Fig. 4(a-v). Computer-drawn plots showing contours of constant vertical velocity v_z (m/sec) as functions of height and time recovered for some of the measurements made in 1970.

MILLSTONE HILL
23-24, FEB. 1970
Vz

-9-5203

110

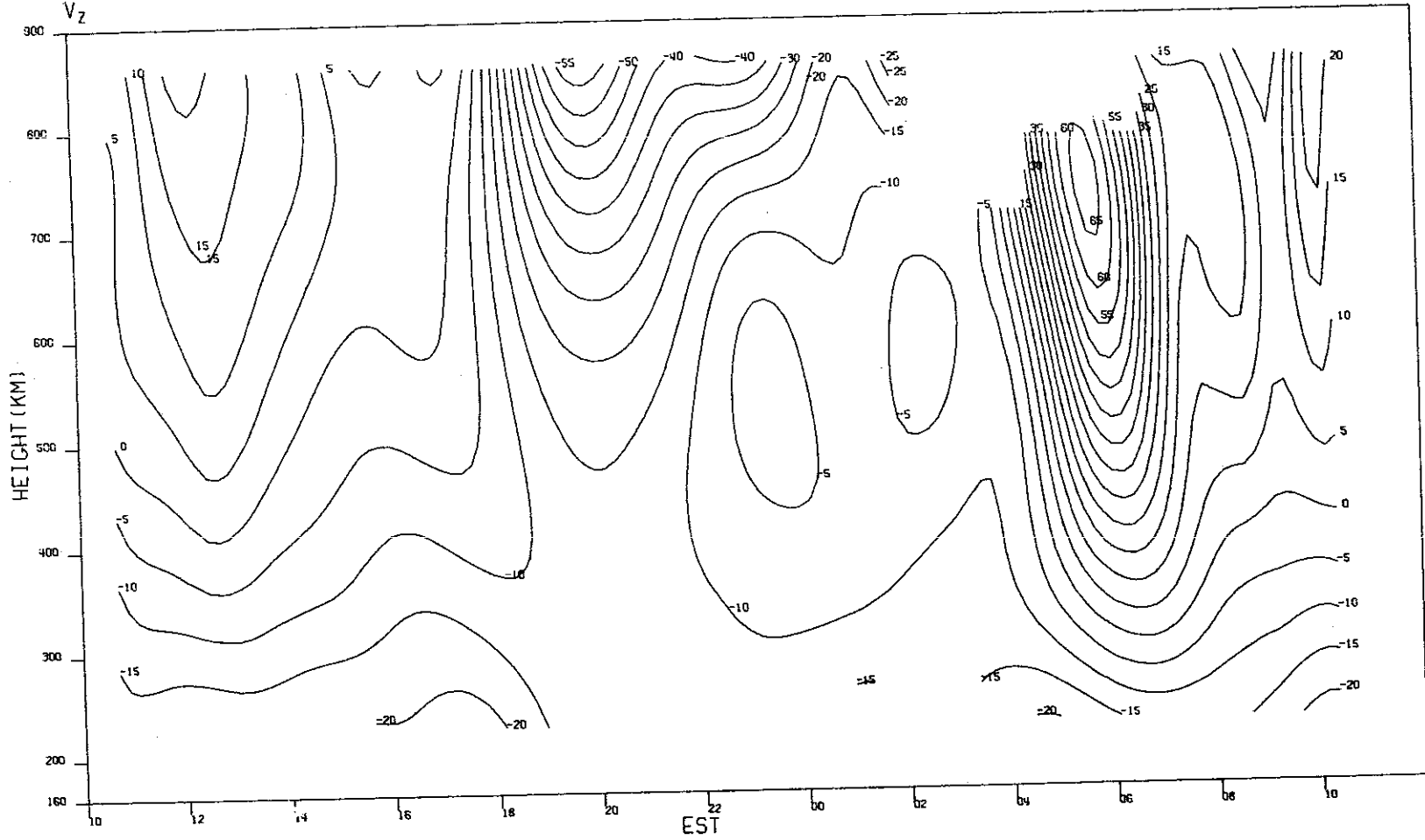


(b)

Fig. 4(a-v). Continued.

MILLSTONE HILL
17-18, MAR, 1970
V_z

-9-5204



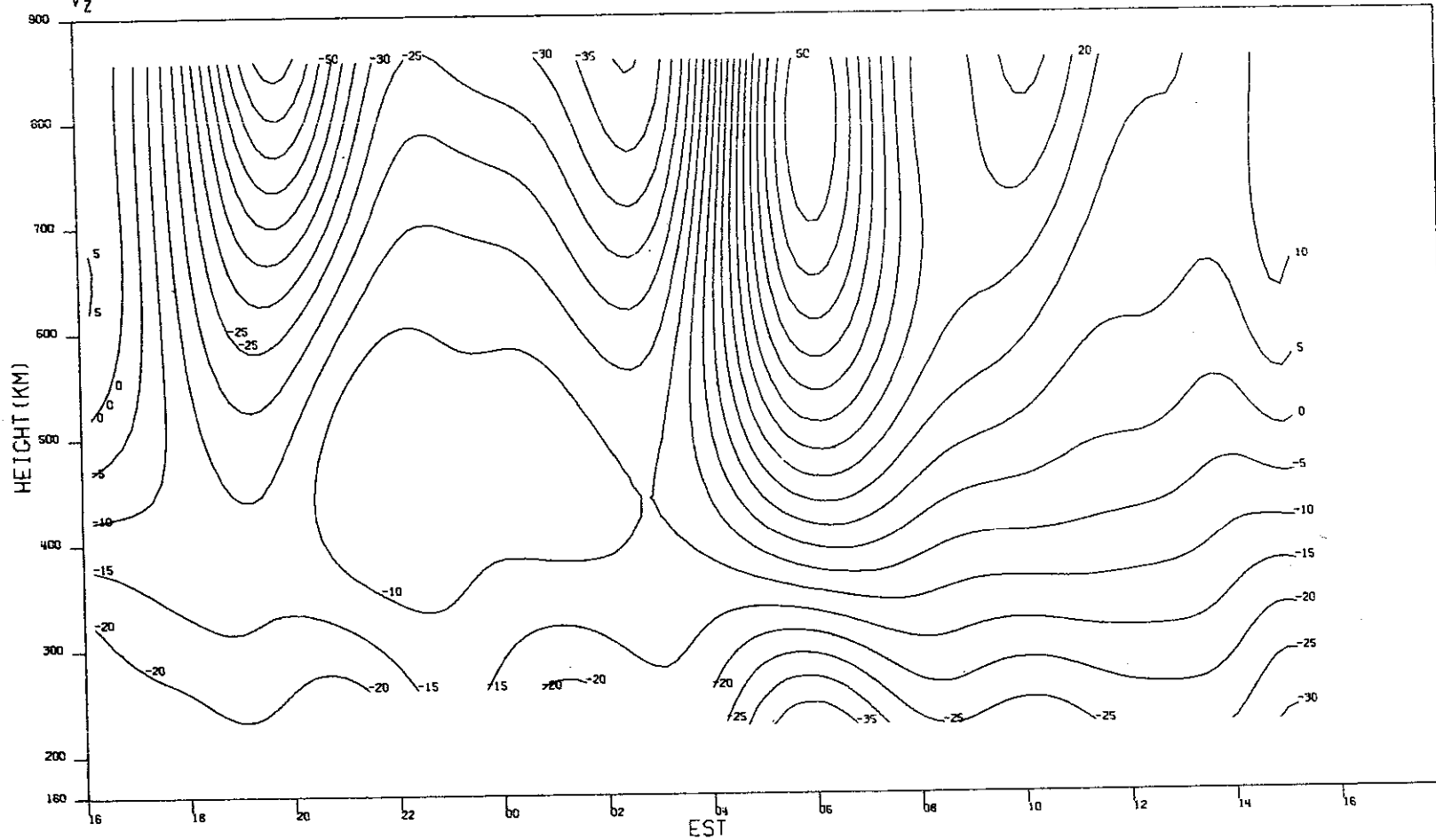
111

(c)

Fig.4(a-v). Continued.

MILLSTONE HILL
23-24, MAR, 1970
Vz

-9-5205



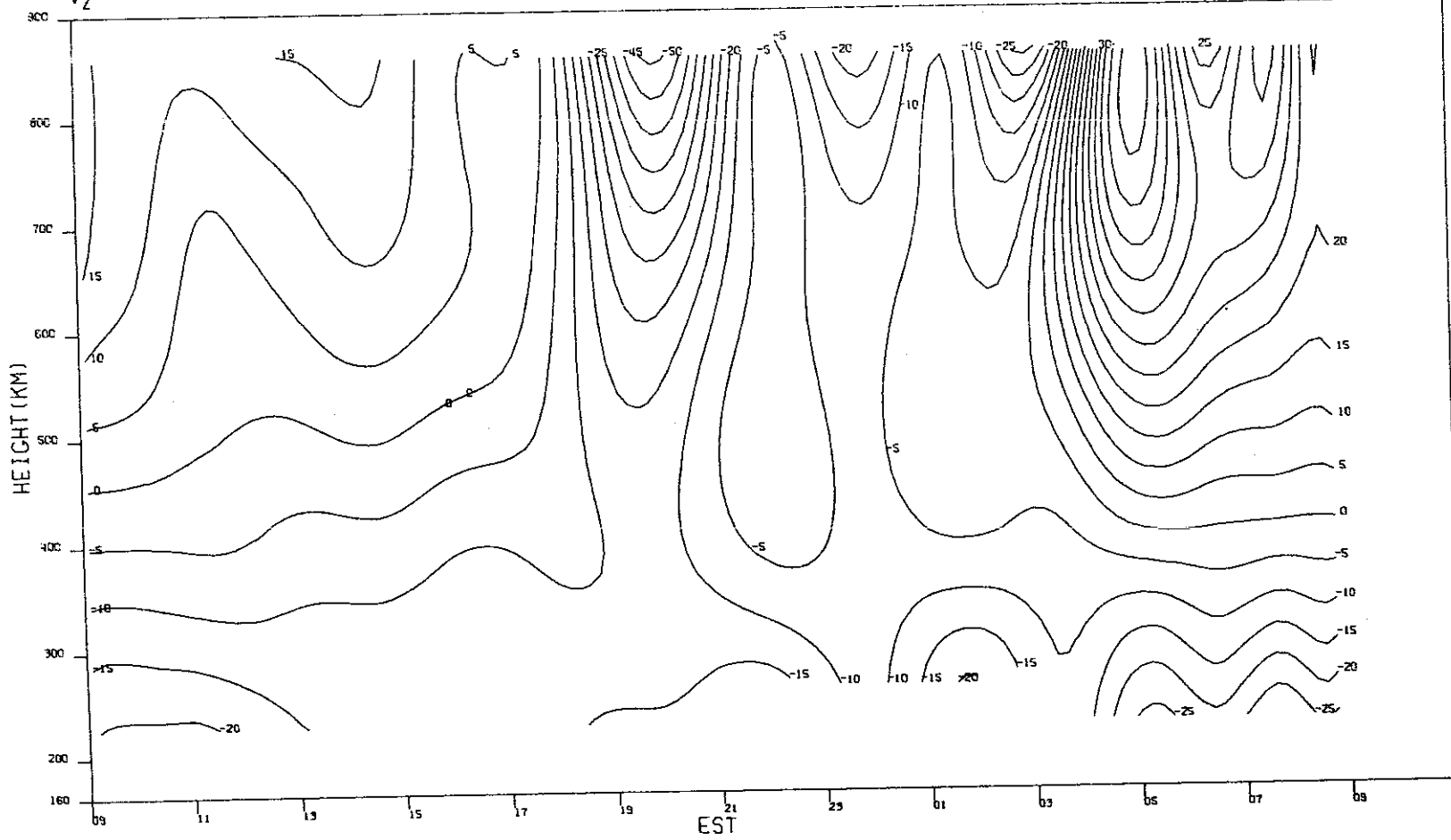
112

(d)

Fig. 4(a-v). Continued.

MILLSTONE HILL
14-15, APR, 1970
Vz

-9-5206



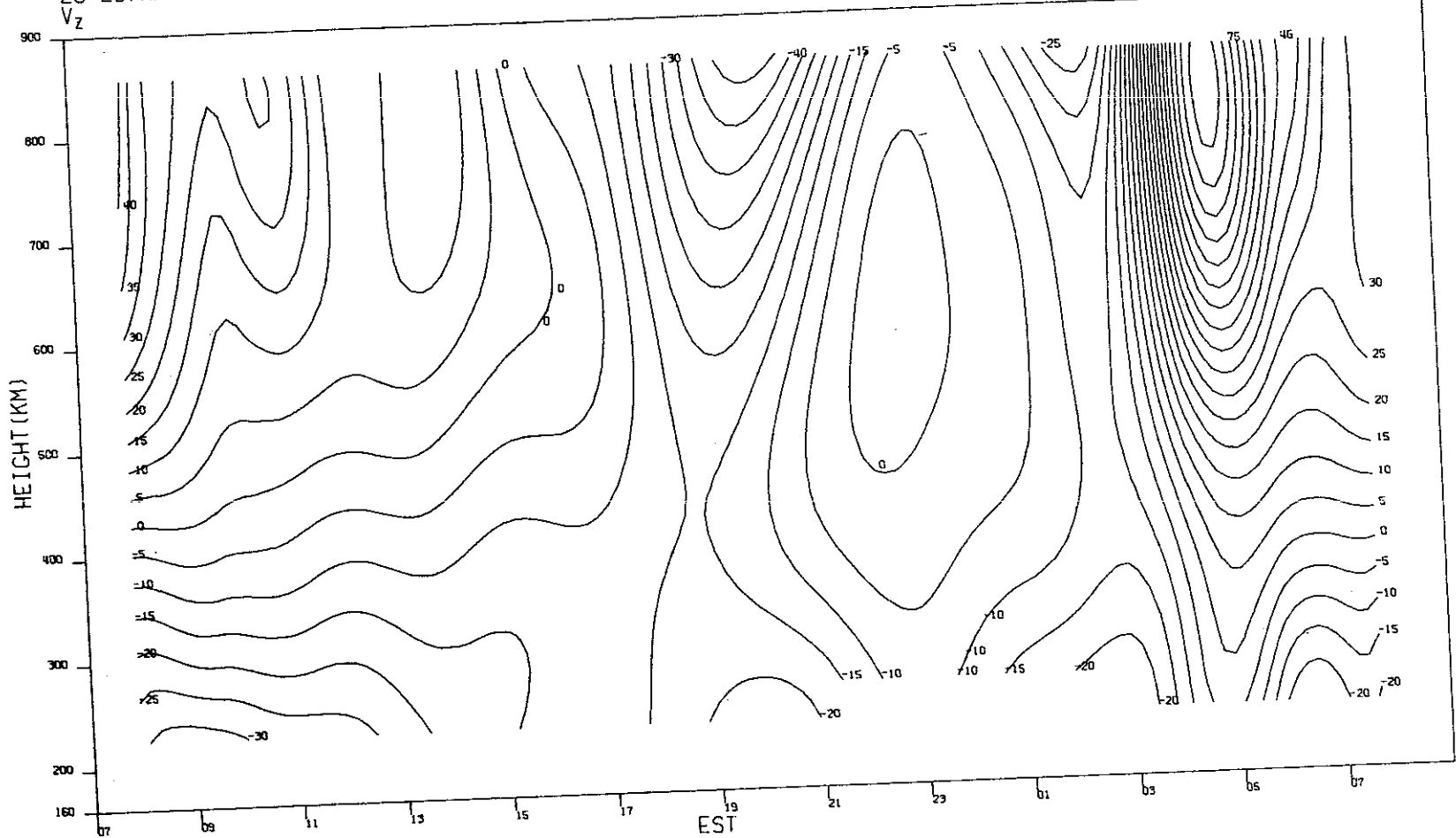
113

(e)

Fig. 4(a-v). Continued.

MILLSTONE HILL
28-29, APR, 1970

-9-5207



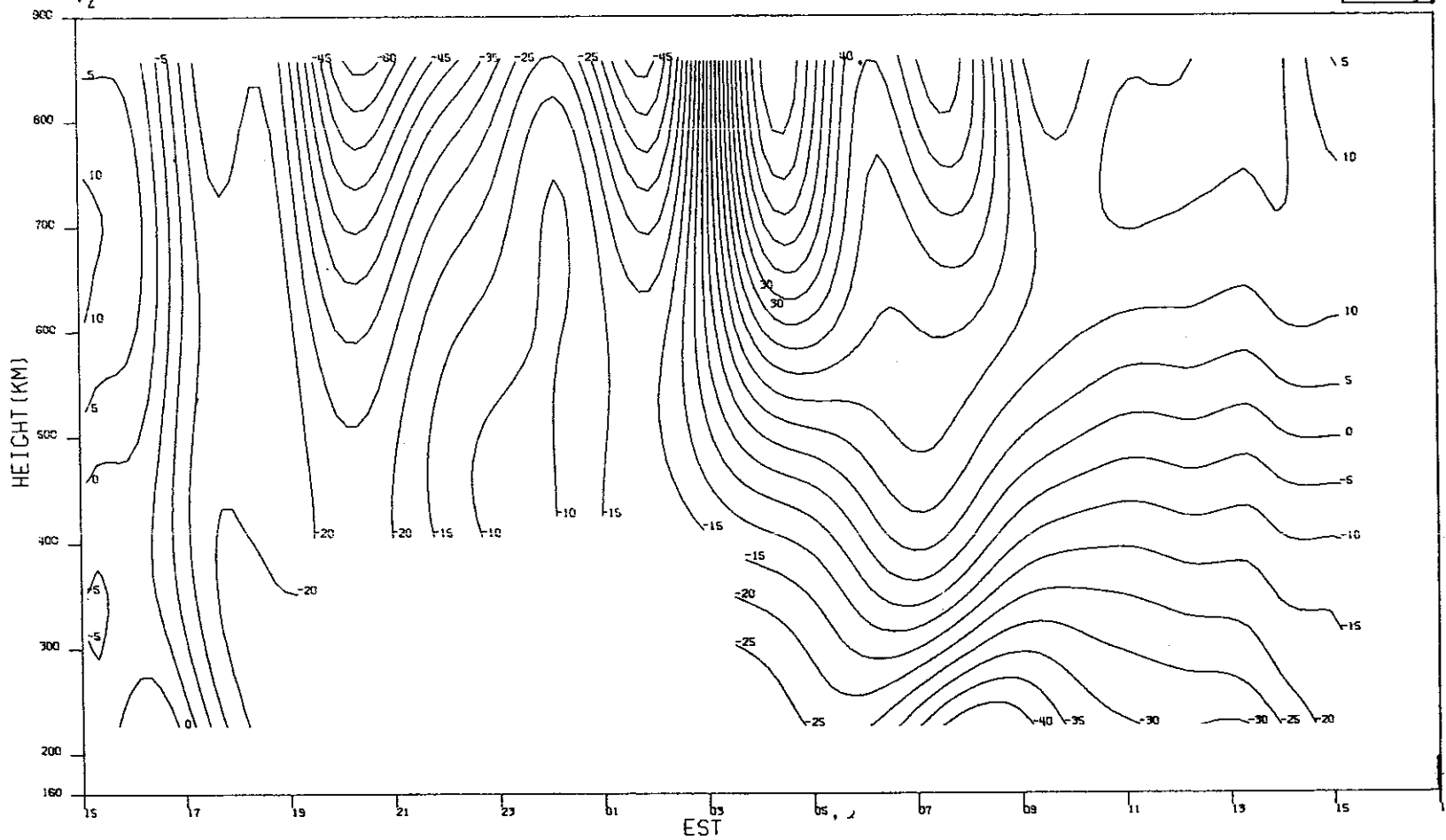
114

(f)

Fig. 4(a-v). Continued.

MILLSTONE HILL
12-13, MAY, 1970
V_z

-9-5208



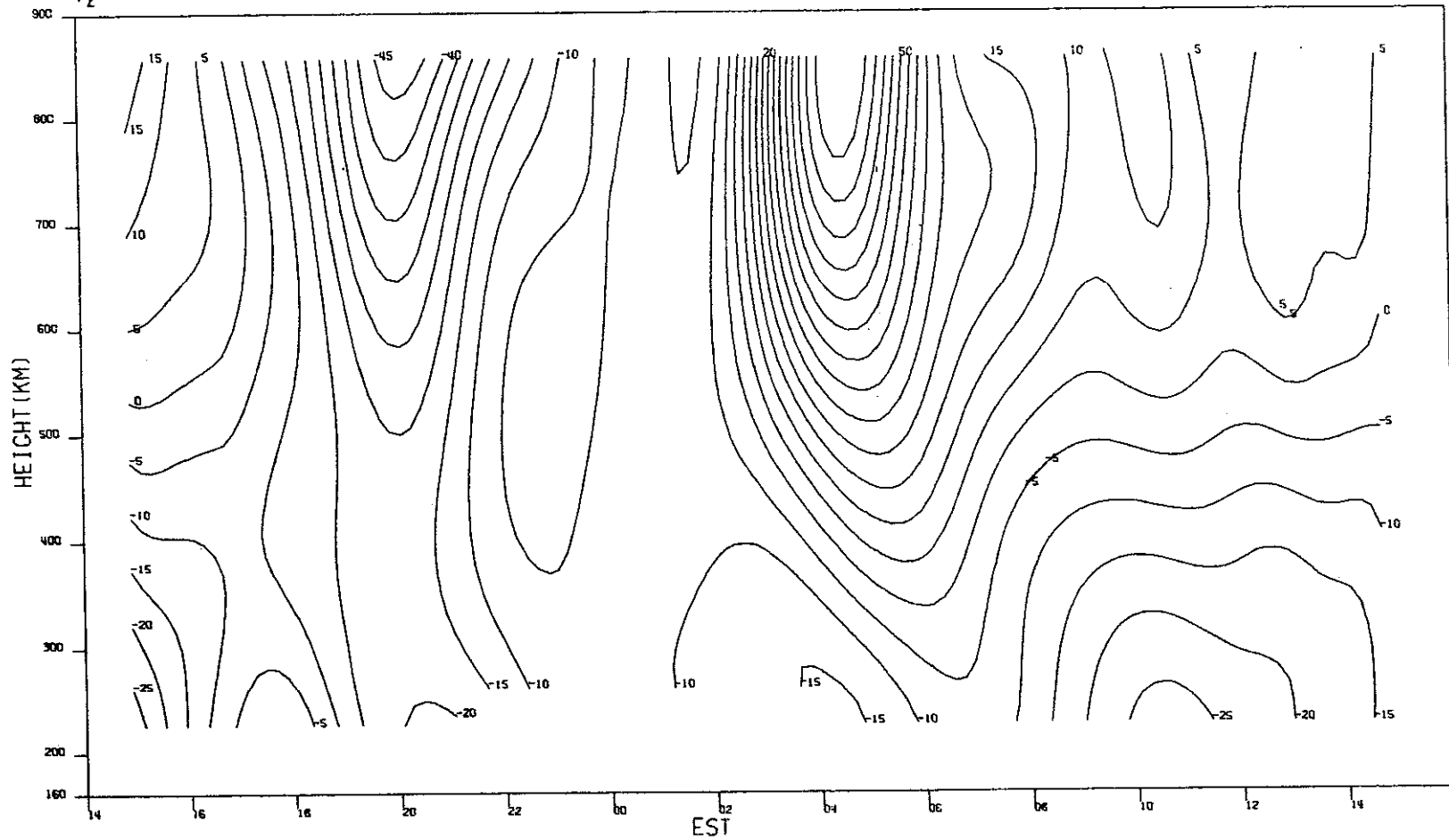
115

(g)

Fig. 4(a-v). Continued.

MILLSTONE HILL
18-19, MAY, 1970
V_z

-9-5209

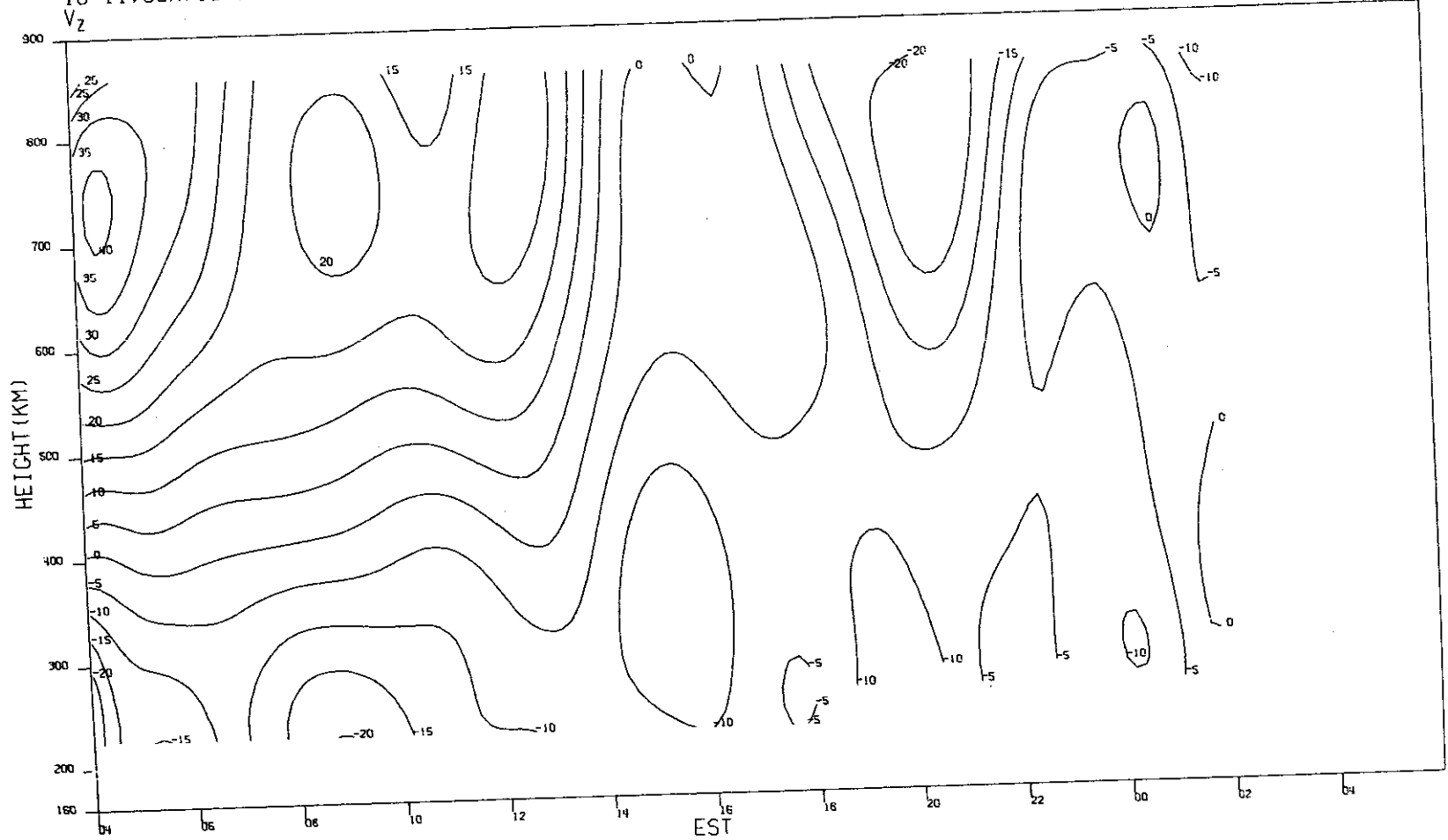


(h)

Fig.4(a-v). Continued.

MILLSTONE HILL
10-11, JUN. 1970
V_z

-9-5210



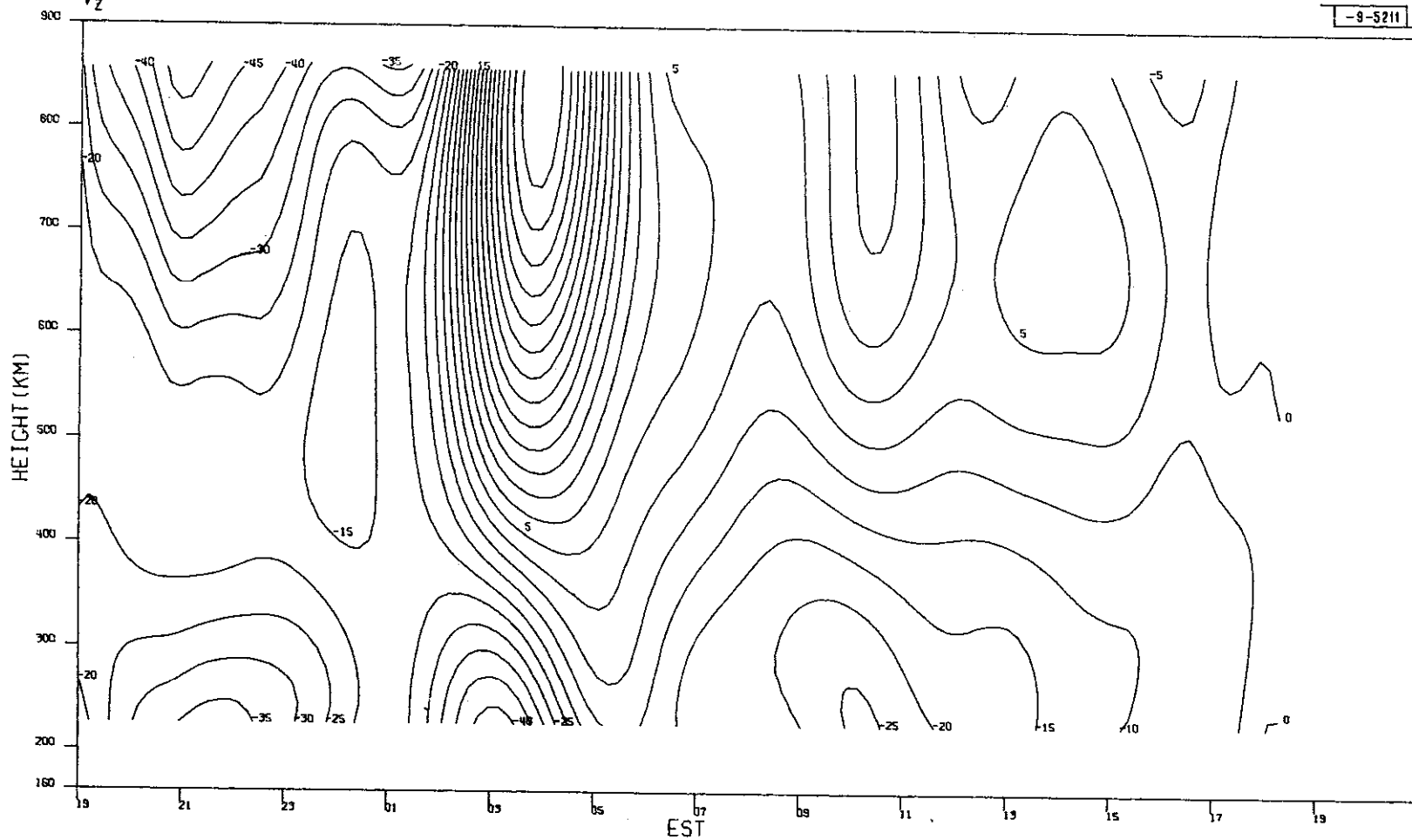
117

(i)

Fig. 4(a-v). Continued.

MILLSTONE HILL
23-24. JUN. 1970
Vz

-9-5211



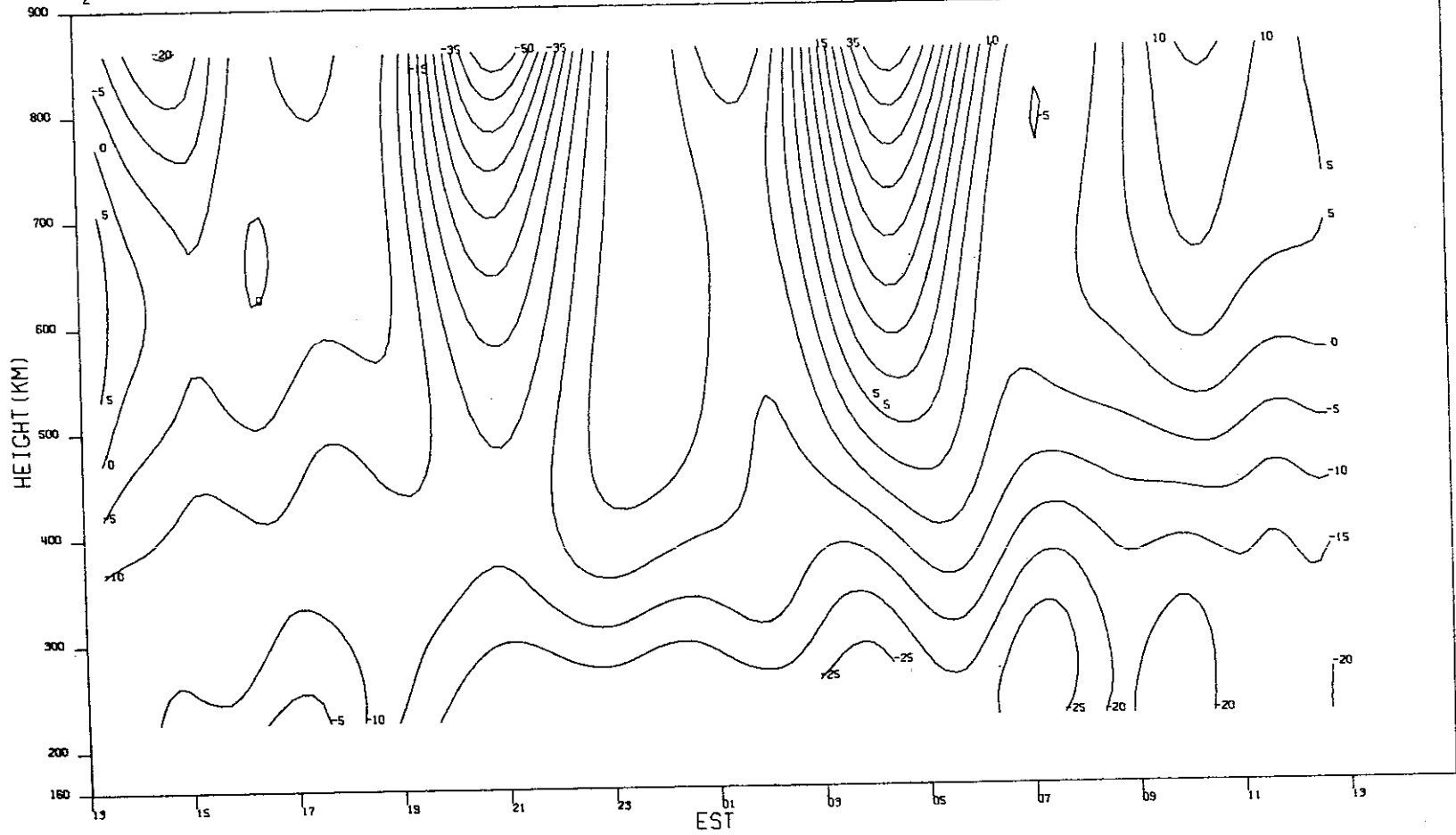
118

(j)

Fig. 4(a-v). Continued.

MILLSTONE HILL
07-08, JUL. 1970
V_z

-9-5212



119

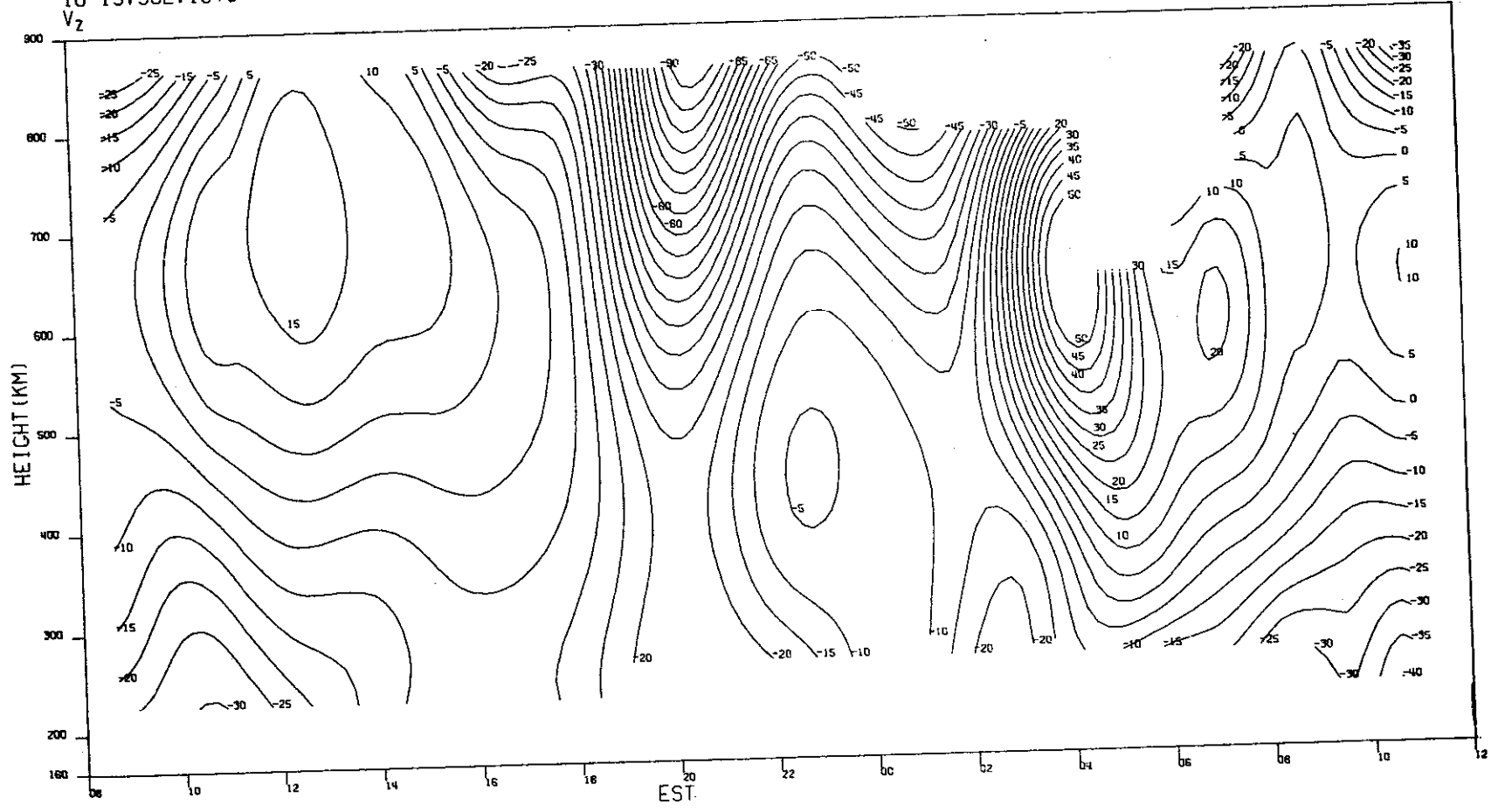
(k)

Fig. 4(a-v). Continued.

MILLSTONE HILL
18-19 JUL. 1970
V₂

-9-5213

120

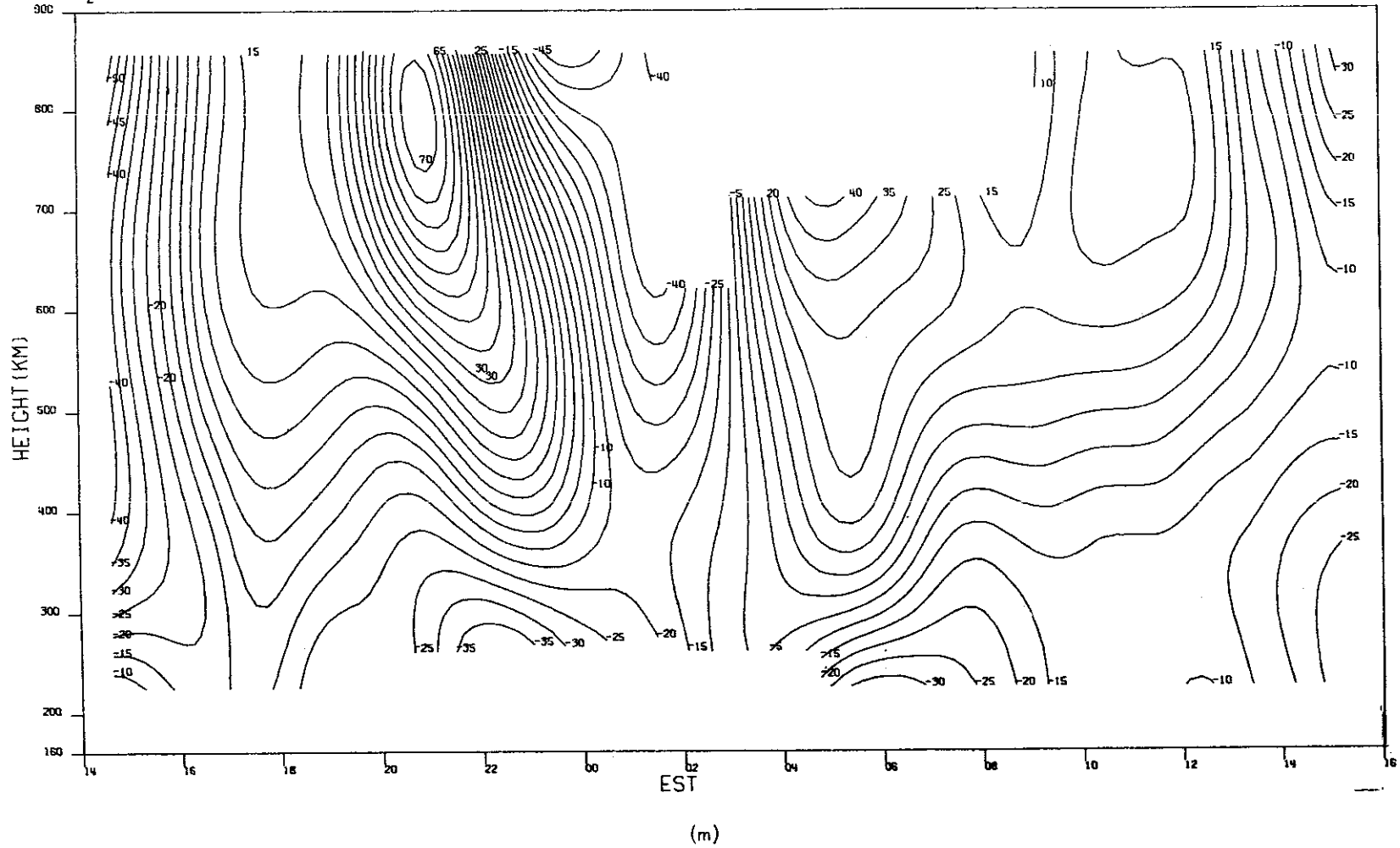


(1)

Fig. 4(a-v). Continued.

MILLSTONE HILL
17-18, AUG. 1970
Vz

-8-5214

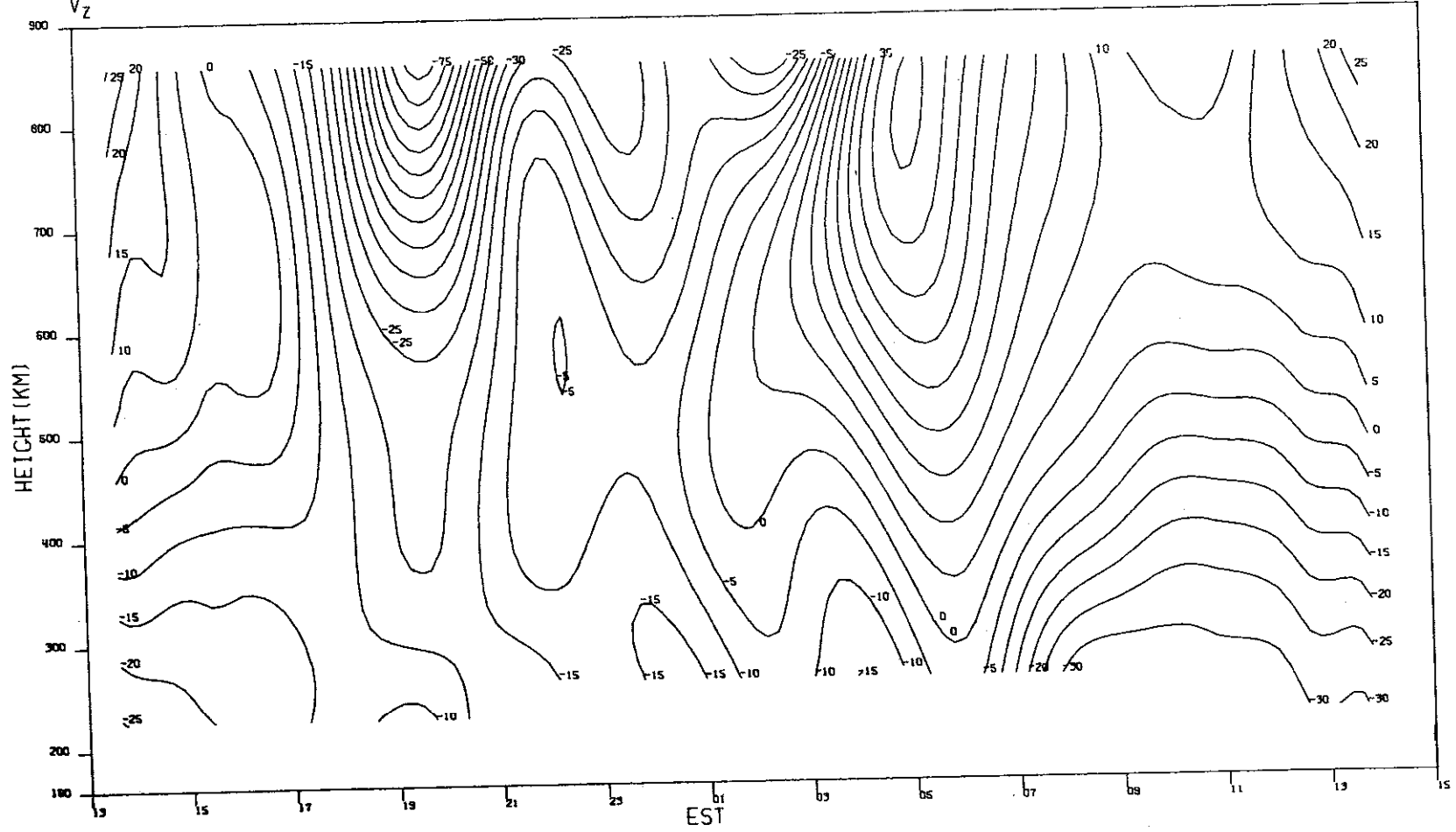


124

Fig. 4(a-v). Continued.

MILLSTONE HILL
24-25, AUG, 1970
V_Z

-9-5215



122

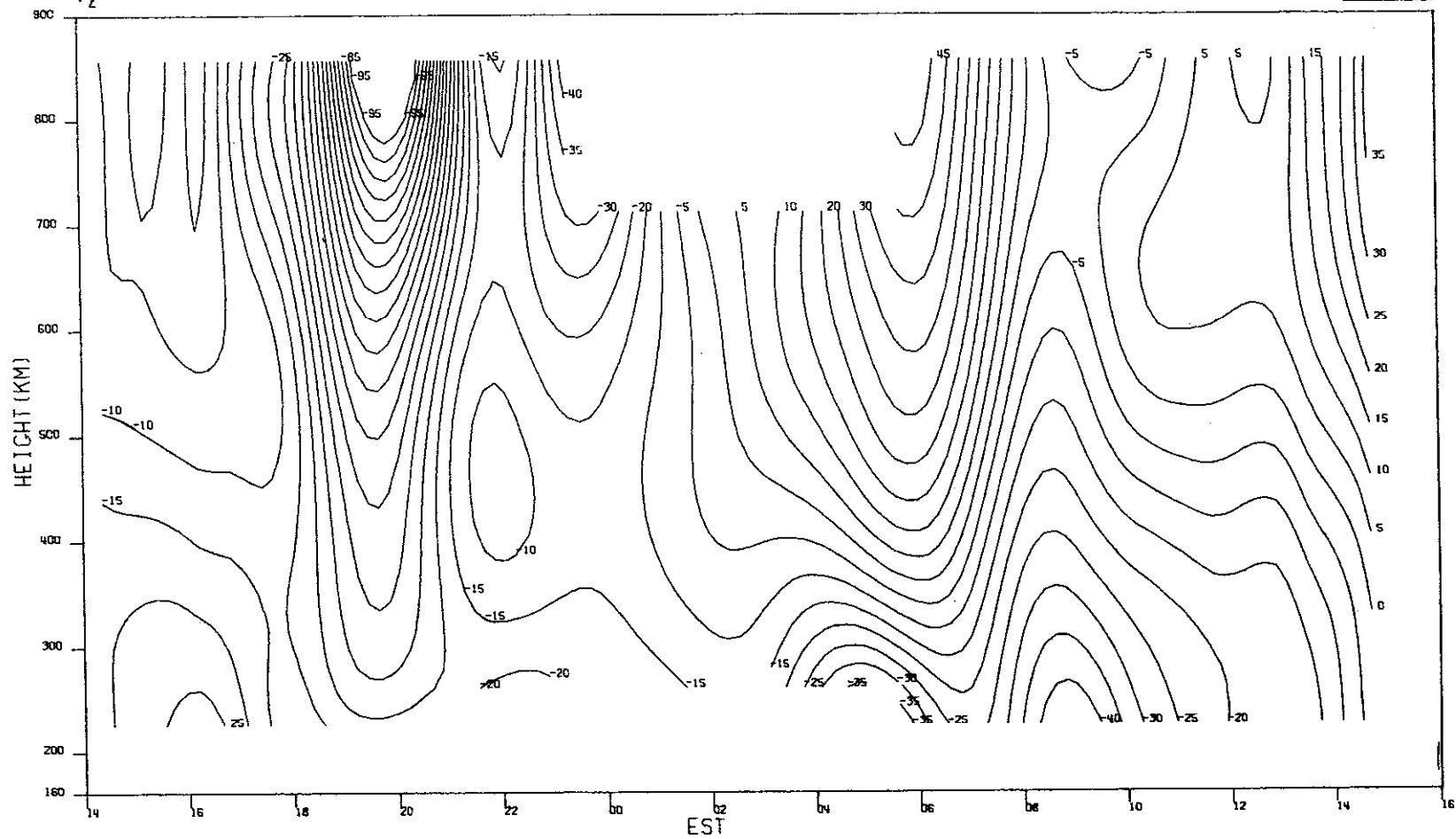
(n)

Fig.4(a-v). Continued.

MILLSTONE HILL
31AUG-01SEP. 1970
V_z

-9-5216

123

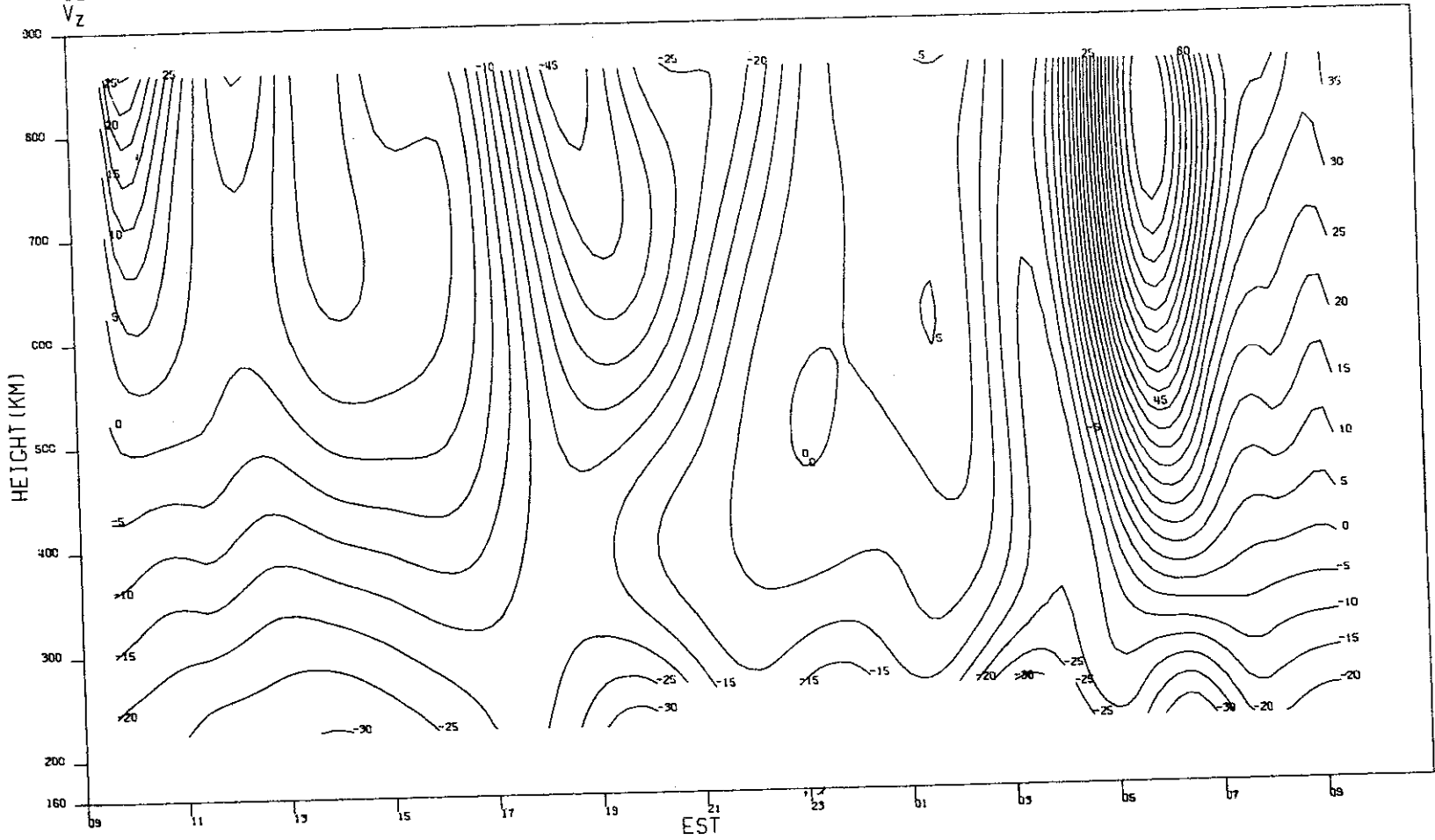


(o)

Fig.4(a-v). Continued.

MILLSTONE HILL
16-17. SEP. 1970

-9-5217



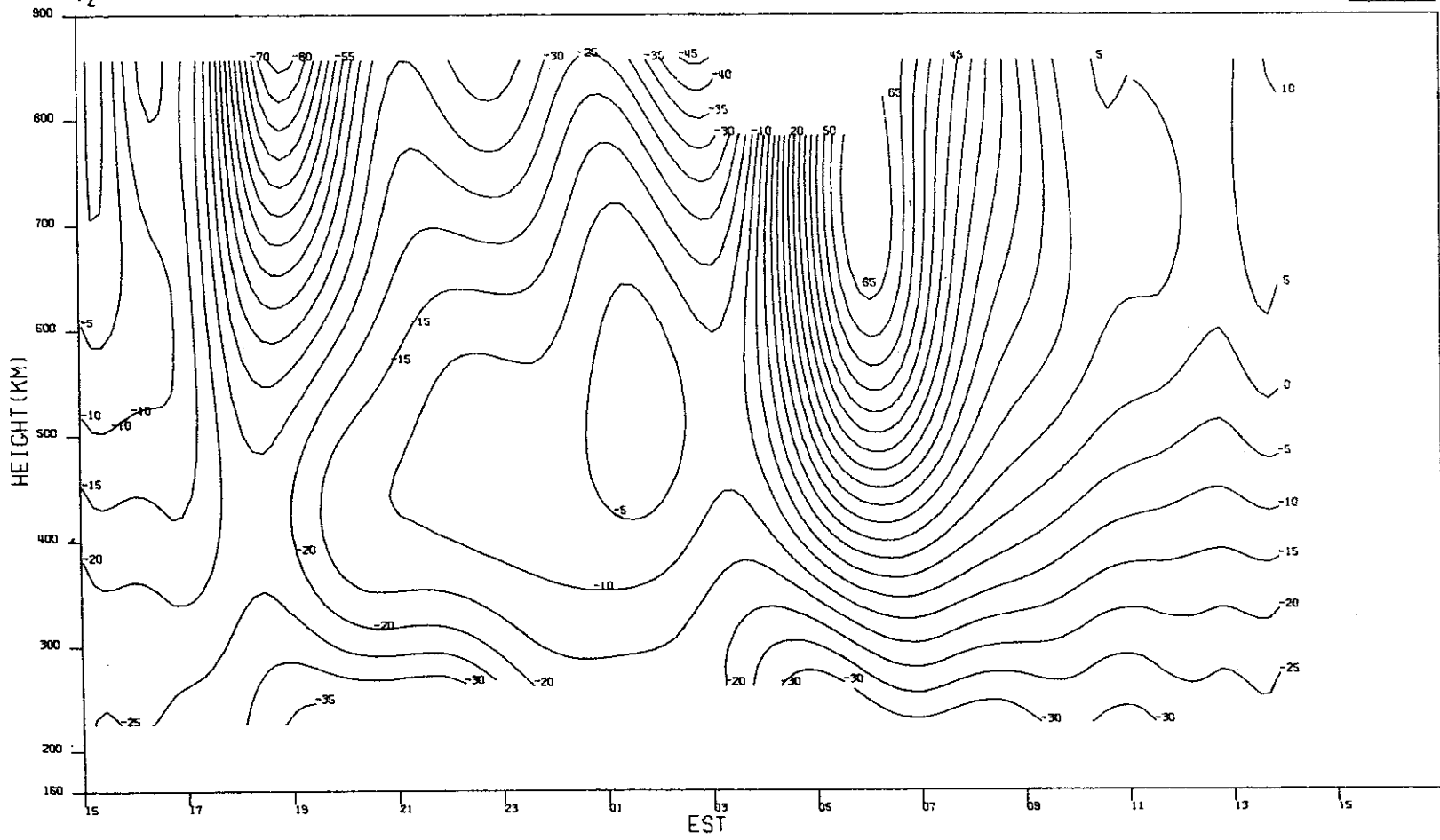
124

(p)

Fig. 4(a-v). Continued.

MILLSTONE HILL
28-29, SEP, 1970
Vz

-9-5218



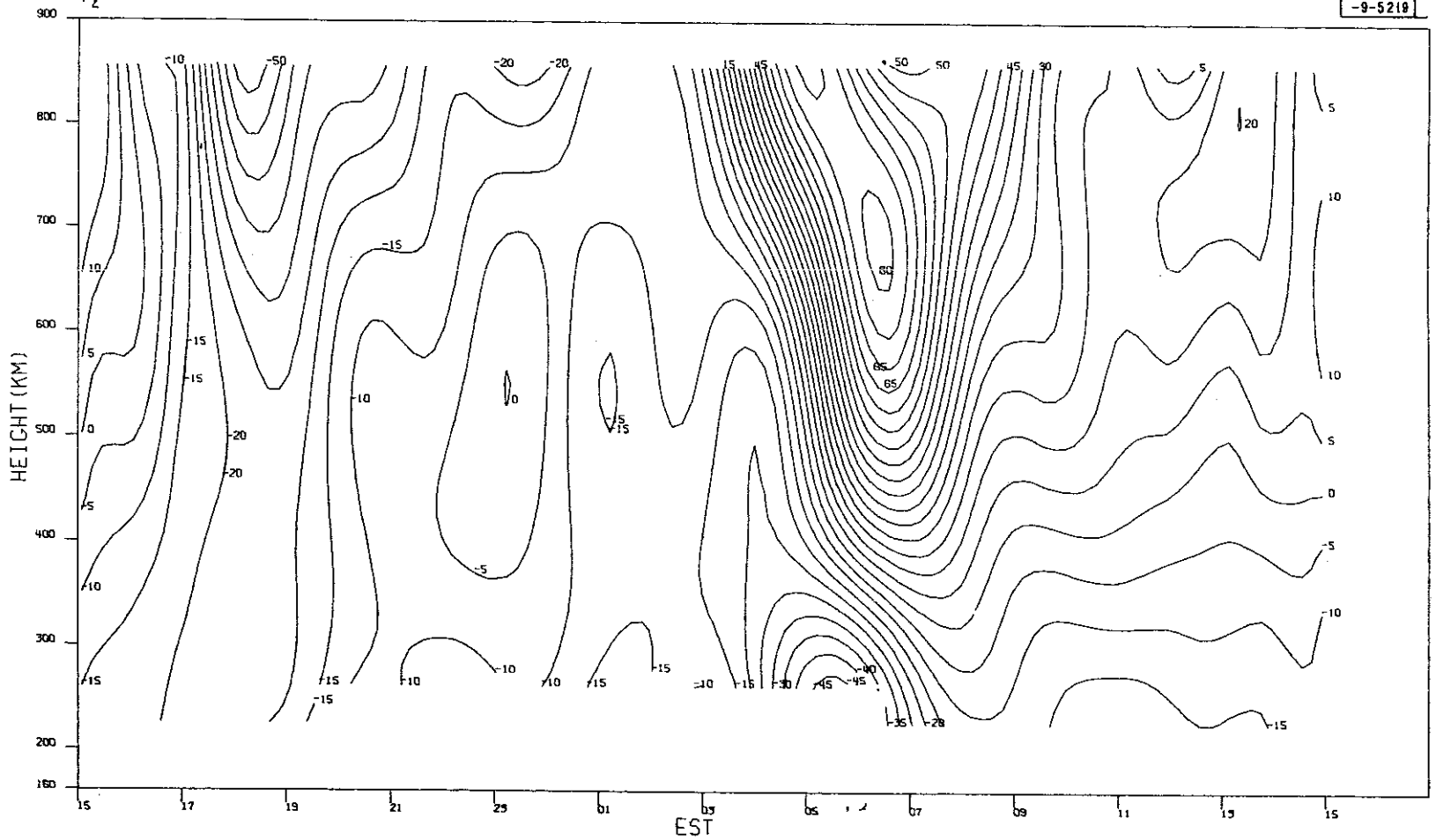
125

(q)

Fig. 4(a-v). Continued.

MILLSTONE HILL
05-06, OCT. 1970
Vz

-9-5219



126

Fig. 4(a-v). Continued.

MILLSTONE HILL
13-14.OCT.1970
V₂

-9-5220

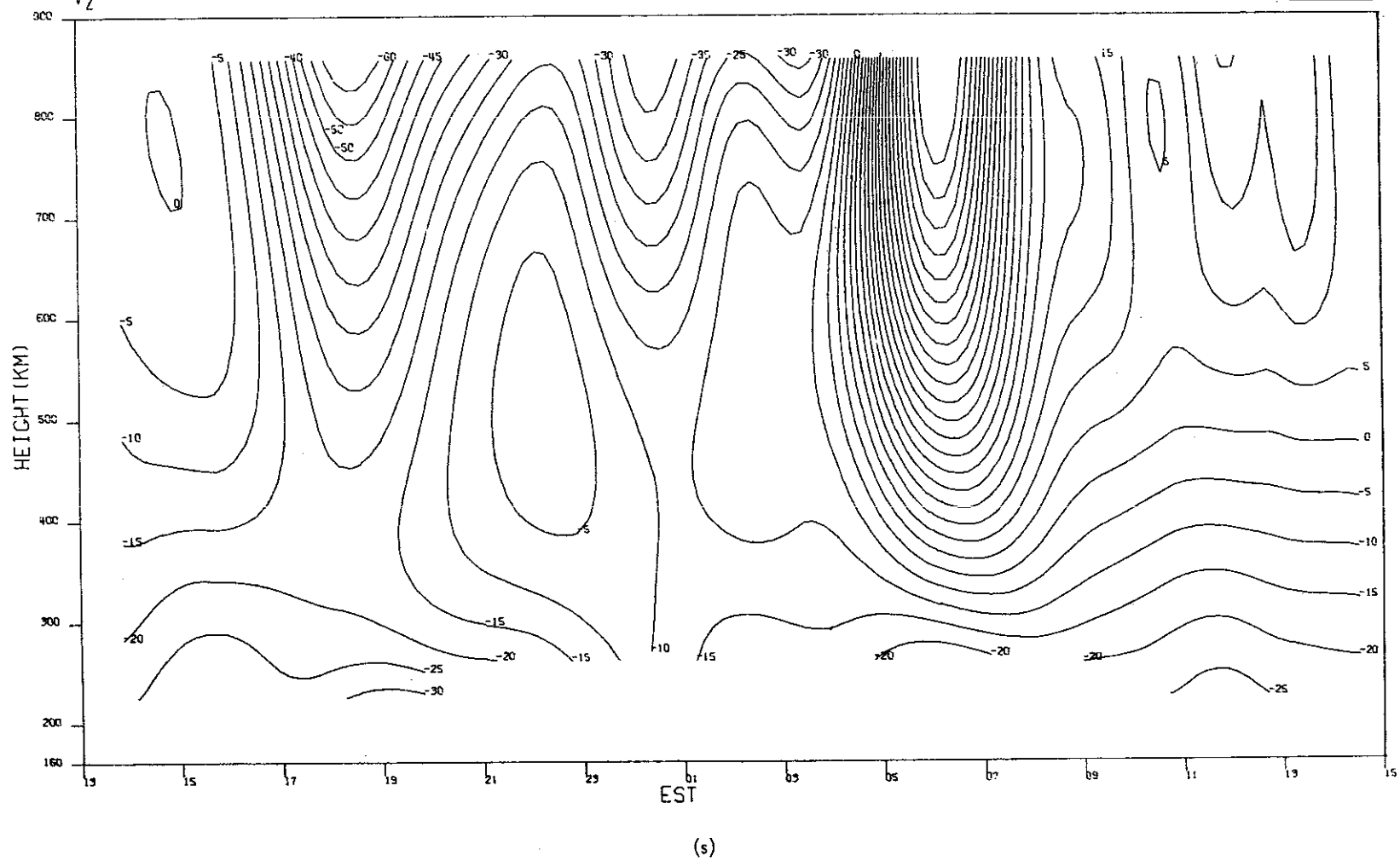
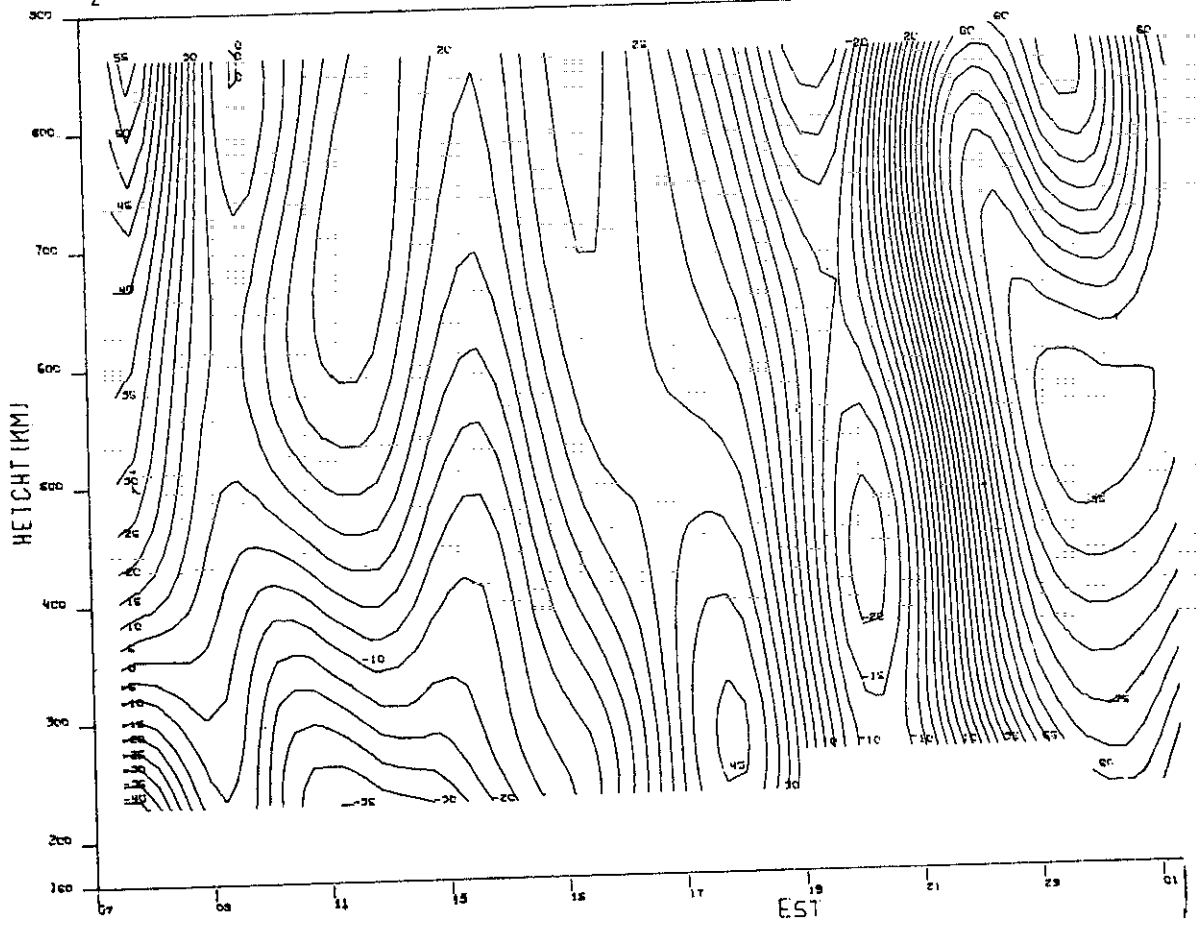


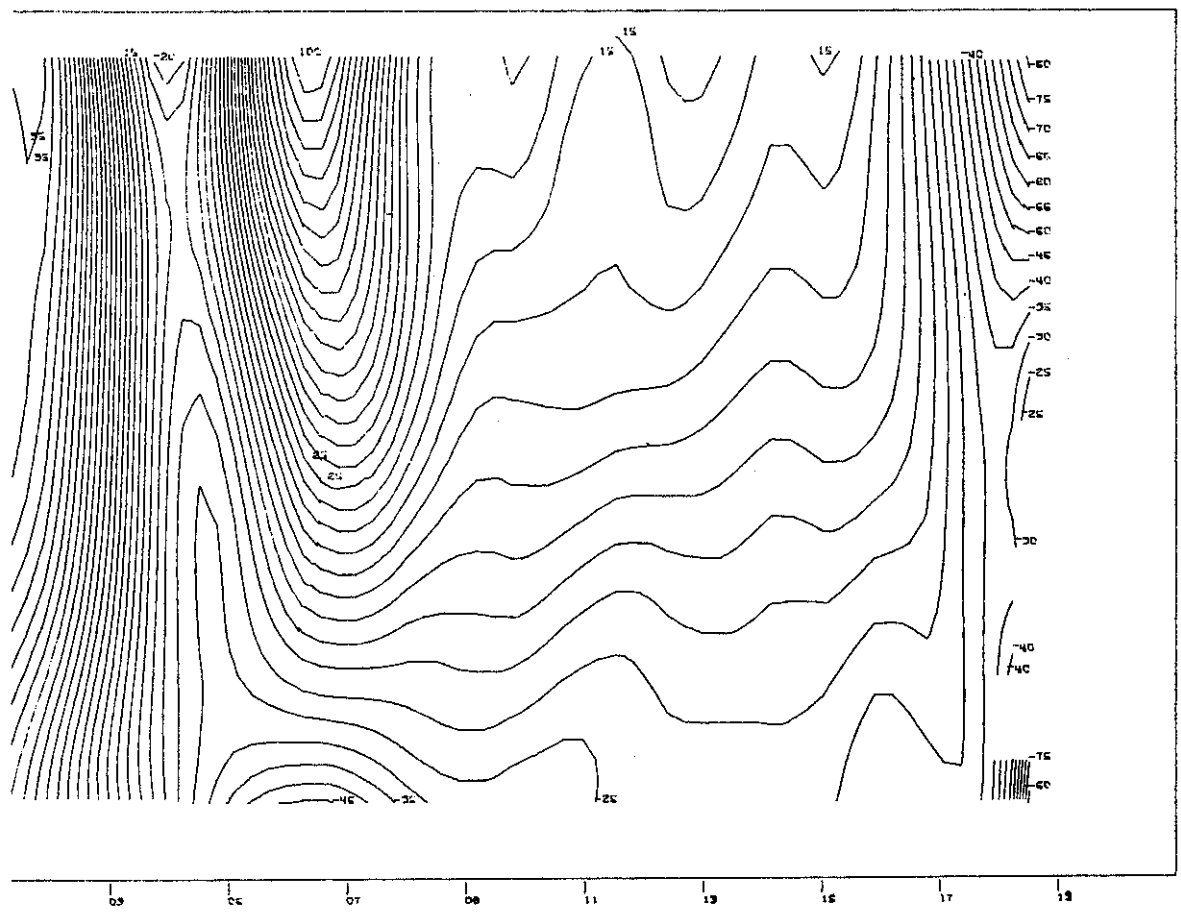
Fig.4(a-v). Continued.

MILLSTONE HILL
31 OCT-01 NOV. 1970
Vz



(t)

Fig. 4(a-v). Continued.



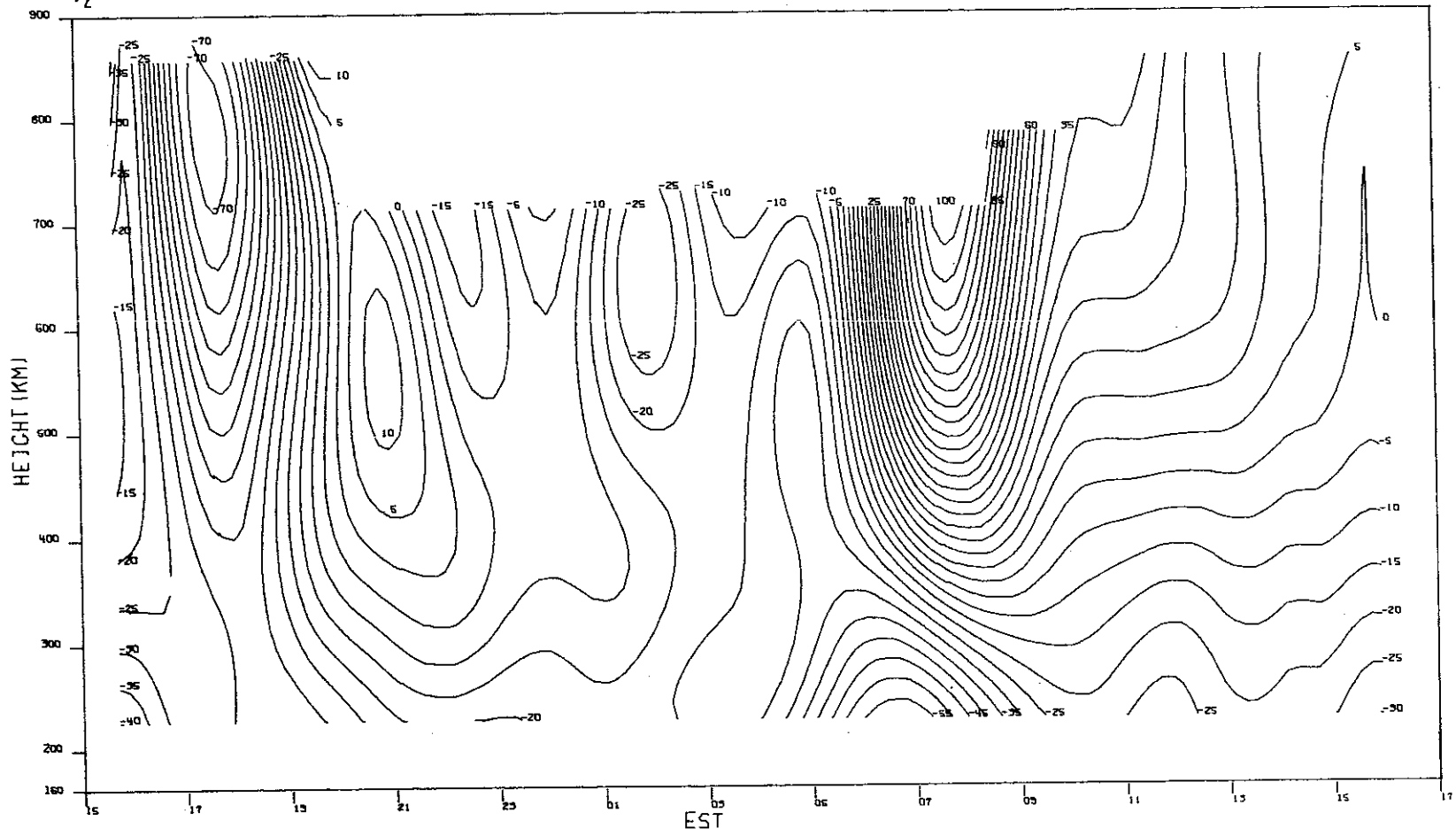
(t)

Fig. 4(a-v). Continued.

MILLSTONE HILL
21-22. DEC. 1970
V_z

-9-5222

130



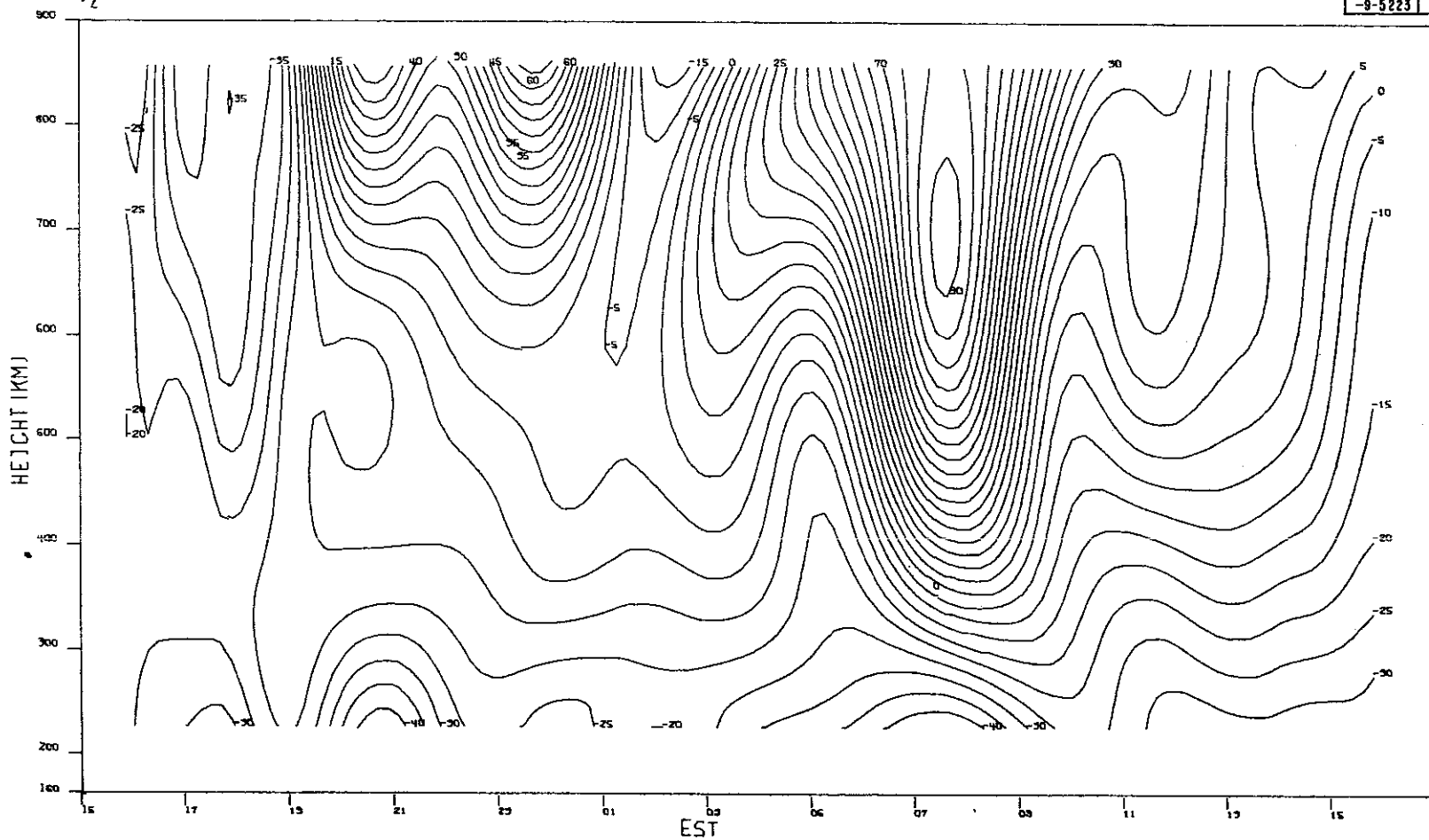
(u)

Fig. 4(a-v). Continued.

MILLSTONE HILL
28-29 DEC. 1970.

V_z

-9-5223



131

(v)

Fig. 4(a-v). Continued.

Here the C-mode results were employed for the nominal altitudes of ≥ 450 km. As we have greater confidence in the C-mode results, this means that the contours drawn for the region above ~ 400 -km altitude are probably more reliable than those below.

The general behavior of the vertical velocity of the plasma over Millstone Hill has been discussed in a series of earlier papers.^{16,32-34} The most striking feature of the contour diagrams is a period of large upward velocity in the region above h_{\max}^{F2} associated with the growth (and thermal expansion) of the layer following sunrise. There is often a fairly well defined period of downward velocity in this region near sunset.

During the daytime, the velocity is usually downward at all altitudes below about 500 km. In this region, ion production exceeds loss so that ions migrate down to lower levels where the recombination rate is higher. Above about 500 km, there is a transition to upward escaping flux, which becomes fully developed by about 700 km. The magnitude of this escape flux in 1969 was the subject of special study.^{7,16} At night in summer, the drift at all levels appears to be directed downward as the layer decays by sinking. In winter there appears to be more variability, though the velocity tends to remain downward. The values obtained for high altitudes (>600 km) at night tend to be very erratic and probably these portions of the contour diagrams should not be trusted.

The vertical velocity observed at Millstone may be represented as the sum of components parallel to and perpendicular to the magnetic field in the north-south (N-S) meridian plane via

$$v_z = 0.96 v_{\parallel} + 0.28 v_{\perp NS} \quad (16)$$

where, in the F-region, the component perpendicular to the magnetic field is related to the east-west (E-W) electric field in

$$v_{\perp} = \frac{\vec{E}_{EW} \times \vec{B}}{B^2} \quad (17)$$

From separate measurements,^{35,36} it appears that on quiet days $V_{\perp NS} < \pm 30$ m/sec. Thus, with some possible small error v_z may be taken as a measure of v_{\parallel} . The velocity observed in the vicinity of h_{\max}^{F2} depends upon the N-S component of the thermospheric wind³³ and this allows the component of the wind to be recovered from incoherent scatter measurements. Salah and Holt³⁷ have examined in detail results for two days in 1970 (23-24 March and 28-29 September) using this approach.

An extension of this work has been the calculation of the zonal wind velocity using the observed diurnal neutral temperature variation to describe the E-W pressure variation. That is, the pressure (temperature) gradients in a local model for the neutral atmosphere (having fixed lower boundary conditions) are simultaneously adjusted to produce the observed diurnal variation of exospheric temperature and meridional winds in the presence of the observed electron concentrations (which establish the ion drag).^{38,39} This analysis has been applied to the results reported by Salah and Holt³⁷ by Roble *et al.*,³⁸ and Antoniadis.³⁹

More recently, Roble⁴⁰ has combined the above neutral calculation with a photochemical model for the ionosphere and was able to reproduce the electron density, and electron and ion temperatures observed at Millstone on 23-24 March 1970. This appears to represent the most complete use of information gathered by the incoherent scatter technique in testing ionospheric theory yet attempted.

ACKNOWLEDGMENTS

The authors are indebted to W. A. Reid, L. B. Hanson, J. H. McNally, D. E. Olden, and others of the staff at Millstone Hill who assisted in operating and maintaining the equipment employed to gather the data reported here. R. F. Julian, J. K. Upham, and Mrs. A. Freeman all contributed to the reduction of the results. During 1970, the incoherent scatter work at Millstone was supported by the U.S. Army as part of a program of radar propagation study. Preparation of this report was supported by the National Science Foundation under Grant GA-42230.

REFERENCES

1. J. V. Evans, "Ionospheric Backscatter Observations at Millstone Hill," Technical Report 374, Lincoln Laboratory, M.I.T. (22 January 1965), DDC AD-616607.
2. _____, "Millstone Hill Thomson Scatter Results for 1964," Technical Report 430, Lincoln Laboratory, M.I.T. (15 November 1967), DDC AD-668436.
3. _____, "Millstone Hill Thomson Scatter Results for 1965," Technical Report 474, Lincoln Laboratory, M.I.T. (18 December 1969), DDC AD-707501.
4. _____, "Millstone Hill Thomson Scatter Results for 1966," Technical Report 481, Lincoln Laboratory, M.I.T. (15 December 1970), DDC AD-725742.
5. _____, "Millstone Hill Thomson Scatter Results for 1967," Technical Report 482, Lincoln Laboratory, M.I.T. (22 July 1971), DDC AD-735727.
6. _____, "Millstone Hill Thomson Scatter Results for 1968," Technical Report 499, Lincoln Laboratory, M.I.T. (23 January 1973), DDC AD-767251/2.
7. _____, "Millstone Hill Thomson Scatter Results for 1969," Technical Report 513, Lincoln Laboratory, M.I.T. (23 July 1974), DDC AD-A008505/0.
8. _____, *Planet. Space Sci.* 13, 1031 (1965), DDC AD-616607.
9. _____, *J. Geophys. Res.* 70, 1175 (1965), DDC AD-614310.
10. _____, *Planet. Space Sci.* 15, 1387 (1967).
11. _____, *Planet. Space Sci.* 18, 1225 (1970), DDC AD-716056.
12. _____, *J. Atmos. Terr. Phys.* 32, 1629 (1970), DDC AD-716057.
13. _____, *J. Geophys. Res.* 75, 4803 and 4815 (1970), DDC AD-714447 and DDC AD-714446, respectively.
14. _____, *Planet. Space Sci.* 21, 763 (1973), DDC AD-772137/6.
15. _____, *J. Atmos. Terr. Phys.* 35, 593 (1973), DDC AD-771877/8.
16. _____, *Planet. Space Sci.* 23, 1461 and 1611 (1975).
17. G. W. Armistead, J. V. Evans, and W. A. Reid, *Radio Sci.* 7, 153 (1972).
18. J. V. Evans, editor, "The Millstone Hill Propagation Study: Progress in FY 1970," Technical Note 1970-20, Lincoln Laboratory, M.I.T. (2 December 1970), DDC AD-717156.
19. J. V. Evans and W. L. Oliver, *Radio Sci.* 1, 103 (1972).
20. W. L. Oliver and S. A. Bowhill, "Investigation of the Ionospheric Response to the Solar Eclipse of 7 March 1970 by the Thomson Scatter Radar Technique at Millstone Hill Ionospheric Observatory," Aeronomy Report 51, Department of Electrical Engineering, University of Illinois, Urbana (1 February 1973).
21. J. E. Salah and J. V. Evans, *Space Research XIII* (Akademie-Verlag, Berlin, 1973), pp. 267-286.
22. J. E. Salah, R. H. Wand, and J. V. Evans, *Radio Sci.* 10, 347 (1975).
23. J. E. Salah, J. V. Evans, and R. H. Wand, *Radio Sci.* 9, 231 (1974); also *J. Atmos. Terr. Phys.* 37, 461 (1975).

24. J.S. Nisbet, *J. Atmos. Sci.* 24, 586 (1967).
25. J.V. Evans, R.F. Julian, and W.A. Reid, "Incoherent Scatter Measurements of F-Region Density, Temperatures, and Vertical Velocity at Millstone Hill," Technical Report 477, Lincoln Laboratory, M.I.T. (6 February 1970), DDC AD-706863.
26. J.P. McClure, W.B. Hanson, A.F. Nagy, R.J. Cicerone, L.H. Brace, M. Baron, P. Bauer, H.C. Carlson, J.V. Evans, G.N. Taylor, and R.F. Woodman, *J. Geophys. Res.* 78, 197 (1973).
27. J. Noxon and J.V. Evans, "Simultaneous Optical and Incoherent Scatter Observations of Two Low-Latitude Auroras," *Planet. Space Sci.* 24, 425 (1976).
28. J.L. Massa, "Theoretical and Experimental Studies of the Ionization Exchange between the Ionosphere and Plasmasphere," Ph. D. Thesis, University of Michigan, Ann Arbor (1974).
29. W.W. Hauck, Jr., "Foundations for Estimation by the Method of Least Squares," Smithsonian Astrophysical Observatory Special Report 340 (27 December 1971).
30. G. Dahlquist, A. Bjorck, and N. Anderson, *Numerical Methods* (Prentice Hall, Englewood Cliffs, New Jersey, 1969), pp. 101-103.
31. M.H. Schultz, *Spline Analysis* (Prentice Hall, Englewood Cliffs, New Jersey, 1973).
32. J.V. Evans, R.A. Brockelman, R.F. Julian, W.A. Reid, and L.A. Carpenter, *Radio Sci.* 5, 27 (1970).
33. J.V. Evans, *Radio Sci.* 6, 609; also 6, 843 (1971).
34. J.V. Evans and J.M. Holt, *Radio Sci.* 6, 855 (1971).
35. J.V. Evans, *J. Geophys. Res.* 77, 2341 (1972).
36. V.W.J.H. Kirchhoff and L.A. Carpenter, *J. Atmos. Terr. Phys.* 37, 419 (1975).
37. J.E. Salah and J.M. Holt, *Radio Sci.* 9, 301 (1974).
38. R.G. Roble, B.A. Emery, J.E. Salah, and O.B. Hays, *J. Geophys. Res.* 79, 2868 (1974).
39. D.A. Antoniadis, *J. Atmos. Terr. Phys.* 38, 187 (1976).
40. R.G. Roble, *Planet. Space Sci.* 23, 1017-1034 (1975).

APPENDIX
RCVR, RCVR1, RCVRP: USERS INSTRUCTIONS, LISTING
AND SAMPLE PRINTED OUTPUT

RCVR, RCVR1, and RCVRP are intended for external distribution and are, therefore, completely self-documented. The user should refer to the following listings for information on the use of these subroutines. These listings include three short test programs to test RCVR, RCVR1, and RCVRP. Each test program first calls SUBROUTINE CREAD to read the card deck generated by INSCON. RCVR, RCVR1, or RCVRP is then called to recover the INSCON fit values at the experimental times and altitudes. The user is not limited to these times and altitudes, but may use any others within the range of the data. Each recovery routine requires two or three additional subroutines:

RCVR: SET, IPL

RCVR1: SET1, IPL

RCVRP: RCVR1, SPLN3A, TRIDAG

Listings of SET, SET1 and IPL are included in this appendix. In the version of these programs intended for external distribution, the INSCON parameters are stored in a labelled COMMON block rather than blank COMMON. An abbreviated example of the printed output produced by the RCVR1 test program follows the listings.

RCVR, RCVR1, RCVRP LISTINGS

C	PROGRAM TEST RCVR	TEST0010
C		TEST0020
C	INSCON IS A FORTRAN PROGRAM WHICH CALCULATES LEAST MEAN SQUARE	TEST0030
C	FITS TO, AND PLOTS CONTOUR DIAGRAMS OF, INCOHERENT SCATTER DATA	TEST0040
C	OBTAINED AT MILLSTONE HILL. THE FIT VALUE CORRESPONDING TO A	TEST0050
C	GIVEN TIME AND ALTITUDE MAY BE RECOVERED BY MEANS OF SUBROUTINES	TEST0060
C	CREAD AND RCVR. FOR EXAMPLE THIS PROGRAM FIRST CALLS CREAD TO	TEST0070
C	READ THE CARD DECK GENERATED BY INSCON. IT THEN CALLS RCVR TO	TEST0080
C	RECOVER THE INSCON FIT VALUES AT THE EXPERIMENTAL TIMES AND	TEST0090
C	ALTITUDES.	TEST0100
C		TEST0110
C	COMMON LABEL, IDAYNO,	TEST0120
	1 KOAT, NX, NY, NPX, NPY, XT, YT, DMAX, DMIN, XMAX, XMIN,	TEST0130
	2 YMAX, YMIN, RELTME, SHIFT, GAMX, DELX, FACX, GAMY, DELY,	TEST0140
	3 FACY, A, SIG, ISTAT	TEST0150
	DIMENSION LABEL(15)	TEST0160
	DIMENSION XT(64), YT(64), GAMX(32), DELX(32), FACX(32), GAMY(32),	TEST0170
	1 DELY(32), FACY(32), A(32,32), SIG(64), ISTAT(64,64)	TEST0180
C		TEST0190
C	10 CALL CREAD	TEST0200
C		TEST0210
C	WRITE(6,101)	TEST0220
C		TEST0230
	DO 20 I=1,NPX	TEST0240
	ITIME = XT(I) + RELTME	TEST0250
	IF(ITIME .GT. 86400) ITIME=ITIME-86400	TEST0260
	IHRS = ITIME/3600	TEST0270
	MINS = (ITIME-IHRS*3600)/60	TEST0280
	ITIME = 10000 + 100*IHRS + MINS	TEST0290
	DO 20 J=1,NPY	TEST0300
	CALL RCVR(XT(I), YT(J), P)	TEST0310
	WRITE(6,201) ITIME, YT(J), P	TEST0320
	20 CONTINUE	TEST0330
	GO TO 10	TEST0340
C		TEST0350
CFORMAT STATEMENTS.....	TEST0360
C	101 FORMAT(1W1, 4X, 4HTIME, 5X, 8HALTITUDE, 8X, 3HFIT)	TEST0370
	201 FORMAT(5X, 14, 5X, F6.0, 5X, F11.5)	TEST0380
C		TEST0390
C	END	TEST0400

	SUBROUTINE RCVR(X, Y, P)	RCV 0010
C		RCV 0020
C	JOHN M. HOLT	RCV 0030
C	MIT LINCOLN LABORATORY	RCV 0040
C	MILLSTONE HILL FIELD STATION	RCV 0050
C	P. O. BOX 73	RCV 0060
C	LEXINGTON, MASSACHUSETTS 02173	RCV 0070
C		RCV 0080
C	RCVR USES THE INSCON FIT PARAMETERS STORED IN COMMON TO RECOVER	RCV 0090
C	THE INSCON FIT VALUE P AT TIME X AND ALTITUDE Y. KOAT INDICATES	RCV 0100
C	THE TYPE OF DATA, FOR EXAMPLE ELECTRON DENSITY. THIS INFORMATION	RCV 0110


```

C      IS ALSO ON THE FIRST CARD OF THE INSCON OUTPUT DECK. X IS IN          RCV 0120
C      SECONDS, WITH X=0 AT THE HOUR PRECEDING THE FIRST EXPERIMENTAL      RCV 0130
C      DATA(RELTME). THE SMALLEST AND LARGEST PERMISSIBLE VALUES OF      RCV 0140
C      X ARE GIVEN BY XMIN AND XMAX. Y IS IN KILOMETERS AND MAY RANGE      RCV 0150
C      FROM YMIN TO YMAX. IF X OR Y IS OUTSIDE THE ALLOWED RANGE, RCVR    RCV 0160
C      RETURNS P=0. THE NPX EXPERIMENTAL VALUES OF X ARE STORED IN XT.    RCV 0170
C      THE NPY EXPERIMENTAL VALUES OF Y ARE STORED IN YT. THE DATA TO    RCV 0180
C      WHICH INSCON FITS AN NX BY NY LEAST MEAN SQUARE POLYNOMIAL RANGE   RCV 0190
C      FROM DMIN TO DMAX. EACH TERM OF THE POLYNOMIAL IS OF THE FORM      RCV 0200
C      PX(I)*PY(J)*A(J,I). THE A(J,I) ARE COEFFICIENTS OUTPUT BY INSCON. RCV 0210
C      THE PX(I) AND PY(J) ARE POLYNOMIALS WHICH ARE ORTHONORMAL OVER    RCV 0220
C      XT(I) AND YT(J) RESPECTIVELY. THEY ARE DEFINED BY RECURSION      RCV 0230
C      COEFFICIENTS GAMX, DELX, FACX, GAMY, DELY, FACY. IF DESIRED A     RCV 0240
C      LOWER ORDER LEAST MEAN SQUARE FIT MAY BE RECOVERED BY DECREASING  RCV 0250
C      NX AND/OR NY. ISTAT(J,I) IS AN NPY BY NPX ARRAY WHICH INDICATES   RCV 0260
C      THE QUALITY OF THE FIT AT (XT(I), YT(J)). IF ISTAT(J,I)=1,       RCV 0270
C      THE FIT IS GOOD. IF ISTAT(J,I)=0, THE FIT MAY BE BAD AND RCVR     RCV 0280
C      RETURNS P=-P. LARGE TIME GAPS IN THE DATA ARE INDICATED BY     RCV 0290
C      ISTAT(J,I)=2. RCVR RETURNS P=-P IF X IS WITHIN THE GAP.          RCV 0300
C      SIG(J) IS THE SQUARE ROOT OF THE MEAN SQUARE DEVIATION ABOUT     RCV 0310
C      THE FIT OF THE DATA AT ALTITUDE YT(J). SHIFT IS A POSITIVE      RCV 0320
C      CONSTANT WHICH IS ADDED BEFORE FITTING TO DATA WHICH TAKES ON   RCV 0330
C      NEGATIVE VALUES.                                               RCV 0340
C                                                                    RCV 0350
C                                                                    RCV 0360
C      COMMON LABEL, IDAYNO,                                           RCV 0370
C      1      KDAT, NX, NY, NPX, NPY, XT, YT, DMAX, DMIN, XMAX, XMIN,    RCV 0380
C      2      YMAX, YMIN, RELTME, SHIFT, GAMX, DELX, FACX, GAMY, DELY,   RCV 0390
C      3      FACY, A, SIG, ISTAT                                       RCV 0400
C      DIMENSION LABEL(15)                                           RCV 0410
C      DIMENSION XT(64), YT(64), GAMX(32), DELX(32), FACX(32), GAMY(32), RCV 0420
C      1      DELY(32), FACY(32), A(32,32), SIG(64), ISTAT(64,64)     RCV 0430
C      DIMENSION PX(32), PY(32)                                       RCV 0440
C                                                                    RCV 0450
C                                                                    RCV 0460
C                                                                    RCV 0470
C                                                                    RCV 0480
C      IF(X .LE. XMAX .AND. X .GE. XMIN .AND.                          RCV 0490
C      1  Y .LE. YMAX .AND. Y .GE. YMIN) GO TO 10                      RCV 0500
C      P = 0.                                                           RCV 0510
C      RETURN                                                           RCV 0520
C      XP = (2.*X-XMAX-XMIN)/(XMAX-XMIN)                               RCV 0530
C      YP = (2.*Y-YMAX-YMIN)/(YMAX-YMIN)                               RCV 0540
C      CALL SET(XP, NX, GAMX, DELX, FACX, PX)                           RCV 0550
C      CALL SET(YP, NY, GAMY, DELY, FACY, PY)                           RCV 0560
C      P = 0.                                                           RCV 0570
C      DO 20 I=1,NX                                                    RCV 0580
C      DO 20 J=1,NY                                                    RCV 0590
C      20 P = P + PX(I)*PY(J)*A(J,I)                                    RCV 0600
C      P = ((DMAX-DMIN)*P+DMAX+DMIN)/2.                                RCV 0610
C      IF(IPL(X,Y) .EQ. 3) P=-P
C      RETURN
C                                                                    RCV 0620
C                                                                    RCV 0630
C                                                                    RCV 0640
C      END

```

```

C      SUBROUTINE CREAD                                               CRED0010
C                                                                    CRED0020
C      CREAD READS THE CARD DECK GENERATED BY INSCON. THE CONTENTS OF  CRED0030

```

```

C THE CARDS ARE STORED IN BLANK COMMON, INSCON PUNCHES CRED0040
C ISTAT(J,I) ONLY IF, GIVEN J, EITHER THERE IS AN I SUCH THAT CRED0050
C ISTAT(J,I) IS NOT 0, OR J=NPY. IF NO CARD IS PRESENT FOR A GIVEN CRED0060
C J, CREAD SETS ISTAT(J,I)=1. CRED0070
C CRED0080
COMMON LABEL, IDAYNO, CRED0090
1 KDAT, NX, NY, NPX, NPY, XT, YT, DMAX, DMIN, XMAX, XMIN, CRED0100
2 YMAX, YMIN, RELTME, SHIFT, GAMX, DELX, FACX, GAMY, DELY, CRED0110
3 FACY, A, SIG, ISTAT CRED0120
DIMENSION LABEL(15) CRED0130
DIMENSION XT(64), YT(64), GAMX(32), DELX(32), FACX(32), GAMY(32), CRED0140
1 DELY(32), FACY(32), A(32,32), SIG(64), ISTAT(64,64), CRED0150
2 IST(64) CRED0160
C CRED0170
READ(5,101) (LABEL(I), I=1,15), IDAYNO, KDAT, NX, NY, NPX, NPY CRED0180
READ(5,201) XT(I), I=1,NPX CRED0190
READ(5,201) YT(J), J=1,NPY CRED0200
READ(5,201) DMAX, DMIN, XMAX, XMIN, YMAX, YMIN, RELTME CRED0210
N = MAX(NX,NY) CRED0220
READ(5,201) GAMX(I), DELX(I), FACX(I), CRED0230
1 GAMY(I), DELY(I), FACY(I), I=1,N CRED0240
DO 10 I=1,NX CRED0250
10 READ(5,201) A(J,I), J=1,NY CRED0260
READ(5,201) SIG(J), J=1,NPY CRED0270
J1 = 1 CRED0280
20 READ(5,301) YP, (IST(I), I=1,NPX) CRED0290
DO 60 J=J1,NPY CRED0300
IF(ABS(YT(J)-YP) .LT. .1 .OR. YT(J) .GE. 9999.9) GO TO 40 CRED0310
DO 30 I=1,NPX CRED0320
30 ISTAT(J,I) = 1 CRED0330
GO TO 60 CRED0340
40 DO 50 I=1,NPX CRED0350
50 ISTAT(J,I) = IST(I) CRED0360
IF(J .EQ. NPY) RETURN CRED0370
J1 = J + 1 CRED0380
GO TO 20 CRED0390
60 CONTINUE CRED0400
C CRED0410
C .....FORMAT STATEMENTS..... CRED0420
101 FORMAT(15A4, 13X, 16/ 5I4) CRED0430
201 FORMAT(6(1X, E12.5)) CRED0440
301 FORMAT(F7.1, 4X, 64I1) CRED0450
C CRED0460
END CRED0470

```

```

-----
SUBROUTINE SET(X, N, GAM, DEL, FAC, P) SET 0010
C SET CALCULATES THE FIRST N ORTHONORMAL POLYNOMIALS SET 0020
C P (DEFINED BY GAM, DEL, FAC) AT ARGUMENT X. SET 0030
C SET 0040
C SET 0050
1 SET 0060
DIMENSION P(1), GAM(1), DEL(1), FAC(1) SET 0070
P(1) = 1. SET 0080
P(2) = X - GAM(2) SET 0090
DO 10 L=3,N

```

```

10 P(L) = (X-GAM(L))*P(L-1) - DEL(L)*P(L-2)          SET 0100
   DO 20 L=1,N                                         SET 0110
20 P(L) = P(L)/FAC(L)                                  SET 0120
   RETURN                                              SET 0130
C                                                       SET 0140
   END                                                SET 0150
-----
FUNCTION IPL(X,Y)                                     IPL 0010
C                                                       IPL 0020
C   IPL DETERMINES WHETHER THE INSCON FIT IS GOOD AT POINT (X,Y).  IPL 0030
C                                                       IPL 0040
COMMON LABEL, IDAYN0,                                IPL 0050
1   KDAT, NX, NY, NPX, NPY, XT, YT, DMAX, DMIN, XMAX, XMIN,  IPL 0060
2   YMAX, YMIN, RELTME, SHIFT, GAMX, DELX, FACX, GAMY, DELY,  IPL 0070
3   FACY, A, SIG, ISTAT                                IPL 0080
DIMENSION LABEL(15)                                   IPL 0090
DIMENSION XT(64), YT(64), GAMX(32), DELX(32), FACX(32), GAMY(32),  IPL 0100
1   DELY(32), FACY(32), A(32,32), SIG(64), ISTAT(64,64)    IPL 0110
C                                                       IPL 0120
   DX = ABS(X-XT(1))                                  IPL 0130
   DO 10 I=2,NPX                                       IPL 0140
   DX1 = ABS(X-XT(I))                                  IPL 0150
   IF(DX1 .GT. DX) GO TO 20                             IPL 0160
10  DX = DX1                                           IPL 0170
20  IP = I - 1                                         IPL 0180
   DY = ABS(Y-YT(1))                                  IPL 0190
   DO 30 J=2,NPY                                       IPL 0200
   DY1 = ABS(Y-YT(J))                                  IPL 0210
   IF(DY1 .GT. DY) GO TO 40                             IPL 0220
30  DY = DY1                                           IPL 0230
40  JP = J - 1                                         IPL 0240
   IF(ISTAT(JP,IP)-1) 50,60,70                         IPL 0250
50  IPL = 3                                           IPL 0260
   RETURN                                              IPL 0270
60  IPL = 2                                           IPL 0280
   RETURN                                              IPL 0290
70  IPL = 2                                           IPL 0300
   IF(X .GT. XT(IP) .AND. ISTAT(JP,IP+1) .EQ. 2 .OR.  IPL 0310
1   X .LT. XT(IP) .AND. ISTAT(JP,IP-1) .EQ. 2) IPL=3    IPL 0320
   RETURN                                              IPL 0330
C                                                       IPL 0340
   END                                                IPL 0350
-----
C   PROGRAM TEST RCVR1                                TEST0010
C                                                       TEST0020
C   INSCON IS A FORTRAN PROGRAM WHICH CALCULATES LEAST MEAN SQUARE  TEST0030
C   FITS TO, AND PLOTS CONTOUR DIAGRAMS OF, INCOHERENT SCATTER DATA  TEST0040
C   OBTAINED AT MILLSTONE HILL. THE FIT VALUE AND FIRST DERIVATIVE  TEST0050
C   VALUES CORRESPONDING TO A GIVEN TIME AND ALTITUDE MAY BE RECOVERED  TEST0060
C   BY MEANS OF SUBROUTINES CREAD AND RCVR1. FOR EXAMPLE THIS PROGRAM  TEST0070
C   FIRST CALLS CREAD TO READ THE CARD DECK GENERATED BY INSCON. IT  TEST0080
C   THEN CALLS RCVR1 TO RECOVER THE INSCON FIT VALUES AND DERIVATIVES  TEST0090
C   AT THE EXPERIMENTAL TIMES AND ALTITUDES.          TEST0100

```

C		TEST0110
	COMMON LABEL, IDAYNO,	TEST0120
1	KDAT, NX, NY, NPX, NPY, XT, YT, DMAX, DMIN, XMAX, XMIN,	TEST0130
2	YMAX, YMIN, RELTME, SHIFT, GAMX, DELX, FACX, GAMY, DELY,	TEST0140
3	FACY, A, SIG, ISTAT	TEST0150
	DIMENSION LABEL(15)	TEST0160
	DIMENSION XT(64), YT(64), GAMX(32), DELX(32), FACX(32), GAMY(32),	TEST0170
1	DELY(32), FACY(32), A(32,32), SIG(64), ISTAT(64,64)	TEST0180
C		TEST0190
10	CALL CREAD	TEST0200
C		TEST0210
	WRITE(6,101)	TEST0220
C		TEST0230
	DO 20 I=1,NPX	TEST0240
	ITIME = XT(I) + RELTME	TEST0250
	IF(ITIME .GT. 86400) ITIME=ITIME-86400	TEST0260
	IHRS = ITIME/3600	TEST0270
	MINS = (ITIME-IHRS*3600)/60	TEST0280
	ITIME = 10000 + 100*IHRS + MINS	TEST0290
	DO 20 J=1,NPY	TEST0300
	CALL RCVR1(XT(I), YT(J), P, PDX, PDY)	TEST0310
	WRITE(6,201) ITIME, YT(J), P, PDX, PDY	TEST0320
20	CONTINUE	TEST0330
	GO TO 10	TEST0340
C		TEST0350
FORMAT STATEMENTS.....	TEST0360
101	FORMAT(1H1, 4X, 4HTIME, 5X, 8HALTITUDE, 8X, 1HP, 13X, 5HDP/DX,	TEST0370
1	11X, 5HDP/DY)	TEST0380
201	FORMAT(5X, 14, 5X, F6.0, F16.5, 4X, E12.5, 4X, E12.5)	TEST0390
C		TEST0400
	END	TEST0410

	SUBROUTINE RCVR1(X, Y, P, PDX, PDY)	RCV10010
C		RCV10020
	JOHN M. HOLT	RCV10030
C	MIT LINCOLN LABORATORY	RCV10040
C	MILLSTONE HILL FIELD STATION	RCV10050
C	P. O. BOX 73	RCV10060
C	LEXINGTON, MASSACHUSETTS 02173	RCV10070
C		RCV10080
C	RCVR1 USES THE INSCON FIT PARAMETERS STORED IN COMMON TO RECOVER	RCV10090
C	THE INSCON FIT VALUE P, AND ITS DERIVATIVES WITH RESPECT TO X AND	RCV10100
C	Y, PDX AND PDY, AT TIME X AND ALTITUDE Y. KDAT INDICATES	RCV10110
C	THE TYPE OF DATA, FOR EXAMPLE ELECTRON DENSITY. THIS INFORMATION	RCV10120
C	IS ALSO ON THE FIRST CARD OF THE INSCON OUTPUT DECK. X IS IN	RCV10130
C	SECONDS, WITH X=0 AT THE HOUR PRECEDING THE FIRST EXPERIMENTAL	RCV10140
C	DATA(RELTME), THE SMALLEST AND LARGEST PERMISSIBLE VALUES OF	RCV10150
C	X ARE GIVEN BY XMIN AND XMAX. Y IS IN KILOMETERS AND MAY RANGE	RCV10160
C	FROM YMIN TO YMAX. IF X OR Y IS OUTSIDE THE ALLOWED RANGE, RCVR1	RCV10170
C	RETURNS P=0. THE NPX EXPERIMENTAL VALUES OF X ARE STORED IN XT.	RCV10180
C	THE NPY EXPERIMENTAL VALUES OF Y ARE STORED IN YT. THE DATA TO	RCV10190
C	WHICH INSCON FITS AN NX BY NY LEAST MEAN SQUARE POLYNOMIAL RANGE	RCV10200
C	FROM DMIN TO DMAX. EACH TERM OF THE POLYNOMIAL IS OF THE FORM	RCV10210
C	PX(I)*PY(J)*A(J,I). THE A(J,I) ARE COEFFICIENTS OUTPUT BY INSCON.	RCV10220

```

C THE PX(I) AND PY(J) ARE POLYNOMIALS WHICH ARE ORTHONORMAL OVER RCV10230
C XT(I) AND YT(J) RESPECTIVELY. THEY ARE DEFINED BY RECURSION RCV10240
C COEFFICIENTS GAMX, DELX, FACX, GAMY, DELY, FACY. IF DESIRED A RCV10250
C LOWER ORDER LEAST MEAN SQUARE FIT MAY BE RECOVERED BY DECREASING RCV10260
C NX AND/OR NY. ISTAT(J,I) IS AN NPY ARRAY WHICH INDICATES RCV10270
C THE QUALITY OF THE FIT AT (XT(I), YT(J)). IF ISTAT(J,I)=1, RCV10280
C THE FIT IS GOOD. IF ISTAT(J,I)=0, THE FIT MAY BE BAD AND RCVR1 RCV10290
C RETURNS P=-P. LARGE TIME GAPS IN THE DATA ARE INDICATED BY RCV10300
C ISTAT(J,I)=2. RCVR1 RETURNS P=-P IF X IS WITHIN THE GAP. RCV10310
C SIG(J) IS THE SQUARE ROOT OF THE MEAN SQUARE DEVIATION ABOUT RCV10310
C THE FIT OF THE DATA AT ALTITUDE YT(J). SHIFT IS A POSITIVE RCV10330
C CONSTANT WHICH IS ADDED BEFORE FITTING TO DATA WHICH TAKES ON RCV10340
C NEGATIVE VALUES. RCV10350
C RCV10360
C COMMON LABEL, IDAYNO, RCV10370
1 KDAT, NX, NY, NPX, NPY, XT, YT, DMAX, DMIN, XMAX, XMIN, RCV10380
2 YMAX, YMIN, RELTME, SHIFT, GAMX, DELX, FACX, GAMY, DELY, RCV10390
3 FACY, A, SIG, ISTAT RCV10400
DIMENSION LABEL(15) RCV10410
DIMENSION XT(64), YT(64), GAMX(32), DELX(32), FACX(32), GAMY(32), RCV10420
1 DELY(32), FACY(32), A(32,32), SIG(64), ISTAT(64,64) RCV10430
DIMENSION PX(32), PY(32), PX1(32), PY1(32) RCV10440
C RCV10450
IF(X .LE. XMAX .AND. X .GE. XMIN .AND. RCV10460
1 Y .LE. YMAX .AND. Y .GE. YMIN) GO TO 10 RCV10470
P = 0. RCV10480
RETURN RCV10490
10 XP = (2.*X-XMAX-XMIN)/(XMAX-XMIN) RCV10500
YP = (2.*Y-YMAX-YMIN)/(YMAX-YMIN) RCV10510
CALL SET1(XP, NX, GAMX, DELX, FACX, PX, PX1) RCV10520
CALL SET1(YP, NY, GAMY, DELY, FACY, PY, PY1) RCV10530
P = 0. RCV10540
PDX = 0. RCV10550
PDY = 0. RCV10560
DO 20 I=1,NX RCV10570
DO 20 J=1,NY RCV10580
P = P + PX(I)*PY(J)*A(J,I) RCV10590
PDX = PDX + PX1(I)*PY(J)*A(J,I) RCV10600
20 PDY = PDY + PX(I)*PY1(J)*A(J,I) RCV10610
P = ((DMAX-DMIN)*P+DMAX+DMIN)/2. RCV10620
PDX = (DMAX-DMIN)*PDX/(XMAX-XMIN) RCV10630
PDY = (DMAX-DMIN)*PDY/(YMAX-YMIN) RCV10640
IF(IPL(X,Y) .EQ. 3) P=-P RCV10650
RETURN RCV10660
C RCV10670
END RCV10680
-----
SUBROUTINE SET1(X, N, GAM, DEL, FAC, P, P1) SET10010
C SET1 CALCULATES THE FIRST N ORTHONORMAL POLYNOMIALS SET10020
C P (DEFINED BY GAM, DEL, FAC) AND THEIR DERIVATIVES P1 AT SET10030
C ARGUMENT X. SET10040
C SET10050
C DIMENSION P(1), P1(1), GAM(1), DEL(1), FAC(1) SET10060
SET10070

```

```

P(1) = 1.
P(2) = X - GAM(2)
P1(1) = 0.
P1(2) = 1.
DO 10 L=3,N
P(L) = (X-GAM(L))*P(L-1) - DEL(L)*P(L-2)
10 P1(L) = P(L-1) + (X-GAM(L))*P1(L-1) - DEL(L)*P1(L-2)
DO 20 L=1,N
P(L) = P(L)/FAC(L)
20 P1(L) = P1(L)/FAC(L)
RETURN
C
END

```

```

SET10080
SET10090
SET10100
SET10110
SET10120
SET10130
SET10140
SET10150
SET10160
SET10170
SET10180
SET10190
SET10200

```

```

C PROGRAM TEST RCVRP
C
C INSCON IS A FORTRAN PROGRAM WHICH CALCULATES LEAST MEAN SQUARE
C FITS TO, AND PLOTS CONTOUR DIAGRAMS OF, INCOHERENT SCATTER DATA
C OBTAINED AT MILLSTONE HILL. THE FIT VALUE AND FIRST DERIVATIVE
C VALUES CORRESPONDING TO A GIVEN TIME AND ALTITUDE MAY BE RECOVERED
C BY MEANS OF SUBROUTINES CREAD AND RCVRP. FOR EXAMPLE THIS PROGRAM
C FIRST CALLS CREAD TO READ THE CARD DECK GENERATED BY INSCON. IT
C THEN CALLS RCVRP TO RECOVER THE INSCON FIT VALUES AND DERIVATIVES
C AT THE EXPERIMENTAL TIMES AND ALTITUDES. A LOCAL SPLINE
C INTERPOLATION PROCEDURE IS USED BY RCVRP TO MAKE THE FIT VALUE AND
C ITS TIME DERIVATIVE PERIODIC.
C
COMMON LABEL, IDAYNO,
1 KDAT, NX, NY, NPX, NPY, XT, YT, DMAX, DMIN, XMAX, XMIN,
2 YMAX, YMIN, RELTME, SHIFT, GAMX, DELX, FACX, GAMY, DELY,
3 FACY, A, SIG, ISTAT
DIMENSION LABEL(15)
DIMENSION XT(64), YT(64), GAMX(32), DELX(32), FACX(32), GAMY(32),
1 DELY(32), FACY(32), A(32,32), SIG(64), ISTAT(64,64)
C
10 CALL CREAD
C
WRITE(6,101)
C
DO 20 I=1,150
RI = I
X = 600.*(RI-1.) - RELTME
IF(X .LT. 0.) X=X+86400.
ITIME = X + RELTME
IF(ITIME .GT. 86400) ITIME=ITIME-86400
IHRS = ITIME/3600
MINS = (ITIME - IHRS*3600)/60
ITIME = 10000 + 100*IHRS + MINS
CALL RCVRP(X, YT(3), P, PDX, PDY, 1, XMIN)
WRITE(6,201) ITIME, YT(3), P, PDX, PDY
20 CONTINUE
GO TO 10
C
C .....FORMAT STATEMENTS.....

```

```

TEST0010
TEST0020
TEST0030
TEST0040
TEST0050
TEST0060
TEST0070
TEST0080
TEST0090
TEST0100
TEST0110
TEST0120
TEST0130
TEST0140
TEST0150
TEST0160
TEST0170
TEST0180
TEST0190
TEST0200
TEST0210
TEST0220
TEST0230
TEST0240
TEST0250
TEST0260
TEST0270
TEST0280
TEST0290
TEST0300
TEST0310
TEST0320
TEST0330
TEST0340
TEST0350
TEST0360
TEST0370
TEST0380
TEST0390
TEST0400

```

101	FORMAT(1H1, 4X, 4HTIME, 5X, 8HALTITUDE, 8X, 1HP, 13X, 5HDP/DX,	TEST0410
1	11X, 5HDP/DY)	TEST0420
201	FORMAT(5X, 14, 5X, F6.0, F16.5, 4X, E12.5, 4X, E12.5)	TEST0430
C		TEST0440
	END	TEST0450

```

SUBROUTINE RCVRP(X, Y, P, PDX, PDY, IND, XS)
C
C RCVRP USES THE INSCON FIT PARAMETERS STORED IN COMMON TO RECOVER
C A PERIODIC APPROXIMATION TO THE INSCON FIT VALUE P, AND ITS
C DERIVATIVES WITH RESPECT TO X AND Y, PDX AND PDY, AT TIME X AND
C ALTITUDE Y. XS IS THE BEGINNING (SECONDS FROM THE MIDNIGHT
C PRECEDING THE FIRST EXPERIMENTAL TIME) OF THE 24 HOUR PERIOD
C ON WHICH THE PERIODIC APPROXIMATION IS TO BE BASED. IF IND=1
C A PERIODIC APPROXIMATION IS CALCULATED BASED ON FIT VALUES
C OBTAINED FROM RCVR1. IF IND=0 RCVRP RETURNS THE ORIGINAL
C NONPERIODIC INSCON FIT VALUES.
C
COMMON LABEL, IDAYNO,
1 KDAT, NX, NY, NPX, NPY, XT, YT, DMAX, DMIN, XMAX, XMIN,
2 YMAX, YMIN, RELTME, SHIFT, GAMX, DELX, FACX, GAMY, DELY,
3 FACY, A, SIG, ISTAT
DIMENSION LABEL(15)
DIMENSION XT(64), YT(64), GAMX(32), DELX(32), FACX(32), GAMY(32),
1 DELY(32), FACY(32), A(32,32), SIG(64), ISTAT(64,64)
DIMENSION XX(7), PP(7), PPDY(7), W(7), PROXIN(7), PPDY(7)
DATA W/0., .166667, .333333, .5, -.333333, -.166667, 0./
C
C .....USE RCVR1 DIRECTLY IF IND=0 OR THE DATA SPANS LESS THAN
C 1 20 HOURS.....
C IF(IND.EQ. 0 .OR. XMAX-XMIN .LT. 72000.)
C 1 CALL RCVR1(X,Y,P,PDX,PDY) ; RETURN
C
C IF(XMAX-XMIN .LT. 86400.) XMN=XMIN
C IF(XMAX-XMIN .GE. 86400.) XMN=XS
C XPR = X
C REPEAT 10, WHILE XPR .GT. XMN+86400.
10 XPR = XPR - 86400.
C REPEAT 20, WHILE XPR .LT. XMN
20 XPR = XPR + 86400.
C IF(XMAX-XMIN .LT. 86400.) GO TO 30
C
C .....IF XMAX-XMIN .GT. 86400. ADD LINEAR TREND TO ALL RECOVERED
C DATA.....
C CALL RCVR1(XMN, Y, P1, PDX1, PDY1)
C CALL RCVR1(XMN+86400., Y, P2, PDX2, PDY2)
C DP = P2 - P1
C DPDX = PDX2 - PDX1
C DPDY = PDY2 - PDY1
C DT = (XPR-XMN)/86400.
C CALL RCVR1(XPR, Y, P, PDX, PDY)
C P = P + DP*DT
C PDX = PDX + DPDX*DT
C PDY = PDY + DPDY*DT
C
RCVP0010
RCVP0020
RCVP0030
RCVP0040
RCVP0050
RCVP0060
RCVP0070
RCVP0080
RCVP0090
RCVP0100
RCVP0110
RCVP0120
RCVP0130
RCVP0140
RCVP0150
RCVP0160
RCVP0170
RCVP0180
RCVP0190
RCVP0200
RCVP0210
RCVP0220
RCVP0230
RCVP0240
RCVP0250
RCVP0260
RCVP0270
RCVP0280
RCVP0290
RCVP0300
RCVP0310
RCVP0320
RCVP0330
RCVP0340
RCVP0350
RCVP0360
RCVP0370
RCVP0380
RCVP0390
RCVP0400
RCVP0410
RCVP0420
RCVP0430
RCVP0440
RCVP0450
RCVP0460
RCVP0470
RCVP0480

```

```

RETURN
C
C .....FIND TIMES XL AND XU, 3 HOURS BEFORE AND 3 HOURS AFTER XC.
C      XL-XU=64800(18 HOURS).
30 XC = XMAX + (86400.-XMAX+XMIN)/2.
C      XL = XC-10800.
C      XU = XC + 10800. - 86400.
C
C .....USE RCVR1 DIRECTLY IF X IS BETWEEN XU AND XL.
C      IF(XPR .GT. XU .AND.XPR .LT. XL) CALL RCVR1(X,Y,P,PDX,PDY) ;
1      RETURN
C
C .....CALCULATE ESTIMATES P1 AND P2 OF P(XC) , AND ESTIMATES
C      PDY1 AND PDY2 OF PDY(XC) FROM P, PDX AND PDY AT EACH
C      BOUNDRY OF THE GAP.....
C      CALL RCVR1(XMAX, Y, P, PDX, PDY)
C      P1 = P + PDX*(XC-XMAX)
C      PDY1 = PDY
C      CALL RCVR1(XMIN, Y, P, PDX, PDY)
C      P2 = P + PDX*(XC-XMIN-86400.)
C      PDY2 = PDY
C      DP = P2 - P1
C      DPDY = PDY2 - PDY1
C
C .....CALCULATE PP(I)=P(XX(I)) AT TIMES XX(1)...XX(N) WHERE
C      XX(1)=XL AND XX(N)=XU AND XX(2)...XX(N-1) ARE AT HOURLY
C      INTERVALS BETWEEN XL AND XU. TIMES XX(I) FOR WHICH DATA
C      DOES NOT EXIST ARE EXCLUDED.
N = 0
DO 40 I=1,7
RI = I
XX(I) = XL + 3600.*(RI-1.)
IF(XX(I) .GT. 86400.) XX(I)=XX(I)-86400.
IF(XX(I) .GT. XMAX .OR. XX(I) .LT. XMIN) GO TO 40
CALL RCVR1(XX(I), Y, PP(I), PPDY(I), PPDY(I))
N = N + 1
XX(N) = XX(I)
IF(N .GT. 1 .AND. XX(N) .LT. XX(N-1)) XX(N)=XX(N)+86400.
PP(N) = PP(I) + W(I)*DP
PPDY(N) = PPDY(I) + W(I)*DPDY
40 CONTINUE
C
C USE CUBIC SPLINE INTERPOLATION BETWEEN THE POINTS PP(XX(I)) TO
C      CALCULATE P(X) AND PDX(X).
C      RLAMO = 1.
C      DO = 6.*((PP(2)-PP(1))/(XX(2)-XX(1))-PPDX(1))/(XX(2)-XX(1))
C      RMUN = 1.
C      DN = 6.*(PPDX(N) - (PP(N)-PP(N-1))/(XX(N)-XX(N-1)))/
1      (XX(N)-XX(N-1))
IF(XPR .LT. XU) XPR=XPR+86400.
CALL SPLN3A(N,1,XX,PP,RLAMO,DO,RMUN,DN,XPR,P,PDX,SS2,PROXIN)
CALL SPLN3A(N,1,XX,PPDY,0.,0.,0.,0.,XPR,PDY,PDX,SS2,PROXIN)
RETURN
C
END
RCVP0490
RCVP0500
RCVP0510
RCVP0520
RCVP0530
RCVP0540
RCVP0550
RCVP0560
RCVP0570
RCVP0580
RCVP0590
RCVP0600
RCVP0610
RCVP0620
RCVP0630
RCVP0640
RCVP0650
RCVP0660
RCVP0670
RCVP0680
RCVP0690
RCVP0700
RCVP0710
RCVP0720
RCVP0730
RCVP0740
RCVP0750
RCVP0760
RCVP0770
RCVP0780
RCVP0790
RCVP0800
RCVP0810
RCVP0820
RCVP0830
RCVP0840
RCVP0850
RCVP0860
RCVP0870
RCVP0880
RCVP0890
RCVP0900
RCVP0910
RCVP0920
RCVP0930
RCVP0940
RCVP0950
RCVP0960
RCVP0970
RCVP0980
RCVP0990
RCVP1000
RCVP1010
RCVP1020
RCVP1030

```


TIME	ALTITUDE	P	DP/DX	DP/DY
2012	150.	-885.56632	-.44337E-02	-.37441E 01
2012	225.	1163.06590	.10711E-01	.88094E 01
2012	300.	1948.94308	-.15981E-01	.10958E 02
2012	375.	2690.71146	-.52171E-01	.83944E 01
2012	450.	3181.53133	-.74241E-01	.47119E 01
2012	525.	3418.26056	-.69387E-01	.18177E 01
2012	600.	3490.43291	-.36018E-01	.34477E 00
2012	675.	3500.16388	.17525E-01	.64399E-01
2012	750.	3512.98395	.75941E-01	.29844E 00
2012	825.	3539.59937	.12163E 00	.33177E 00
2012	900.	3548.58033	.14103E 00	-.17540E 00
2012	975.	-3509.97670	.13266E 00	-.77509E 00
2012	1050.	-3469.86119	.11684E 00	.18073E 00
2012	1125.	-3655.79992	.14710E 00	.59526E 01
2039	150.	-880.71529	-.23849E-02	-.33525E 01
2039	225.	1175.30152	.45780E-02	.88205E 01
2039	300.	1944.72735	.62258E-02	.10536E 02
2039	375.	2647.09170	-.10216E-01	.78268E 01
2039	450.	3101.70718	-.33848E-01	.43732E 01
2039	525.	3331.02952	-.46180E-01	.19918E 01
2039	600.	3438.90297	-.32600E-01	.11175E 01
2039	675.	3525.12140	.10787E-01	.12881E 01
2039	750.	3636.30546	.74926E-01	.16286E 01
2039	825.	3753.09551	.14021E 00	.13351E 01
2039	900.	3813.66047	.18348E 00	.15971E 00
2039	975.	-3773.52254	.18967E 00	-.11061E 01
2039	1050.	-3701.69777	.16804E 00	-.14678E 00
2039	1125.	-3913.15259	.17308E 00	.73615E 01
2104	150.	-876.57853	-.33654E-02	-.37017E 01
2104	225.	1176.92096	.25657E-02	.90782E 01
2104	300.	1957.07819	.70942E-02	.10497E 02
2104	375.	2641.10716	-.18783E-02	.74082E 01
2104	450.	3059.48564	-.25048E-01	.38936E 01
2104	525.	3263.26924	-.44557E-01	.18506E 01
2104	600.	3382.11590	-.42789E-01	.15755E 01
2104	675.	3526.17767	-.11179E-01	.23493E 01
2104	750.	3731.86008	.45812E-01	.30221E 01
2104	825.	3951.44887	.11158E 00	.25979E 01
2104	900.	4086.60412	.16308E 00	.82016E 00
2104	975.	-4065.72192	.18142E 00	-.12440E 01
2104	1050.	-3965.16338	.16726E 00	-.61860E 00
2104	1125.	-4174.35110	.16108E 00	.81662E 01
2133	150.	-868.30834	-.64208E-02	-.43161E 01
2133	225.	1165.43042	-.10628E-01	.93250E 01

BIBLIOGRAPHIC DATA SHEET	1. Report No.	2.	3. Recipient's Accession No.
	4. Title and Subtitle Millstone Hill Thomson Scatter Results for 1970		5. Report Date 11 May 1976
7. Author(s) John V. Evans and John M. Holt	9. Performing Organization Name and Address Lincoln Laboratory, M.I. T. P.O. Box 73 Lexington, MA 02173		6.
12. Sponsoring Organization Name and Address National Science Foundation RANN Directorate Washington, DC 20550		10. Project/Task/Work Unit No.	8. Performing Organization Rept. No. Technical Report 522
15. Supplementary Notes		11. Contract/Grant No. GA-42230	13. Type of Report & Period Covered Technical Report
16. Abstracts During 1970, the incoherent scatter radar at Millstone Hill (42.6°N, 71.5°W) was employed to measure the electron density, electron and ion temperatures, and vertical velocity of the ions in the F-region over periods of 24 hours on an average of twice per month. The observations spanned the height interval 200 to 900 km, approximately, and achieved a time resolution of about 30 minutes. This report presents the results of these measurements in a set of contour diagrams.		14.	
17. Key Words and Document Analysis. 17a. Descriptors Millstone radar F-region diurnal variations electron density ionospheric scatter seasonal variations temperature effects spectrum analyzers			
7b. Identifiers/Open-Ended Terms			
7c. COSATI Field/Group			
8. Availability Statement		19. Security Class (This Report) UNCLASSIFIED	21. 152
		20. Security Class (This Page) UNCLASSIFIED	22. Price